The Use of Modified Oligonucleotides to Investigate Biological Applications for Triple Helix Formation

Thesis by

Joseph Gerard Hacia

In Partial Fulfillment of the Requirements

for the Degree of

Doctor of Philosophy

California Institute of Technology

Pasadena, California

1995

(submitted January 16, 1995)

Acknowledgments

I would like to express my deepest gratitude to both of my advisors Barbara Wold and Peter Dervan. They have contributed equally towards making graduate school a challenging and rewarding intellectual experience. Peter's intelligence, leadership, and professionalism have made a lasting impression on me. Barbara's sharp intellect, creativity, and genuine enthusiasm towards science will never be forgotten. Both Peter and Barbara supported me through both the good and bad times and provided me with a tremendous amount of freedom in designing my experiments. The scientific environment and equipment were always of the highest caliber. It is easy to take for granted Barbara's and Peter's diverse scientific interests. It is a real privilege to have studied under their guidance and I hope to maintain their high scientific standards.

I would also like to thank my thesis committee members: Professors Guiseppe Attardi, William J. Dunphy, and Alexander Varshavsky. I appreciate the scientific discussions that I had with them and the interest that they took in me. I was fortunate enough to rotate through Dr. Attardi's laboratory and get to know Salil, Nalini, Giovanni, and Ram who are all great scientists and great friends.

During my undergraduate days at Rutgers University I was had the privilege to conduct research in the laboratory of Dr. Masayori Inouye. All the people in his laboratory were very helpful and great teachers. In particular, Giafen Chen and Claude Lerner spent a great deal of time teaching me the basics of molecular biology and were very supportive and patient. I will always admire Dr. Inouye's great intelligence and creativity. He provided the highest standards of scientific research and integrity that I will always try to emulate.

In both the Dervan group and Wold group I met a number of extremely talented postdoctoral fellows and graduate students who are also very genuine human beings. David Horne was a much appreciated friend during my first two years. He taught me a great deal about chemistry and how to be a good scientist. The time that he spent with me and my Mom will never by forgotten. Kent Gates and I spent many hours talking about science and life in general. This was always the most fun part of my day and I appreciate his support and advise. I was fortunate to share a laboratory with Steve Woski during my final three years at Caltech. Coming to work every day was infinitely more enjoyable and rewarding knowing that he was nearby. Dinners with Steve and his wife Kori were real fun and provided a much needed break from the lab. Some of my fondest memories are of late night treks to vending machines on campus with Eldon Baird to grab some food. Eldon provided much appreciated help with his computer expertise and stimulating discussions. Dinners and late night beers with Milan Mrksich were great fun and helped raise my spirits during difficult times. Milan is a bright and hard working normal guy who is also a loyal friend. Paul Garrity is always entertaining to talk to and provided excellent experimental advise. He is one of the most bright and talented scientists that anyone could encounter. I also thank all other members past and present of both groups and wish them all well in whatever they choose to do in life.

The help and friendship of many other people at Caltech is greatly appreciated. Susan Horvath and the rest of the microchemical facility is an incredible resource base and generously helped me with oligonucleotide synthesis. Jeff Sampson and Peggy Saks, along with the rest of the Abelson group, taught me a great deal about RNA biochemistry. Henry Lester and Norman Davidson generously provided oocytes for experimentation. Mike Quick was incredibly patient and willing to teach me the basics of microinjection

techniques. Cathy Murphy and Michael Arkin are good friends from the Barton group and helped make the Beckman Institute a great place to work. Oocyte experiments with Tim Johann were fun and intellectually stimulating.

A number of people outside of Caltech greatly contributed to my intellectual development during graduate school. James Hetfield, Lars Ulrich, Kirk Hammet, Cliff Burton, and Jason Newsted provided many hours of stimulating late night discussion and had a major influence on my experimental designs. Late nights at Millikan library with Dewey Simmons provided some of my most vivid memories and embody the essence of the Caltech experience.

Finally and most importantly I would like to thank my family for all the love and support that they have given me throughout my life. I have been blessed by God to have the best parents that anyone could ever hope for. My Mom always was and always will be my best friend in the world. Her kind and generous spirit and sense of humor through good times and bad have made an indelible mark on me and all the people around her. I hope to face life with a fraction of her courage, perseverance, and wisdom. My Dad was always there to support and provide for us. His dedication and love will always be remembered and provides me with a model for my life. My brother Frank's numerous sacrifices that enabled me to get the best education will never be forgotten. He has always put others before himself and I could never repay what he has done for me. My sisters Mary and Grace have provided a great deal of support and guidance during my life. I love them all, especially Mom, and dedicate my work to them.

To Mom and Dad with love

ABSTRACT

Oligonucleotide-directed triple helix formation was assayed for potential biological applications. Unmodified pyrimidine-rich oligodeoxyribonucleotides were found to block the progress of primer extension by DNA polymerase *in vitro* through triple helix formation. Klenow fragment polymerization was obstructed at sites that map near the proximal boundary between duplex and triplex. Among a family of related three-stranded structures, longer triplexes were more effective polymerase inhibitors than shorter complexes. One such complex provided an effective polymerase blockade for at least twenty minutes.

Chemical modifications enhanced both triple helix formation and the nuclease resistance of pyrimidine-rich and purine-rich oligonucleotides. Unmodified purine-rich and pyrimidine-rich oligonucleotides containing a diastereomeric mixture of phosphorothioate or stereoregular (all *R*P) phosphorothioate linkages were tested for triple helix formation by quantitative DNase I footprinting analysis. Both purine-rich and pyrimidine-rich phosphorothioate oligonucleotides containing modified nucleosides formed triple helical complexes *in vitro* under physiological ionic conditions. Pyrimidine-rich oligoribonucleotides as well as 2'-OMe oligoribonucleotides bound DNA with high affinity. Only purine-rich oligodeoxyribonucleotides had significant affinity for double-helical DNA.

Small uridine-rich oligoribonucleotides were overexpressed in *E. coli* for *in vivo* triple helix formation studies using a low-copy number plasmid target site. Micromolar intracellular concentrations of intact oligoribonucleotide were generated; however, *in vivo* footprinting analysis indicated that no triple helical complexes formed. β-galactosidase activity assays further indicated

that the presence of the uridine-rich RNA did not inhibit transcription of a chimeric *lacZ* gene in which the triple helix target site was inserted.

Modified nuclease-resistant pyrimidine-rich and purine-rich oligonucleotides were tested for triple helix formation on *Xenopus* oocyte minichromosomes. *In vivo* footprinting analysis showed that none of the oligonucleotides formed triple helical complexes with the target site. A modified oligonucleotide, which directed an alkylation reaction to a specific guanosine residue on duplex DNA *in vitro*, did not react *in vivo* with the target minichromosomes. Further chemical modifications will have to be made to facilitate *in vivo* triple helix formation.

Table of Contents

List of Figures and Tables

Chapter I

Figures

Chapter II

Tables

Figures

Chapter III

Tables

Figures

Chapter IV

Table

Figures

Chapter V

Tables

Figures

Chapter VI

Tables

Figures

Chapter VII

Tables

Figures

Chapter I

Introduction to Oligonucleotide-Directed Triple Helix Formation

Polymeric Pyrimidine-Rich Triple Helical Complexes. Shortly after the discovery of structure of the DNA double helix by Watson and Crick, the first report of triple-stranded polynucleotide structures, consisting of two equivalents of poly (U) and one equivalent of poly (A), was made by Rich and co-workers (Felsenfeld et al., 1957). In the years following this report, a number of other pyrimidine-rich triple-helical complexes comprised of polydeoxyribonucleotide and polyribonucleotide mixtures were discovered using spectroscopic techniques (Rich, 1958; Rich, 1960; Riley et al., 1966; Blake et al., 1967; Felsenfeld & Miles, 1967; Michelson et al., 1967; Cassani et al., 1969; Murray & Morgan, 1973). In addition to triple helical complexes involving duplexes with A•T/U Watson-Crick base pairing, triple helices comprised of two strands of poly (C) bound to guanine oligoribonucleotides under acidic conditions were found (Lipsett, 1963; Howard et al., 1964; Lipsett, 1964; Thiele & Guschlbauer, 1971). Further experimentation proved that triple helices can form with the homopolymeric duplex poly (dT-dC)• poly (dG-dA) and either poly (U-C) or poly (dT-dC) third strand polynucleotides (Morgan & Wells, 1968; Lee et al., 1979). Analysis of x-ray fiber diffraction patterns generated from poly (A) • 2 poly (U) and poly (dA) • 2 (dT) triple helical complexes gave the first high resolution information about the structure of these polymeric triple helices (Arnott & Selsing, 1972; Arnott & Bond, 1973; Arnott et al., 1973; Arnott & Seling, 1974; Arnott et al., 1976). Structural models were proposed suggesting that the Watson-Crick

base-paired double helix was bound by the third strand polynucleotide forming specific hydrogen bonds to exposed purines in the major groove (Figure 1). These hydrogen bonds were designated Hoogsteen hydrogen bonds after the pioneering work of Kelvin Hoogsteen who provided the first crystallographic evidence of base triplets formed with uracil and adenine (Rich, 1958; Hoogsteen, 1959). The triple helical structure was consistent with proposals of the two polypyrimidine strands being in an antiparallel orientation with respect to one another and with all the bases being in the *anti* conformation.

Polymeric Purine-Rich Triple Helical Complexes. Although there have been a wealth of studies involving pyrimidine-rich polymeric triple helices, less work has been done examining triple helical complexes formed with two purine polynucleotide strands. Lipsett first reported the discovery of triple-stranded polynucleotide structures consisting of two equivalents of poly (G) and one equivalent of poly (C) under neutral pH conditions (Lipsett, 1964). This claim was later supported by additional spectroscopic evidence of other workers (Mark & Thiele, 1978). Later Fresco and co-workers reported length-dependent polymeric triple stranded structures consisting of two equivalents of poly (A) and one equivalent of poly (U) (Broitman et al., 1987).

Pyrimidine-Rich Oligonucleotide Directed Triple Helix Formation. Oligonucleotides were first utilized to form localized sequence-specific triple helical complexes with double-helical DNA through the pioneering work of Moser and Dervan (Moser & Dervan, 1987). Pyrimidine-rich oligodeoxyribonucleotides ranging from 11 nt to 15 nt in length bound to specific homopyrimidine-homopurine tracts on kilobase size plasmid

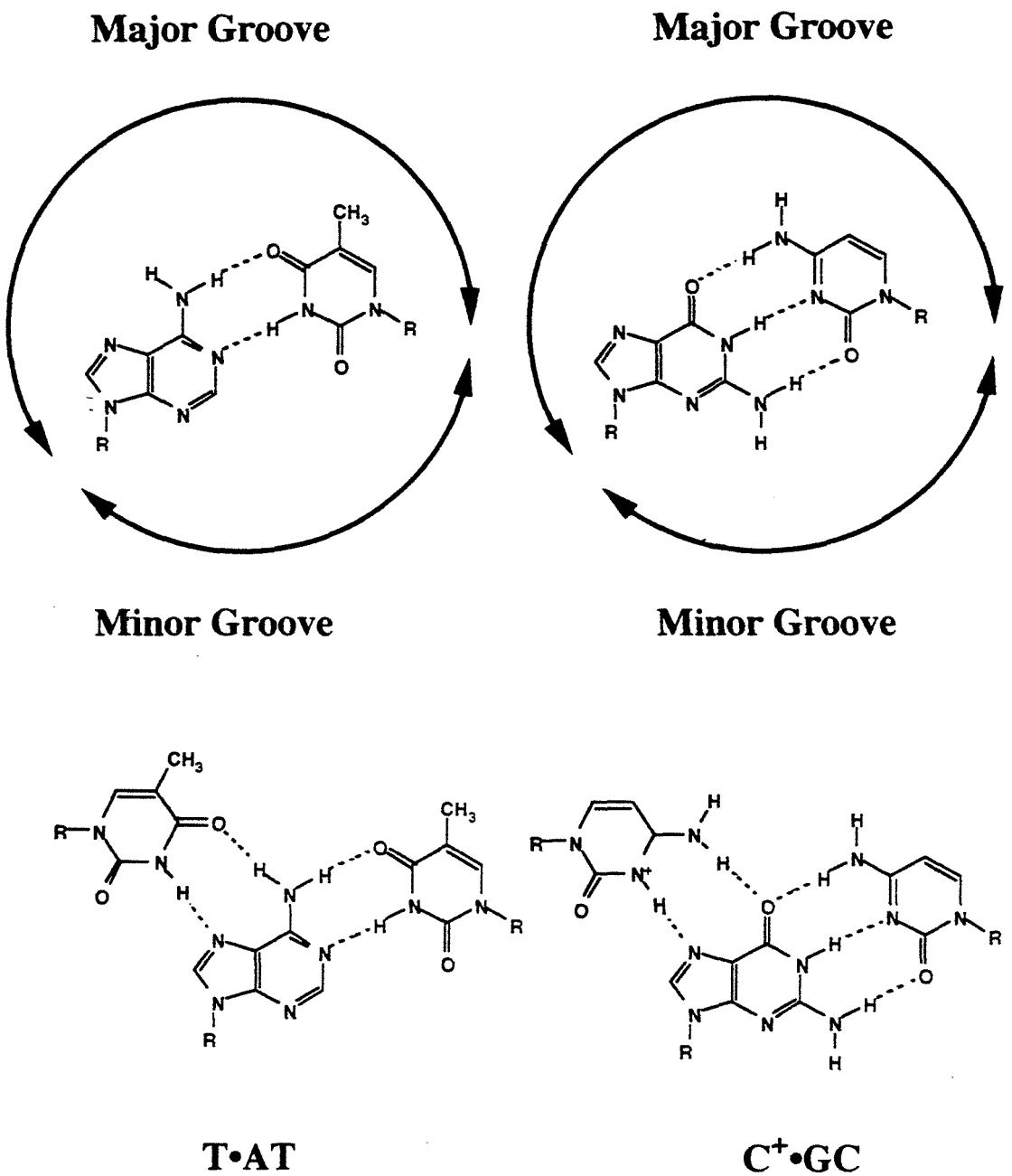

Figure 1. Pyrimidine•Purine•Pyrimidine Base Triplets.

restriction fragments through the formation of both T•AT and C^+•GC base triplets. An EDTA•Fe(II) chelate, a redox activatable DNA cleaving agent, was tethered to the triple helix forming oligonucleotides to create a sequence-specific chemical nuclease (Dreyer & Dervan, 1985). The pattern of DNA cleavage generated through triple helix formation established that the third strand oligonucleotide bound in a parallel orientation relative to the purine-rich strand in the major groove of the double-helical target. It was later found that G•TA triplets may be incorporated into triple helical complexes formed by otherwise pyrimidine-rich oligonucleotides (Griffin & Dervan, 1989). However, the stability of G•TA triplets may be subject to sequence composition effects (Kiessling et al., 1992).

Purine-Rich Oligonucleotide Directed Triple Helix Formation. Complementing work involving pyrimidine-rich oligonucleotides, other studies have focused on the use of purine-rich oligonucleotides to form triple helical complexes. Hogan and co-workers first demonstrated that a guanine-rich oligonucleotide could bind *in vitro* to a natural guanine-rich sequence in the promoter of the human c-*myc* gene (Cooney et al., 1988). The purine-rich oligonucleotide was proposed to bind in a parallel orientation relative to the purine-rich strand of the double helical DNA target site through the formation of G•GC and A•AT base triplets (Figure 2). However, it was later shown by Beal and Dervan through affinity cleavage analysis that purine-rich third strand oligonucleotides bind in an antiparallel orientation relative to the purine-rich strand of the double helical DNA target site (Beal & Dervan, 1991). Furthermore this study provided evidence for T•AT as well as G•GC and A•AT base triplets in this triple helical structural motif.

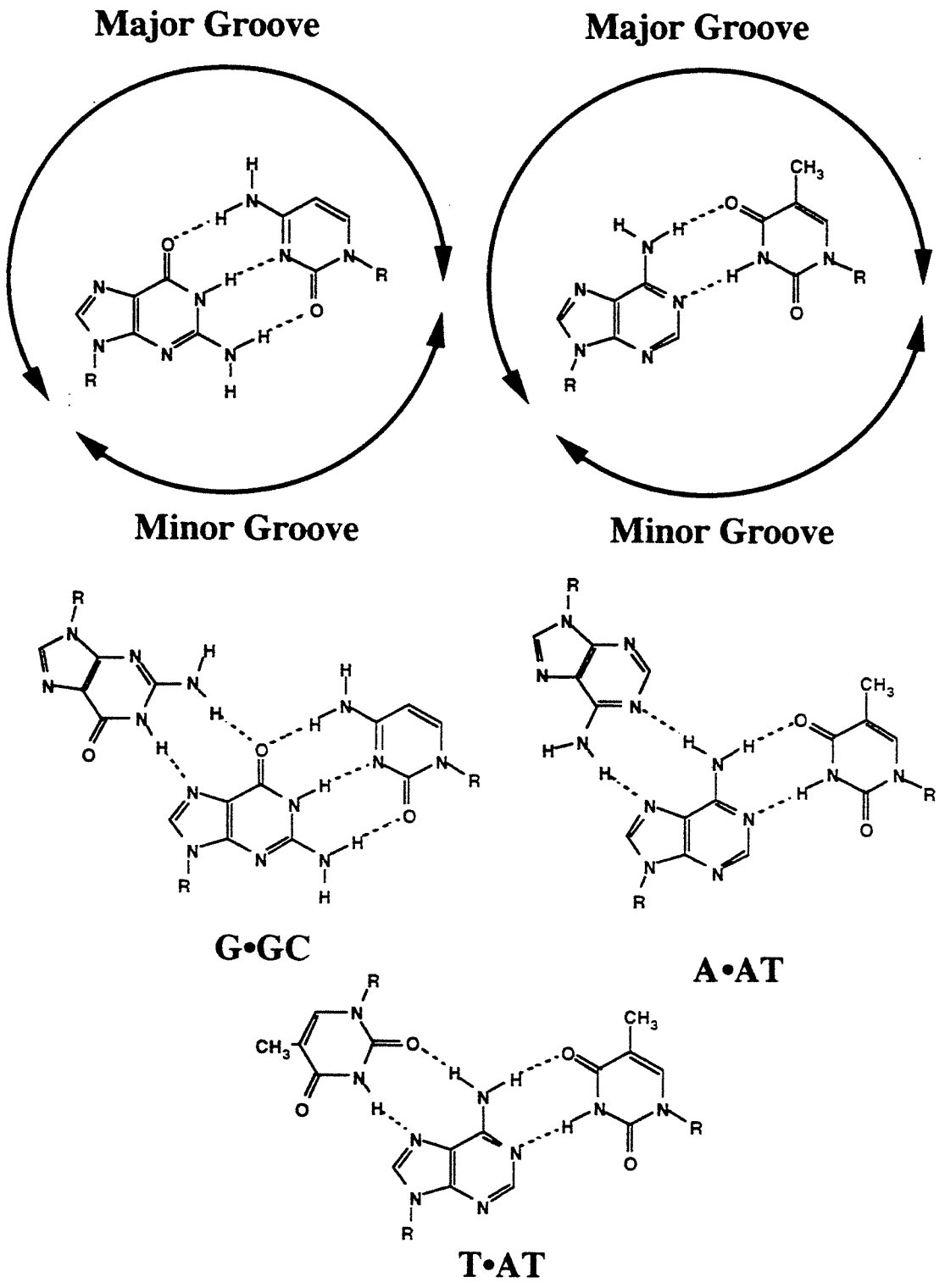

Figure 2. Purine•Purine•Pyrimidine Base Triplets.

Alternate-Strand Triple Helix Formation. Besides recognizing purine-rich tracts present on one strand of duplex DNA, oligonucleotide-directed triple helix formation has been utilized to bind adjacent purine-rich sequences present on opposite strands of the double helix. The first report of alternate-strand triple helix formation was made by Horne and Dervan (Horne & Dervan, 1990). Two separate pyrimidine-rich oligonucleotide recognition units were joined by their 3'-end termini with an abasic nucleoside linker to generate a oligonucleotide capable of binding adjacent purine-rich sequences on opposite strands of the 5'-$(Purine)_x(Pyrimidine)_y$-3' target site. The abasic linker crosses the major groove to allow the binding of two oligonucleotide recognition units to each half-site. Further work optimized linkers necessary for this class of alternate strand triple helix formation (Froehler et al., 1992). Another approach uses a third strand consisting of purine and pyrimidine blocks which recognize purines in the target duplex by switching strands at the junction between purine-rich and pyrimidine-rich tracts while maintaining the required strand polarity (Beal & Dervan, 1992; Jayasena & Johnston, 1992; Jayasena & Johnston, 1993). Both 5'-$(Purine)_x(Pyrimidine)_y$-3' and 5'-$(Pyrimidine)_x(Purine)_y$ DNA sequences theoretically can be targeted using this strategy.

NMR Studies of Triple Helical Complexes. NMR studies have provided high resolution structures of a variety of triple helical complexes. In 1989 Feigon and co-workers presented NMR structural data for an 8mer triple helical complex formed between 2 homopyrimidine $d(T\text{-}C)_4$ and one homopurine $d(G\text{-}A)_4$ strands (Rajagopal & Feigon, 1989a; Rajagopal & Feigon, 1989b). Hoogsteen hydrogen-bonding schemes were confirmed for T•AT and C^+•GC base triplets. Patel and co-workers presented similar NMR data for an 11mer

triple helical complex composed of two pyrimidine strands and one purine strand (de los Santos et al., 1989; Live et al., 1991). These studies relied on hybridizing three distinct oligodeoxyribonucleotides together to form the complex.

In 1990 Feigon presented NMR structural data for an intramolecular triple helix formed from a single DNA strand (Sklenar & Feigon, 1990). The triple helical region consisted of two pyrimidine tracts and one purine tract. Such structures also have been characterized through chemical footprinting techniques (Haner & Dervan, 1990). Results of NMR studies on such structures lead to the assignment of the sugar conformation of the pyrimidine and purine tracts involved in complex formation. Analysis of the sugar puckers revealed that the triple helical sugars are predominantly of the S-type (close to C2'-*endo*) (Macaya et al., 1992a; Macaya et al., 1992b). However some of the Hoogsteen base-paired cytosines were of the N-type (close to C3'-*endo*). The dominant of S-type sugar conformation is consistent with the sugar conformation normally found in B-DNA (Saenger, 1984). This contrasts models derived from fiber diffraction studies in which all three strands had sugars of the N-type characteristic of A-form DNA (Arnott & Selsing, 1974). Feigon and co-workers have used such structures to measure the stability of GC mismatches in the third strand of intramolecular triplexes by NMR and UV melting analysis (Macaya et al., 1991).

Other NMR studies have focused on the structure of pyrimidine-rich intramolecular triple helices containing a G•TA base triplet. Patel and co-workers have found that the third strand guanosine adopts a predominantly N-type sugar conformation and uses the hydrogen bonding scheme depicted in Figure 3 (Radhakrishnan et al., 1991b; Radhakrishnan et al., 1991c; Radhakrishnan et al., 1992a; Radhakrishnan et al., 1992b; Radhakrishnan &

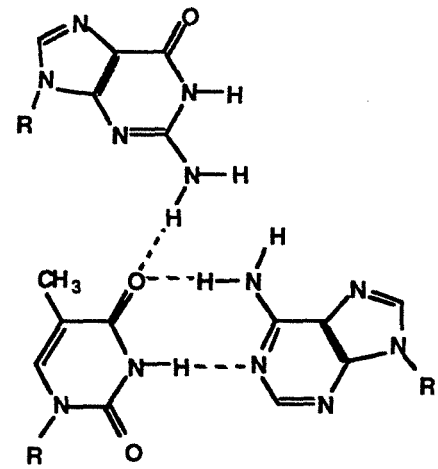

Figure 3. Hydrogen bonding pattern of a G•TA triplet.

Patel, 1994). Futhermore, the presence of guanosine in the otherwise homopyrimidine strand does not cause major structural distortions. Feigon and co-workers have proposed the same hydrogen-bonding scheme and similar structural data (Wang et al., 1992). A NMR solution structure of a py•pu•py DNA triple helix containing a guanine in the third strand is shown in figure 4 (Patel & Radhakrishnan, 1994).

Structural data on purine•purine•pyrimidine intramolecular triple helical structures also has been gathered through NMR studies. Patel and co-workers confirmed reverse hydrogn-bonding interactions between the purine third strand and the purine strand of the Watson-Crick helix (Radhakrishnan et al., 1991a; Radhakrishnan et al., 1993; Radhakrishnan & Patel, 1993a; Radhakrishnan & Patel, 1993b). These studies revealed that the guanine residues adopt S-type sugar conformations ranging from *C1'-exo* to *C3'-exo* while in most cases the thymines adopt *C-4'-exo* conformations. Complexes formed with the nonisomorphic base triplets G•GC and T•AT displayed structural deformations at d(TpG) and d(GpT) steps. A NMR solution structure of a purine•purine•pyrimidine intramolecular DNA triple helix is

Figure 4. NMR structural model of a pyrimidine•purine•pyrimidine intramolecular triple helix containing a central G•TA triplet (Patel & Radhakrishnan, 1994). The purine-rich and pyrimidine-rich strands of the double-helical target are depicted in blue and green, respectively. The third pyrimidine-rich strand is depicted in red.

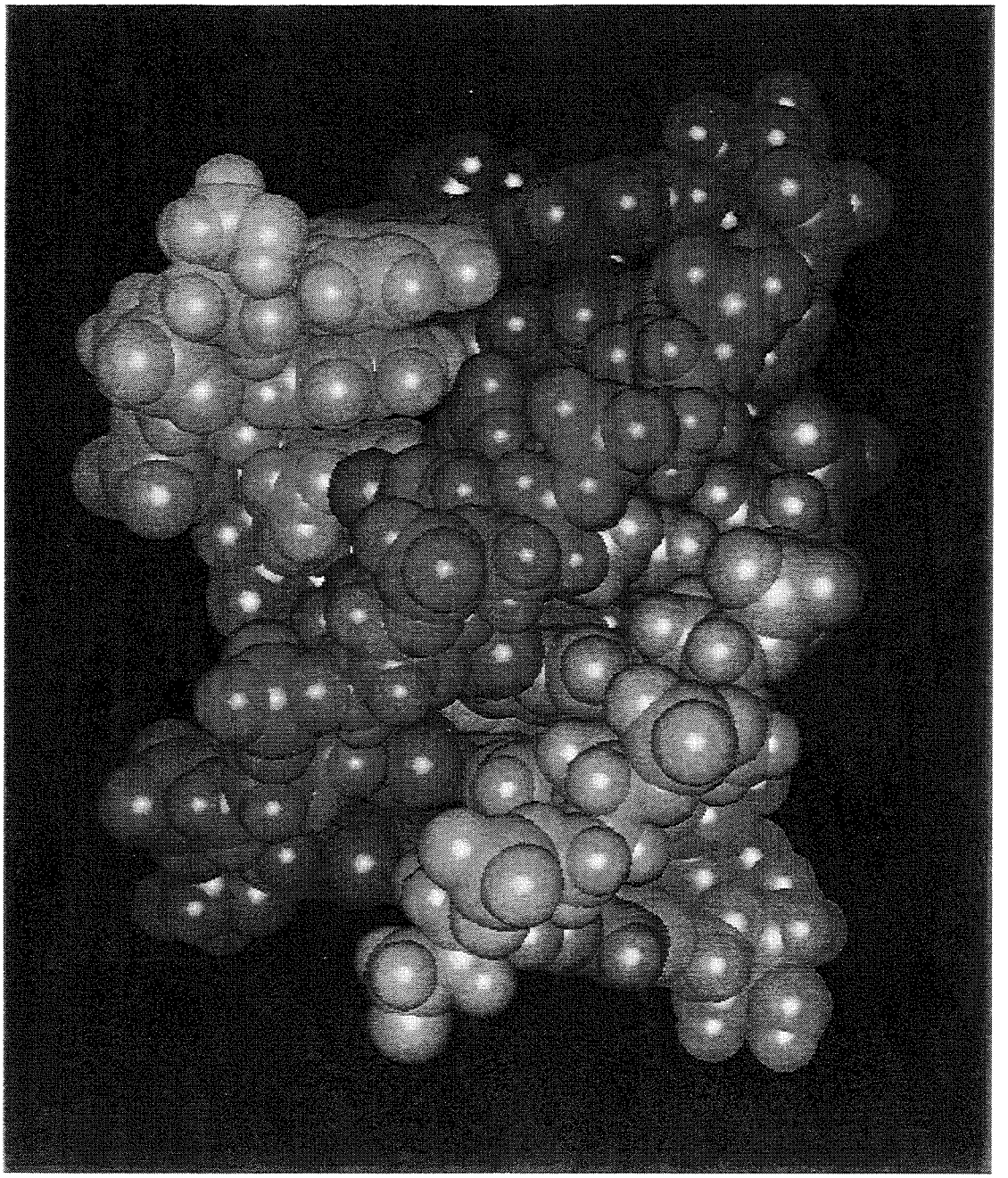

Figure 5. NMR structural model of a purine•purine•pyrimidine intramolecular triple helix (Radhakrishnan & Patel, 1993b). The purine-rich and pyrimidine-rich strands of the double-helical target are depicted in blue and green, respectively. The third purine-rich strand is depicted in red.

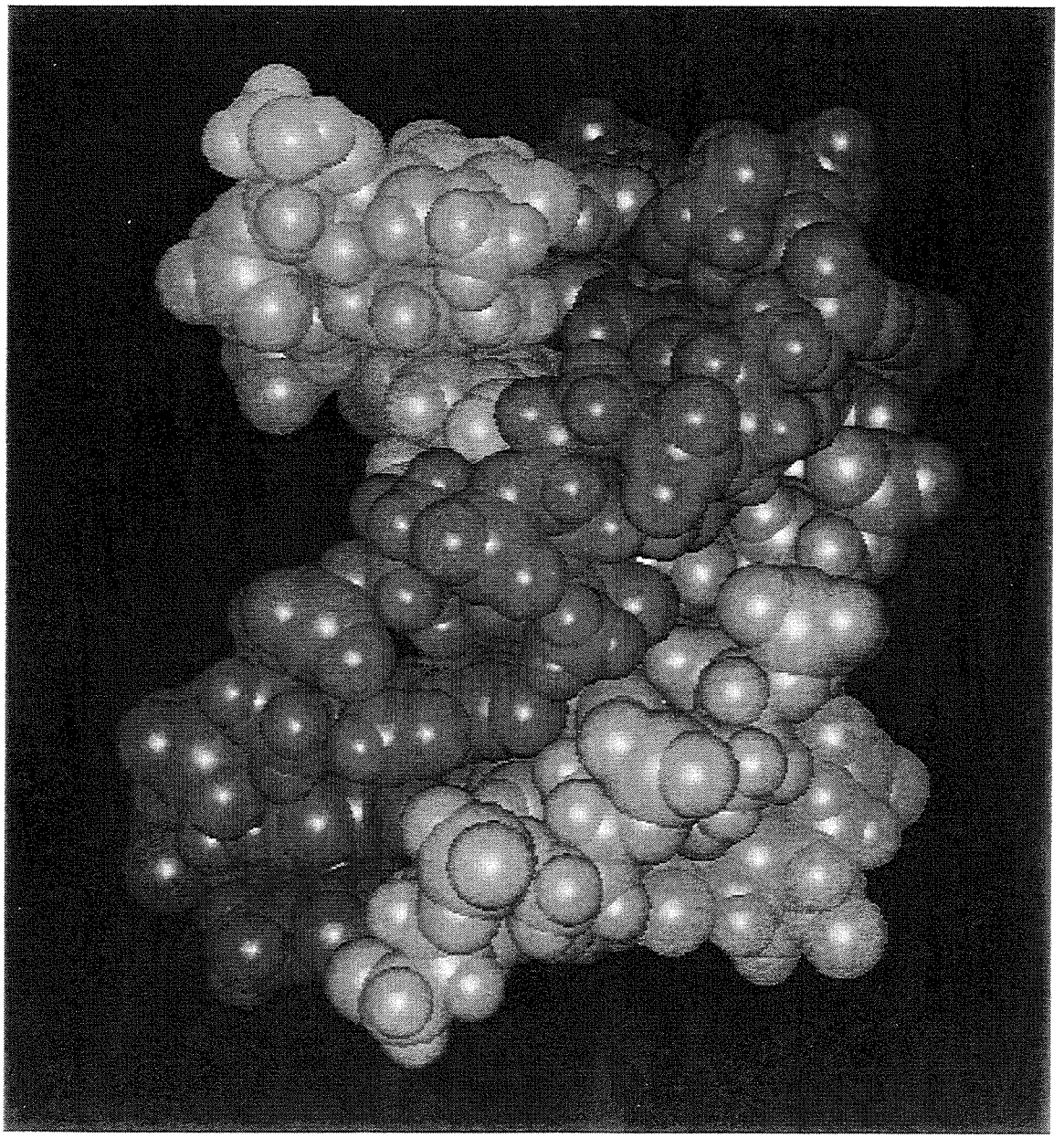

shown in figure 5 (Patel & Radhakrishnan, 1993b).

Cooperative Oligonucleotide-Directed Triple Helix Formation. Cooperative interactions between DNA binding molecules increase the sequence specificity of the recognition process as well as the sensitivity of the binding equilibrium to concentration changes. Cooperative interactions between pyrimidine-rich oligonucleotides binding to adjacent sites on double-helical DNA were first reported by Strobel and Dervan (Strobel & Dervan, 1989). These observations were extended by incorporating a dimerization domain to the ends of the oligonucleotides which are juxtaposed upon triple helix formation (Distefano et al., 1991). Dimerization occurs through the formation of Watson-Crick base-pairing to create a mini-helix projecting away from the target site and a Y-shaped triple helical complex. The stability of such complexes can be controlled through the binding of a small molecule such as echinomycin to the mini-helix dimerization domain (Distefano & Dervan, 1992). The energetics of cooperatively binding pyrimidine-rich oligonucleotides has been rigorously measured by quantitative affinity cleavage titrations (Colocci et al., 1993; Colocci & Dervan, 1994). A 20-fold enhancement in equilibrium association constant is realized for an 11 nt pyrimidine oligonucleotide binding in the presence of a neighboring site using T•AT and $^{m}C^{+}$•GC base triplets (Colocci et al., 1993). Recent experiments have maximized the extent of these cooperative interactions. Colocci and Dervan demonstrated that the inclusion of the modified nucleoside 5-(1-propynyl)-2'-deoxyuridine into oligonucleotides allowed greater than 40-fold enhancement in the binding of two neighboring 8-mer oligonucleotides (Colocci & Dervan, 1994).

The Use of Oligonucleotide-Directed Triple Helix Formation to Cleave Genomic DNA. The development of site-specific DNA cleaving agents is important to the field of chromosome mapping as well as for gene isolation and sequencing (Dervan, 1990). Oligonucleotide-directed triple helix formation was used to cleave λ genomic DNA at a single site by Strobel and Dervan (Strobel et al., 1988). A pyrimidine-rich oligonucleotide-EDTA•Fe(II) conjugate bound to a unique 18-bp site on the 48.5 kbp λ genome and effected cleavage to yield two DNA fragments, 39.1 and 9.4 kbp. This affinity cleavage technique later was expanded for use on yeast genomic DNA (Strobel & Dervan, 1990). A pyrimidine-rich oligonucleotide-EDTA conjugate bound a unique engineered 20-bp sequence inserted into the 340-kilobase pair chromosome III of *Saccharomyces cerevisae*. Cleavage was shown to be specific for the chromosome III target site and produced two new DNA fragments, approximately 110 and 230 kbp. A chemical-enzymatic technique for genomic DNA cleavage utilizing oligonucleotide-directed triple helix formation was introduced in 1991 by Strobel and Dervan (Strobel & Dervan, 1991). In the first step of this strategy, triple helix formation protects a specific site on double-helical DNA from modification by a methyltransferase. When the genomic DNA is digested by a restriction endonuclease which recognizes the same sequence as the methyltransferase, only the site that was protected from methylation by triple helix formation will be cleaved. A pyrimidine-rich oligonucleotide bound to an engineered 24-bp homopurine tract overlapping an EcoR I site in the 340-kilobase pair chromosome III of *Saccharomyces cerevisae.* The triple helix protected the site from methylation by EcoR I methylase and upon disruption of the triple helix allow EcoR I endonuclease to specifically cleave a unique site with greater than 95% efficiency. A similar approach later was used on human genomic DNA

(Strobel et al, 1991). A pyrimidine-rich oligonucleotide protected a 16-bp target site on human chromosome 4 (situated between genetic marker D4S10 and the telomere) from methylation at an overlapping Alu I methylase site. Restriction endonuclease Sst I digested the single unmethylated site to yield a unique 4 Mbp cleavage product with a 80 - 90% yield. A nonenzymatic approach towards the site-specific cleavage of genomic DNA was presented by Povsic, Strobel, and Dervan (Povsic et al., 1992). A N-bromoacetyl-modified pyrimidine-rich oligonucleotide was used to specifically alkylate two specific guanines present on opposite strands of yeast chromosomal DNA. After depurination of the alkylated sites, specific double-stranded cleavage occurred in 85-90% yield.

BIBLIOGRAPHY

Arnott, S., & Bond, P. J. (1973) *Nature New Biol. 244*, 99-101.

Arnott, S., Bond, P. J., Selsing, E., & Smith, P. J. C. (1976) *Nucleic Acids Res. 3*, 2459-2470.

Arnott, S., Hukins, D. W. L., Dover, S. D., Fuller, W., & Hodgson, A. R. (1973) *J. Mol. Biol. 81*, 107-122.

Arnott, S., & Selsing, E. (1972) *Biochem. Biophys. Res. Commun. 47*, 1504-1510.

Arnott, S. & Selsing, E. (1974) *J. Mol. Biol. 88*, 509-521.

Beal, P. A. & Dervan, P. B. (1991) *Science 251*, 1360-1363.

Beal, P. A., & Dervan, P. B. (1992) *J. Am. Chem. Soc. 114*, 4976-4982.

Blake, R. D., Massoulie, J., & Fresco, J. R. (1967) *J. Mol. Biol. 30*, 291-308.

Broitman, S. L., Im, D. D., & Fresco, J. R. (1987) *Proc. Natl. Acad. Sci. U. S. A. 84*, 5120-5124.

Cassani, G. R., & Bollum, F. J. (1969) *Biochemistry 8*, 3928-3936.

Colocci, N., & Dervan, P. B. (1994) *J. Am. Chem. Soc. 116*, 785-786.

Colocci, N., Distefano, M D., & Dervan, P. B. (1993) *J. Am. Chem. Soc. 115*, 4468-4473.

Cooney, M., Czernuszewicz, G., Postel, E. H., Flint, S. J., & Hogan, M. E. (1988) *Science 241*, 456-459.

de los Santos, C., Rosen, M., & Patel, D. (1989) *Biochemistry 28*, 7282-7289.

Dervan, P. B. (1990) in *Human Genome Initiative and DNA Recombination* (Sarma, R. H., & Sarma, M. H., Eds.) pp 37-49, Adenine Press, Guilderland, NY.

Distefano, M. D., & Dervan, P. B. (1992) *J. Am. Chem. Soc. 114*, 11006-11007.

Distefano, M. D., Shin, J. A., & Dervan, P. B. (1991) *J. Am. Chem Soc. 113*, 5901-5902.

Dreyer, G. B., & Dervan, P. B. (1985) *Proc. Natl. Acad. Sci. 82*, 968-972.

Felsenfeld, G., Davies, D. R., & Rich, A. (1957) *J. Am. Chem. Soc. 79*, 2023-2024.

Felsenfeld, G., & Miles, H. T. (1967) *Annu. Rev. Biochem. 36*, 407-448.

Froehler, B. C., Terhorst, T., Shaw, J. P., & McCurdy, S. N. (1992) *Biochemistry 31*, 1603-1609.

Griffin, L. C. & Dervan, P. B. (1989) *Science 245*, 967-971.

Haner, R. & Dervan, P. B. (1990) *Biochemistry 29*, 9761-9765.

Hoögsteen, K. (1959) *Acta Crystallogr. 12*, 822-823.

Horne, D. A. & Dervan, P. B. (1990) *J. Am. Chem. Soc. 112*, 2435-2437.

Howard, F. B., Frazier, J., Lipsett, M. N., & Miles, H. T. (1964) *Biophys. Biochem. Res. Commun. 17*, 93-102.

Jayasena, S. D., & Johnston, B. H. (1992) *J. Am. Chem. Soc. 114*, 1470-1478.

Jayasena, S. D., & Johnston, B. H. (1993) *Biochemistry 32*, 2800-2807.

Kiessling, L. L., Griffin, L. C., & Dervan, P. B. (1992) *Biochemistry 31*, 2829-2834.

Lee, J. S., Johnson, D. A., & Morgan, A. R. (1979) *Nucleic Acids Res. 6*, 3073-3091.

Lipsett, M. N. (1963) *Biophys. Res. Commun. 11*, 224-228.

Lipsett, M. N. (1964) *J. Biol. Chem. 239*, 1256-1260.

Live, D. H., Radhakrishnan, I., Misra, V., & Patel, D. J. (1991) *J. Am. Chem. Soc. 113*, 3073-3091.

Macaya, R., Gilbert, D. E., Malek, S., Sinsheimer, J. S., & Feigon (1991) *Science 254*, 270-276.

Macaya, R. F., Schultze, P., & Feigon, J. (1992a) *J. Am. Chem. Soc. 114*, 781-783.

Macaya, R., Wang, E., Schultze, P., Sklenar, V., & Feigon, J. (1992b) *J. Mol. Biol. 225*, 755-773.

Mark, C., & Thiele, D. (1978) *Nucleic Acids Res. 5*, 1017-1028.

Michelson, A. M., Massoulie, J., & Guschlbaur, W. (1967) *Prog. Nucleic Acids Res. Mol. Biol. 6*, 83-141.

Morgan, A. R., & Wells, R. D. (1968) *J. Mol. Biol. 37*, 63-80.

Moser, H. E., & Dervan, P. B. (1987) *Science 238*, 645-650.

Murray, N. L., & Morgan, A. R. (1973) *Can. J. Biochem. 51*, 436-449.

Povsic, T. J., Strobel, S. A., & Dervan, P. B. (1992) *J. Am. Chem. Soc. 114*, 5941-5945.

Radhakrishnan, I., de los Santos, C., & Patel, D. J. (1991a) *J. Mol. Biol. 221*, 1403-1418.

Radhakrishnan, I., de los Santos, C., & Patel, D. J. (1993) *J. Mol. Biol. 234*, 188-197.

Radhakrishnan, I., Gao, X., de los Santos, C., Live, D., & Patel, D. J. (1991b) *Biochemistry 30*, 9022-9030.

Radhakrishnan, I., & Patel, D. J. (1993a) *J. Am. Chem. Soc. 115*, 1615-1617.

Radhakrishnan, I., & Patel, D. J. (1993b) *Structure 1*, 135-152.

Radhakrishnan, I., & Patel, D. J. (1994) *Structure 2*, 17-32.

Radhakrishnan, I., Patel, D., & Gao, X. (1991c) *J. Am. Chem. Soc. 113*, 8542-8544.

Radhakrishnan, I., Patel, D., & Gao, X. (1992a) *Biochemistry 31*, 2514-2523.

Radhakrishnan, I., Patel, D. J., Veal, J. M., & Gao, X. (1992b) *J. Am. Chem. Soc. 114*, 6913-6915.

Rajagopal, P., & Feigon, J. (1989a) *Biochemistry 28*, 7859-7870.

Rajagopal, P., & Feigon, J. (1989b) *Nature 339*, 637-640.

Rich , A. (1958) *Nature 181*, 521-525.

Rich, A. (1960) *Proc. Natl. Acad. Sci. U. S. A. 46*, 1044-1053.

Riley, M., Maling, B., & Chamberlin, M. J. (1966) *J. Mol. Biol. 20*, 359-389.

Saenger, W. (1984) *Principles of Nucleic Acid Structure*, Springer-Verlag, New York.

Sklenar, V., & Feigon, J. (1990) *Nature 345*, 836-838.

Strobel, S. A., & Dervan, P. B. (1989) *J. Am. Chem. Soc. 111*, 7286-7287.

Strobel, S. A., Douchette-Stamm, L A., Riba, L., Housman, D. E., & Dervan, P. B. (1991) *Science 254*, 1639.

Strobel, S. A., Moser, H. E., & Dervan, P. B. (1988) *J. Am. Chem. Soc. 110*, 7927-7929.

Strobel, S. A., & Dervan, P. B. (1990) *Science 249*, 73-75.

Strobel, S. A., & Dervan, P. B. (1991) *Nature 350*, 172-174.

Thiele, D., & Guschlbauer, W. (1971) *Biopolymers 10*, 143-157.

Wang, E., Malek, S., & Feigon, J. (1992) *Biochemistry 31*, 4838-4846.

Chapter II

Energetics of Triple Helix Formation With Oligonucleotides Containing Modified Sugars

INTRODUCTION

Both pyrimidine-rich and purine-rich oligodeoxyribonucleotides can hybridize to specific DNA sequences through triple helix formation. Pyrimidine-rich oligodeoxyribonucleotides bind in a parallel orientation to purine-rich strands in the major groove of the double helix by forming specific Hoogsteen hydrogen bonds (T•AT and C^+•GC base triplets) (Moser & Dervan, 1987; Le Doan et al., 1987; Rajagopal & Feigon, 1989; de los Santos et al., 1989). Purine-rich oligodeoxyribonucleotides bind in an antiparallel orientation relative to purine-rich strands in the major groove of the double helix by forming specific reverse Hoogsteen hydrogen bonds (G•GC and T•AT or A•AT base triplets) (Beal & Dervan, 1991; Chen, 1991; Pilch et al., 1991; Durland et al., 1991; Radhakrishnan & Patel, 1993).

In this chapter results obtained from quantitative Ava I endonuclease protection studies examining the ability of both modified pyrimidine-rich and purine-rich oligonucleotides to form triple-helical complexes are presented. Several pyrimidine-rich oligonucleotides with modified sugars had high affinity for double helical DNA. In contrast, only purine-rich oligodeoxyribonucleotides formed stable triple helical complexes. Moreover, the effect of modifying hybridization conditions, such as

increasing pH, on triple helix formation was examined. These results have implications for the design of *in vivo* triple helix forming oligonucleotides as well as for the structures of different classes of triple helices.

EXPERIMENTAL PROCEDURES

Materials. All DNA synthesis reagents were obtained from Applied Biosystems Inc. except for 5-methylcytosine and inosine phosphoramidites obtained from Cruachem. Phosphoramidites for the chemical synthesis of RNA oligonucleotides were obtained from Biogenix. Restriction endonuclease Ava I (10U/μL) and ribonucleoside triphosphates were obtained from Pharmacia. Tetrabutylammonium fluoride in tetrahydrofuran was obtained from Aldrich. All other restriction enzymes, snake venom phosphodiesterase, and calf intestine alkaline phosphatase were purchased from Boehringer Mannheim.

Plasmid Target Site. The 6363-bp pMTCAT-TH1 construct contains the mouse metallothionein I promoter modified by site-directed mutagenesis to contain a 21-bp homopurine triple helix target site (figure 1) (Maher et al., 1989). The 21-bp homopurine run partially overlaps one of two Ava I restriction endonuclease sites found on the construct. A ribbon model depicting two possible triple helix structures that can occupy this site are shown schematically in Figure 1.

Chemical Synthesis of Oligodeoxyribonucleotides. The oligodeoxyribonucleotides used in this study are shown in Tables 1 and 2. All oligodeoxyribonucleotides as well as 2'-OMe oligonucleotides were prepared on an Applied Biosystems 380B DNA Synthesizer with β-cyanoethyl phosphoramidites. Abasic β-cyanoethyl phosphoramidite were kindly provided by Dr. David Horne (Horne & Dervan, 1991). 2'-OMe β-cyanoethyl phosphoramidites were the gift of Dr. Robert Haner

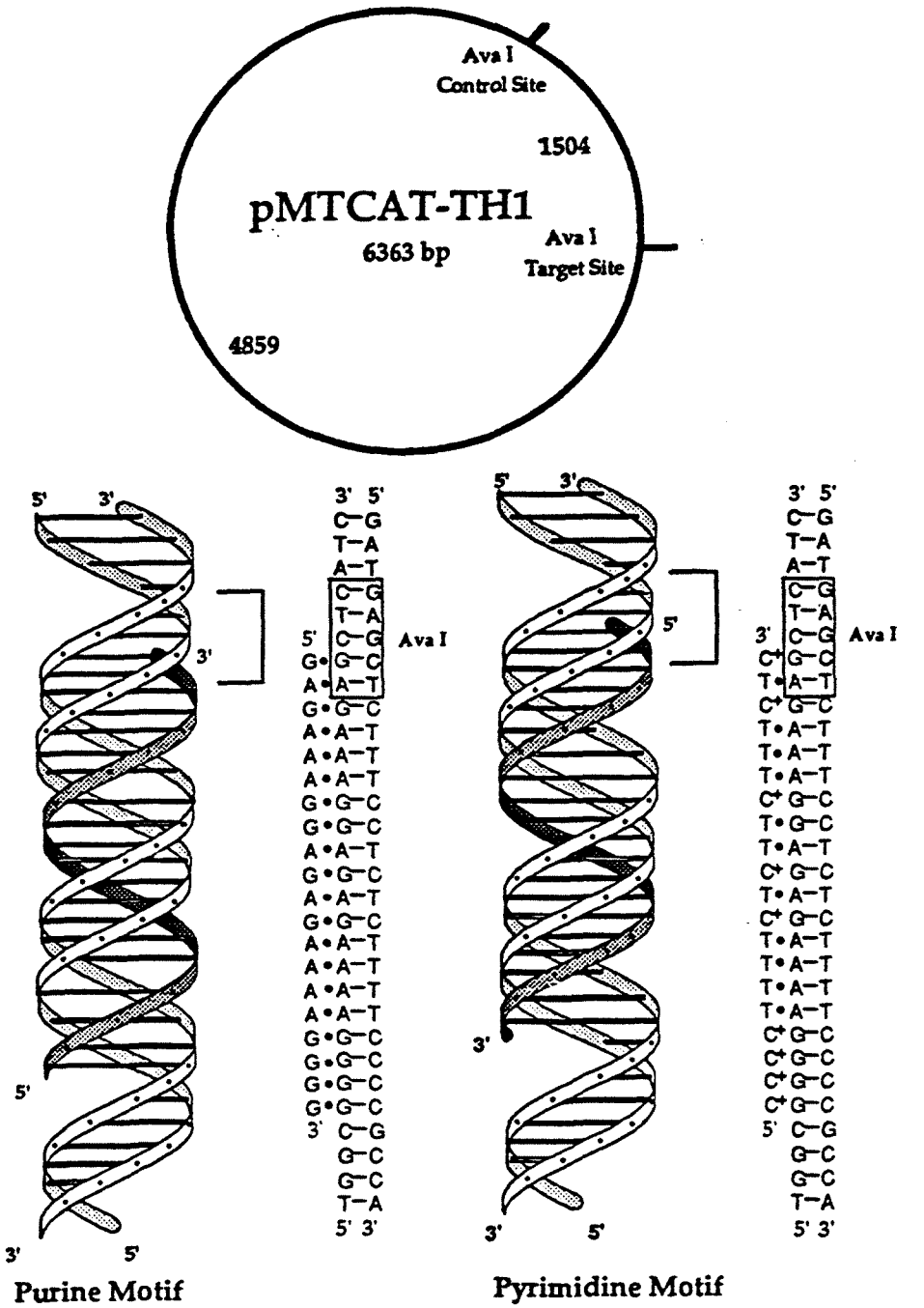

Figure 1: Restriction map of pMTCAT-TH1 and schematic representation of the triple helical complexes involving oligonucleotides **Pu1** and **Py1**. In the ribbon model of these complexes, the Ava I recognition site overlapping the 21-bp homopurine sequence is indicated by a bracket (center) and by a box (right). (-) indicates Watson-Crick hydrogen-bonded base pairing while (•) and (+) indicate Hoogsteen hydrogen bonds for the complex involving oligonucleotide **Py1**. (•) indicates reverse Hoogsteen hydrogen bonds for the complex involving oligonucleotide **Pu1**.

(Haner & Dervan, unpublished observations). Oligonucleotides were purified by denaturing polyacrylamide gel electrophoresis, visualized by UV shadowing, and electroeluted from gel slices using an Elu-trap apparatus (Schleicher & Schuell). They were ethanol precipitated and resuspended in 0.5X TE before storing at -80 °C. The concentration of oligonucleotides were determined by A_{260} measurements using the following molar extinction coefficients: 15,400 (A), 11,700 (G), 7,300 (C), 8,800 (T), 5,800 (^{m}C), and 12,300 (I).

Enzymatic Synthesis of Oligoribonucleotides. Oligonucleotides **Py4** and **Pu3** were enzymatically synthesized by T7 *in vitro* transcription on a chemically synthesized oligodeoxyribonucleotide template (Milligan et al. 1987). To 100 pmoles of T7 promoter oligonucleotide **T7PRO** 5'-TA ATACGACTCACTATAG-3' was added 100 pmoles of either template **YRNA** 5'-GGGGAAAAAGAGAGGAAAGAGCTCCCTATAGTGAGTCG TATTA-3' or template **RRNA** 5'-CTCTTTCCTCTCTTTTTCCCCTATAGT GAGTCGTATTA-3' in a 50 µL total volume of 1X STE (10 mM NaCl, 10 mM Tris-Cl pH 8.0, and 1 mM EDTA). The mixture was heated to 90 °C for one minute and oligonucleotides were annealled by cooling to room temperature over the course of one hour. T7 RNA polymerase *in vitro* transcription reactions were assembled by adding 50 µL of annealed template to 50 µL of 10X T7 RNA Polymerase Transcription Buffer (250 mM $MgCl_2$, 500 mM Tris-Cl pH 8.0, 50 mM DTT, 2 mM spermidine), 10 µL of 1M DTT, 50 µL of 40 mM NTP mix (40 mM ATP, 40 mM UTP, 40 mM CTP, 40 mM GTP) and 340 µL of Milli-Q water. The transcription reaction was initiated by adding 40 µL of 70U/µL T7 RNA polymerase and incubated at 37 °C for 12 hours. The reactions were extracted with an equal

Table 1. Pyrimidine-rich oligonucleotides tested[a]

Oligo	Sequence
	5'- G A G A A A G G A G A G A A A A G G G G-3'
	3'- C T C T T T C C T C T C T T T T C C C C-5'
Py1	5'-dCdTdCdTdTdTdCdCdTdCdTdCdTdTdTdTdTdCdCdCdC-3'
	m m m m m m m m m
Py2	5'-dCdTdCdTdTdTdCdCdTdCdTdCdTdTdTdTdTdCdCdCdC-3'
	m b m b b b m m b m b m b b b b b m m m
Py3	5'-dCdUdCdUdUdUdCdCdUdCdUdCdUdUdUdUdUdCdCdCdC-3'
	m m m m m m m m m
Py4	5'-rCrTrCrTrTrTrCrCrTrCrTrCrTrTrTrTrTrCrCrCrC-3'
Py5	5'-rCrUrCrUrUrUrCrCrUrCrUrCrUrUrUrUrUrCrCrCrC-3'
Py6	5'-rUrUrCrCrCrCrUrCrUrUrCrUrUrUrUrUrCrUrCrCrUrC-3'
Py7	5'-dTdTdCdCdCdCdTdCdTdTdCdTdTdTdTdCdTdCdCdTdC-3'
	m m m m m m m m
Py8	5'-dCdTdCdTdTdTdCdCdTdCdTdCdTdTdTdTdTdCdCdC-3'
	m m m m m m m
Py9	5'-dCdTdCdTdTdTdCdCdTdCdTdCdTdTdTdTdTdCdC-3'
	m m m m m m
Py10	5'-dCdTdCdTdTdTdCdCdTdCdTdCdTdTdTdTdTdC-3'
	m m m m m m
Py11	5'-dCdTdCdTdTdTdCdCdTdCdTdCdTdTdTdTdT-3'
	m m m m m m
Py12	5'-dCdTdCdTdTdTdCdCdTdCdTdCdTdTdTdT-3'

Key: d = 2'-deoxyribose, r = ribose, r = 2'-OMe-ribose, ^{m}C = 5-methylcytidine, ^{b}U = 5-bromouridine.

volume of phenol : chloroform : isoamyl alcohol (25 : 24 : 1) and then with an equal volume of chloroform. The volume was brought to 2 mL with Milli-Q water and exhaustively dialyzed against Milli-Q water overnight. Reactions were lyophilized and resuspended in 100 µL of 1X TE. Reactions containing template **YRNA** were treated with 1 uL of 10 U/µL RNase T1 followed by incubation at 37 °C for 1 hour prior to organic extraction and desalting. Oligonucleotides were purified by denaturing polyacrylamide gel electrophoresis, visualized by UV shadowing, and electroeluted from

Table 2. Purine-rich oligonucleotides tested[a]

Oligo	Sequence
	5'- G A G A A A G G A G A G A A A A A G G G G-3'
	3'- C T C T T T C C T C T C T T T T T C C C C-5'
Pu1	5'-dGdAdGdAdAdAdGdGdAdGdAdGdAdAdAdAdAdGdGdGdG-3'
Pu2	5'-dGdTdGdTdTdTdGdGdTdGdTdGdTdTdTdTdTdGdGdGdG-3'
Pu3	5'-rGrArGrArArArGrGrArGrArGrArArArArArArGrGrGrG-3'
	b b b b b b b b b b b b b
Pu4	5'-dGdUdGdUdUdUdGdGdUdGdUdGdUdUdUdUdUdGdGdGdG-3'
Pu5	5'-dGdCdGdCdCdCdGdGdCdGdCdGdCdCdCdCdCdGdGdGdG-3'
	m m m m m m m m m m m m m
Pu6	5'-dGdCdGdCdCdCdGdGdCdGdCdGdCdCdCdCdCdGdGdGdG-3'
Pu7	5'-dGdIdGdIdIdIdGdGdIdGdIdGdIdIdIdIdIdGdGdGdG-3'
Pu8	5'-dGdØdGdØdØdØdGdGdØdGdØdGdØdØdØdØdØdGdGdGdG-3'
Pu9	5'-dGdAdGdAdAdAdGdGdAdGdAdGdAdAdAdAdAdGdGdGdG-3'
Pu10	5'-dGdTdGdTdTdTdGdGdTdGdTdGdTdTdTdTdTdGdGdGdG-3'
Pu11	5'-rGrArGrArArArGrGrArGrArGrArArArArArArGrGrGrG-3'

[a]Key: d = 2'-deoxyribose, r = ribose, r = 2'-OMe-ribose, [m]C = 5-methylcytidine, [b]U = 5-bromouridine, I = inosine, Ø = abasic.

gel slices using an Elu-trap apparatus (Schleicher & Schuell). They were ethanol precipitated and resuspended in 0.5X TE before storing at -80 °C. After ethanol precipitation, oligoribonucleotide **Pu3** was dephosphorylated utilizing RNase free calf intestine alkaline phosphatase and then desalted as above (Sambrook et al., 1989).

Chemical Synthesis of Oligoribonucleotides. Oligoribonucleotides **Py5** and **Pu3** also were prepared on an Applied Biosystems 380B DNA Synthesizer with 2'-hydroxyl protected tertbutyl dimethyl silyl β-

cyanoethyl phosphoramidites. The oligoribonucleotides were deblocked and purified under standard conditions (Usman et al., 1987). The solid support from a typical 1 μmole RNA synthesis was removed from the synthesis vessel and treated with 2 mL of 3 : 1 ammonium hydroxide : ethanol solution and incubated at 55 °C for 8 - 12 hours. The solution was dried in a Speed-Vac (Savant) and resuspended in 2 mL of tetrabutylammonium fluoride/tetrahydrofuran. After a 48 hour room temperature incubation, the reaction was quenched by adding 20 μL of 2M triethylamine acetate pH 7.0 and evaporated to an oil in a Speed-Vac (Savant). The residue was resuspended in 2 mL of Milli-Q water and dialyzed against water Oligoribonucleotides were concentrated through lyophilization, purified by denaturing polyacrylamide gel electrophoresis, visualized by UV shadowing, and electroeluted from gel slices using an Elu-trap apparatus (Schleicher & Schuell). They were ethanol precipitated and resuspended in 0.5X TE before storing at -80 °C. The concentration was determined by A_{260} measurements using the following molar extinction coefficients: 15,400 (A), 11,700 (G), 7,300 (C), and 10,000 (U).

Enzymatic Degradation of Chemically Synthesized Oligoribonucleotides. The purity of chemically synthesized oligonucleotides was confirmed by HPLC nucleotide and nucleoside analysis (McLaughlin et al., 1981; Usman et al., 1987; Wang et al., 1990). For nucleotide analysis, to 10 nmoles of oligoribonucleotide was added 2.5 μL of 1M Tris-Cl pH 8.1, 5 μL of 1M $MgCl_2$, and 10 U of snake venom phosphodiesterase in a 50 μL total volume. The reaction was incubated at 37 °C for 2 hours before concentrating in a Speed-Vac to dryness. The products were resuspended in 10 μL of Milli-Q water before analysis by

HPLC anion exchange chromatography using a Vydac N3033 Anion Exchange Column. Figure 2 shows a HPLC trace of four nucleotide standards (adenosine 5'-monophosphate, cytidine 5'-monophosphate, guanosine 5'-monophosphate, and uridine 5'-monophosphate) along with their retention times of 0.886, 2.007, 3.799 and 8.549 minutes respectively. Figure 3 shows a HPLC trace of the nucleotide analysis of chemically synthesized oligonucleotide **Py5**. The digestion pattern shows the expected products cytidine 5'-monophosphate and uridine 5'-monophosphate, which elute at 0.831 and 3.285 minutes respectively, indicating that the oligonucleotide is free from detectable chemical modifications.

For nucleoside analysis, to 10 nmoles of oligoribonucleotide was added 2.5 μL of 1M Tris-Cl pH 8.1, 5 μL of 1M $MgCl_2$, 10 U of snake venom phosphodiesterase, and 10 U of calf intestine alkaline phosphatase in a 50 μL total volume. The reaction was incubated at 37 °C for 2 hours before concentrating in a Speed-Vac to dryness. The reaction products were resuspended in 10 μL of Milli-Q water before analysis by HPLC reverse phase chromatography using a Brownlee Labs C18 Reverse Phase Column. Figure 4 shows a HPLC trace of the four nucleoside standards (cytidine, uracil, guanidine, and adenine) along with their retention times of 3.721, 4.504, 7.177, and 10.530 minutes respectively. Figure 5 shows a HPLC trace of the nucleoside analysis of chemically synthesized oligonucleotide **Py5**. The digestion pattern shows the expected products cytidine and uridine, which elute at 3.721 and 4.504 minutes respectively, indicating that the oligonucleotide is free from detectable chemical modifications.

Oligonucleotide Association Reaction. Binding reactions include

Figure 2: HPLC analysis of nucleotide standards. A ten nanomole mixture of the four nucleotide standards adenosine 5'-monophosphate, cytidine 5'-monophosphate, guanosine 5'-monophosphate, and uridine 5'-monophosphate was injected onto a Vydac 303NT Anion Exchange column using an isocratic run of 50 mM NaH_2PO_4, pH3.0 at 1 mL/minute. Analysis of the HPLC trace indicates retention times of 0.886, 2.007, 3.799 and 8.549 minutes for adenosine 5'-monophosphate, cytidine 5'-monophosphate, guanosine 5'-monophosphate, and uridine 5'-monophosphate, respectively.

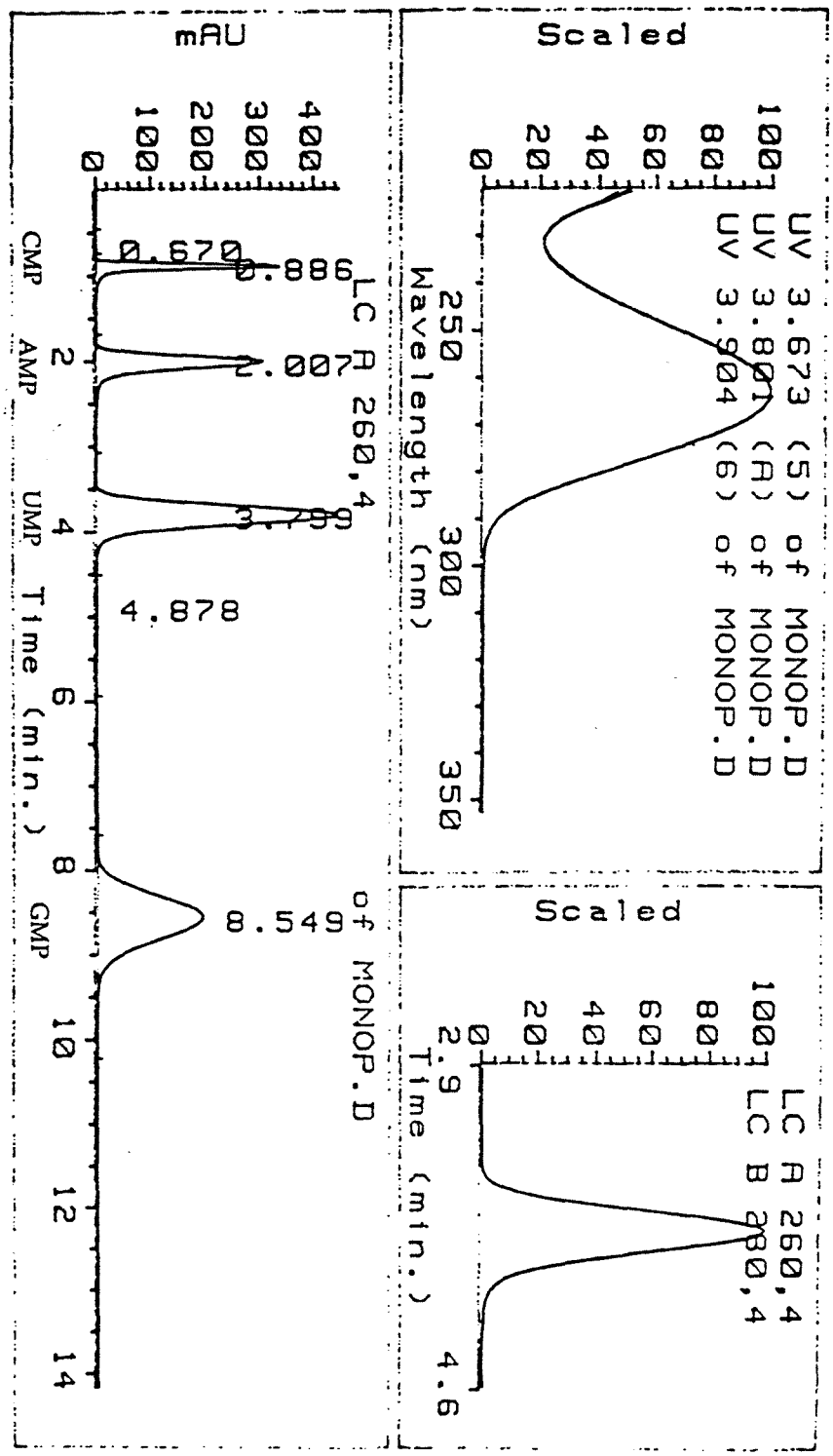

Figure 2. HPLC Analysis of Nucleotide Standards.

Figure 3: HPLC analysis of nucleotides derived from digestion of oligonucleotide **Py5**. Three nmoles of oligonucleotide **Py5** were digested with snake venom phosphodiesterase as described. The reaction was dried in a Speed-Vac and resuspended in 10 μL of Milli-Q water. A 5 μL volume of sample was injected onto the anion exchange column as described in Figure 2. Analysis of the HPLC trace indicated the presence of expected products cytidine 5'-monophosphate and uridine 5'-monophosphate, which elute at 0.831 and 3.285 minutes respectively, along with cytosine which elutes at 0.595 minutes.

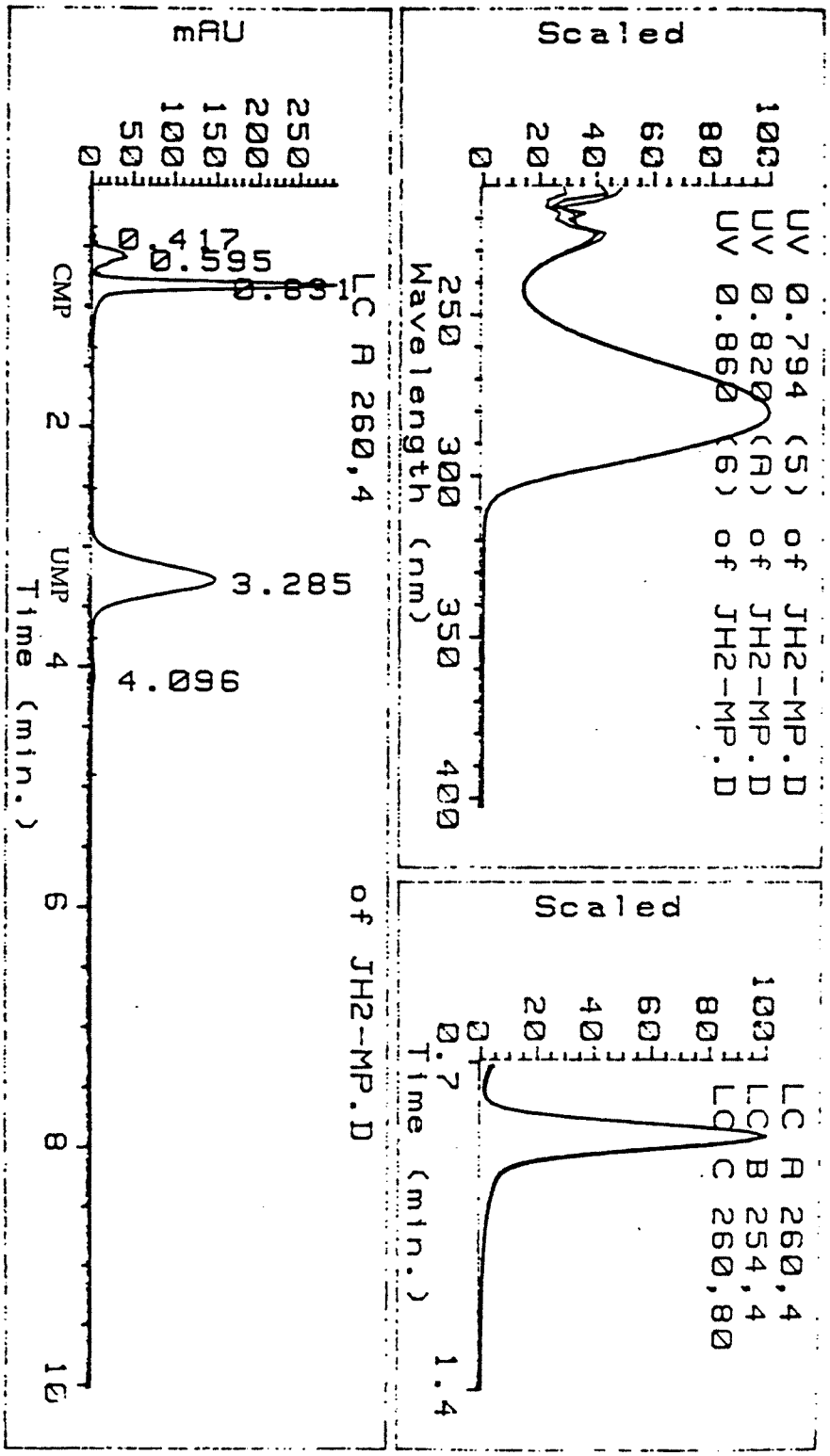

Figure 3. HPLC Nucleotide Analysis of Digested Oligonucleotide Py5.

Figure 4: HPLC analysis of nucleoside standards. A ten nmole mixture of the four nucleoside standards cytidine, uracil, guanidine, and adenine were injected onto a Brownlee Labs C18 Reverse Phase column using the following analytical conditions: T(0) = 10 mM Ammonium Phosphate pH 5.1/ 2.5% MeOH, T(3) = 10 mM Ammonium Phosphate pH 5.1/ 2.5% MeOH, T(3.1) = 10 mM Ammonium Phosphate pH 5.1/ 8.0 % MeOH with a constant flow rate of 1 mL/minute. Analysis of the HPLC trace indicates retention times of 3.721, 4.504, 7.177, and 10.530 minutes for cytidine, uracil, guanidine, and adenine respectively.

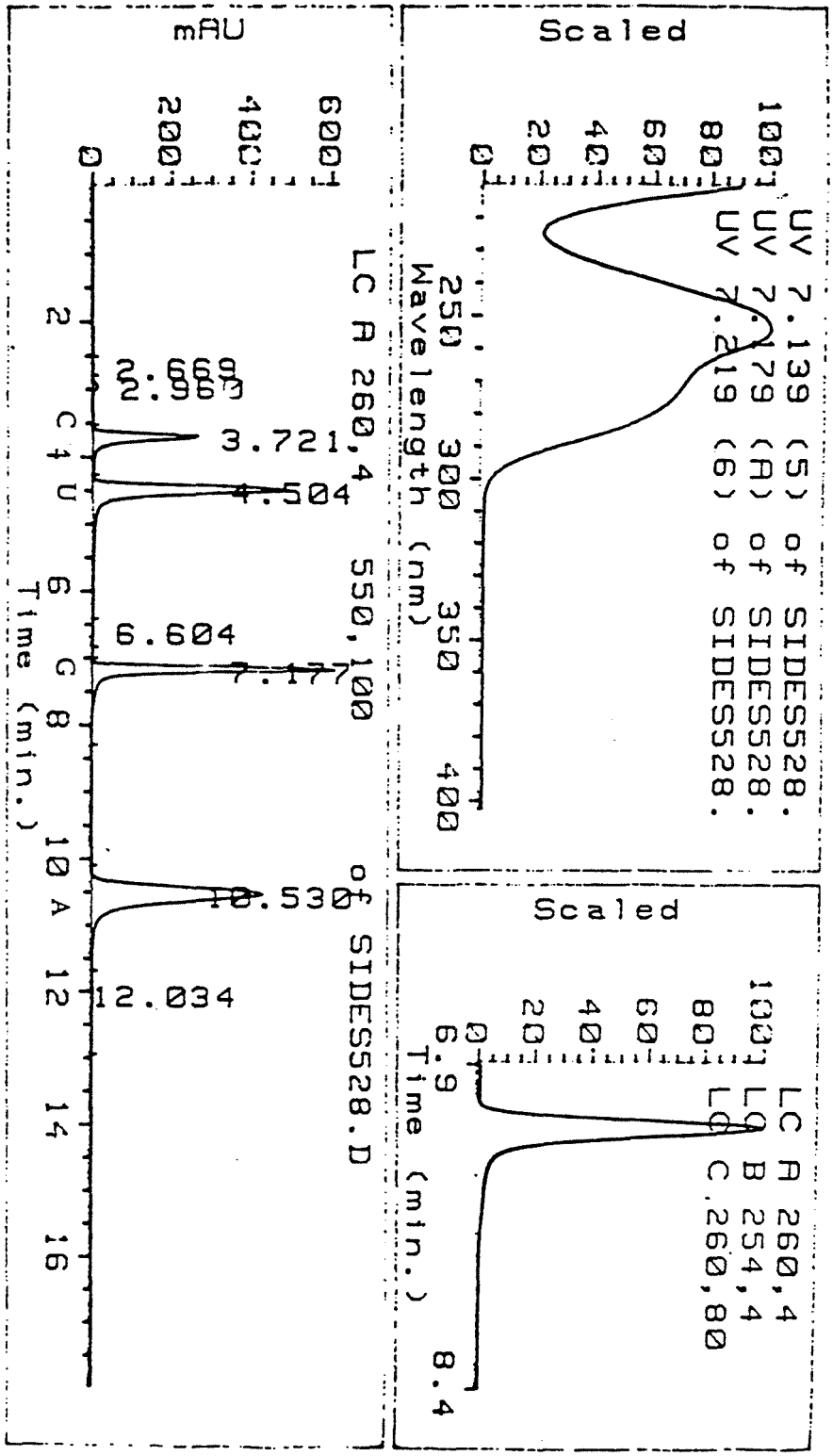

Figure 4. HPLC Analysis of Nucleoside Standards.

Figure 5: HPLC analysis of nucleosides derived from digested oligonucleotide **Py5**. Three nmoles of oligonucleotide **Py5** were digested with snake venom phosphodiesterase and dephosphorylated with calf intestine alkaline phosphatase as described in the Experimental Section. The reaction was dried in a Speed-Vac and resuspended in 10 μL of Milli-Q water. A 5 μL volume of sample was injected onto the reverse phase column as described in Figure 4. Analysis of the HPLC trace indicates the presence of the expected products cytidine and uridine, which elute at 3.721 and 4.504 minutes respectively.

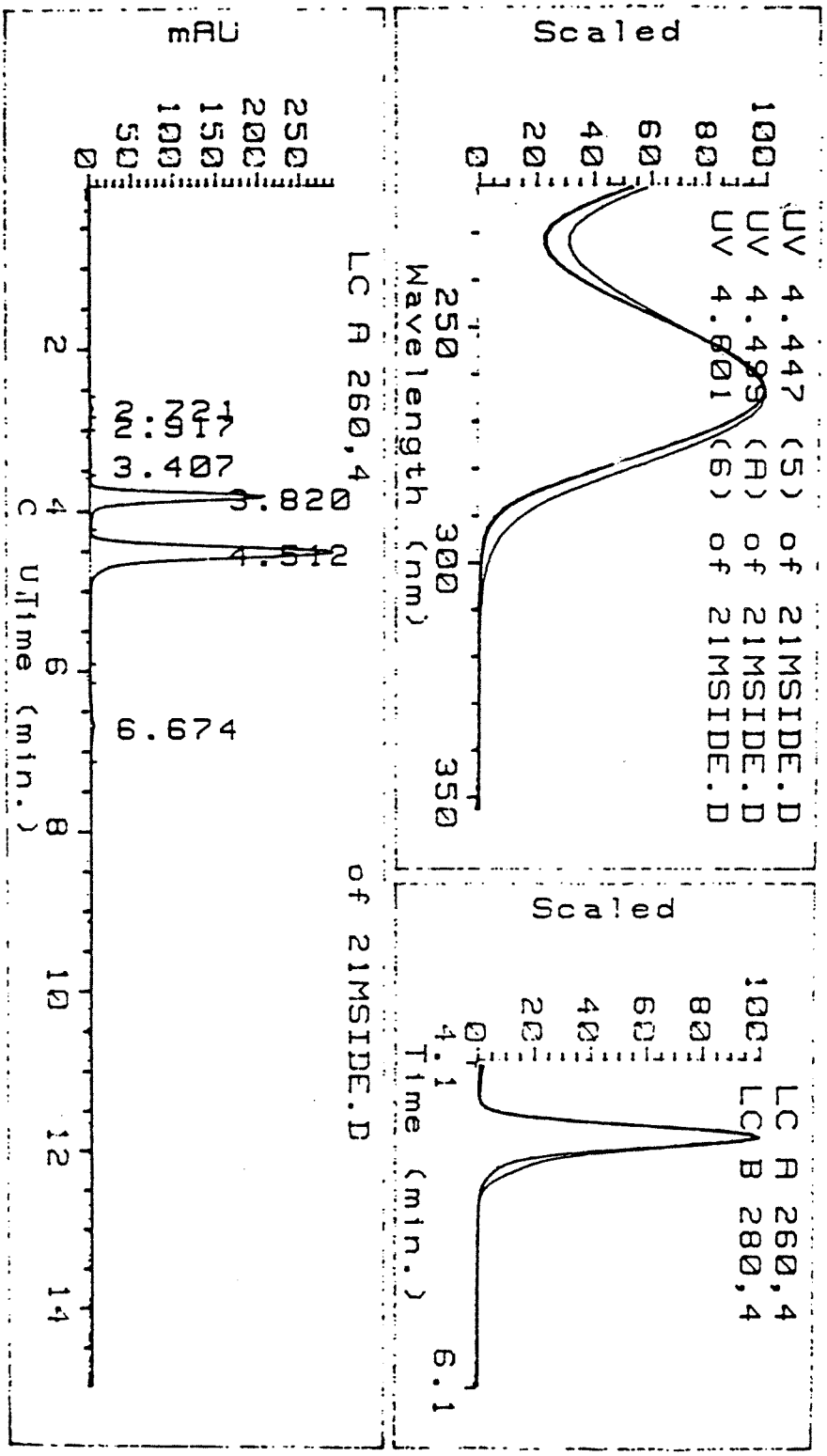

Figure 5. HPLC Nucleoside Analysis of Digested Oligonucleotide Py5.

pMTCAT-TH1 supercoiled DNA (100 ng), oligonucleotide, and association buffer in a 25 μL final volume. Association buffer contains 25 mM Tris-Acetate pH 6.8, 70 mM sodium chloride, 20 mM magnesium chloride, 400 μM spermine tetrachloride, 10 mM β-mercaptoethanol, and 0.1 mg/mL bovine serum albumin (Maher et al., 1989). Buffer pH refers to the 10-fold concentrated stock buffer solution at 22 °C. For pH-variation experiments, 25 mM Tris-Acetate was used at the indicated pH values. Reactions were incubated in a 37 °C oven for 12 hours with no visible evidence of evaporation.

Ava I Endonuclease Protection Assay. The Ava I endonuclease assay was used to measure the extent of triple-helix formation at the 21-bp homopurine target site of supercoiled pMTCAT-TH1 (Maher et al., 1989) When an oligonucleotide is bound to the homopurine tract the overlapping Ava I restriction sequence is protected from Ava I digestion. Another Ava I site elsewhere on the plasmid serves as an internal control for nonspecific inhibition of Ava I cleavage. Ava I (15 units) was added to the binding reactions and digestion proceeded at 37 °C for 12 minutes. Digestions were terminated by adding 10 μL of 1X Stop Buffer (1X TAE, 100 mM EDTA, 56% glycerol, 0.2% SDS, and 1% bromophenol blue) and electrophoresed on a 1.5% agarose, 1X TAE gel.

Quantitation. Plasmid DNA was visualized by ethidium bromide fluorescence. Photographic images obtained on Polaroid type 55 positive/negative film were quantitated on an LKB Ultrascan XL scanning densitometer. The extents of Ava I protection at the homopurine site is reflected by the differential observed fluorescence between DNA fragments

of 1504, 4859, and 6363-bp. The fraction Ava I protection (F) is defined as:

$$F = A(6363)/(A(6363)+A(4859)+A(1504))$$

where A(fragment size) is the peak area. The percent Ava I protection is given by 100F and is an experimental measure of the fraction of double helical target sites occupied by bound third strand oligonucleotide.

Data Analysis. Oligonucleotide binding experimental data were analyzed using a program to find the best fitting sigmoidal curve (Kaleidagraph version 3.01, Albeck Software). The program utilized the following function to determine the best fit:

$$Y_{fit} = (Y_{min}+(Y_{max}-Y_{min})(X\text{^}HC)(Kd\text{^}HC))/ (1+(X\text{^}HC)(Kd\text{^}HC))$$

where Y_{fit} is a measure of % Ava I inhibition, Y_{min} is the minimum % Ava I inhibition, Y_{max} is the maximum % Ava I inhibition, Y_{max} is the maximum % Ava I inhibition, X is the concentration of oligonucleotide, and HC is a measure of the Hill coefficient. Estimates of these parameters are entered into the program which calculates a best fit through an iterative process that requires evaluating the partial derivative of the function with respect to each parameter. This function is derived from relationships applied to quantitative footprinting studies (Brenowitz et al., 1986).

Quantitation of photographs is dependent upon the linearity of film response relative to the fluorescent intensity of DNA fragments. The film response has been shown to be nonlinear for substantially different DNA

fragments (Pulleyblank et al., 1977). Calculations were made such that measurements were not substantially influenced by the shape of the film response curve (Maher et al., 1990).

RESULTS

Design of a Duplex DNA Target Site and Corresponding Third Strand Oligonucleotides. To examine how third strand sequence composition as well as backbone modifications effect triple helix formation, a 21-bp homopurine tract in a supercoiled plasmid was designed to act as a target site. The homopurine tract contains 11 adenines and 10 guanosines for recognition by either Hoogsteen or reverse Hoogsteen hydrogen bonding. Furthermore, the sequence contains five contiguous adenines as well as four contiguous guanosines which can serve as nucleation sites for either parallel or antiparallel triple helical complexes. Potential third-strand oligonucleotides are shown in Table 1 and Table 2. Reagents **Py1 - Py5** are designed to occupy the target site through Hoogsteen hydrogen bonding interactions and bind in the parallel orientation shown. Reagents **Py6 - Py7**, which are not expected to bind to the target site, measure nonspecific inhibition of Ava I endonuclease. Reagents **Pu1 - Pu4** are designed to occupy the target site through reverse Hoogsteen hydrogen bonding interactions and bind in the antiparallel orientation shown. Reagents **Pu5 - Pu8** assay the effect of noncannonical base triplet involving AT base pairs on triple helix formation. Reagents **Pu9 - Pu10**, which are not expected to bind to the target site, again control for nonspecific inhibition of Ava I endonuclease.

Triple Helix Formation With Modified Pyrimidine-Rich Oligonucleotides. Results of Ava I endonuclease protection assays examining the binding affinities of various pyrimidine-rich third strand oligonucleotides for the target site are shown in Table 3. Oligonucleotide

Py1 (containing dT and dC nucleosides) has weak affinity for the target site with an apparent association constant of 2.4 X 10^5. An approximate 500-fold enhancement in binding affinity is caused by introducing 5-methyl-2'-deoxycytosine to produce oligonucleotide **Py2** (containing dT and $d^{me}C$ nucleosides). However, replacing the thymidines in **Py2** with 5-bromo-2'-deoxyuridines to create **Py3** (containing d^bU and d^mC nucleosides) decreases binding affinity by approximately a factor of six. As shown in Figure 2, changing oligodeoxyribonucleotide **Py1** to its oligoribonucleotide analog **Py5** (containing rU and rC nucleosides) causes an approximate 12-fold increase in binding affinity. Modifying oligonucleotide **Py2** to its oligoribo-(2'-OMe)-nucleotide analog **Py4** (containing 2'-OMe T and 2'-OMe ^mC nucleosides) does not significantly change affinity for the binding site. Mismatch control oligonucleotides **Py6** and **Py7** do not have measurable affinity for the target site.

Triple Helix Formation With Purine-Rich Oligonucleotides. The results of Ava I endonuclease protection assays examining purine-rich third strand oligonucleotides are shown in Table 4. Oligonucleotide **Pu1** (containing dG and dA nucleosides) has moderate affinity for the target site with an apparent association constant of 1.1 X 10^7. In contrast, oligonucleotide **Pu2** (containing dG and dT nucleosides), which binds AT base pairs with T•AT base triplets, does not have measurable affinity for the target site. Altering the oligonucleotide backbone of **Pu1** to make the oligoribonucleotide analog **Pu3** or the 2'-OMe oligoribonucleotide analog **Pu11** inhibits triple helix formation. Unlike oligonucleotide **Pu2**, oligonucleotide **Pu4** (containing dG and d^bU nucleosides) has measurable affinity for the target site. Oligonucleotides **Pu5** and **Pu6** (containing dG

and either dC or $d^{m}C$ nucleosides, respectively) both have negligible affinity for the target site as do oligonucleotides **Pu7** and **Pu8** (containing dG and either dI or abasic nucleosides, respectively). Mismatch control oligonucleotides **Pu9** and **Pu10** lack measurable affinity for the target site.

pH Dependence of Triple Helix Stability Using Pyrimidine-Rich Oligonucleotides. To examine the effect of pH on the formation of different triple helical structures, third strand oligonucleotides were allowed to equilibrate with the target site under a range of pH conditions. Pyrimidine-rich oligonucleotides **Py1 - Py5** as well as purine-rich oligonucleotides **Pu1** and **Pu4** were incubated with pMTCAT-TH1 at concentrations that produce 70% - 90% occupancy of the double-helical target site under pH 6.8 buffer conditions. In this concentration range, the assay is sensitive to changes in complex stability. Oligonucleotide **Py1** and **Py5** both show a substantial decrease in triple helix formation when increasing the pH from 6.8 to 7.2. Under higher pH condtions, there is negligible triple helix formation. Oligonucleotides **Py2** and **Py3** show a strong pH dependence on target site occupancy; however, the inclusion of ^{m}C nucleosides in these third strands lessens the severity of this effect. In contrast, oligonucleotide **Py5** (present at 1 μM) has a less dramatic decrease in binding affinity for the homopurine tract at higher pH. It is not until the interval between pH 7.4 - 7.6 that this 2'-OMe third strand has significantly lessened affinity for the target site (figures 7 and 8).

pH Dependence of Triple Helix Stability Using Purine-Rich Oligonucleotides. The pH dependence of triple helical complexes formed

Figure 6: Results of an Ava I endonuclease protection assay determining the relative binding affinity of oligonucleotide **Py5** for the 21-bp homopurine target site. A photograph of an ethidium bromide stained agarose gel is shown after electrophoretic separation of pMTCAT-TH1 fragments. The concentration of oligonucleotide **Py5** is given above each lane. All assays were performed under standard conditions.

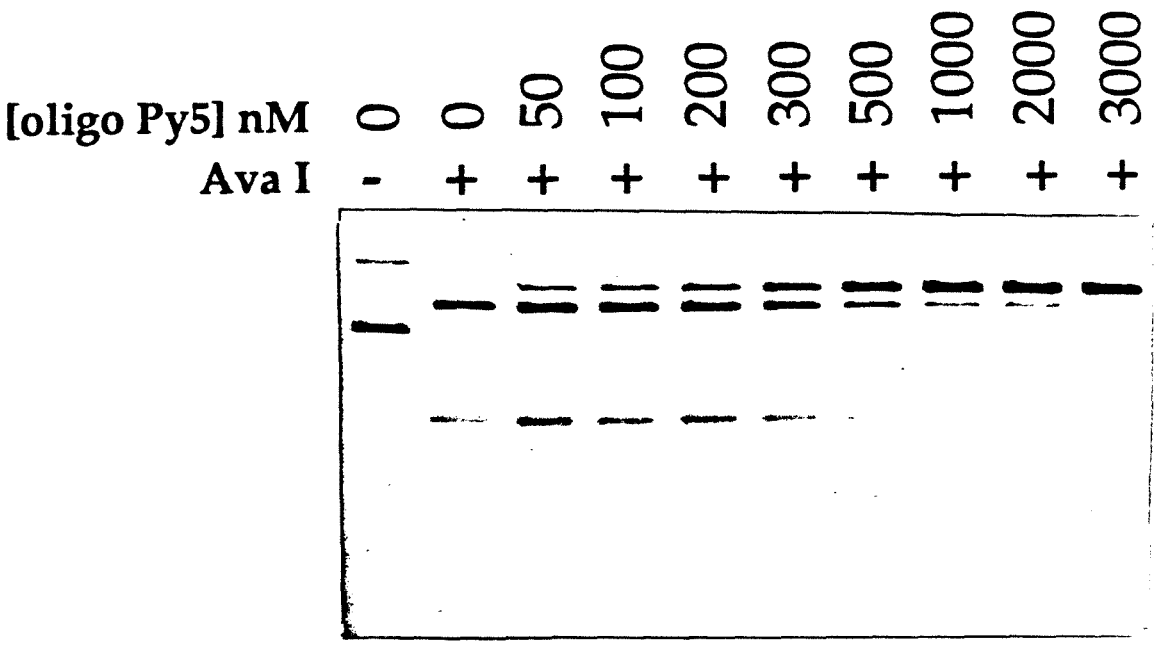
[oligo Py5] nM
Ava I
0
0
50
100
200
300
500
1000
2000
3000
-
+
+
+
+
+
+
+
+
+

Table 3. Equilibrium association constants for pyrimidine-rich oligonucleotides[a]

oligonucleotide	K (M^{-1})	ΔG (kcal mol^{-1})
Py1	2.4 (± 0.3) X 10^5	- 7.6 (± 0.1)
Py2	1.2 (± 0.2) X 10^8	-11.4 (± 0.1)
Py3	1.9 (± 0.1) X 10^7	-10.3 (± 0.1)
Py4	1.2 (± 0.1) X 10^8	-11.4 (± 0.1)
Py5	2.9 (± 0.2) X 10^6	- 9.1 (± 0.1)
Py6	<1.0 X 10^5	
Py7	<1.0 X 10^5	
Py8	2.0 (± 0.1) X 10^8	-11.7 (± 0.1)
Py9	2.1 (± 0.1) X 10^8	-11.8 (± 0.1)
Py10	1.9 (± 0.2) X 10^8	-11.7 (± 0.1)
Py11	2.0 (± 0.2) X 10^8	-11.7 (± 0.1)
Py12	6.1 (± 0.5) X 10^7	-11.0 (± 0.1)

[a]Values reported in the table are mean values measured from four repetitions of Ava I endonuclease protection experiments performed in association buffer I (25 mM Tris-Acetate pH 6.8, 70 mM sodium chloride, 20 mM magnesium chloride, 400 μM spermine tetrachloride, 10 mM β-mercaptoethanol, and 0.1 mg/mL bovine serum albumin, 37 °C)

with purine-rich oligonucleotides was determined in the same way as pyrimidine-rich oligonucleotides. Oligonucleotide **Pu1** shows identical affinity for the target site across the pH range studied. In contrast, oligonucleotide **Pu4** shows a decrease in binding affinity for the target site under higher pH conditions.

Length Dependence of Pyrimidine-Rich Oligonucleotide Directed Triple Helix Stability. To examine the relative energetic contribution of the four 3'-terminal triplets (3 $^{m}C^{+}$•GC and 1 C^{+}•GC) towards the triple helix formation in oligonucleotide **Py2**, oligonucleotides **Py8** - **Py11** were designed to contain successive deletions of the 3'-end terminal nucleotides. Oligonucleotide **Py8** (lacking 1 ^{m}C•GC triplet) has slightly

Table 4. Equilibrium Association Constants for Purine-Rich Oligonucleotides[a]

oligonucleotide	K (M^{-1})	ΔG (kcal mol^{-1})
Pu1	1.1 (± 0.2) X 10^7	-10.0 (± 0.1)
Pu2	<1.0 X 10^5	
Pu3	<1.0 X 10^5	
Pu4	1.0 (± 0.3) X 10^5	- 7.1 (± 0.1)
Pu5	<1.0 X 10^5	
Pu6	<1.0 X 10^5	
Pu7	<1.0 X 10^5	
Pu8	<1.0 X 10^5	
Pu9	<1.0 X 10^5	
Pu10	<1.0 X 10^5	
Pu11	<1.0 X 10^5	

[a]Values reported in the table are mean values measured from four repetitions of Ava I endonuclease protection experiments performed in association buffer I (25 mM Tris-Acetate pH 6.8, 70 mM sodium chloride, 20 mM magnesium chloride, 400 μM spermine tetrachloride, 10 mM β-mercaptoethanol, and 0.1 mg/mL bovine serum albumin, 37 °C)

higher affinity for the target site (100 nM) than oligonucleotide **Py2** although it is shorter in length (20 nt as opposed to 19 nt). Oligonucleotides **Py9**, **Py10**, and **Py11** (19 nt, 18 nt, and 17 nt in length respectively) all have similar affinity for the target site as oligonucleotide **Py8**. However, deleting a terminal 3'-end T•AT triplet from oligonucleotide **Py11** (to form oligonucleotide **Py12**) causes a 4-fold decrease in binding affinity.

Figure 7: (A) Results of an Ava I endonuclease protection assay determining the affinity of oligonucleotide **Py4** for the target plasmid pMTCAT-TH1 as a function of pH. The concentration of oligonucleotide **Py4** is held constant at 20 nM. All assays were performed under standard conditions with the indicated pH of the reaction held constant with 25 mM Tris-OAc.

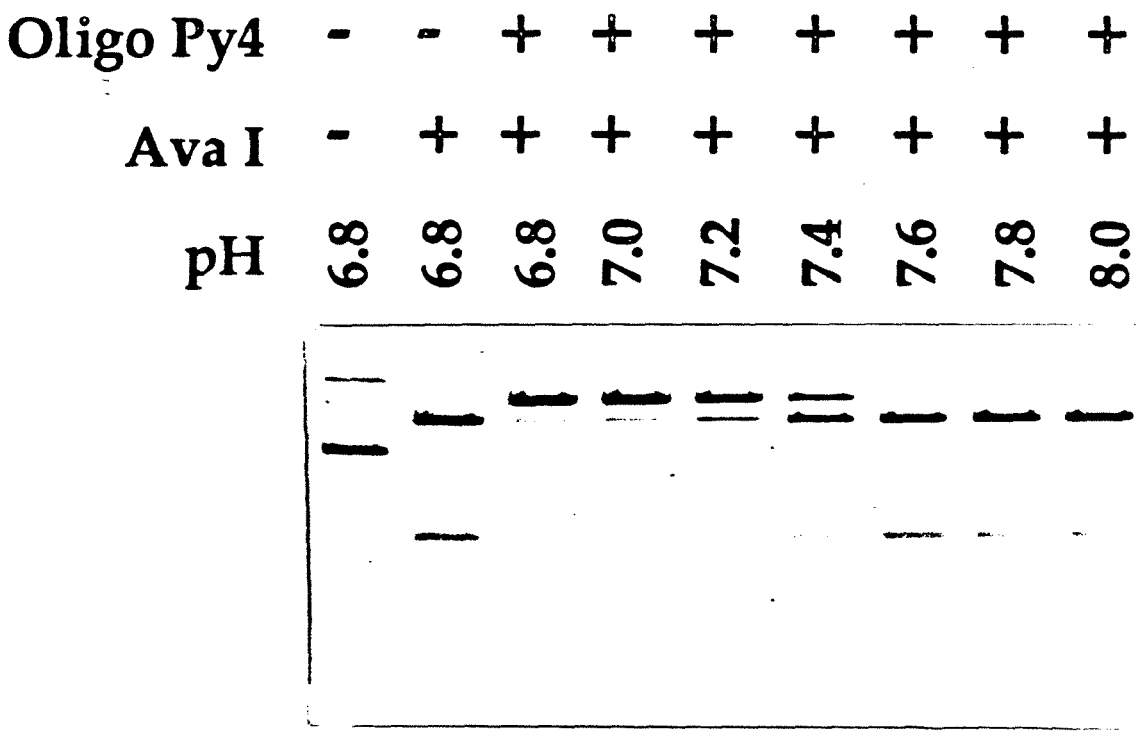
Oligo Py4 - - + + + + + + +
Ava I - + + + + + + + +
pH 6.8 6.8 6.8 7.0 7.2 7.4 7.6 7.8 8.0

Figure 8. Plot of the data collected from four repetitions of Ava I endonuclease protection assays determining the extent of triple helix formation under different pH conditions. Symbols used: ■ = oligonucleotide **Py1** (10 mM), ○ = oligonucleotide **Py2** (20 nM), ▲ = oligonucleotide **Py3** (100 nM), ● = oligonucleotide **Py4** (20 nM), ❑ = oligonucleotide **Py5** (1 μM), ◆ = oligonucleotide **Pu1** (500 nM), ✖ = oligonucleotide **Pu4** (20 mM). Horizontal error bars represent the standard error of the mean.

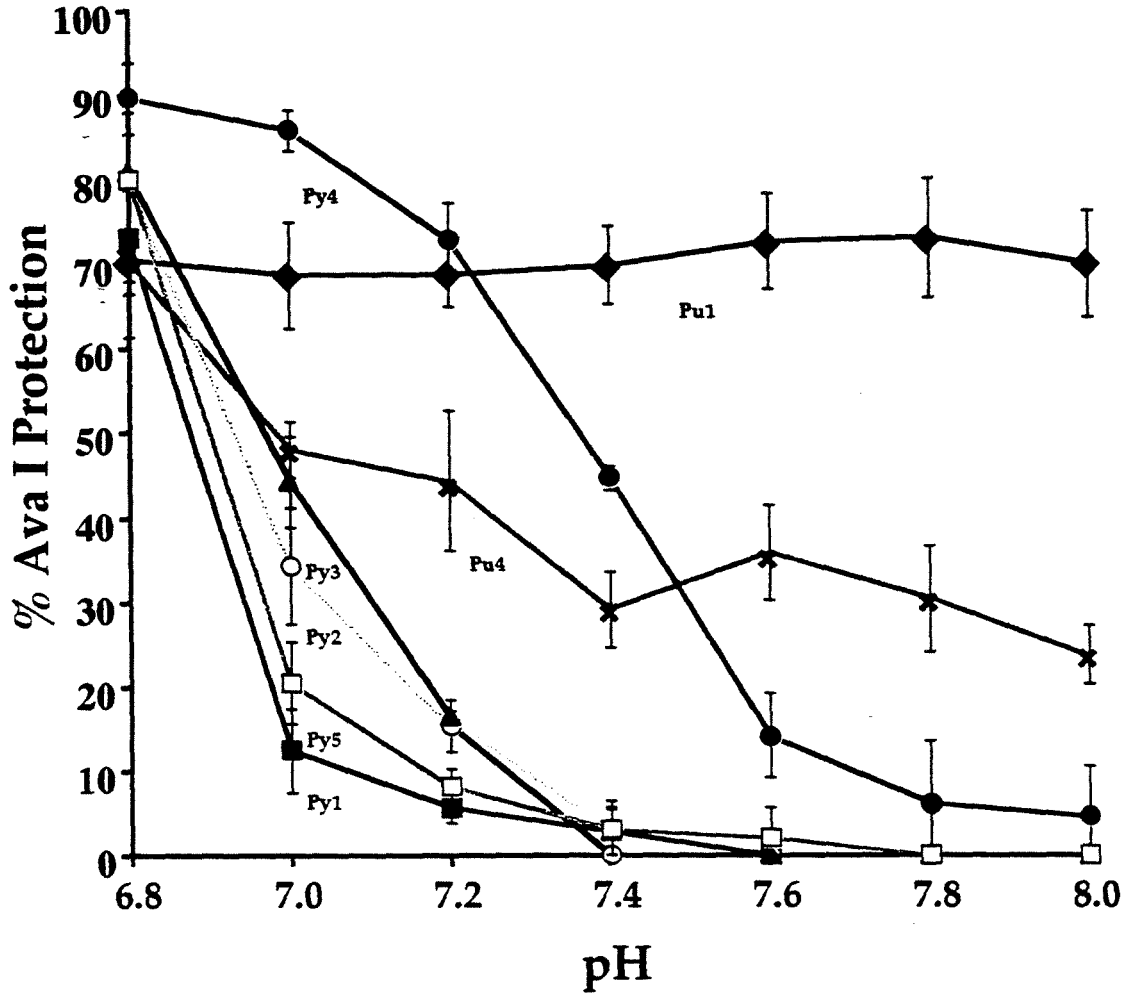

Figure 8. pH Dependence of Triple Helix Formation.

DISCUSSION

Pyrimidine-rich and purine-rich oligonucleotides displayed various affinities for the double-helical target site depending on nucleoside and backbone composition. Additional differences in binding affinities were found under different hybridization conditions. Although chemical modifications can substantially increase oligonucleotide affinity for double helical DNA, it is not yet possible to predict their influence on the energetics of triple helix formation under all conditions. Moreover, sequence composition effects can play a major role in determining the stability of triple helical complexes.

The Effect of Backbone Composition on Pyrimidine-Rich Oligonucleotide-Directed Triple Helix Formation. Modifications made to the sugar component of pyrimidine-rich oligonucleotide phosphodiester backbones enhanced triple helix formation. For example, oligoribonucleotide **Py4** has substantially higher affinity for the target site relative to the oligodeoxyribonucleotide analog **Py1**. However, there is an equivalent decrease in the formation of both triple helical complexes due to increases in pH. The 2'-OH and 2'-OMe groups alter the sugar conformation from the C-2' endo type found in oligodeoxyribonucleotides to the C-3' endo type (Saenger, 1984). NMR studies demonstrated that the pyrimidine-rich third strands tend to have sugars in the C-3' endo conformation in triple helical complexes (Macaya et al., 1982). These sugars may preorganize the oligonucleotide to entropically favor triple helix formation or allow for a more energetically favorable placement of the third strand in the major groove. Furthermore, the 2'-OH group may

act as an additional hydrogen bond donors or acceptors in these triple helices. Alternatively these analogs may favor the binding of stabilizing cations to the complexes. Crothers and co-workers have confirmed that RNA third strand oligonucleotides have higher affinity for double helical DNA relative to DNA third strand oligonucleotides (Roberts & Crothers, 1992). Similar results were reported by Helene and co-workers (Escude et al., 1993). Nevertheless, Han and Dervan reported that both RNA and DNA third strands had equivalent affinity for a DNA target site (Han & Dervan, 1993). Therefore, it is difficult to draw definitive conclusions from these studies unless a number of different sequences and ionic conditions are examined for each oligonucleotide modification.

The 2'-OMe oligonucleotide **Py5** binds with similar affinity to the double helical target site at pH 6.8 as does its oligodeoxyribonucleotide analog **Py2**. Interestingly, the 2'-OMe oligonucleotide shows significantly higher affinity for the homopurine tract at higher pH than does the oligodeoxyribonucleotide. A number of theories may be proposed to account for these observations. The 2'-OMe groups may effect the protonation N3 of the 5-methylcytosine nucleosides either through interactions with the base or by trapping the nucleoside in a protonated state through altered solvent accessibility. These structural explanations are non-exclusive, and the relative contributions of each will require further biophysical studies.

Possible Explanations for the Differing Stabilities of Pyrimidine-Rich Oligonucleotide-Directed Triple Helices of Various Lengths. Although oligonucleotide **Py2** is designed to recognize a 21-bp homopurine tract of double-helical DNA, it has marginally lower affinity for the target site

than oligonucleotides **Py9 - Py11** which lack subsets of the final four 3'-end base triplets (Table 3). This implies that the final four C^+•GC or $^mC^+$•GC base triplets of oligonucleotide **Py2** are not contributing to the free energy of triple helix formation. However, deleting a 3'-end terminal T•AT triplet from oligonucleotide **Py11** to create oligonucleotide **Py12** causes a substantial three fold decrease in binding affinity. This demonstrates that the 3'-end terminal T•AT triplet makes a significant energetic contribution towards complex stability. The higher stability of 3'-end terminal T•AT triplets relative to 3'-end terminal C^+•GC or $^mC^+$•GC triplets may be due to the assay conditions. Acidic pH favors triple-helix formation by pyrimidine-rich oligonucleotides containing cytosine and 5-methylcytosine (Lee et al., 1984; Povsic & Dervan, 1989; Plum et al., 1990; Xodo et al., 1991). This is due to the required protonation of N3 of cytosine and 5-methylcytosine to form a Hoogsteen hydrogen bond with N7 of guanosine. Under the pH 6.8 assay conditions, the cytosines and 5-methylcytosines are not fully protonated and thus are not as stable as the T•AT triplets. Furthermore, there may be electrostatic repulsion between adjacent protonated $^mC^+$•GC triplets that could offset the positive energetic contributions of triplet formation such as hydrogen bond formation and stacking interactions. Therefore, the four 3'-end terminal $^mC^+$•GC and C^+•GC triplets of oligonucleotide **Py2** most probably are not binding to the target site.

The Effect of Backbone Composition on Purine-Rich Oligonucleotide-Directed Triple Helix Formation. In contrast to pyrimidine-rich oligonucleotides, only purine-rich oligodeoxyribonucleotides are capable of forming triple helical complexes with double-helical DNA. Purine-rich

oligoribonucleotides, as well as 2'-OMe oligonucleotides, do not have significant affinity for the 21-bp homopurine tract. Although there does not appear to be any obvious physical basis for this observation, a number of possible explanations may be proposed. The 2'-OH or 2'-OMe groups may cause steric hindrance that prevents triple helix formation. These groups alter the sugar conformation from the C-2' endo type found in oligodeoxyribonucleotides to C-3' endo type found in oligoribonucleotides. This change in sugar conformation may cause a less favorable placement of the third stand in the major groove due to negative steric interactions, disruption of waters binding in the triple helical grooves, or disruption of shielding cations binding to the triple helical complex. Furthermore, these modifications may promote intramolecular oligonucleotide self-associations that compete with binding to the double-helical target site. Again these non-exclusive structural implications await further clarifying biophysical studies.

The Recognition of AT Base Pairs By Guanine-Rich Oligonucleotides. The relative stability of triple helical complexes comprised of G•GC triplets as well as triplets containing AT Watson-Crick base pairs were examined. Antiparallel triple helical complexes were most stabilized by A•AT triplets followed by ^{b}U•AT triplets. Triple helices containing ^{m}C^{+}•GC and C^{+}•GC triplets displayed very weak complex formation while oligodeoxyribonucleotides designed for T•AT, I•AT, or ϕ•AT recognition have no detectable affinity for the target site. It is suprising that T•AT triplets are not compatable with G•GC triplets in this target sequence given that T•AT and A•AT triplets are relatively interchangeable in guanine-rich triple helices (Beal & Dervan, 1991; Beal & Dervan, 1992).

Like most reported sequences capable of forming triple helices with guanine-rich oligonucleotides, this homopurine tract contains four continuous guanines that can act as a triple helix nucleation site. However, unlike many of these other sequences, the homopurine tract studied is not overwhelmingly guanine-rich (55% GC and 45% AT base pairs). Furthermore the sequence contains five contiguous adenines, adjacent to the four contiguous guanines, that can serve as a nucleation site for pyrimidine-rich oligonucleotide-directed triple helix formation (Figure 8). Thymidine-rich oligonucleotides preferentially form parallel stranded triple helical complexes since Hoogsteen hydrogen bonds (found in parallel complexes) are more energetically favorable than reverse Hoogsteen hydrogen bonds (found in antiparallel complexes). Oligonucleotide **Pu2**, containing guanosine and thymidine nucleosides, may not bind to the target site since the five continuous thymidines can nucleate a parallel triple helix at the adenine rich site that competes with the adjacent nucleation of the antiparallel triple helix (Figure 8). Oligonucleotide **Pu1** can participate in an antiparallel triple helix since A•AT triplets do not favor competing structures such as a parallel triple helix.

One would predict from this model that modifying the T•AT triplet to favor a reverse Hoogsteen over a Hoogsteen hydrogen bond pattern may stabilize antiparallel guanine-rich triple helix formation. Introducing electron-withdrawing groups, such as bromine, off the 5-position of thymidine makes O2 a stronger hydrogen bond acceptor than O4 (Saenger, 1984). Since reverse Hoogsteen hydrogen-bonded T•AT triplets utilize O2 of thymidine as a hydrogen bond acceptor while Hoogsteen hydrogen-bonded T•AT triplets utilize O4 of thymidine as a hydrogen bond acceptor,

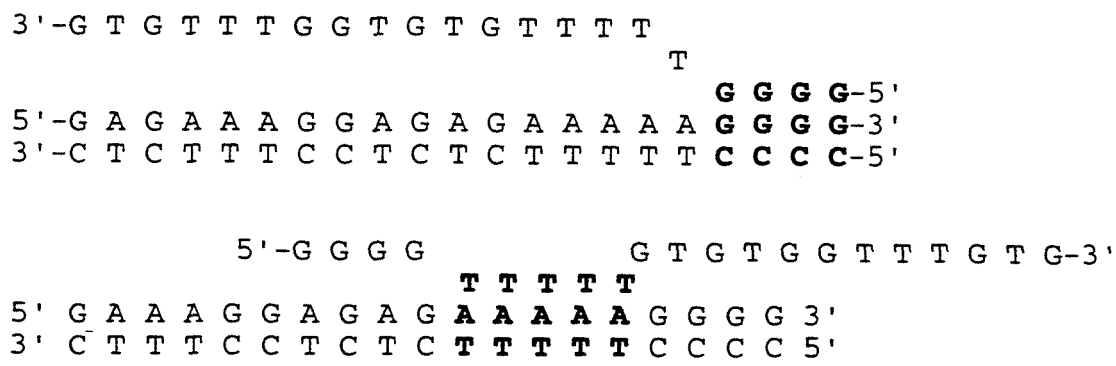

Figure 8 : Potential sites of nucleation for both antiparallel and parallel triple helical complex formation involving oligonucleotide **Pu2**. Potential base triplets are shown in bold.

one can propose that 5-bromouridine forms a stronger reverse Hoogsteen, as opposed to Hoogsteen, hydrogen-bonded triplets with AT base pairs (Saenger, 1984). In keeping with this prediction, oligonucleotide **Pu4** forms a moderately stable antiparallel triple helix through the formation of G•GC and ^{b}U•AT base triplets. For antiparallel triple helical complexes it appears that A•AT triplets will be less effected by the sequence composition of the target site than T•AT triplets.

pH Dependence of Purine-Rich Oligonucleotide-Directed Triple Helices. Since the reverse Hoogsteen hydrogen bonds formed in antiparallel triple helices are not protonation dependent, it is expected that triple helix formation will not be sensitive to changes in pH. Oligonucleotide **Pu1**, capable of forming G•GC and A•AT triplets, has equivalent affinity for the double helical target site over a wide range of pH values. Curiously, oligonucleotide **Pu4**, capable of forming G•GC and ^{b}U•AT triplets, shows a moderate decrease in triple helix formation under conditions of increasing pH. This may reflect a pH dependence associated

with ^{b}U•AT triplet formation which is not readily explicable by the reverse Hoogsteen hydrogen bond scheme. pH-dependent changes in the tautomeric form of 5-bromouridine that either stabilize or destabilize triplet formation could possibly account for this phenomenon.

BIBLIOGRAPHY

Beal, P. A. & Dervan, P. B. (1991) *Science 251,* 1360-1363.

Beal, P. A., & Dervan, P. B. (1992) *Nucleic Acids Res. 20,* 2773-2776.

Brenowitz, M., Senear, D. F., Shea, M. A., & Ackers, G. K. (1986) *Proc. Natl. Acad. Sci. U. S. A. 83,* 8462-8466.

Chen, F. -M. (1991) *Biochemistry 30,* 4472-4479.

de los Santos, C., Rosen, M., & Patel, D. (1989) *Biochemistry 28,* 7282-7289.

Durland, R. H., Kessler, D. J., Gunnell, S., Duvic, M., Pettitt, B. M. & Hogan, M. E. (1991) *Biochemistry 30,* 9246-9255.

Escude, C., Francois, J.-C., Sun, J.-S., Ott, G., Sprinzl, M., Garestier, T., & Helene, C. (1993) *Nucleic Acids Res. 21,* 5547-5553.

Han, H. & Dervan, P. B. (1993) *Proc. Natl. Acad. Sci. 90,* 3806-3810.

Horne, D. A. & Dervan, P. B. (1991) *Nucleic Acids Res. 19,* 4963-4965.

Le Doan, T., Perrouault, L., Praseuth, D., Habhoub, N., Decout, J.-L., Thuong, N. T., Lhomme, J., & Helene, C. (1987) *Nucleic Acids Res. 15,* 7749-7760.

Lee, J. S., Johnson, D. A., & Morgan, A. R. (1979) *Nucleic Acids Res. 6*, 3073-3091.

Macaya, R., Wang, E., Schultze, P., Sklenar, V., & Feigon, J. (1992) *J. Mol. Biol. 225*, 755-773.

Maher, L. J., III, Wold, B., & Dervan, P. B. (1989) *Science 245*, 725-730.

Maher, L. J., III, Dervan, P. B., Wold, B. J. (1990) *Biochemistry 29*, 8820-8826.

McLaughlin, L. W., Cramer, F., & Sprinzl, M. (1981) *Anal. Biochem. 112*, 60-69.

Milligan, J. F., Groebe, D. R., Witherell, G. W., & Uhlenbeck, O. C. (1987) *Nucleic Acids Res. 15*, 8783-8798.

Moser, H. E., & Dervan, P. B. (1987) *Science 238*, 645-650.

Pilch, D. S., Levenson, C., & Shafer, R. H. (1991) *Biochemistry 30*, 6081-6087.

Plum, G. E., Park, Y.-W., Singleton, S. F., Dervan, P. B., & Breslaur, K. J. (1990) *Proc. Natl. Acad. Sci. 87*, 9436-9440.

Povsic, T. J., & Dervan, P. B. (1989) *J. Am. Chem. Soc. 111*, 3059-3061.

Pulleyblank, D. E., Shure, M., & Vinograd, J. (1977) *Nucleic Acids Res. 4,* 1409-1418.

Radhakrishnan, I., & Patel, D. J. (1993) *Structure 1,* 135-152.

Rajagopal, P., & Feigon, J. (1989) *Nature 339,* 637-640.

Roberts, R. W., & Crothers, D. M. (1992) *Science 258,* 1463-1466.

Saenger, W. (1984) *Principles of Nucleic Acid Structure,* Springer-Verlag, New York.

Sambrook, J., Fritsch, E. F., & Maniatis, T. (1989) *Molecular Cloning, A Laboratory Manual,* 2nd ed., Cold Spring Harbor Laboratory, Cold Spring Harbor, NY.

Usman, N., Oglivie, K. K., Jiang, M. Y., Cedergren, R. J. (1987) *J. Am. Chem. Soc. 109,* 7845-7854.

Wang, Y. Y., Lyttle, M. H., Borer, P. N. (1990) *Nucleic Acids Res. 18,* 3347-3352.

Xodo, L. E., Manzini, G., Quadrifoglio, F., van der Marel, G. A., & van Boom, J. H. (1991) *Nucleic Acids Res. 19,* 5625-5631.

Chapter III

Screening For Oligoribonucleotide Species Which Bind Double-Helical DNA

INTRODUCTION

Screening randomized oligonucleotide libraries though selection and amplification techniques has lead to the discovery of high-affinity oligonucleotide ligands to a wide range of molecular targets. Oligonucleotides have been found which have high affinity for proteins as well as for small molecules. The success of these selection techniques hinges on the ability of short nucleic acids to form rigid secondary structures and adopt a large number of different conformations. These structures may provide a novel means of recognizing specific sequences of double-stranded nucleic acids.

The sequence-specific recognition of double-helical DNA by oligoribonucleotides can be accomplished only through triple helix formation. Pyrimidine-rich oligoribonucleotides bind in the major groove of DNA at homopurine target sites through the formation of U•AT and rC^+•GC base triplets (Roberts & Crothers, 1992; Escude et al., 1993; Han & Dervan, 1993). As shown in Chapter 1 purine-rich oligoribonucleotides cannot recognize double helical DNA through the formation of G•GC with T•AT or A•AT base triplets. This limits RNA-directed triple helix formation under nonacidic conditions to adenine-rich homopurine tracts.

In this study, we attempt to screen and select for oligoribonucleotide species in a randomized library which display affinity for double-helical plasmid DNA. Multiple rounds of positive and negative selection steps were performed in the screening process under different hybridization conditions. Some oligodeoxyribonucleotide analogs of selected RNA species altered the activity of the restriction endonuclease Sca I apparently without binding to the target plasmid. However, no oligoribonucleotides were found that had significant affinity for the plasmid DNA target. It may be necessary to use less stringent binding conditions as well as increased randomized nucleotide positions in order to find novel oligoribonucleotides that have affinity for DNA.

EXPERIMENTAL PROCEDURES

Materials. All DNA synthesis reagents were obtained from Applied Biosystems Inc. except for Chemical Phosphorylation Reagent obtained from Glen Research. Restriction enzymes, T4 polynucleotide kinase, T4 DNA ligase, and DNase I were purchased from Boehringer Mannheim. r*Tth* Thermostable RT-PCR Kit and the RT-PCR Kit were obtained from Perkin-Elmer Cetus. Spun Columns were obtained from Pharmacia. Sequenase Version 2.0 DNA Sequencing Kit was purchased from U. S. Biochemicals. Adenosine 5'- [γ^{32}P] - triphosphate and deoxyadenosine - [α^{32}P] - triphosphate were obtained from New England Nuclear.

Synthesis of Oligodeoxyriboucleotides. Oligodeoxyribonucleotides were synthesized on an Applied Biosystems Model 380B DNA synthesizer using β-cyanoethyl phosphoramidite chemistry. Positions of random sequence composition were generated by placing equimolar amounts of all four phosphoramidites (dA, dC, dG, and dT) on a designated DNA synthesizer port and delivering this mixture to the solid support during the appropriate coupling cycles. Oligonucleotides were purified by denaturing polyacrylamide gel electrophoresis, visualized by UV shadowing, and electroeluted from gel slices using an Elu-trap apparatus (Schleicher & Schuell). They were ethanol precipitated and resuspended in 0.5X TE before storing at -80 °C. The concentration of oligonucleotides were determined by A_{260} measurements using the following molar extinction coefficients: 15,400 (A), 11,700 (G), 7,300 (C), 8,800 (T), and 10,800 (randomized sequence).

Plasmid Construction. The plasmid pCROSS I was obtained by cloning the oligonucleotides 5'-pAGCTTGACGTCTTTTTTTCGGAGGGGGAGTACTG-3' and 5'-pGATCCAGTACTCCCCCTCCGAAAAAAAGACGTCA-3' into the large Hind III/BamH I restriction fragment of pBSIISK+ (Stratagene). Large scale preparation of plasmid was performed using Qiagen purification kits. The sequence of the insert was confirmed by dideoxynucleotide sequencing.

Chemical Synthesis of Oligoribonucleotides. Indicated oligoribonucleotides were prepared on an Applied Biosystems 380B DNA Synthesizer using 2'-hydroxyl protected tertbutyl dimethyl silyl β-cyanoethyl phosphoramidites. Oligoribonucleotides were deblocked and purified under standard conditions (Usman et al., 1987; Wu et al., 1989). The solid support from a typical 1 μmole RNA synthesis was removed from the column and treated with 2 mL of 3 : 1 ammonium hydroxide : ethanol solution and incubated at 55 °C for 12 hours. The solution was dried in a Speed-Vac (Savant) and resuspended in 2 mL of tetrabutylammonium fluoride/tetrahydrofuran. After a 48 hour room temperature incubation, the reaction was quenched by adding 20 μL of 2M triethylamine acetate pH 7.0 and evaporated to an oil in a Speed-Vac (Savant). The residue was resuspended in 2 mL of Milli-Q water and exhaustively dialyzed against water. The oligoribonucleotide was concentrated through lyophilization, purified by denaturing polyacrylamide gel electrophoresis, visualized by UV shadowing, and electroeluted from gel slices using an Elu-trap apparatus (Schleicher & Schuell). It was ethanol precipitated and resuspended in 0.5X TE before storing at -80 °C. The concentration of the oligonucleotide was determined by A_{260} measurements using the following molar extinction coefficients: 15,400 (A), 11,700 (G), 7,300 (C), and 10,000 (U).

Enzymatic Synthesis of Oligoribonucleotides. Oligoribonucleotides were synthesized by T7 RNA polymerase *in vitro* transcription reactions using standard protocols (Milligan et al., 1987). To 10 pmoles of T7 promoter oligonucleotide **T7PRO** 5'-TAATACGACTCACTATAG-3' was added 10 pmoles of template in a final 50 µL volume of 1 X STE (10 mM NaCl, 10 mM Tris-Cl pH 8.0, and 1 mM EDTA). The mixture was heated to 90 °C for one minute and oligonucleotides were annealled by slow cooling to room temperature over the course of one hour. The transcription reaction was assembled by adding 50 µL of annealed template to 50 µL of 10X T7 RNA Polymerase Transcription Buffer (250 mM $MgCl_2$, 500 mM Tris-Cl pH 8.0, 50 mM DTT, 2 mM spermidine), 10 µL of 1M DTT, 50 µL of 40 mM NTP mix (40 mM ATP, 40 mM UTP, 40 mM CTP, 40 mM GTP) and 340 µL of Milli-Q water. The reaction was initiated by adding 40 µL of 70U/µL T7 RNA polymerase and incubating at 37 °C for 12 hours. The reactions were extracted with an equal volume of phenol : chloroform : isoamyl alcohol (25 : 24 : 1) and then with an equal volume of chloroform. The volume was brought to 2 mL with Milli-Q water and dialyzed against Milli-Q water. The reaction was lyophilized and resuspended in 100 µL of 1X TE. Oligoribonucleotides were purified by denaturing polyacrylamide gel electrophoresis, visualized by UV shadowing, and electroeluted from gel slices using an Elu-trap apparatus (Schleicher & Schuell). They were ethanol precipitated and resuspended in 0.5X TE before storing at -80 °C.

Oligonucleotide Selection Scheme: The 89-nt long oligonucleotide **RTEMP** 5'-CCTTGGCTTCTGCAGTTGACTCCTANNNNNNNNNNNNNNNNNNNNNNNNNTGGAGCACTGTCTAGAGACTCCTATAGTGAGTCGTATTA-3' served as a template for a 5 mL T7 RNA polymerase *in vitro* transcription

reaction. Appoximately 1 μmole of a population of 72-nt long RNA transcripts was generated that contains a 25-nt long randomized tract. As indicated in Table I, supercoiled plasmid DNA (pCROSS I for positive selection steps and pBSIISK$^+$ for negative selection steps) and the indicated oligonucleotide were incubated in a 20 μL total volume of 1X Selection Buffer for 24 hours at 37 °C. The reaction was applied to a Pharmacia Spun Column equilibrated with 2 X 10 mL of 1X Selection Buffer. The column was placed over a 15 mL Falcon tube and centrifuged at 10,000Xg for 2 minutes. Flow-through was collected in the 15 mL tube and 1 mL of 1X Selection Buffer was applied to the column. Again the column was centrifuged at 10,000Xg for 2 minutes and the eluate 1+ was collected and desalted by ethanol precipitation. The column was washed with 2 mL of 1X Selection Buffer and eluate 1- was collected and desalted as above. The nucleic acid pellet was resuspended in 0.5 mL of 0.5X TE. The nucleic acid mixture derived from eluate 1+ or eluate 1- was subject to a RT-PCR reaction.

RT-PCR using M-MLV Reverse Transcriptase. RT-PCR reactions were assembled in a 650 μL pre-siliconized microfuge tube by combining 10 fmoles of oligoribonucleotide, 4 μL of 25 mM $MgCl_2$, 8 μL of 2.5 mM dNTP mix (containing all four dNTPs), 2 μL of 10X PCR Buffer II (100 mM Tris-HCl, pH 8.3, 500 mM KCl), 1 μL of 20U/μL RNase Inhibitor, 100 pmoles of primer **RT1** 5'-CCTTGGCTTCTGCAGTTGACTCCTA-3', and 1 μL of 50U/μL Moloney Murine Leukemia Virus (M-MLV) Reverse Transcriptase in a 20 μL total volume. The solution was covered with 100 μL of mineral oil and incubated at 55 °C for 20 minutes. Subsequently the solution was incubated at 99 °C for 5 minutes and finally at 5 °C for 10 minutes. During this time a PCR Master Mix was assembled by combining 4 μL of 25 mM MgCl2, 8 μL of 10X PCR

Buffer II, and 0.5 µL of 2.5U/µL AmpliTaq DNA polymerase in a 78 µL total volume. After the incubations, 78 µL of PCR Master Mix was added under oil to the reaction followed by 1 µL of 100 µM primer **RT2** 5'-TAATACGACTCA CTATAGGAGTCTCTAGACAGTGCTCCA-3'. The reaction was placed in a thermocycler and subject to 25 rounds of amplification using the following cycle : 95 °C (denaturation) for 1 minute, 60 °C (annealing) for 1 minute, and 72 °C (extension) for 2 minutes. Samples were rescued from under oil and 10 µL of Stop Buffer (1X TAE, 100 mM EDTA, 56% glycerol, 0.2% SDS, and 1% bromophenol blue) was added to each. Reactions were electrophoresed on 1.5% agarose gels in 1X TAE buffer. Amplification products were excised and eluted from the gel slice.

RT-PCR Reactions Using a Thermostable Reverse Transcriptase. RT-PCR reactions were assembled in a 650 µL pre-siliconized microfuge tube by combining 10 fmoles of oligoribonucleotide, 2 µL of 10 mM $MnCl_2$, 2 µL of 2 mM dNTP mix (containing all four dNTPs), 2 µL of 10X r*Tth* Reverse Transcriptase Buffer (100 mM Tris-HCl, pH 8.3, 900 mM KCl), 100 pmoles of primer **RT1** 5'-CCTTGGCTTCTGCAGTTGACTCCTA-3', and 2 µL of 2.5U/µL r*Tth* DNA polymerase in a 20 µL total volume. The solution was covered with 100 µL of mineral oil and incubated at 70 °C for 20 minutes. PCR Master Mix was assembled by combining 8 µL of 10X Chelating Buffer (50% glycerol (v/v), 100 mM Tris-HCl, pH 8.3, 1 M KCl, 7.5 mM EGTA, 0.5% Tween 20), 10 µL of 25 mM $MgCl_2$, and 100 pmoles of primer **R T 2** 5'-TAATACGACTCACTATAGGA GTCTCTAGACAGTGCTCCA-3' in a 80 µL total volume. After the incubation, 80 µL of PCR Master Mix was added under oil to the reaction and briefly spun in a microcentrifuge. The reaction was placed in a thermocycler and subject to 25 rounds of amplification using

the following cycle : 95 °C (denaturation) for 1 minute, 60 °C (annealing) for 1 minute, and 72 °C (extension) for 2 minutes. Samples were rescued from under oil and 10 µL of Stop Buffer (1X TAE, 100 mM EDTA, 56% glycerol, 0.2% SDS, and 1% bromophenol blue) was added to each. Reactions were electrophoresed on 1.5% agarose gels in 1X TAE buffer. Amplification products were excised and eluted from the gel slice.

Sequence Determination of Amplified Templates. To determine the sequences of the amplified templates, purified RT-PCR products were digested with the restriction enzymes Pst I and Xba I and subcloned into the large fragment Pst I/Xba I restriction fragment of pBSIISK$^+$ (Stratagene). Plasmid DNA was isolated from individual isolated transformant colonies using a Qiagen plasmid miniprep DNA kit and the sequences of individual inserts were determined by dideoxynucleotide sequencing. Twelve different clones from rounds 4, 5, 6, 7 and 8 using both MMLV and rTH RT-PCR methodology were sequenced from scheme 1. This gave sequence information for 96 different selected oligoribonucleotide sequences.

Gel Filtration Analysis of Oligoribonucleotide Binding. Individual oligoribonucleotides and oligoribonucleotide populations were tested for co-elution with plasmid DNA on gel filtration columns. Hybridization reactions were assembled by combining 20 pmoles of selected 5'-end labeled oligonucleotide (10,000 cpm/pmole) and 1 µg of pCROSS I in a 20 µL volume of 1X Selection Buffer. When analyzing RNA populations, 20 pmoles of 5'-end labeled RNA pool (10,000 cpm/pmole) was used in place of individual oligoribonucleotide. The reactions were equilibrated for 12 hours at 37 °C. Each reaction was applied to an individual gel filtration column. The flow-

through fraction as well as the eluate from a 50 µL column wash with 1X Selection Buffer were combined and radioactivity was measured in a scintillation counter (Beckman Instruments). The same procedure was carried out in the absence of plasmid DNA to define the amount of backround signal derived from incorrectly fractionated RNA.

Sca I Endonuclease Protection Assay. Sca I endonuclease assays measured the extent of triple-helix formation at the 21 bp homopurine target site in supercoiled pCROSS I. In theory, when an oligonucleotide is bound to the target site the overlapping Sca I restriction sequence is protected from Sca I digestion. A distinct Sca I site located elsewhere on the plasmid was designed to serve as an internal control for nonspecific inhibition of Sca I cleavage. Binding reactions contained 100 ng of pCROSS I along with oligonucleotide in a 20 µL volume of 1X Selection buffer. They were incubated in a 37 °C oven in an insulated container for 12 hours with no evidence of evaporation. Sca I (15 units) was added to the binding reactions and digestion was proceeded at 37 °C for 12 minutes. Digestions were terminated by adding 10 µL of 1X Stop Buffer (1X TAE, 100 mM EDTA, 56% glycerol, 0.2% SDS, and 1% bromophenol blue) and electrophoresed on a 1.5% agarose, 1X TAE gels.

In Vitro DNase I Footprinting. Either the 320-bp Kpn I-Pvu II restriction fragment of pCROSS I or the 330-bp BsaH I-Ssp I restriction fragment of pBSIISK$^+$ was 3'-end labeled with deoxyadenosine - [α^{32}P] - triphosphate, and chemical sequencing reactions were carried out by standard procedures (Sambrook et al., 1989). Labeled DNA (50,000 cpm) and the indicated oligonucleotide were incubated in a 20 µL total volume of 1X Selection Buffer (25 mM PIPES pH 6.8, 70 mM NaCl, 20 mM $MgCl_2$, 1 mM Spermine, 100

μg/mL BSA, and 1 mM β-mercaptoethanol) for 24 hours at 37 °C. Prior to addition of 2 μL of DNase I (0.01 U/mL in 1X TE) , 1 μL of 100 mM $CaCl_2$ was added to the reaction. Digestion proceeded for 2 minutes at room temperature before termination by ethanol precipitation and resuspension in Sequenase Stop Buffer (95% formamide, 20 mM EDTA, 0.05% Bromophenol Blue, 0.05% Xylene Cyanol FF). The samples were analyzed by electrophoresis on 8% denaturing polyacrylamide gels. Gels were dried and placed on film or photostimulable phosphor imaging plates and quantitated as described (Singleton & Dervan, 1992).

In Vitro MPE•F(II) Footprinting. Either the 320-bp Kpn I-Pvu II restriction fragment of pCROSS I or the 330-bp BsaHI-SspI restriction fragment of pBSIISK$^+$ was 3'-end labeled with deoxyadenosine - [α^{32}P] - triphosphate, and chemical sequencing reactions were carried out (Sambrook et al., 1989). Labeled DNA (50,000 cpm) and the indicated oligonucleotide were incubated in a 20 μL total volume of 1X Selection Buffer for 24 hours at 37 °C. To a freshly prepared stock solution of 10 mM MPE was added an equivalent volume of freshly prepared 10 mM ferrous ammonium sulfate to generate a 5 mM stock solution of MPE•Fe(II). A 2 μL volume of 5 mM MPE•Fe(II) was added to the hybridization reactions and allowed to incubate at room temperature for 2 minutes. Footprinting reactions were initiated by adding 2 μL of 10 mM DTT to the samples and proceeded for 20 minutes at room temperature. The reactions were terminated by ethanol precipitation and resuspended in Sequenase Stop Buffer. The samples were analyzed by electrophoresis on 8% denaturing polyacrylamide gels. Gels were dried and placed on film or photostimulable phosphor imaging plates and quantitated as described (Singleton & Dervan, 1992).

In Vitro DMS Footprinting. Either the 320-bp Kpn I-Pvu II restriction fragment of pCROSS I or the 330-bp BsaHI-SspI restriction fragment of pBSIISK$^+$ was 3'-end with deoxyadenosine - [α^{32}P] - triphosphate, and chemical sequencing reactions were carried out by standard procedures (Sambrook et al., 1989). Labeled DNA (50,000 cpm) and the indicated oligonucleotide were incubated in a 20 µL total volume of 1X Selection Buffer for 24 hours at 37 °C. When indicated, 2 µL of 2% DMS was added to the reaction and incubated at room temperature for 4 minutes. The footprinting reaction was terminated by adding 50 µL of DMS stop solution (10 mM β-mercaptoethanol and10 mM Tris-Cl pH 8.0) and 750 µL of ethanol. Reactions were incubated on dry ice for 15 minutes prior to centrifugation at 4 °C for 20 minutes. Supernatants were discarded and the pellets were washed with 70% ethanol prior to drying in a Speed-Vac. The pellets were resuspended in 80 µL of 10% piperidine and incubated at 90 °C for 30 minutes. The reactions were cooled to room temperature, spun briefly in a microcentrifuge, and dried in a Speed-Vac. The pellets were resuspended in 100 µL of Milli-Q water and dried again in a Speed-Vac prior to resuspension in 10 µL of Sequenase Stop Buffer. The samples were analyzed by electrophoresis on 8% denaturing polyacrylamide gels. Gels were dried and placed on film or photostimulable phosphor imaging plates and quantitated as described (Singleton & Dervan, 1992).

RESULTS

Design of an Experimental System to Select for RNA Species That Can Bind to Double Helical DNA. To select for oligoribonucleotides that have strong affinity for a specific substrate, it is important to separate binding from nonbinding species and enrich for binders by reiterating this process. Figure 1 depicts the general scheme by which the randomized RNA library was treated to select for individuals with high affinity for double helical DNA. Individual species that have affinity for the plasmid pTARGET are separated from those that had no affinity by gel filtration chromatography. The gel filtration column separates high molecular weight species such as plasmid DNA from lower molecular weight species such as small oligoribonucleotides. Oligoribonucleotides that bind to the plasmid elute with the plasmid fraction and are from the unbound oligoribonucleotides which are retained longer on the column. In theory, the co-eluting RNA will be substantially enriched for species that have affinity for any of the sequences present in the plasmid. This process is called positive selection since it indiscriminately selects for DNA binding species.

In the process of negative selection, molecules that sequence specifically bind to distinct DNA species are enriched. Parental plasmid lacking the target site of interest, depicted as pΔTarget in Figure 1, is allowed to hybridize with the RNA pool and then applied to a gel filtration column. The unbound RNA fraction, retained longer on the column, is enriched in RNA species that have affinity for the target site containing plasmid but lack affinity for the parental plasmid. This will separate those species that bind to other sequences found on the plasmid.

Multiple rounds of positive and negative selection were performed on

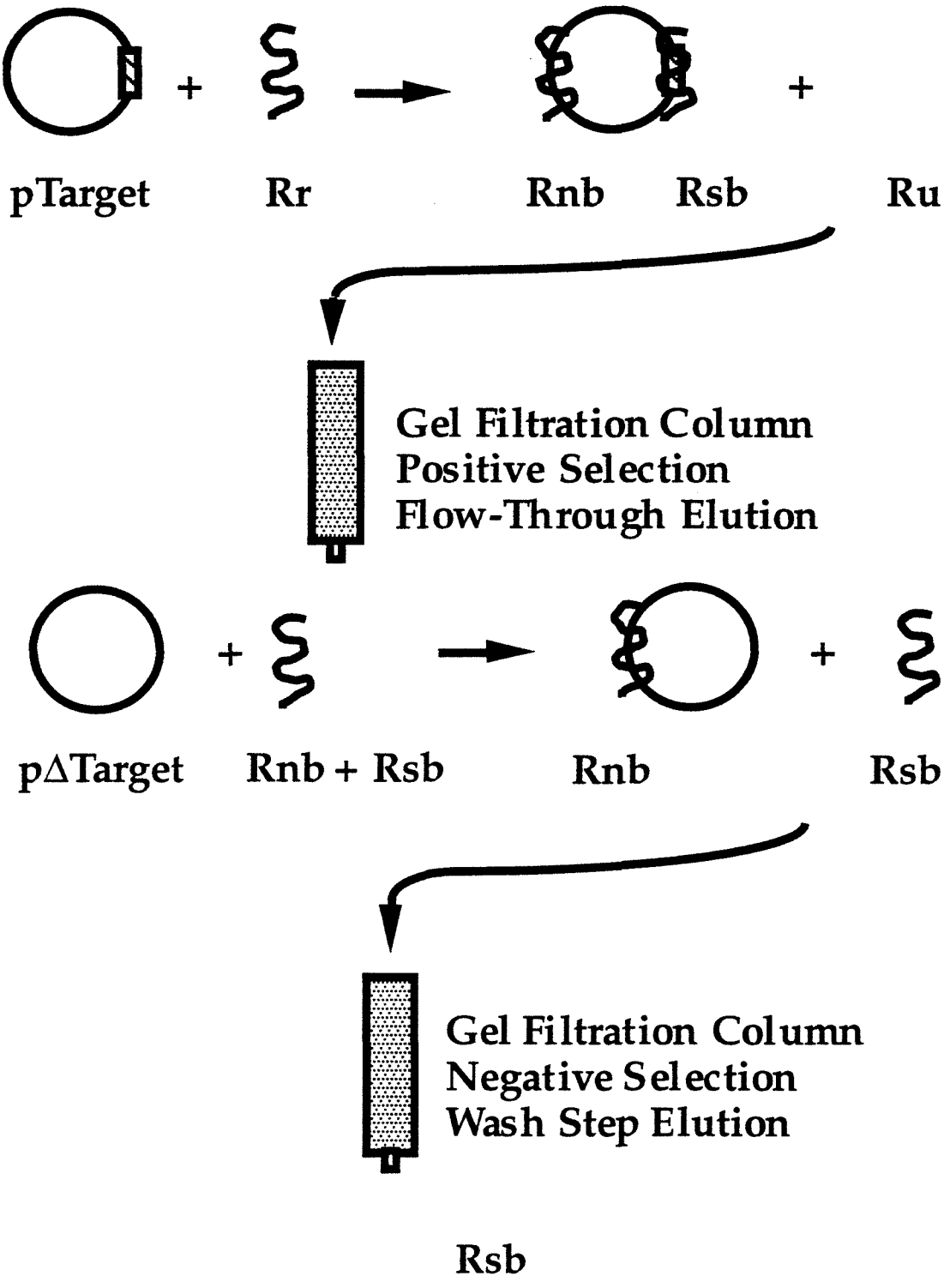

Figure 1: *In vitro* separation scheme. Key: Rr = RNA pool, Rnb = nonspecific RNA binding, Rsb = specific RNA binding, Ru = RNA unbound

nucleic acids fractions through cycles of reverse transcription and PCR amplification of the cDNA products (Figure 2). A random oligoribonucleotide library is generated through an *in vitro* T7 RNA polymerase transcription reaction on a DNA template containing a stretch of random nucleotide sequence. The template is complementarity to the T7 promoter oligonucleotide and has regions of defined sequences upstream and downstream of the randomized segment. An oligodeoxyribonucleotide primer complementary to the T7 promoter and downstream sequences is hybridized to the DNA template and used for an *in vitro* transcription reaction. The oligoribonucleotide population generated is fractionated by gel filtration chromatography. RNA fractions are converted to complementary DNAs (cDNAs) through reverse transcription reactions. The cDNA population is converted back to T7 RNA polymerase templates through PCR reactions using the reverse transcriptase and transcription primers. It is important for the T7 promoter oligodeoxyribonucleotide primer to contain sequence downstream of the T7 site complementary to the cDNA to allow the first round of priming to occur. The sequence information provided by the T7 promoter region of the oligodeoxyribonucleotide is lost during the transcription reaction since the polymerase only transcribes the sequence downstream of the promoter. However, the first round of PCR regenerates this T7 promoter sequence information using these primers. This allows the amplification products to be used for another cycle of transcription, fractionation, cDNA synthesis, and reamplification.

The plasmid pCROSS I was used as the DNA target for positive selection steps with its parent plasmid pBSIISK+ used for negative selection steps. The specific sequence of interest in pCROSS I is a 20-bp site target site (figure 3). Oligodeoxyribonucleotides with a 5'-purine-rich domain linked by at least

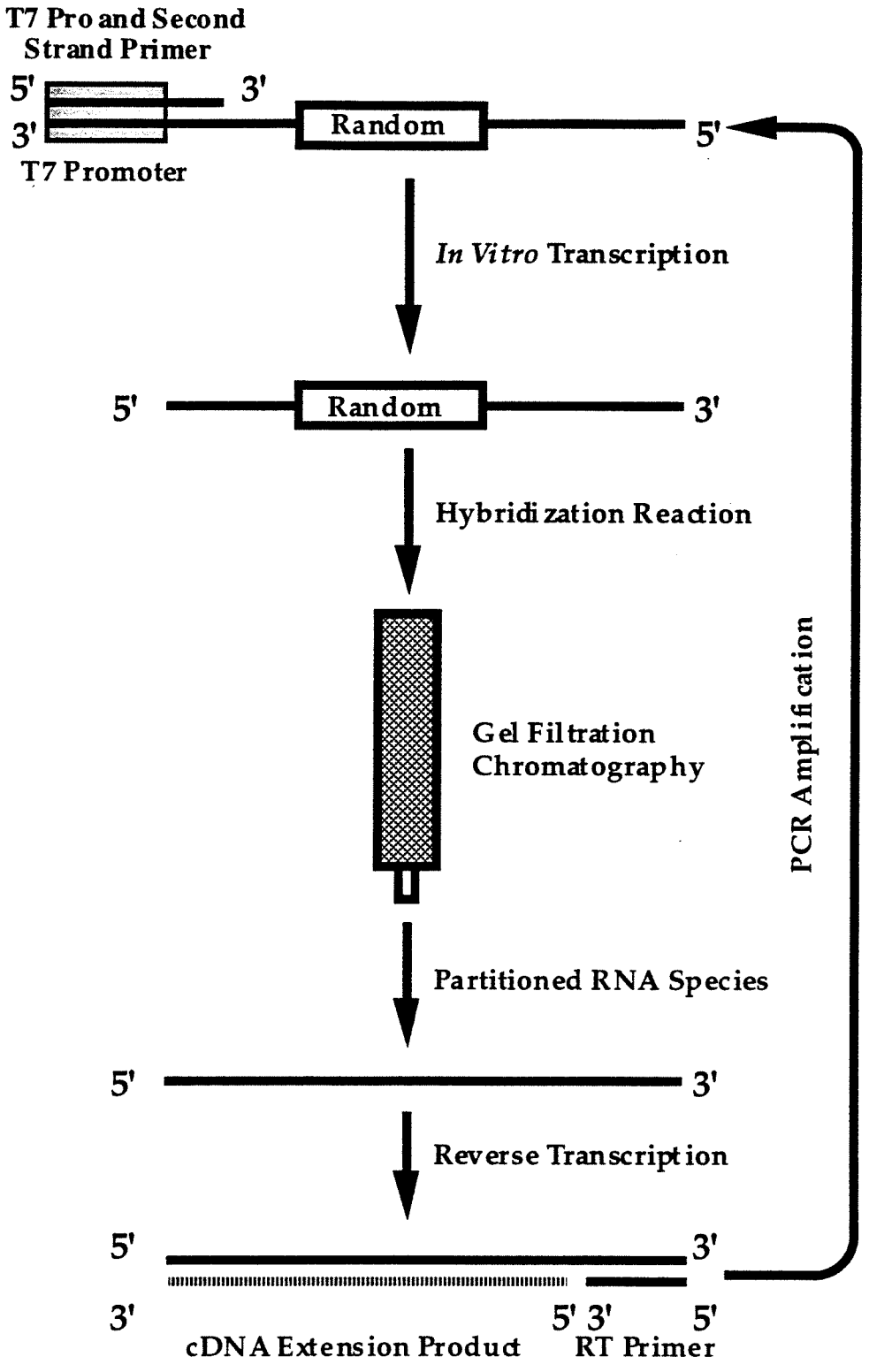

Figure 2: *In vitro* selection and amplification scheme.

two nucleotides to a 3'-pyrimidine-rich domain occupy such sites by forming Hoogsteen-hydrogen bonded base triplets one strand and reverse Hoogsteen-hydrogen bonded base triplets on the other strand of the helix (Beal & Dervan, 1992). While the adenine-rich half-site should be recognized by a uridine-rich oligoribonucleotide , the guanine-rich half-site probably will not be recognized by RNA, as shown in Chapter 1. Therefore, only oligoribonucleotides that could occupy the target site through non-triple helical interactions would be recovered in a functional selection process.

Another important variable is the amount of random sequence to incorporate into the oligoribonucleotide pool. For N number of random nucleotide positions in an oligonucleotide, there is 4^N possible different sequences. In this experiment, 25 randomized positions were used which represents approximately 1.1 X 10^{15} different sequences. To represent every one of these sequences in a population, a minimum of 1.9 nmoles of oligoribonucleotide would have to be made. This is well within the limits of DNA template synthesis as well as *in vitro* transcription reactions. The initial transcription reaction used 20 nmoles of DNA template to ensure that a majority of the oligodeoxyribonucleotide population was represented at least one time. Since ten nanomoles of randomized oligoribonucleotide pool was used in the first round of positive selection, a majority of the oligoribonucleotide population is theoretically represented.

The buffer conditions under which the RNA population hybridizes with the target DNA is crucial to the selection process. In scheme A, moderately stringent ionic conditions (25 mM PIPES pH 6.8, 70 mM NaCl, 20 mM $MgCl_2$, 1 mM spermine, 100 μg/mL BSA, and 1 mM β-mercaptoethanol) were used. Similar ionic conditions were used in selection scheme B with the omission of BSA. This was done to prevent selection for RNA species which have affinity

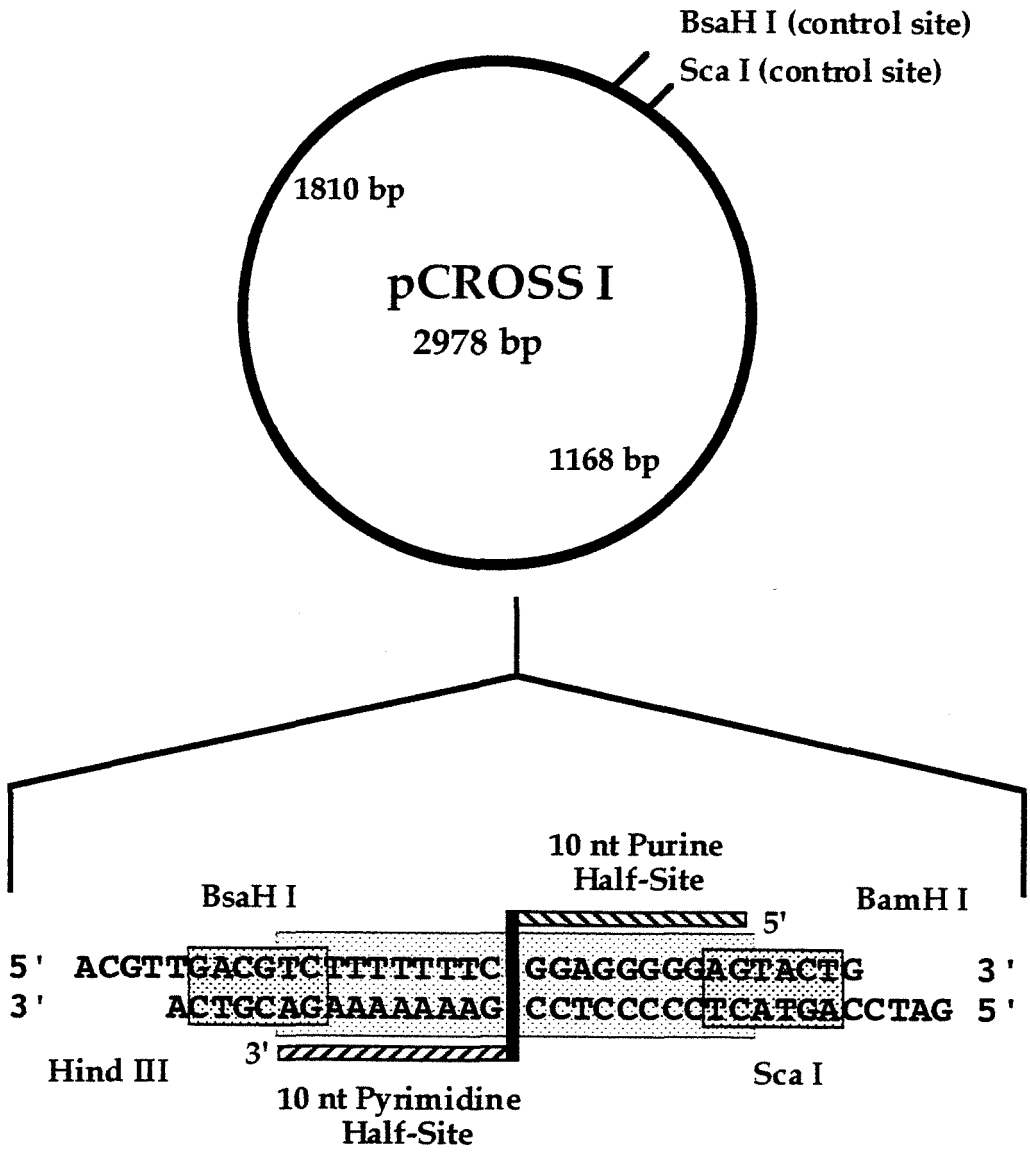

Figure 3: Partial restriction map of the plasmid pCROSS I.

for this protein. These conditions are similar to those used to promote triple helix formation in Chapter 1. Initial rounds of hybridization for positive selection were carried out at 37 °C while more stringent rounds were carried out at 42 °C. The ratio of RNA pool to target site DNA in the hybridization reaction also plays an important role in the selection process. For rounds of positive selection, a 10^3-10^4 fold excess of RNA pool over target was used, as

shown in Table I. This provides a competitive environment so that only tight DNA binders would be selected. For rounds of negative selection, a 10-fold excess of RNA to plasmid DNA was used (Table I). This ratio was designed to provide a nonspecific DNA sequence reservoir to soak up non-specific DNA binders in the population.

Oligonucleotide Nomenclature. The sequence of the selected oligoribonucleotides was determined from the sequences of cloned templates. Some of these oligoribonucleotide species, as well as their oligodeoxyribonucleotide analogs, were synthesized (Table I). Oligonucleotides are designated first by the round of selection from which they were isolated followed by the number of the clone from which they originated. Thirdly, they are named by the type of reverse transcriptase used in the amplification procedure, M for murine Moloney leukemia virus or Th for thermostable reverse transcriptase. Next, they were designated by the selection pathway utilized as shown in Figure 1. Finally, they are designated as either ribo -(R) or deoxyribo-(D) oligonucleotides along with the length of the clone in nucleotides. Oligonucleotides were made either representing the full length generated RNA (72mer) or only the randomized region (25mer). For example, the oligonucleotide **7-1-M-AR72** is a 72mer oligoribonucleotide derived from the first clone of round seven using MMLV reverse transcriptase and selection pathway A (Table I).

Gel Filtration Analysis of Oligonucleotides and Oligoribonucleotide Pools. Individual oligoribonucleotides and their oligodeoxyribonucleotide analogs selected in Round 7, using either MMLV or rTh reverse transcriptases, were tested for binding to the target plasmid pCROSS I by gel filtration analysis as

Table I. Hybridization conditions[a]

Round	Type	RNA	Plasmid	Ratio[b]	Temp.
1A	+	10 nmole	200 ng pCROSS I	50,000	37° C
2A	+	1 nmole	100 ng pCROSS I	10,000	37° C
3A	+	1 nmole	100 ng pCROSS I	10,000	37° C
4A	-	10 pmole	1 mg pBSIISK+	10	37° C
5A	-	10 pmole	1 mg pBSIISK+	10	37° C
6A	+	10 pmole	10 ng pCROSS I	1,000	47° C
7A	+	10 pmole	1 ng pCROSS I	10,000	47° C
1B	+	10 nmole	200 ng pCROSS I	50,000	37° C
2B	+	1 nmole	100 ng pCROSS I	10,000	37° C
3B	+	1 nmole	100 ng pCROSS I	10,000	37° C
4B	+	1 nmole	100 ng pCROSS I	10,000	37° C
5B	+	1 nmole	100 ng pCROSS I	10,000	37° C
6B	+	1 nmole	100 ng pCROSS I	10,000	37° C
7B	+	1 nmole	100 ng pCROSS I	10,000	37° C
8B	+	1 nmole	100 ng pCROSS I	10,000	37° C

[a]All hybridization reaction were allowed in equilibrate for 24 hours in 1X Selection Buffer (25 mM PIPES pH 6.8, 70 mM NaCl, 20 mM $MgCl_2$, 1 mM spermine, 100 μg/ml BSA, and 1 mM β-mercaptoethanol). In the case of rounds 1A-8A 1X Selection Buffer without BSA was used. [b]The approximate molar ratio of RNA to plasmid DNA in the reaction.

shown in Table III. None of the oligoribonucleotide or oligodeoxyribonucleotide clones from round seven of scheme A appeared to elute with either the target plasmid pCROSS I or the nonspecific plasmid pBSIISK+. Gel filtration analysis on labeled RNA pools from scheme B also showed that there is no measurable enrichment for DNA binders in the population with up to ten steps of positive selection (Table IV).

Inhibition of Sca I Restriction Endonuclease By Selected Oligonucleotides. A number of different oligodeoxyribonucleotide analogs of selected oligoribonucleotides inhibited Sca I cleavage of pCROSS I DNA preferentially

Table II. Sequences of selected oligonucleotides[a]

Oligonucleotide	Sequence
7-1-M-A	5'-CGCUCCCGGCUUCCCCUUGCUAUCC-3'
7-2-M-A	5'-CUACCUUUGUGCCGUGGCUGCCCCC-3'
7-5-M-A	5'-UUCUCUCCUAUGGUUCCCGUUGUCU-3'
7-8-M-A	5'-UGUUCGGUGACUCUGCCGACGUUUG-3'
7-1-Th-A	5'-UGUCUUGGGCCACCCUGGCACGCGG-3'
7-3-Th-A	5'-GGAGGCAGGCCGCAGUCGCCCGUGG-3'
7-5-Th-A	5'-CAGUUGUCUCCUAACCGGCCUCCCC-3'
7-7-Th-A	5'-CUGCCGAGCGUGCUAGGUGCGAAGC-3'

[a]The sequence of the 25-nt randomized region is given for each oligonucleotide. The complete sequence of each oligonucleotide in all cases contains the 5'-leader sequence 5'-GGAGUCUCUAGACAGUGCUCCA-3' as well as the 3'-trailer sequence 5'-UAGGAGUCAACUGCAGAAGCCAAGG-3'.

at one restriction site. Figure 4 shows the results of Sca I protection assays utilizing the DNA analogs of several oligoribonucleotides selected from round 7 of scheme A. Lanes 1-8 all show a complete disappearance of supercoiled DNA, when compared to the untreated lane 18. There appears to be a bias towards linearized DNA product as opposed to the expected double-cut species found in lane 17. Higher molecular weight plasmid DNA products are present in all these lanes, but are most visible in lanes 7 and 8. These products are dependent upon the presence of Sca I in the reaction (data not shown). In lanes 9-16 there is a complete disappearance of supercoiled DNA. However, lane 16 shows a bias towards single cut plasmid DNA with a faint appearance of higher molecular weight products. Similar, but less prominent, results are also shown in lanes 11, 12, and 14. None of the full-legth 72mer or shortened 25mer oligoribonucleotides were able to effect Sca I cleavage patterns (data not shown).

Table III. Gel filtration analysis of selected oligonucleotides[a]

Oligo Species	CPM Elutedw/ pCROSS I	CPM Eluted w/ pBSIISK+
7-1-M-AR72	5.9×10^2	5.2×10^2
7-1-M-AD72	4.8×10^2	4.9×10^2
7-2-M-AR72	4.7×10^2	5.0×10^2
7-2-M-AD72	7.1×10^2	7.7×10^2
7-5-M-AR72	8.4×10^2	7.2×10^2
7-5-M-AD72	7.8×10^2	6.8×10^2
7-8-M-AR72	5.8×10^2	7.1×10^2
7-8-M-AD72	4.9×10^2	5.2×10^2
7-1-Th-AR72	7.7×10^2	7.2×10^2
7-1-Th-AD72	5.4×10^2	5.7×10^2
7-3-Th-AR72	6.2×10^2	5.9×10^2
7-3-Th-AD72	7.8×10^2	6.2×10^2
7-5-Th-AR72	6.2×10^2	7.5×10^2
7-5-Th-AD72	5.3×10^2	6.1×10^2
7-7-Th-AR72	5.9×10^2	6.4×10^2
7-7-Th-AD72	5.5×10^2	5.9×10^2

[a]Values reported in the table are mean values measured from three repetitions of gel filtration chromatography experiments performed in 1X Selection Buffer (25 mM PIPES pH 6.8, 70 mM NaCl, 20 mM $MgCl_2$, 1 mM spermine, 100 μg/mL BSA, and 1 mM β-mercaptoethanol) with 1×10^6 cpm labelled oligonucleotide.

In Vitro Footprinting of Selected Oligoribonucleotides. As shown in Figure 5, none of the tested oligoribonucleotide species or their oligodeoxyribonucleotide analogs appear to protect the target site of interest from DNase I digestion. Similar results were found using DMS and MPE•Fe(II) as footprinting reagents (data not shown). Since the oligodeoxyribonucleotide analogs effect cleavage of the plasmid by Sca I, the 330-bp BsaH I-Ssp I restriction fragment of pBSIISK+, containing the Sca I control sequence found in pCROSS I, was used in footprinting analysis. Again no oligonucleotide-dependent protection of the target site or other sequences on the fragment was detected using DNase I, DMS, or MPE•Fe(II)

TABLE IV. Gel filtration analysis of oligoribonucleotide pools[a]

RNA Pool	CPM w/DNA	CPM w/o DNA	ΔCPM Retained
1-R-Th-2	9.1×10^2	8.0×10^2	1.1×10^2
2-R-Th-2	8.8×10^2	9.8×10^2	0
3-R-Th-2	7.2×10^2	8.2×10^2	0
4-R-Th-2	9.5×10^2	9.8×10^2	0
5-R-Th-2	9.3×10^2	9.2×10^2	10
6-R-Th-2	8.5×10^2	7.6×10^2	90
7-R-Th-2	7.7×10^2	1.0×10^3	0
8-R-Th-2	7.4×10^2	6.8×10^2	60
9-R-Th-2	9.0×10^3	8.0×10^2	1.0×10^2
10-R-Th-2	9.9×10^2	8.7×10^2	1.2×10^2

[a]Values reported in the table are mean values measured from three repetitions of gel filtration chromatography experiments performed in 1X Selection Buffer (25 mM PIPES pH 6.8, 70 mM NaCl, 20 mM $MgCl_2$, 1 mM spermine, 100 μg/mL BSA, and 1 mM β-mercaptoethanol) with 1×10^6 cpm labelled oligonucleotide pool.

as footprinting reagents (data not shown).

FIGURE 4: Results of a Sca I endonuclease protection assay determining the stability of triple helical complexes formed between indictaed oligodeoxyribonucleotides and the target plasmid pCROSS I. The concentration of oligodeoxyribonucleotides are held constant at 1 μM. All assays were performed under standard conditions. Lane 1, oligonucleotide **7-1-M-AD72**; lane 2, oligonucleotide **7-2-M-D72**; lane 3, oligonucleotide **7-5-M-AD72**; lane 4, oligonucleotide **7-8-M-AD72**; lane 5, oligonucleotide **7-1-Th-AD72**; lane 6, oligonucleotide **7-3-Th-AD72**; lane 7, oligonucleotide **7-5-Th-AD72**; lane 8, oligonucleotide **7-7-Th-AD72**; Lane 9, oligonucleotide **7-1-M-1D25**; lane 10, oligonucleotide **7-2-M-D25**; lane 11, oligonucleotide **7-5-M-1D25**; lane 12, oligonucleotide **7-8-M-1D25**; lane 13, oligonucleotide **7-1-Th-1D25**; lane 14, oligonucleotide **7-3-Th-1D25**; lane 15, oligonucleotide **7-5-Th-1D25**; lane 16, oligonucleotide **7-7-Th-1D25**; lane 17, no oligonucleotide; lane 18, no enzyme.

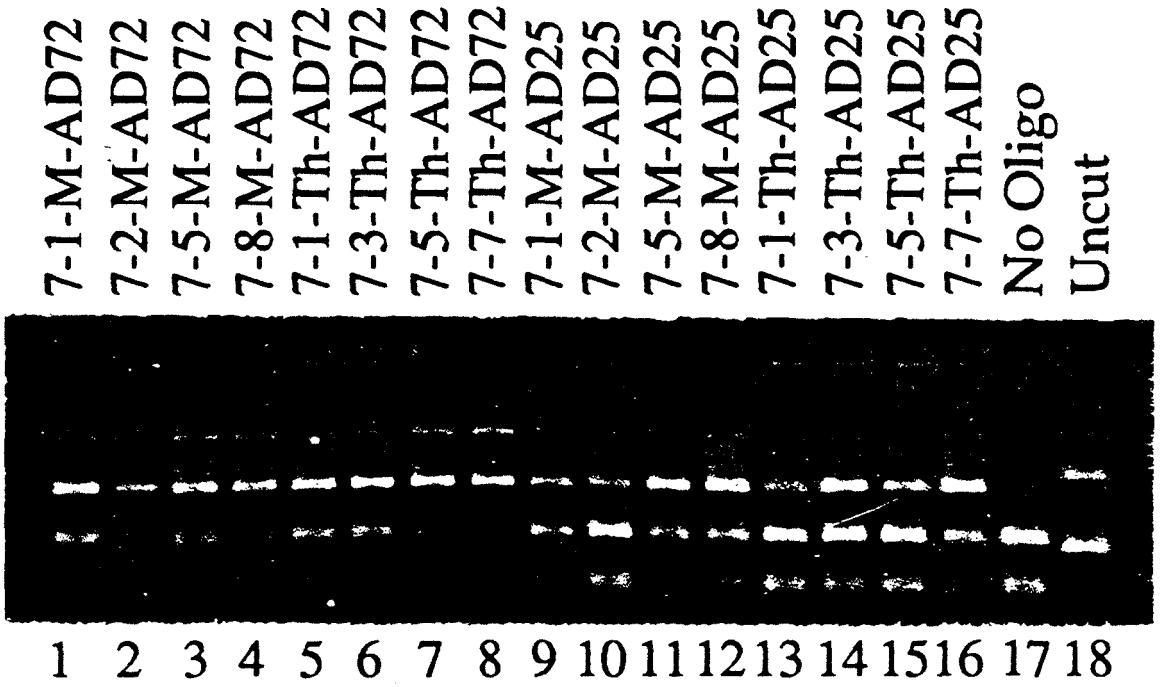
7-1-M-AD72
7-2-M-AD72
7-5-M-AD72
7-8-M-AD72
7-1-Th-AD72
7-3-Th-AD72
7-5-Th-AD72
7-7-Th-AD72
7-1-M-AD25
7-2-M-AD25
7-5-M-AD25
7-8-M-AD25
7-1-Th-AD25
7-3-Th-AD25
7-5-Th-AD25
7-7-Th-AD25
No Oligo
Uncut
1 2 3 4 5 6 7 8 9 10 11 12 13 14 15 16 17 18

FIGURE 5: Autoradiogram of an 8% denaturing polyacrylamide gel showing DNase I footprinting assays performed on the 320-bp Kpn I-Pvu II restriction fragment of pCROSS I with the indicated oligonucleotides. Lane 1, C + T; Lane 2, no oligonucleotide; Lane 3, oligonucleotide **7-1-M-AD72**; lane 4, oligonucleotide **7-1-M-R72**; lane 5, oligonucleotide **7-2-M-AD72**; lane 6, oligonucleotide **7-2-M-AR72**; lane 7, oligonucleotide **7-5-M-AD72**; lane 8, oligonucleotide **7-5-M-AR72**; lane 9, oligonucleotide **7-8-M-AD72**; lane 10, oligonucleotide **7-8-M-AD72**; lane 10, no oligonucleotide; lane 11, oligonucleotide **7-1-Th-AD72**; lane 12, oligonucleotide **7-2-M-AR72**; lane 13, oligonucleotide **7-3-Th-AD72**; lane 14, oligonucleotide **7-3-Th-AR72**; lane 15, oligonucleotide **7-5-Th-AD72**; lane 16, oligonucleotide **7-5-Th-AR72**; lane 17, oligonucleotide **7-7-Th-AD72**; lane 18, oligonucleotide **7-7-Th-AR72**; lane 19, no oligonucleotide; lane 20, no DNase I.

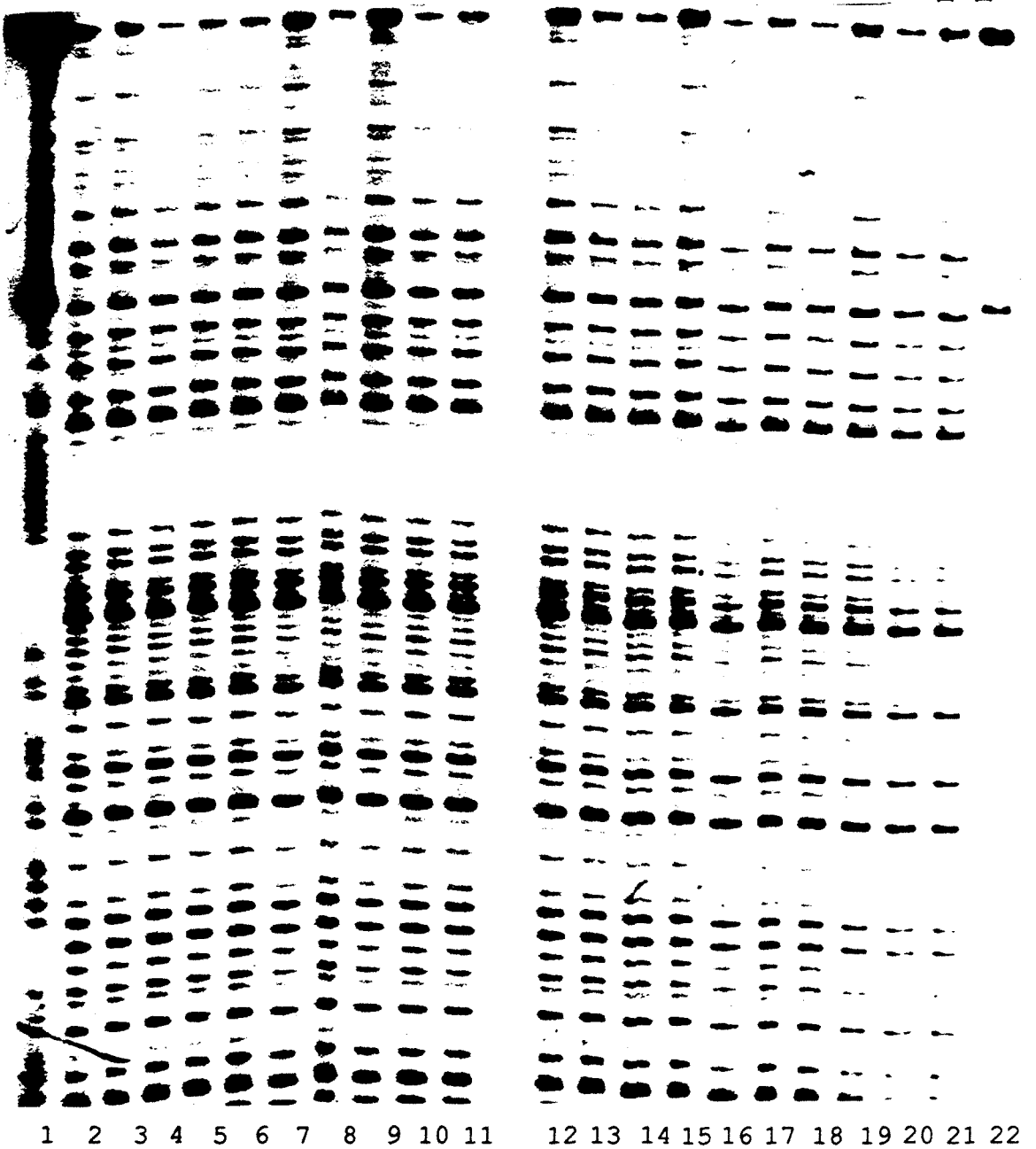
C + T
No Oligo
7-1-M-AD72
7-1-M-AR72
7-2-M-AD72
7-2-M-AR72
7-5-M-AD72
7-5-M-AR72
7-8-M-AD72
7-8-M-AR72
No Oligo
No Oligo
7-1-Th-AD72
7-1-Th-AR72
7-3-Th-AD72
7-3-Th-AR72
7-5-Th-AD72
7-5-Th-AR72
7-7-Th-AD72
7-7-Th-AR72
No Oligo
No DNase I
1 2 3 4 5 6 7 8 9 10 11
12 13 14 15 16 17 18 19 20 21 22

DISCUSSION

Possible Reasons for the Inability to Select for Oligoribonucleotides With Affinity for Double Helical DNA. There are many possible reasons why no oligoribonucleotides with measurable binding affinity to the target plasmid were found in the population. It is likely that the selection conditions were too stringent to allow oligoribonucleotide binding. Since the hybridization reaction was done under conditions close to neutral pH, potential triple-helix forming oligoribonucleotides would not have significant affinity for guanine-rich homopurine tracts. Triple helices containing $rC^+ \bullet GC$ triplets were shown in Chapter 1 at higher pH ranges. This will bias triple helix selection towards uridine-rich sequences. However, T7 RNA polymerase has difficulty in transcribing oligoribonucleotides with five or more contiguous uridines with high fidelity (Milligan et al., 1987). This will cause uridine-rich sequences to be underrepresented in the selection pool.

Another likely possibility is that non-triple helical DNA binding molecules are not significantly represented in the population. Triple helix formation is the only known way in which oligoribonucleotides can bind double helical DNA. Since both the DNA target site and the oligoribonucleotide pool are polyanions, coulombic repulsions may present a significant barrier towards non-triple helical hybridization. Furthermore, such molecules may hybridize only under a narrow range of ionic conditions that are unpredictable. Several other hydridization buffers would need to be tested in order to rule out this possibility.

The amount of randomized sequence in the population is another important variable. Non-cannonical interactions between RNA and duplex DNA may require large structural RNA motifs. Since the RNAs are 68-nt

long with 25 randomized positions, the number and types of different structures that can be formed is limited. RNA pools with greater than 100 randomized positions may be needed to generate sufficient structural diversity to find novel binding species. However, only an infinitesimal percentage of the population will be represented in this RNA pool.

Another major variable is the means by which the RNA pool is fractionated for individuals that can or cannot bind to double helical DNA. Gel filtration chromatography separated plasmid DNA from the oligoribonucleotide pool. Nonspecific oligoribonucleotides were separated greater than 99.9% from plasmid DNA using the gel filtration column. This should provide sufficient partitioning of RNA species for successful selection. Nevertheless, more efficient separation may be accomplished through gel shift techniques. Hybridization reactions applied to either nondenaturing polyacylamide or agarose gels will provide almost quantitative separation of bound and unbound species. However, RNA extraction from the gel matrix may be inefficient and complexes may be unstable to gel electrophoresis. Alternatively, separation can be achieved using affinity chromatography. Double-helical DNA target sites may be attached to a solid support and used as a target site. A study using such a strategy is described in the next section.

The DNA target site is another important variable to be considered. Oligoribonucleotides were initially screened for specific binding to a 20-bp target sequence through rounds of positive and negative selection. After no enrichment was detected, a second attempt was made using eight consecutive positive selection steps for oligoribonucleotides that could bind anywhere on pCROSS I. Although this strategy did not produce measurable enrichment for DNA binders, it seems likely that presenting a large number of target sequences will be important for a successful screening procedure. If

noncannonical RNA-mediated nucleic acid interactions exist, most probably they will be subject to sequence composition effects. By providing a large number of different target sites the likelihood that a sequence favorable to non-cannonical hybridization is present increases. Larger DNA samples such as λ DNA or cosmids may favor the selection of novel RNA interactions.

Report of Selecting DNA Binding Oligoribonucleotides From a Random Population. Schultz and co-workers reported an experimental design that selected for individual RNA molecules, from a large population of sequences, which bound to a 16-base pair homopurine DNA sequence through triple helix formation (Pei et al., 1991). An 89-nt RNA pool was generated that contained a contiguous run of 50 randomized nucleotides representing approximately 10^{10} to 10^{12} different RNA species. Separation of DNA binding species was accomplished by immobilizing a 25-bp DNA fragment containing the homopurine tract onto a thio-Sepharose support and using this resin as an affinity column. RNA transcripts were hybridized to the affinity column under nonstringent conditions (2 M NaCl, pH 5.5) for 1 hour at room temperature. Unbound oligoribonucleotide were washed away by treating with binding buffer and bound RNA was eluted with a low-salt buffer (50 mM Tris-HCl, pH 8.0, 1 mM EDTA). The eluted RNA was used as a template for cDNA synthesis and subsequently amplified through PCR with a primer that contains the T7 RNA polymerase promoter sequence. The selected templates were transcribed and the RNA population was treated to a second round of selection as stated above. During the next three rounds of selection, bound RNA species eluted from the affinity column (positive selection) were passed next though an underivatized thio-Sepharose column under identical

conditions to remove RNA with affinity for the thio-Sepharose support (negative selection).

After the five rounds of selection, DNA templates were subcloned and individual clones were sequenced. Of the 17 clones reported, 14 contained stretches of homopyrimidine sequences that had significant Hoogsteen-hydrogen bonding complementarity to the homopurine target sequence. It was proposed that nonstandard triplets such as C^+(C)•AT, U•GC, A•AT, and G•GC triplets were forming between selected RNA species and the target site. The authors also suggested that triple helical complexes could accommodate a number of secondary structural elements such as interior loops and, to a lesser degree, hairpin loops. Individual RNA species were derivatized with staphylococcal nuclease to create affinity cleaving analogs cleaved the DNA target site under permissive conditions.

The selected RNA species most likely will not have measurable affinity for the target site at neutral pH and moderate cation concentrations. Under the nonstringent hybridization and affinity cleavage conditions, there is high tolerance of mismatches in the triple helical complexes. It is well established for third strand oligodeoxyribonucleotides that mismatched triplets have a destabilizing effect towards triple helix formation (Griffin & Dervan, 1989; Mergny et al., 1991; Roberts & Crothers, 1991; Beal & Dervan, 1992b; Singleton & Dervan, 1992; Fossella et al., 1993). More stringent hybridization conditions will probably reveal that the proposed noncannonical RNA triplets are energetically unfavorable and that secondary structures inhibit triple helix formation.

Interestingly, no RNA species were selected that could bind the target site through non-triple helical interactions. This suggests that if RNA species with different binding modes do exist, then they are relatively rare species in

the population. It is still a significant challenge to select for RNA species that can bind under more stringent conditions and provide new leads towards recognizing double helical DNA.

Reports of Selecting Oligonucleotides that Bind Proteins From a Random Population. Oligoribonucleotides with high affinity for a variety of different protein have been found by screening randomized RNA libraries. Tuerk and Gold made the first report of these experiments by selecting for RNA ligands with high affinity for T4 DNA polymerase (Tuerk & Gold, 1990). The authors later used mathematical and computer simulation analysis to propose modifications to their protocol that enhance the selection efficiency (Irvine et al., 1991).

Other studies have focused on selecting RNA species with affinity for human immunodeficiency virus I (HIV-1) proteins (Tuerk & MacDougal-Waugh, 1993). Oligoribonucleotides with a pseudoknot consensus sequence had high affinity for HIV-1 reverse transcriptase (Tuerk et al., 1992). Selected RNAs proved to be inhibitory to HIV-1 reverse transcriptase activity and one particular species did not inhibit the activity of other reverse transcriptases from Moloney murine leukemia virus and avian myeloblastosis virus. Oligoribonucleotides with high affinity for the HIV-1 Tat protein also have been selected (Tuerk & MacDougal-Waugh, 1993). By examining the results of selection experiments, Szostak and co-workers proposed that non-Watson-Crick G•G base pairs contribute to Rev binding to the natural Rev-responsive element (*RRE*) (Bartel et al., 1991). Additional studies have expanded the number of RNA species that have high affinity for this protein (Giver et al., 1993; Jensen et al., 1994).

Other RNA-protein interactions have been studied using selection procedures similar to the one first proposed by Tuerk and Gold. Some studies have focused on selecting RNA ligands for *E. coli* and bacteriophage proteins such as the bacteriophage R17 coat protein and *E. coli* rho factor (Schneider et al., 1992; Schneider et al., 1993). Others have examined binding to mammalian growth factors such as basic fibroblast growth factor (bFGF) and vascular endothelial growth factor (VEGF) (Jellinek et al., 1993; Jellinek et al., 1994). Both single-stranded DNA and RNA oligonucleotides with affinity for human thrombin have been found. The selected oligodeoxyribonucleotides were guanine-rich and later shown to form G-quartet structures (Bock et al., 1992; Macaya et al., 1993; Wang et al., 1993). Selected oligoribonucleotides were shown to adopt two different classes of stem-loop structures unrelated to G-quartet formation. This may be due to the different selection conditions were used as well as the inherent differences between RNA and DNA ligands.

Reports of Selecting Oligonucleotides that Bind Small Molecules From a Random Population. Oligoribonucleotides that bind specifically to small molecules have been isolated through *in vitro* selection experiments. The first report of such species was made by the elegant work of Ellington and Szostak (Ellington & Szostak, 1990). RNAs were isolated that bound to several dyes, such as Cibracon Blue, which mimic metabolic cofactors. The selected RNAs were highly specific for the substrate dye and that most bore no recognizable sequence similarity to one another. The authors concluded that there are numerous independent solutions to the problem of oligoribonucleotide-directed dye binding. The authors also reported the results of similar selections carried out with single-stranded DNA pools (Ellington & Szostak,

1992). Analogous results were found except in one case a common 18 nt sequence, which was presented as the capping loop of a larger stem-loop structure, was overrepresented. The authors surmised that smaller sequence motifs may dominate a selection process over longer and better sequences due to the statistical overrepresentation of the smaller sequences in the population.

Studies have identified RNA molecules that can bind with high specificity to other types of small molecules. Szostak and co-workers found RNAs with high affinity for ATP as well as for vitamin B_{12} (Sassanfar & Szostak, 1993; Lorsch & Szostak, 1994). In addition, RNAs with specific affinity for the amino acids D-tryptophan, L-arginine, L-valine, and D-arginine have been isolated (Famulok & Szostak, 1992; Famulok, 1994; Connell et al., 1994; Majerfeld & Yarus, 1994). Finally, a small RNA with remarkable discrimination for theophylline has been reported (Jenison et al., 1994). In all these cases, the selection procedures produced a single RNA sequence motif, in contrast to the original studies of Ellington and Szostak. The highly stringent conditions of the selection procedures may have caused this to occur.

Based on data gathered from these selection studies, Ellington has estimated that nucleic acid structures that can bind several different sizes and types of small ligands can be constructed from 17 to 23 fixed nucleotide positions (Ellington, 1994). He also proposed that tighter binding RNA species usually have higher specificity apparently due to the increase in specific contacts with the ligand. In general, larger molecules were found to be bound somewhat better than smaller ones. The tightest binding RNA species all recognize nucleotides or at least ligands that contain heterocyclic

rings. None of the amino acid-binding RNA species display this level of affinity or specificity.

Possible Reasons for Oligodeoxyribonucleotide-Dependent Inhibition of Sca I Endonuclease. Although *in vitro* footprinting analysis shows that none of the tested oligonucleotides bind to either of the Sca I sites present on pCROSS I, some of oligodeoxyribonucleotide species cause the enzyme to preferentially cleave the substrate only once. This contrasts control experiments where the enzyme efficiently cleaves both Sca I sites. One possible explanation is that there is nonspecific inhibition of the enzyme by the oligodeoxyribonucleotide. However, this would be expected to produce a mixture of products in which the linearized fragment is not overwhelmingly overrepresented. Sca I may cleave one of the recognition sites faster than the other due to flanking sequence effects. For example, the restriction endonuclease EcoR I is known to have different substrate specificity for targets adjacent to oligopurine tracts (Venditti et al., 1991). Any bias in target site cleavage may be exacerbated by nonspecific enzyme inhibitors. This could cause the preferential appearance of linearized product. An alternative explanation involves oligodeoxyribonucleotide binding to the restriction enzyme to alter its cleavage specificity. Further experimentation is needed to provide a definitve explanation for these observations.

The formation of higher molecular weight products resulting from Sca I digestion reactions performed in the presence of oligodeoxyribonucleotides is difficult to explain. It would appear that the oligodeoxyribonucleotide activates ligase or topisomerase activity present in the Sca I enzyme preparation. This activity may be latent to the Sca I protein itself or a contaminant from the isolation procedure. It has been characterized as a type

II restriction endonuclease with no unusual addtional enzymatic properties (Kita et al., 1985). The activity which gives rise to the higher molecular weight species is dependent on the sequence of the oligodeoxynucleotide and is not stimulated by the oligoribonucleotide analogs.

BIBLIOGRAPHY

Bartel, D. P., Zapp, M. L., Green, M. R., & Szostak, J. W. (1991) *Cell 67*, 529-536.

Beal, P. A., & Dervan, P. B. (1992a) *J. Am. Chem. Soc. 114*, 4976-4982.

Beal, P. A., & Dervan, P. B. (1992b) *Nucleic Acids Res. 20*, 2773-2776.

Bock, L. C., Griffin, L. C., Latham, J. A., Vermaas, E. H., & Toole, J. J. (1992) *Nature 355*, 564-566.

Connell, G. J., Illangesekare, M., & Yarus, M. (1993) *Biochemistry 32*, 5497-5502.

Ellington, A. D. (1994) *Berichte Der Bunsen Gesellschaft Fur Physikalische Chemie 98*, 1115-1121.

Ellington, A. D., & Szostak, J. W. (1990) *Nature 346*, 818-822.

Ellington, A. D., & Szostak, J. W. (1992) *Nature 355*, 850-852.

Escude, C., Francois, J.-C., Sun, J.-S., Ott, G., Sprinzl, M., Garestier, T., & Helene, C. (1993) *Nucleic Acids Res. 21*, 5547-5553.

Famulok, M. (1994) *J. Am . Chem. Soc. 116*, 1698-1706.

Famulok, M., & Szostak, J. W. (1992) *J. Am. Chem. Soc. 114*, 3990-3991.

Fossella, J. A., Kim, Y. J., Shih, H., Richards, E. G., & Fresco, J. R. (1993) *Nucleic Acids Res. 21*, 4511-4515.

Giver, L., Bartel, D. P., Zapp, M. L., Green, M. R., & Ellington, A. D. (1993) *Gene 137*, 19-24.

Griffin, L. C., & Dervan, P. B. (1989) *Science 245*, 967-971.

Han, H. & Dervan, P. B. (1993) *Proc. Natl. Acad. Sci. 90*, 3806-3810.

Irvine, D., Tuerk, C., & Gold, L. (1991) *J. Mol. Biol. 222*, 739-761.

Jellinek, D., Green, L. S., Bell, C., & Janjic, N. (1994) *Biochemistry 33*, 10450-10456.

Jellinek, D., Lynott, C. K., Rifkin, D. B., & Janjic, N. (1993) *Proc. Natl. Acad. Sci. U. S. A. 90*, 11227-11231.

Jenison, R. D., Gill, S. C., Pardi, A., & Polisky, B. (1994) *Science 263*, 1425-1429.

Jensen, K. B., Green, L., MacDougal-Waugh, S., & Tuerk, C. (1994) *J. Mol. Biol. 235*, 237-247.

Kita, K., Hiraoka, N., Kimizuka, F., Obayashi, A., Kojima, H., Takahashi, H., & Saito, H. (1985) *Nucleic Acids Res. 13*, 7015-7024.

Lorsch, J. R., & Szostak, J. W. (1994) *Biochemistry 33*, 973-982.

Macaya, R. F., Schultze, P., Smith, F. W., Roe, J. A., & Feigon, J. (1993) *Proc. Natl. Acad. Sci. U. S. A. 90*, 3745-3749.

Majerfeld, I., & Yarus, M. (1994) *Nature Struct. Biol. 1*, 287-292.

Mergny, J. L., Sun, J. S., Rougee, M., Montenay-Garestier, T., Barcelo, F., Chomilier, F., & Helene, C. (1991) *Biochemistry 30*, 9791-9798.

Milligan, J. F., Groebe, D. R., Witherell, G. W., & Uhlenbeck, O. C. (1987) *Nucleic Acids Res. 15*, 8783-8798.

Pei, D., Ulrich, H. D., & Schultz, P. G. (1991) *Science 253*, 1410-1411.

Roberts, R. W., & Crothers, D. M. (1991) *Proc. Natl. Acad. Sci. U. S. A. 88*, 9397-9401.

Roberts, R. W., & Crothers, D. M. (1992) *Science 258*, 1463-1466.

Sambrook, J., Fritsch, E. F., & Maniatis, T. (1989) *Molecular Cloning, A Laboratory Manual*, 2nd ed., Cold Spring Harbor Laboratory, Cold Spring Harbor, NY.

Sassanfar, M., & Szostak, J. W. (1993) *Nature 364*, 550.

Scheider, D., Gold, L., & Platt, T. (1993) *FASEB J. 7*, 201-207.

Scheider, D., Tuerk, C., & Gold, L. (1992) *J. Mol. Biol. 228*, 862-869.

Singleton, S. F., & Dervan, P. B. (1992) *J. Am. Chem. Soc. 114*, 6957-6965.

Tuerk, C., & Gold, L. (1990) *Science 249*, 505-510.

Tuerk, C., & MacDougal-Waugh, S. (1993) *Gene 137*, 33-39.

Tuerk, C., MacDougal, S., & Gold, L. (1992) *Proc. Natl. Acad. Sci. U. S. A. 89*, 6988-6992.

Venditti, S., & Wells, R. D. (1991) *J. Biol. Chem. 266*, 6786-6790.

Wang, K. Y., McCurdy, S., Shea, R. G., Swaminathan, S., & Bolton, P. H. (1993) *Biochemistry 32*, 1899-1904.

Chapter IV

In Vivo Footprinting Analysis for RNA-Directed Triple Helix Formation

INTRODUCTION

Specific interactions between nucleic acids and proteins mediate the control of gene expression in all organisms. In one of their most important roles, nucleic acids serve as information-bearing macromolecules which encode for polypeptide gene products. Nature has utilized RNA as an intermediary in the information transfer process between the expression of genes encoded on DNA and the production of polypeptides. In addition, RNA provides crucial structural information for a variety of biological processes such as translation. Although RNA serves a large number of diverse functions, it has yet to be shown that specific interactions between native double-helical DNA and RNA can occur *in vivo* and be used to modulate biological processes such as gene expression or replication.

The only known means of sequence-specific recognition of native double-helical DNA by RNA is through oligoribonucleotide-directed triple helix formation. Pyrimidine-rich oligoribonucleotides bind in the major groove of DNA at homopurine target sites through the formation of U•AT and rC^{+}•GC base triplets (Roberts & Crothers, 1992; Escude et al., 1993; Han & Dervan, 1993). Oligodeoxyribonucleotide-directed triple helix formation has been used *in vitro* to inhibit DNA binding proteins such as restriction endonucleases, methylases, and transcription factors from recognizing their binding sites (Maher et al., 1989; Maher et al., 1990; Maher et al., 1992; Strobel

& Dervan, 1991). Furthermore, *in vitro* transcription and primer extension reactions have been specifically modulated (Young et al., 1991; Maher et al., 1992; Duval-Valentin et al., 1993; Maher, 1992; Hacia et al., 1994).

Although triple helix formation has been used with great success *in vitro*, there is no definitive evidence that these structures can form within a cell. One possible explanation involves delivery of third strand nucleic acid to the target site. In this study, we examine the ability of oligoribonucleotides overexpressed in a prokaryotic cell to form triple helical complexes with a plasmid target site through *in vivo* footprinting experiments. Although intact oligoribonucleotide was produced in micromolar concentrations *in vivo*, there was no evidence of triple helix formation. Nevertheless, this system demonstrates that small unstructured oligoribonucleotides can be overproduced in *E. coli* and can encourage further studies for *in vivo* oligoribonucleotide-directed triple helix fomation.

EXPERIMENTAL PROCEDURES

Materials. All DNA synthesis reagents were obtained from Applied Biosystems Inc. except for Chemical Phosphorylation Reagent obtained from Glen Research. Tetrabutylammonium fluoride in tetrahydrofuran was obtained from Aldrich. All other restriction enzymes, T4 polynucleotide kinase, and T4 DNA ligase were purchased from Boehringer Mannheim. Sequenase Version 2.0 DNA polymerase was purchased from U. S. Biochemicals. Ampicillin, kanamycin sulfate, and tetracycline hydrochloride were obtained from Boehringer Mannheim. Thiamine hydrochloride was obtained from Sigma. Adenosine 5'- [γ^{32}P] - triphosphate and deoxyadenosine - [α^{32}P] - triphosphate were obtained from New England Nuclear. The *E. coli* strain 8117 f'11 was a generous gift from Dr. Benno Muller-Hill. The *E. coli* strain CG103 was a generous gift from Dr. Dennis Arvidson. The plasmid pSRW 21 was a generous gift from Dr. Christopher M. Thomas. The plasmid p177MmCAU was a generous gift from Dr. Ladonne Schulman. The plasmid pPD16.51 was a generous gift from Dr. Andrew Fire.

Chemical Synthesis of Oligodeoxyribonucleotides. Oligodeoxyribonucleotides were prepared on an Applied Biosystems 380B DNA Synthesizer with β-cyanoethyl phosphoramidites. Oligodeoxyribonucleotides were purified by denaturing polyacrylamide gel electrophoresis, visualized by UV shadowing, and electroeluted from gel slices using an Elu-trap apparatus (Schleicher & Schuell). They were ethanol precipitated and resuspended in 0.5X TE before storing at -80 °C. The concentration of oligonucleotides were determined by A_{260} measurements using the following molar extinction coefficients: 15,400

(A), 11,700 (G), 7,300 (C), and 8,800 (T).

Chemical Synthesis of Oligoribonucleotides. Oligoribonucleotide **RNAY1** was prepared on an Applied Biosystems 380B DNA Synthesizer with 2' -hydroxyl protected tertbutyl dimethyl silyl β-cyanoethyl phosphoramidites. The oligoribonucleotide was deblocked and purified under essentially standard conditions (Usman et al., 1987; Wu et al., 1989). The solid support from a 1 μmole RNA synthesis was removed from the synthesis vessle and treated with 2 mL of 3 : 1 ammonium hydroxide : ethanol solution and incubated at 55 °C for 8 - 12 hours. The solution was dried in a Speed-Vac (Savant) and resuspended in 2 mL of tetrabutylammonium fluoride/tetrahydrofuran. After a 48 hour room temperature incubation, the reaction was quenched by adding 20 μL of 2M triethylamine acetate pH 7.0 and evaporated to an oil in a Speed-Vac (Savant). The residue was resuspended in 2 mL of Milli-Q water and dialyzed against water. Oligoribonucleotide **RNAY1** was concentrated through lyophilization, purified by denaturing polyacrylamide gel electrophoresis, visualized by UV shadowing, and electroeluted from gel slices using an Elu-trap apparatus (Schleicher & Schuell). It was ethanol precipitated and resuspended in 0.5X TE before storing at -80 °C. The concentration of the oligoribonucleotide was determined by A_{260} measurements using the following molar extinction coefficients: 15,400 (A), 11,700 (G), 7,300 (C), and 10,000 (U).

Construction of Triple Helix Target Site Plasmid The plasmid pTER I was obtained by cloning the oligonucleotides **UCT1** 5'-pTCGACTTTTTTTCTTTTT CTTTCTTTTTTTTTTTTGGCGCATG-3' and **UCT2** 5'-pCGCCAAAAAAAAA AAAGAAAGAAAAAGAAAAAAAG-3' into the large Sal I/Sph I restriction

fragment of pUC19. The plasmid pLTC1.1 was obtained by ligating the purified 2375-bp Pvu II fragment from pTER I to the purified large 3620-bp Hinc II/Fsp I restriction fragment from pACYC177. pLTC 1.1 was digested with BstE II and the 5'-overhanging ends were filled in using Sequenase 2.0 DNA polymerase. Subsequently, the linearized plasmid pLTC 1.1 was digested with Xba I and a 3.1 kbp restriction fragment was purified on an 1.5% agarose gel. The purified 4244-bp Msc I/Xba I restriction fragment from pPD16.51, containing the complete coding sequence of β-galactosidase, was ligated to the 3.1 kbp BstE II/Xba I fragment from pLTC1.1 to yield the plasmid pBLUE. Plasmid DNA was isolated using Qiagen purification kits and the sequences of all inserts were confirmed by dideoxynucleotide sequencing.

Construction of RNA Expression Plasmid. The plasmid pTRE I was obtained by ligating the purified large 1949-bp Sma I fragment from pmMCAU177 into the purified large 2513-bp Pvu II fragment from pBSIIKS+. The plasmid pTRE2 was obtained by cloning the oligonucleotides **TRET** 5'-pAATTCTTTTTTTTTTTCTTTCTTTTTCTTTTTTTCGAGCT-3' and **TREA** 5'-pCGAAAAAAAGAAAAAGAAAGAAAAAAAAAAAAG-3' into the large EcoR I/Sac I fragment of pTRE I. The plasmid pLARSI was obtained by cloning the 1530-bp Ssp I/Nae I restriction fragment from pSRW21 into the large 4281-bp Ssp I fragment of pTRE 2. Large scale preparation of plasmid DNA were performed using Qiagen purification kits. The sequence of all inserts were confirmed by dideoxynucleotide sequencing.

Strain Construction. The strain MTL-1 Δ(lac-pro) ΔtrpR ara⁻ thi⁻ reca:tn10 (F' 11 lac i^{Q1}pro) was generated by episomal transfer of F'11 from 8117 F'11

Δ(lac-pro) nalA thi⁻ supE (F' 11 lac i^{Q}pro) to CG103 Δ(lac-pro) ΔtrpR ara⁻ thi⁻ reca:tn10 using standard methods (Besse, et al., 1986; Oehler et al., 1990; Miller, 1992). The strain 8117 F'11 was grown to an OD_{600} value of 0.7 in 5 mL of 1X M9 minimal media supplemented with 0.0005% thiamine hydrochloride and 0.2% glycerol (Davis et al., 1980). Likewise, the strain CG 103 was grown to an OD_{600} value of 0.7 in 5 mL of 1X M9 minimal media supplemented with 0.0005% thiamine hydrochloride, 0.2% glycerol, and 15 μg/mL tetracycline. A 1 mL aliqout of each culture was removed and placed in a single 10 mL culture tube. The new culture was incubated without mixing at 37 °C for 2 hours. Afterwards 0.1, 0.01, and 0.001 dilutions of culture were plated on 1X M9 agar plates containing 0.2% glycerol, 0.0005% thiamine hydrocholoride and 15 μg/mL tetracycline. Plates were incubated at 37 °C for 36 hours to allow for the appearance of colonies. Ten candidate colonies were picked and restreaked two times on plates containing same selective media to yield eight individually isolated colonies of MTL-1.

Bacterial Culture and Induction Conditions. The strain MTL-1 was grown in 1X M9 minimal media supplemented with 0.2% glycerol, 0.0005% thiamine hydrochloride, 0.05% casamino acids, and 15 μg/mL tetracycline in a 37 °C incubator shaking at 200 rpm. Cultures were kept well aerated by growing in 0.2 volume of the culture flask capacity with the flask's lid loosely closed. MTL-1/pBLUE and MTL-1/pLARSI were grown under identical conditions as MTL-1 with the addition of either 100 μg/mL ampicillin or 50 μg/mL kanamycin, respectively. MTL-1/pBLUE, pLARSI was grown under identical conditions as MTL-1 with the addition of both 100 μg/mL ampicillin and 50 μg/mL kanamycin. When indicated, cultures were induced by adding a 0.01 volume of 8 mg/mL 3-β-indoleacrylic acid (IAA) in ethanol when the culture

reached an OD_{600} value of 0.7 or repressed by being grown in the presence of 40 μg/mL tryptophan. Additionally, when indicated cultures were induced through the addition of a 0.01 volume of 10 mM isopropyl-β-D-thiogalactopyranoside (IPTG) when the culture reached an OD_{600} value of 0.7.

In Vitro MPE•Fe(II) Footprinting With Labeled Fragments. The 438-bp Afl III-EcoR I restriction fragment of pTER I was 3'-end labeled with deoxyadenosine - [α^{32}P] - triphosphate and chemical sequencing reactions were carried out by standard procedures (Sambrook et al., 1989). Labeled DNA (50,000 cpm) and the indicated concentration of oligonucleotide **RNAY1** were assembled in 20 μL of 1X *E. coli* Buffer (20 mM Tris-Cl pH 7.5, 250 mM KCl, 70 mM NaCl, 4 mM $MgCl_2$), or 1X *E. coli* MagnesiumBuffer (20 mM Tris-Cl pH 7.5, 250 mM KCl, 70 mM NaCl, 40 mM $MgCl_2$), or 1X *E. coli* Reaction Buffer (20 mM Tris-OAc pH 6.8, 250 mM KCl, 70 mM NaCl, 4 mM $MgCl_2$) and equilibrated for 4 hours at 37 °C. A 1 μL volume of freshly prepared 50 mM MPE•Fe(II) solution was added to each solution equilibrated for one minute at 25 °C prior to adding 1 μL of 50 mM DTT. The cleavage reaction proceeded for 15 minutes at 25 °C prior to being quenched by adding 20 μL of 3 M NaOAc pH 4.8, 180 μL of Milli-Q water, and 510 μL of ethanol. The reactions were stored for 15 minutes at -80 °C before microcentrifugation for 20 minutes at 4 °C. The DNA pellet was washed with 500 μL of 70% ethanol before drying under vaccuum and resuspension in 10 μL of Sequenase Stop Buffer (95% formamide, 20 mM EDTA, 0.05% Bromophenol Blue, 0.05% Xylene Cyanol FF). Samples were electrophoresed on 8% denaturing polyacrylamide gels followed by phosphorimager analysis.

In Vitro DMS Footprinting With Labeled Fragments. The 438-bp Afl III-EcoR I restriction fragment of pTER I was 3'-end labeled with deoxyadenosine - [α^{32}P] - triphosphate, and chemical sequencing reactions were carried out by standard procedures (Sambrook et al., 1989). Labeled DNA (50,000 cpm) and the indicated concentration of oligonucleotide **RNAY1** were assembled in 20 µL of 1X *E. coli* Buffer (20 mM Tris-Cl pH 7.5, 250 mM KCl, 70 mM NaCl, 4 mM $MgCl_2$), or 1X *E. coli* MagnesiumBuffer (20 mM Tris-Cl pH 7.5, 250 mM KCl, 70 mM NaCl, 40 mM $MgCl_2$), or 1X *E. coli* Reaction Buffer (20 mM Tris-OAc pH 6.8, 250 mM KCl, 70 mM NaCl, 4 mM $MgCl_2$) and equilibrated for 4 hours at 37 °C. A 4 µL volume of freshly prepared 2% DMS was added and reacted for 15 minutes at 25 °C. Afterwards, 10 µL of DMS Stop Solution was added along with 785 µL of ethanol (Sambrook et al., 1989). The reaction was incubated for 20 minutes at -80 °C, microcentrifuged for 20 minutes at 4 °C, and the resulting DNA pellet was washed with 70% ethanol before being dried under vaccuum. Samples were resuspended in 10 µL of Sequenase Stop Buffer (95% formamide, 20 mM EDTA, 0.05% Bromophenol Blue, 0.05% Xylene Cyanol FF) and electrophoresed on 8% denaturing polyacrylamide gels followed by phosphorimager analysis.

In Vitro DEPC Footprinting With Labeled Fragments. The 438-bp Afl III-EcoR I restriction fragment of pTER I was 3'-end labeled with deoxyadenosine - [α^{32}P] - triphosphate, and chemical sequencing reactions were carried out by standard procedures (Sambrook et al., 1989). Labeled DNA (50,000 cpm) and the indicated concentration of oligonucleotide **RNAY1** were assembled in 20 µL of 1X *E. coli* Buffer (20 mM Tris-Cl pH 7.5, 250 mM KCl, 70 mM NaCl, 4 mM $MgCl_2$), or 1X *E. coli* MagnesiumBuffer (20 mM Tris-Cl pH 7.5, 250 mM KCl, 70 mM NaCl, 40 mM $MgCl_2$), or 1X *E. coli* Reaction Buffer (20 mM Tris-

OAc pH 6.8, 250 mM KCl, 70 mM NaCl, 4 mM $MgCl_2$) and allowed to equilibrate for 4 hours at 37 °C. A 4 µL volume of DEPC was added and reacted for 15 minutes at 25 °C. Afterwards, 10 µL of DMS Stop Solution was added along with 785 µL of ethanol (Sambrook et al., 1989). The reaction was incubated for 20 minutes at -80 °C, microcentrifuged for 20 minutes at 4 °C, and the resulting DNA pellet was washed with 70% ethanol before being dried under vaccuum. Samples were resuspended in 10 µL of Sequenase Stop Buffer (95% formamide, 20 mM EDTA, 0.05% Bromophenol Blue, 0.05% Xylene Cyanol FF) and electrophoresed on 8% denaturing polyacrylamide gels followed by phosphorimager analysis.

RNA Isolation from E. coli Cultures. Total RNA was isolated from *E. coli* cultures according to the method of Summers (Summers, 1970). A 50 mL volume of *E. coli* culture, grown to an OD_{600} of 0.70, was centrifuged at 3,000 rpm at 4 °C for 10 minutes in a JA-20 rotor. The supernatant was carefully removed and the cell pellet was resuspended in 50 mL of Protoplasting Buffer (15 mM Tris-Cl pH 8.0, 0.45 M sucrose, 8 mM EDTA) and 400 µL of 50 mg/mL lysozyme was added. The solution was incubated for 15 minutes at 4 °C prior to centrifugation at 3,000 rpm for 5 minutes at 4 °C. The protoplasts were resuspended in 0.5 mL of Lysis Buffer (30 mM Tris-Cl pH 7.4, 100 mM NaCl, 5 mM EDTA, 1% SDS, 100 mg/mL proteinase K) prior to the addition of 75 µL of DEPC and incubated for 5 minutes at 37 °C. The lystate was chilled on ice and 1.25 mL of saturated NaCl was added. The solution was gently mixed by inversion to produce a substantial precipitate. The mixture was incubated for 10 minutes on ice and centrifuged at 18,000 rpm in a JA-20 rotor for 20 minutes at 4 °C. The supernatant was transferred to a fresh 50 mL centrifuge tube and 5 mL of ice-cold ethanol was added. The solution was

incubated at -20 °C for 8 hours and centrifuged at 18,000 rpm for 20 minutes at 4 °C. The pellet was rinsed twice with 5 mL of ice-cold 70% ethanol and briefly dried through lyophiliztion. The pellet was redissolved in 1 mL of Milli-Q water and stored at -80 °C. The concentration of the isolated RNA was determined by spectoscopic measurments (Sambrook et al., 1989).

Northern Blot Analysis. Approximately 5 μg samples of isolated RNA, resuspended in 25 μL of Sequenase Stop Buffer, were loaded per lane on a denaturing 15% polyacrylamide gel. Samples were electrophoresed and the RNA was transferred from the polyacylamide matirx to a Nytran Nylon Transfer and Immobilization Membrane (Schleicher & Schuell) through a PosiBlot 30-30 Pressure Blotter (Stratagene). After transfer, the RNA was cross-linked to the nylon membrane using a Stratalinker UV Crosslinker (Stratagene). Hybridization steps were done using standard methodology (Sambrook et al., 1989). The membrane was placed in a hybridization bag and covered with 0.2 mL/cm^2 prehybrization/hybridization Buffer (6X SSPE, 5X Denhardt's reagent (0.1% Ficoll, 0.1% polyvinylpyrrolidone, and 0.1% BSA), 0.5% SDS, 100 mg/mL denatured, fragmented salmon sperm DNA) for 2 hours at 42 °C. The prehybridization/hybridization buffer was removed and replaced with fresh prehybridization/hybridization buffer containing 1 X 10^7 cpm of ^{32}P 5'-end labeled oligonucleotide **H1** 5'-AGCTCGAAAAAAAGA AAAAGAAAGAAAAAAAAAAAAGAATT-3'. The hybridization reaction proceeded for 8 hours at 50 °C. After this time, the hybridization/prehybridization solution was removed and replaced with 1 X SSPE, 0.1% SDS for a 20 minute room temperature incubation. The filter was washed twice for 20 minutes at 50 °C with 0.2 X SSPE, 0.1% SDS. The filter was exposed either to X-ray film or subject to phosphorimager analysis.

β–galactosidase Assay. *E. coli* cells were cultured in 1X M9 media supplemented with 0.05% casamino acids as well as the appropriate antibiotics to an OD_{600} of 0.70. Cultures were induced with the addition of 0.01 volume of 10 mM IPTG or 0.01 volume of 8 mg/mL IAA (in ethanol) when indicated. After the indicated incubation period, 0.5 mL of culture were withdrawn and added to 0.5 mL of Z buffer (60 mM $Na_2HPO_4 \bullet 7H_2O$, 40 mM $NaH_2PO_4 \bullet H_20$, 10 mM KCl, 1 mM $MgSO_4 \bullet 7H_2O$, 50 mM β-mercaptoethanol, pH 7.0). Two drops of chloroform and one drop of 0.1% SDS solution was added to each assay mixture. The tubes were vortexed for 10 seconds and placed in a 28 °C heat block for 5 minutes. The reaction was initiated by adding 0.2 mL of ONPG (4 mg/mL in 100 mM phosphate buffer pH 7.0) to each tube followed by a gentle mixing. The reactions were stopped by the addition of 0.5 mL of a 1M Na_2CO_3 solution after a medium yellow color developed or after 8 hours if no yellow color developed. Afterward, OD_{420} readings were taken for each tube. The activity of β-galactosidase was determined as follows:

$$\text{Units of } \beta\text{-galactosidase} = \frac{1000 \times (OD_{420} - 1.75 \times OD_{550})}{(\text{time (min)}) \times (\text{volume of culture used}) \times OD_{600}}$$

Primer Extension Analysis. Primer extension reactions were assembled in a 650 µL microfuge tube by combining 30 µL of reisolated plasmid, 7 µL of dNTP mix (2.5 mM in each dNTP), 7 µL of 10X *Pfu* Polymerase Buffer (20 mM Tris-Cl (pH 8.5), 100 mM $(NH_4)_2SO_4$, 20 mM $MgCl_2$, 1 mg/mL BSA, 1% Triton X-100), the indicated ^{32}P 5'-end-labeled primer (100,000 cpm) , and 1 U

of Pfu DNA polymerase in a 70 µL total volume. Primer **RYP1** 5'-CGACGTTGTAA AACGACGG-3' was used to analyze the 31-bp homopurine tract. A PCR wax gem (Perkin Elmer-Cetus) was placed on top of the reaction and the microfuge tube was placed in a thermocycler. The reactions were subjected to three cycles of primer extension (99 °C denaturation for 1 minute, 68 °C annealing for 1 minute, and 74 °C extension for 2 minutes) after which they were removed from under the wax layer and transferred to a fresh 1.5 mL microfuge tube. To each reaction was added 330 µL of Milli-Q water, 40 µL of 3M NaOAc pH 5.2, and 1 mL of ethanol prior to a 20 minute incubation at -80 °C. The reactions were centrifuged at 4 °C for 20 minutes and the pellets were washed with 70% ethanol. The samples were dried in a Speed-Vac and resuspended in 10 µL of 1X Stop Buffer (1X TAE, 100 mM EDTA, 56% glycerol, 0.2% SDS, and 1% bromophenol blue) prior to storage at -80 °C. The samples were analyzed by electrophoresis on 8% denaturing polyacrylamide gels. Gels were dried and placed on film or photostimulable phosphor imaging plates and quantitated as described (Singleton & Dervan, 1992).

In Vitro Methylation Reaction. *In vitro* methylation reactions were assembled by combining 250 ng of pBLUE, 2 µL of 10X *E. coli* Reaction Buffer (200 mM Tris-Cl pH 7.4, 2.5 M KCl, 700 mM NaCl, 40 mM $MgCl_2$), and 2 µL of a 200 mM solution of the indicated oligonucleotide in a 20 µL total volume. When indicated, 2 µL of 10X Triple Helix Buffer (100 mM NaCl, 1 mM spermine, 25 mM Tris-OAc, pH 6.8) was used in place of 10X *E. coli* Reaction Buffer. A 2 µL volume of a 10% DMS solution was added to the reaction and incubated for four minutes at room temperature. The reaction was terminated by adding 50 µL of DMS stop solution (10 mM β-mercaptoethanol, 10 mM Tris-

Cl pH 8.0) and 750 µL of ethanol. Reactions were incubated on dry ice for 15 minutes prior to microcentrifugation at 4 °C for 20 minutes. Supernatants were discarded and the pellets were washed with 70% ethanol prior to drying in a Speed-Vac. The pellets were resuspended in 80 µL of 10% piperidine and incubated at 90 °C for 30 minutes. The reactions were spun briefly in a microcentrifuge and dried in a Speed-Vac. The pellets were resuspended in 100 µL of Milli-Q water and dried again in a Speed-Vac prior to final resuspension in 10 µL Milli-Q water. Samples were evaluated by primer extension analysis as described above.

DMS In Vivo Footprinting Protocol. A 400 mL *E. coli* cell culture was grown to an OD_{600} reading of 0.7. The culture was transferred to two sterile 250 mL centrifuge bottles and spun in a JA-10 rotor at 2,500 rpm for 10 minutes. The pellet was resuspended in 50 mL of growth media and 14 µL of DMS was added to the culture. The solution was incubated at 37 °C for 5 minutes afterwhich 400 mL of ice cold 0.1 M Phosphate Buffer pH 7.0 was added. The solution was centrifuge in a JA-10 rotor at 2,500 rpm for 10 minutes. The pellet was resuspended in 3 mL of Digestion Buffer (25% sucrose, 50 mM Tris-Cl pH 8.0) and 10 mg of lysozyme was added. The solution was incubated for 5 minutes on ice prior to adding 5 mL of 0.5 M EDTA pH 8.0. Then the solution was incubated for 5 minutes on ice prior to adding 15 mL of Triton Lysis Solution (50 mM Tris-Cl pH 8.0, 10% Triton X-100, 60 mM EDTA). The solution was centrifuged at 18,000 rpm in a JA-20 rotor for 30 minutes at 4 °C. The supernatant was transferred to a fresh 50 mL centrifuge tube and 400 mL of a 5 mg/mL RNase A solution was added and incubated for 30 minutes at 37 °C. Afterwards, 8 mL of 2.55 M KOAc pH 5.5 was added and the solution was centrifuged in a JA-20 for 30 minutes at 18,000 rpm. The

supernatant was loaded onto two separate Qiagen TIP-500 columns, which were preequilibrated with 30 mL each of QBT Buffer. The columns were washed with 25 mL of QC Buffer and the DNA was eluted with 10 mL of QF Buffer per column. The eluates were combined into a single 50-mL centrifuge tube and 25 mL of isopropanol was added along with 5 µL of glycogen. The solution was centrifuged at 18,000 rpm for 30 minutes and the pellet was washed with 5 mL of 70 % ethanol prior to resuspension in 2 mL of Milli-Q water. The sample was extracted twice with an equal volume of phenol : chloroform : isoamyl alcohol (25 : 24 : 1). A 200 µL volume of 3M NaOAc pH 5.5 was added in addition to 5 mL of ethanol. The sample was incubated at -80 °C for 1 hour prior to recentrifugation at 18,000 rpm for 30 minutes. The pellet was washed with 5 mL of 70% ethanol and dried briefly under vacuum. The pellet was reuspended in 0.2 mL of 0.5X TE prior to storage at -80 °C.

RESULTS

Design of an Experimental System to Assay for In Vivo Triple Helix Formation. To examine whether and to what extent oligoribonucleotides can form triple helical complexes *in vivo* with a DNA target site, an experimental system using *E. coli* cell culture was developed (Figure 1). Two plasmids were introduced into an *E. coli* strain one of which overexpressed of a small uridine-rich RNA with other providing a low copy number target site located within a tightly regulated β-galactosidase reporter gene. Since the potential third strand oligoribonucleotide is generated *in situ* difficulties associated with the cellular delivery are circumvented. Triple helix formation was assayed either through *in vivo* footprinting experiments or transcriptional inhibition studies measuring the expression of the β-galactosidase reporter gene.

The plasmid pBLUE was designed to provide a target site for triple helix formation as well as a sensitive assay system for triple helix-mediated transcriptional inhibition studies. This plasmid contains a 31-bp adenine-rich homopurine tract located downstream of a lac promoter expressing a chimeric full length and enzymatically active β-galactosidase gene (figure 2). The effect of overexpressing the uridine-rich oligoribonucleotide on β-galactosidase activity can be easily measured (Miller, 1992). If triple helical complexes form at the target site and can inhibit trancriptional elongation, then it would be expected that β-galactosidase activity would decrease upon induction of RNA expression. This is a low copy number plasmid minimizes the number of triple helical target sites per cell. pBLUE derives a p15A origin of replication from pACYC177 which supports approximately 15-20 copies of the plasmid per cell genome (Martinez et al., 1988). Furthermore, the p15A

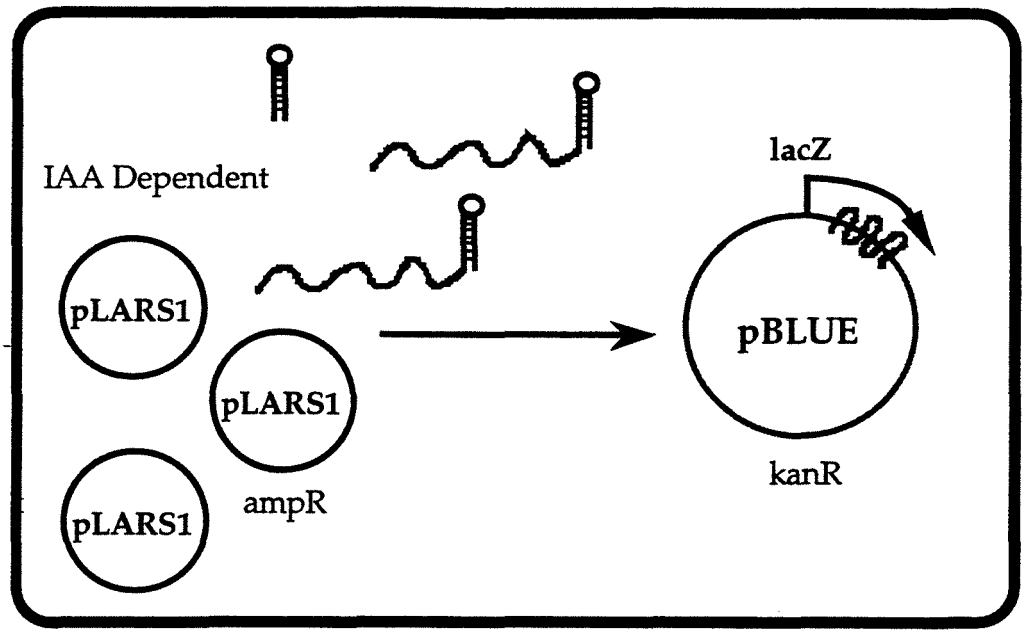

Figure 1. General *in vivo* triple helix experimental design.

origin is compatable with high copy number pUC19-ColE1 origin plasmids, which are necessary for the overexpression of the uridine-rich RNA in this study (Martinez et al., 1988). Finally, this plasmid carries a *kan*^{r} gene which allows for selective growth in the presence of kanamycin.

pLARSI is a high-copy number vector designed to overexpress a small uridine-rich RNA under the control of the *trp* promoter (figure 3). The *trp* promoter was chosen to regulate RNA production because it allows high levels of expression of downstream genes and is regulated independently from the *lac* operon system (Nichols & Yanofsky, 1990; Yansura & Henner, 1990). It can be repressed by supplementing growth media with the aporepressor tryptophan (Warne et al., 1986). Expression is induced by adding 3-β-indoleacrylic acid (IAA) to the culture media. IAA is a tryptophan analog that binds to the Trp repressor protein and inhibits it from binding to the trp operator sequence thus allowing the promoter to become

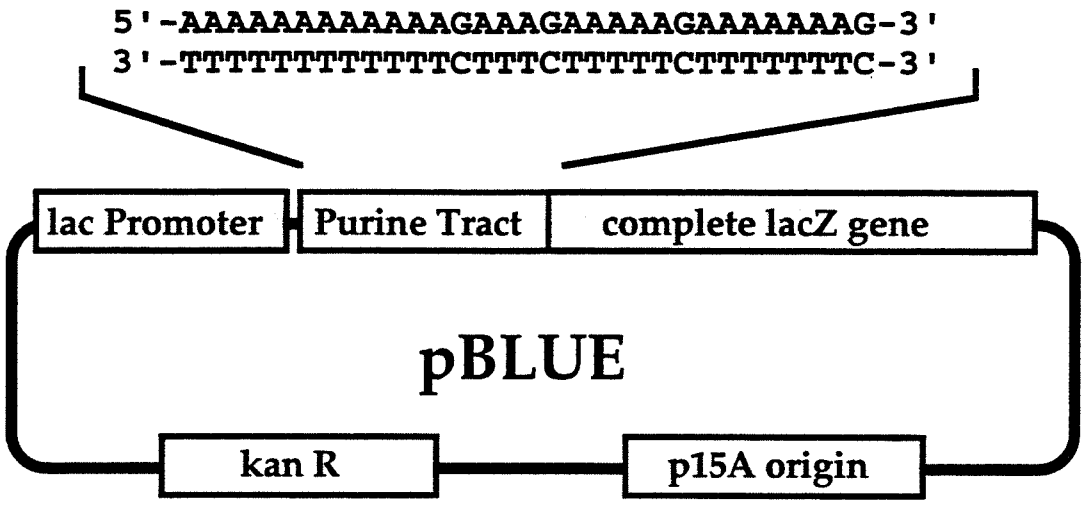

Figure 2. General schematic of the triple helix target plasmid pBLUE.

transcriptionally active. Furthermore it is important that the RNA species is small so that it can bind to the target without steric interference or topological constraints. The transcribed RNA is kept small due to the presence of a strong *rrnC* transcriptional termination sequence downstream of the trp promoter. Such terminators are thought to work through the formation of RNA hairpin structures in the nascent transcript that halt RNA chain elongation (Rosenberg & Court, 1979; von Hippel et al., 1984; Platt et al., 1986; Telesnitsky & Chamberlin, 1989).

The trp promoter system allows one to study of the effect of uridine-richRNA production on the expression of the synthetic *lacZ* reporter gene. Normally the *trp* promoter is tightly regulated by the *trp* repressor protein produced by chromosomal copies of the *trpR* gene. It has been estimated that *E. coli* strains grown in the absence of tryptophan carry approximately 375 Trp repressor dimers per cell giving an intracellular concentration of 850 nM Trp repressor protein (Gunsalas et al., 1986). However, high copy number plasmids, such as the pUC series, carrying the *trp* promoter are not tightly

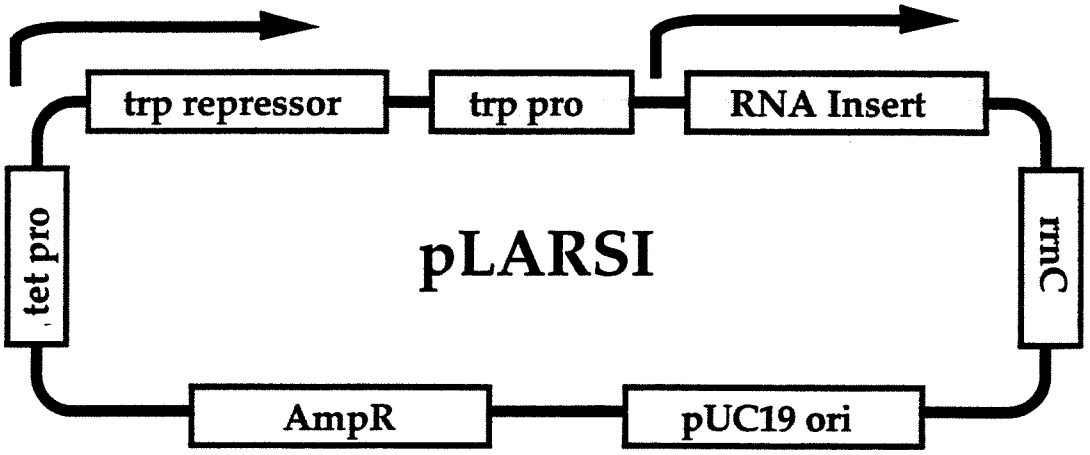

Figure 3. General schematic of the RNA expression vector pLARSI.

regulated due to limiting amounts of cellular Trp repressor protein (Warne et al., 1986; Latta et al., 1990). To circumvent this problem, a copy of the *trpR* gene under the control of a constituative and strong tetracycline promoter was introduced into pLARSI. This provides the high levels of Trp repressor protein in the *E. coli* cell necessary for tight regulation of a *trp* promoter present on a high copy number plasmid (Warne et al., 1986). The Trp repressor protein was expressed under control of the tetracycline promoter because the natural *trpR* gene has an operator similar to the trp operon site to which the Trp repressor protein can bind in the presence of the co-repressor tryptophan to autoregulate its own synthesis (Gunsalas et al., 1979; Gunsalas & Yanofsky, 1979; Bogosian et al., 1984; Paluh & Yanofsky, 1986; Kelley & Yanofsky, 1982). Therefore, it is not possible to overexpress large quanities of the Trp repressor protein in cells by using plasmids carrying the *trpR* gene under the control of its natural promoter (Paluh & Yanofsky, 1986). Finally, this plasmid carries the amp^r gene which allows for selective growth in the presence of ampicillin.

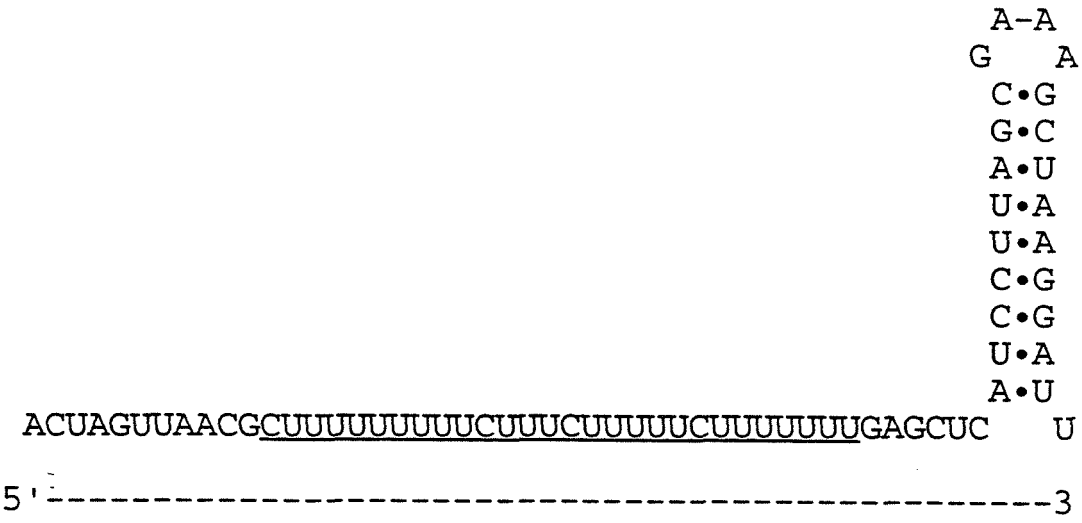

Figure 4: Sequence and potential secondary structure of the 68-nt oligoribonucleotide **RNAY1**. The 31-bp homopyrimidine tract is underlined.

A pyrimidine-rich third strand oligoribonucleotide was chosen for triple helix formation based on the results in Chapter 1. A purine-rich oligoribonucleotide did not have measurable affinity for a DNA target site in contrast to the high affinity displayed by its oligodeoxyribonucleotide counterpart. On the other hand, a pyrimidine-rich oligoribonucleotide had more than ten-fold greater affinity for a target site than its oligodeoxyribonucleotide counterpart. The expected sequence and potential secondary structure of the pyrimidine-rich RNA generated in this study is shown in figure 4. Since phage RNA polymerases have difficulty in transcribing uridine-rich oligoribonucleotides, it was important to consider the maximal amount of contiguous uridines that could be made *in vivo* with high fidelity (Milligan et al., 1987). A uridine-rich RNA species will maximize the amount of stabilizing U•AT triplets in a potential triple helical complex and minimize the amount of pH sensitive rC^+•GC triplets. In the Genbank data base, the *E. coli* papB mRNA was found to contain a string of nine contiguous uridines in its coding region. It is likely that the *E. coli* can

accurately transcribe up to nine contiguous uridines on a DNA template. Furthermore, genetic studies have indicated that *E. coli* can transcribe templates containing up to nine contiguous uridines *in vivo* with high fidelity (Wagner et al., 1990). Only when greater than nine uridines are transcribed does the accuracy of transcription begin to significantly decrease, primilarily through polymerase stuttering on the template. Since the designed RNA contains runs of nine, three, five, and seven uridines, it is likely that *E. coli* transcribe this species with high fidelity *in vivo.*

To maintain high intracellular levels of the uridine-rich oligoribonucleotide, it is important that it is actively transcribed and has a relatively long half-life. While most *E. coli* mRNA species are very unstable with half-lives on the order of one to two minutes others have half-lives of greater than thirty minutes (Newbury et al., 1987; Baga et al., 1988; Melefors & von Gabain, 1988). There are a number of redundent pathways for RNA degradation in *E. coli* (Deutscher et al., 1984; Zaniewski et al., 1984; Deutscher, 1985; Deutscher et al., 1985; Donovan & Kushner, 1986; Ariano et al., 1988; Mackie, 1989; Babitzke & Kushner, 1991). Most degradation is initiated through the action of 3'-exonucleases with endonucleases providing the remainder of cellular nucleolytic activity. There are no reports of 5'-exonuclease activity in the cell (Belasco & Higgins, 1988). Some longer lived mRNA species in *E. coli* are stabilized through the presence of 3'-stem loop structures called repetitive extragenic palidromic (REP) elements (Stern et al., 1984; Newbury et al., 1987; Higgins et al., 1988; Plamann & Stauffer, 1990). These structures may interfere with 3'-endonuclease activity either by presenting a steric blockade or by masking the 3'-end terminus of the RNA species (McLaren et al., 1991). In addition, protein factors may bind to this element and inhibit nuclease degradation. The pyrimidine-rich RNA species

used in this study has a 3'-end stem loop structure that serves as a stabilizing element (figure 1).

The strain MTL-1 was constructed to produce an *E. coli* cell that has a deleted chromosomal *lac* operon but could still tightly control the expression of β-galactosidase reporter gene on a low-copy number plasmid by an overexpressed *lacI* gene (figure 5). Since the chimeric *lacZ* gene on pBLUE serves as a reporter gene to assay the effect of triple helix formation on transcriptional elongation. β-galactosidase protein produced by the chromosomal copy of the *lacZ* gene could create backround signal which complicates experimental interpretation. The overexpression of the lac repressor protein, mediated by the $laci^{QL}$ gene found on an f' episome, prevents leaky expression of the *lacZ* gene in the absence of IPTG inducer (Muller-Hill, 1975). The f' episome is maintained because it allows the cell, with its deleted genomic copy of the proline operon, to grow in the absence of proline. Since this episome provides tight regulation of the lac promoter, the triple helix target site is free from transcribing *E. coli* RNA polymerase under controlled conditions. T7 as well as *E. coli* RNA polymerases can unwind triple helical complexes (Young et al., 1991; Duval-Valentin et al., 1992; Maher, 1992). Therefore a homopurine tract present in a transcriptionally inert region of *E. coli* DNA provides an attractive target site for triple helix formation.

The chromosomal copy of the *trpR* gene was disrupted to prevent confusion associated with the intracellular levels of trp repressor derived from the gene present on the plasmid pLARSI or on the genome. The genomic copy of the *trpR* gene will be subject to autoregulation from the high cellular levels of the Trp repressor protein produced from pLARSI. By eliminating the genomic copy, constant levels of the *trp* repressor may be

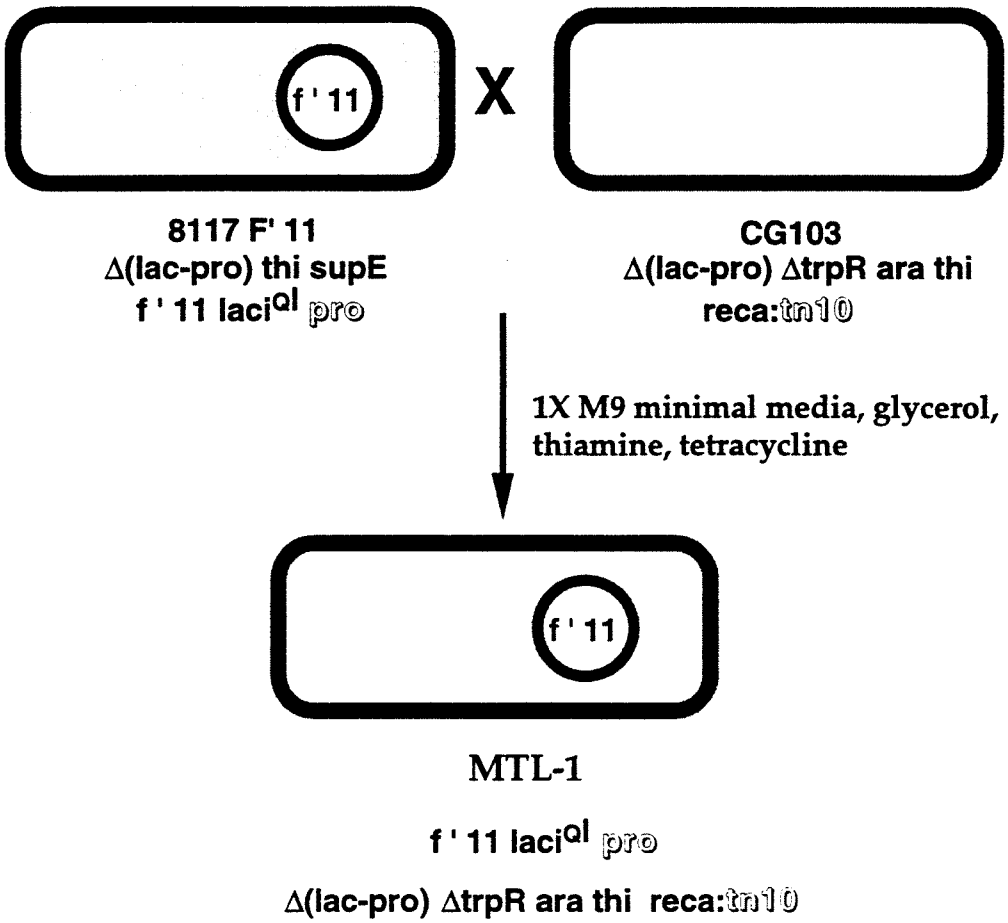

Figure 5. General scheme for the production of *E. coli* host strain MTL-1.

made through the expression of the plasmid copy of the gene. Furthermore, it is necessary for the *recA* gene to be disrupted to prevent recombination between the two plasmids and genomic DNA. This was accomplished by the insertion of the tn10 transposon into the *recA* gene. This insertion is maintained by growing the strain in the presence of tetracycline since the tn10 insertion contains the gene encoding for tetracycline resistance.

In vivo footprinting experiments were chosen as the primary analytical techniques for determining if oligoribonucleotide-directed triple helical complexes formed on plasmid DNA in *E. coli* cells. Previous studies have shown that *E. coli* is amenable to *in vivo* footprinting analysis utilizing a

number of DNA damaging agents such as DMS and $KMnO_4$ (Borowiec & Gralla, 1986; Borowiec et al., 1987; Flashner & Gralla, 1988; Sasse-Dwight & Gralla, 1988; Ohlsen & Gralla, 1992). In this study, dimethyl sulfate was chosen as the *in vivo* footprinting reagent of choice. Dimethyl sulfate agent preferentially methylates N7 of guanine in the major groove of the double helix. Being a small and relatively lipophilc molecule, it readily crosses cell membranes from both prokaryotic and eukaryotic organisms. Triple helix formation protects N7 of guanine from *in vitro* methylation by alkylating agents through the formation of either specific Hoogsteen or reverse Hoogsteen hydrogen bonds. *In vivo* triple helix formation can be detected by determining the protection of specific guanines in the target site from *in vivo* methylation.

Determination of E. coli Physiological Ionic Conditions. The intracellular concentration of sodium and potassium in *E. coli* cells has been estimated to be approximately 70 mM and 250 mM respectively (Castle et al., 1986a; Castle et al 1986b; Richey et al., 1987; Cayley et al., 1991). The intracellular concentration of magnesium has been determined to be approximately 4 mM (Hurwitz & Rosano, 1967; Lusk et al., 1968; Park et al., 1976). Putrescine is the most abundant polyamine with an intracellular concentration of 10 mM, followed by spermidine which is present at 2 mM concentration (Munro et al., 1972). Spermine has not been found to be present in significant level in *E. coli*. The intracellular pH of *E. coli* cells growing logarithically in pH 7.2 media is approximately pH 7.8 (Repaske & Adler, 1981; Zilberstein et al., 1984; Booth, 1985; Krulwich et al., 1985). Intracellular conditions are known to significantly vary from different strains and culture conditions. However,

these reports provide guidance for modeling an *in vitro* binding assay that approximates the *in vivo E. coli* intracellular ionic environment.

In Vitro Footprinting of the Homopurine Tract Under Physiological Ionic Conditions. To determine the approximate affinity of the overexpressed uridine-rich RNA being overexpressed in *E. coli* for the triple helix target site, a number of *in vitro* footprinting experiments using different footprinting reagents were conducted. Figure 6 shows the results of such experiments using MPE•Fe(II), DMS, and DEPC as footprinting reagents. A restriction fragment derived from pTER I which carries a 31-bp homopurine tract identical to the one found on pBLUE was used for analysis. This plasmid is more easily available in larger quantities than pBLUE due to its high-copy number. Lanes 2-7 depict MPE•Fe(II) footprinting analysis of the target site. Under *E. coli* physiological salt conditions, oligoribonucleotide **RNAY1** does not occupy the target site (compare lanes 2 and 3). Making the hybridization conditions less stringent either by increasing magnesium concentrations or lowering the pH did not rescue binding to the target site (compare lanes 4 and 5 and also lanes 6 and 7). Similar results were obtained using DMS as a footprinting reagent. Under physiological conditions (lanes 9 and 10) or less stringent hybridization conditions (lanes 11-14), there is no oligoribonucleotide-dependent protection of the guanines in the target site. Finally, DEPC was used as an *in vitro* footprinting agent based on a report by Helene and co-workers which indicated that triple helix formation may induce DEPC hypersensitive sites at the 3'-end junction of the complex (Collier et al., 1991). Lanes 16-21 show that under a variety of hybridization conditions, no hypersensitivities associated with triple helix formation are evident. Oligoribonucleotide **RNAY1** does not appear to have appreciable

affinity for the target site under physiological ionic conditions.

Overexpression of a Small Uridine-Rich Oligoribonucleotide In Vivo. The overexpression of the small uridine-rich RNA upon IAA induction is demonstrated through Northern Blot analysis (Figure 3). Lanes 2-6 show *in vitro* synthesized **RNAY1** loaded in four different concentrations. The chemically synthesized RNA is an intact single species and the amount of radioactive signal generated in each lane is proportional to the molar amount of oligoribonucleotide loaded. These lanes serve as standards to quantitate the amount of uridine-rich RNA generated *in vivo*. Lane 1 contains total RNA isolated from MTL-1/pBLUE, pLARSI cultures grown with tryptophan repression. As expected, there are very low levels of uridine-rich RNA of the appropriate size under these conditions. Lane 7 shows total RNA isolated from MTL-1/pBLUE after IAA induction. Predictably, there is no detectable levels of uridine-rich RNA. Lanes 8 and 9 contain total RNA isolated from MTL-1/pBLUE, pLARSI cultures at either 2, or 4 hours after IAA induction, respectively. This demonstrates the presence of a small RNA of approximately the expected molecular weight. The equivalent signals generated 2 and 4 hours after induction of the trp promoter signifies that the RNA is fully induced at the 2 hour time point and remains at high intracellular levels for several hours. Comparing the signals in lane 7 and 8 to that in lane 1 indicates that there is an approximately 250-fold induction in the level of uridine-rich RNA upon IAA stimulation. The trp promoter present of pLARSI is tightly regulated by the overexpressed Trp repressor protein. Furthermore, by comparing the amount of signal generated in lanes 7 and 8 with the signal generated in the standard lanes 2-5, the total intracellular concentration of the uridine-rich RNA can be approximated.

Figure 6: Autoradiogram of an 8% denaturing polyacrylamide gel showing results of *in vitro* footprinting reactions performed on the 438-bp Afl III-EcoR I restriction fragment of pTER I. Lanes 1, 8, and 15, A + G specific chemical sequencing lanes; Lanes 2 and 3, MPE•Fe(II) footprinting reactions performed in 1X *E. coli* Buffer in the absence or presence of 5 μM **RNAY1**, respectively. Lanes 4 and 5, MPE•Fe(II) footprinting reactions performed in 1X *E. coli* Magnesium Buffer in the absence or presence of 5 μM **RNAY1**, respectively. Lanes 6 and 7, MPE•Fe(II) footprinting reactions performed in 1X *E. coli* pH6.8 Buffer in the absence or presence of 5 μM **RNAY1**, respectively. Lanes 9 and 10, DMS footprinting reactions performed in 1X *E. coli* Buffer in the absence or presence of 5 μM **RNAY1**, respectively. Lanes 11 and 12, DMS footprinting reactions performed in 1X *E. coli* Magnesium Buffer in the absence or presence of 5 μM **RNAY1**, respectively. Lanes 13 and 14, DMS footprinting reactions performed in 1X *E. coli* pH 6.8 Buffer in the absence or presence of 5 μM **RNAY1**, respectively. Lanes 16 and 17, DEPC footprinting reactions performed in 1X *E. coli Buffe*r in the absence or presence of 5 μM **RNAY1**, respectively. Lanes 18 and 19, DEPC footprinting reactions performed in 1X *E. coli Buffe*r in the absence or presence of 5 μM **RNAY1**, respectively. Lanes 20 and 21, DEPC footprinting reactions performed in 1X *E. coli* pH 6.8 Buffer in the absence or presence of 5 μM **RNAY1**, respectively.

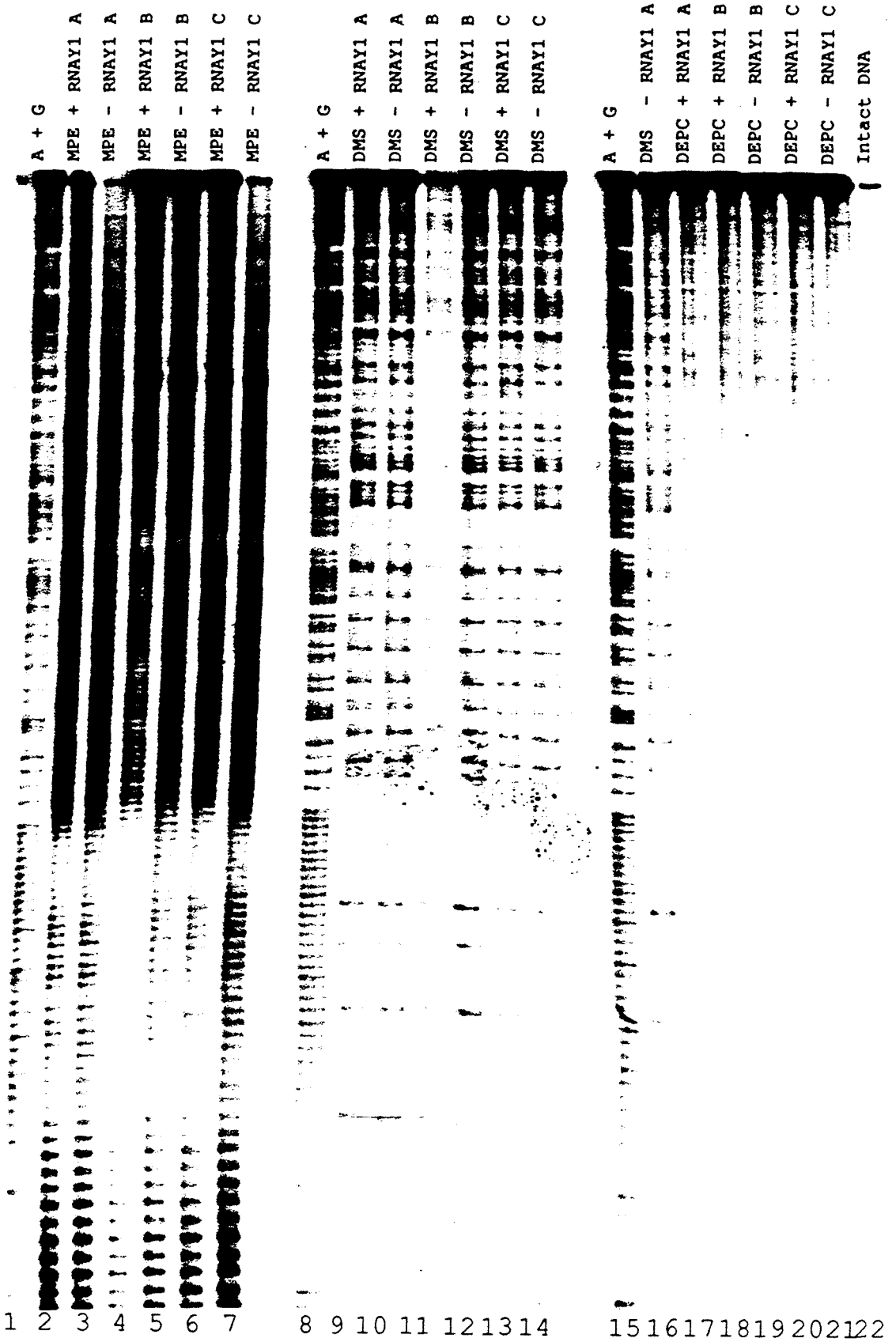
A + G
MPE + RNAY1 A
MPE - RNAY1 A
MPE + RNAY1 B
MPE - RNAY1 B
MPE + RNAY1 C
MPE - RNAY1 C
A + G
DMS + RNAY1 A
DMS - RNAY1 A
DMS + RNAY1 B
DMS - RNAY1 B
DMS + RNAY1 C
DMS - RNAY1 C
A + G
DMS - RNAY1 A
DEPC + RNAY1 A
DEPC + RNAY1 B
DEPC - RNAY1 B
DEPC + RNAY1 C
DEPC - RNAY1 C
Intact DNA
1 2 3 4 5 6 7 8 9 10 11 12 13 14 15 16 17 18 19 20 21 22

Phosphorimager analysis indicated that there is approximately 400 fmoles of isolated oligoribonucleotide in lanes 7 and 8 respectively. This amount of RNA was isolated from 8 X 10^7 cells, given that an OD_{600} reading of 0.7 indicates a concentration of 3.5 X 10^8 cells/mL culture, to yield a ratio of 5 X 10^{-21} moles (or 3,000 molecules) of RNA per bacterium . Since the volume of an *E. coli* cell is approximately 1 X 10^{-15} L, the approximate concentration of the uridine-rich RNA per cell is 5 μM after IAA induction. Prior to this induction, there is a 50 nM uridine-rich RNA intracellular concentration. These are conservative estimates of the intracellular concentration since it is assumed that there is complete recovery of the uridine-rich RNA from *E. coli* cultures.

Effect of Oligoribonucleotide Overexpression on the β–galactosidase Reporter Gene. Table 1 lists the results of experiments measuring the effect of inducing oligoribonucleotide **RNAY1** expression on β-galactosidase expression. In all cases, in the absence of IPTG induction, there is virtually no detectable production of β-galactosidase protein. This demonstrates that the lac promoter is tightly regulated by the excess lac repressor protein present in MTL-1 due to the f'11 $lacI^{QL}$ gene. When the hybrid *lacZ* gene is induced, pretreatment with either tryptophan or IAA does not significantly alter the amount of active β-galactosidase produced. This shows that overexpression of the uridine-rich RNA has no effect on reporter gene expression.

In Vivo Footprinting of Triple Helical Target Sites in the Presence of a Pyrimidine-Rich Oligoribonucleotide. Figure 8 shows the results of DMS *in vivo* footprinting experiments examining the effect of overexpressing a small uridine-rich oligoribonucleotide on *in vivo* triple helix formation. Lane 1

Figure 7: Autoradiogram showing results of northern blot analysis of RNA isolated from cultures of MTL-1/pBLUE and MTL-1/pBLUE, pLARSI. In these cases, approximately 5 µg of total RNA isolated from bacterial cultures were electrophoresed on a 15% denaturing polyacrylamide gel and transferred to Nytran Nylon Transfer and Immobilization Membrane. The membrane was probed with 5'-end labeled oligonucleotide **H1** as described. Lane 1, total RNA isolated from MTL-1/pBLUE, pLARSI with tryptophan repression; Lane 2, total RNA isolated from MTL-1/pBlue with IAA induction supplemented with 100 fmoles of **RNAY1**; Lane 3, total RNA isolated from MTL-1/pBlue with IAA induction supplemented with 75 fmoles of **RNAY1**; Lane 4, total RNA isolated from MTL-1/pBlue with IAA induction supplemented with 50 fmoles of **RNAY1**; Lane 5, total RNA isolated from MTL-1/pBlue with IAA induction supplemented with 25 fmoles of **RNAY1**; Lane 6, total RNA isolated from MTL-1/pBlue with IAA induction supplemented with 25 fmoles of **RNAY1**; Lane 7, total RNA isolated from MTL-1/pBlue with IAA induction; Lane 8, total RNA isolated from MTL-1/pBLUE, pLARSI 2 hours after IAA induction; Lane 9, total RNA isolated from MTL-1/pBLUE, pLARSI 4 hours after IAA induction.

IAA	-	+	+	+	+	+	+	+	+
trp	+	-	-	-	-	-	-	-	-
pLARSI	+	-	-	-	-	-	-	+	+
pBLUE	+	+	+	+	+	+	+	+	+
RNAY1	-	+	+	+	+	+	-	-	-

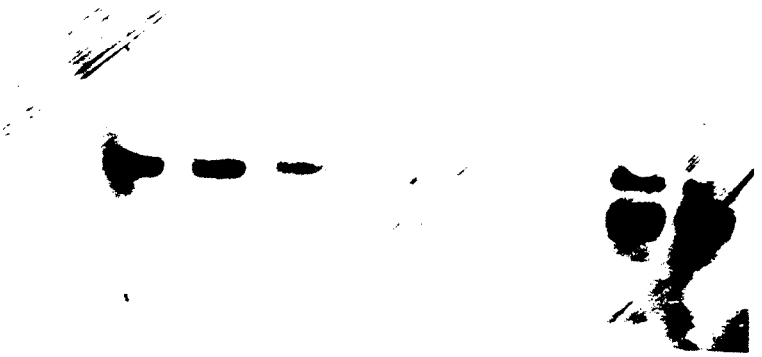

1 2 3 4 5 6 7 8 9

Table 1: Effect of RNA induction on β-galactosidase activity[a]

Strain	IAA	Trp	IPTG	Units
MTL-1/pBLUE	-	+	-	1 (± 1)
MTL-1/pBLUE	+	-	-	1 (± 1)
MTL-1/pBLUE	-	+	+	256 (± 8)
MTL-1/pBLUE	+	-	+	261 (± 7)
MTL-1/pBLUE, pLARSI	-	+	-	1 (± 1)
MTL-1/pBLUE,pLARSI	+	-	-	1 (± 1)
MTL-1/pBLUE, pLARSI	-	+	+	249 (± 9)
MTL-1/pBLUE, pLARSI	+	-	+	252 (± 7)

[a]Values reported in the table are mean values measured from three repetitions of β-galactosidase activity experiments. + IAA indicates the addition of 80 μg/mL 3-β-indoleacrylic acid three hours prior to activity measurement. + IPTG indicates the addition of 100 μM isopropyl-β-D-thiogalactopyranoside one hour prior to activity measurement. Units indicates β-galactosidase activity reported in Miller units.

depicts primer extension analysis of *in vitro* methylation in the absence of oligoribonucleotide **RNAY1**. Lanes 2 and 3 depict *in vitro* methylation of the target site pBLUE in the presence of 5 μM **RNAY1** under physiological conditions (lane 2) or permissive hybridization conditions (lane 3). Oligoribonucleotide **RNAY1** binds tightly to the target site under permissive conditions but does not occupy the target site under stringent conditions. This result is in good agreement with the results presented in figure 6. Lane 4 depicts the *in vivo* methylation pattern of pBLUE present in MTL-1/pBLUE. Lane 5 shows the methylation pattern of pBLUE present in MTL-1/pBLUE, pLARSI with tryptophan repression. Lanes 6 and 7 depict the methylation

pattern of pBLUE present in MTL-1/pBLUE, pLARS I, 2 and 4 hours after induction with IAA. In all cases, the presence of pLARSI, regardless if the culture is induced or not induced by IAA, does not alter the methylation pattern of the guanines present in the triple helix target site. It does not appear likely that the oligoribonucleotide **RNAY1** forms *in vivo* triple helical complexes with its cognate binding site present on pBLUE.

Figure 8: Autoradiogram of an 8% denaturing polyacrylamide gel showing results of *in vivo* footprinting reactions on *E. coli* strain MTL-1/pBLUE, pLars 1. When indicated, cultures were induced by adding 4 mL of 5 mg/mL 3-β-indoleacrylic acid to 400 mL of culture media. All samples were generated through primer extension reactions on reisolated pBLUE using 5'-end labeled primer **RYP1**. Lane 1, *in vitro* DMS footprinting reaction in 1X *E. coli* Buffer; lane 2, *in vitro* DMS footprinting reaction with 5 μM **RNAY1** in 1X *E. coli* Buffer; lane 3, *in vitro* DMS footprinting reaction with 5 μM **RNAY1** in 1X Triple Helix Buffer; lane 4, *in vivo* DMS footprinting reaction with MTL-1/pBLUE with IAA induction; lane 5, *in vivo* DMS footprinting reaction with MTL-1/pBLUE, pLARSI with tryptophan repression; lane 6, *in vivo* footprinting reaction with MTL-1/pBLUE, pLARSI 2 hours after IAA induction; lane 7, *in vivo* DMS footprinting reaction with MTL-1/pBLUE, pLARSI 4 hours after IAA induction.

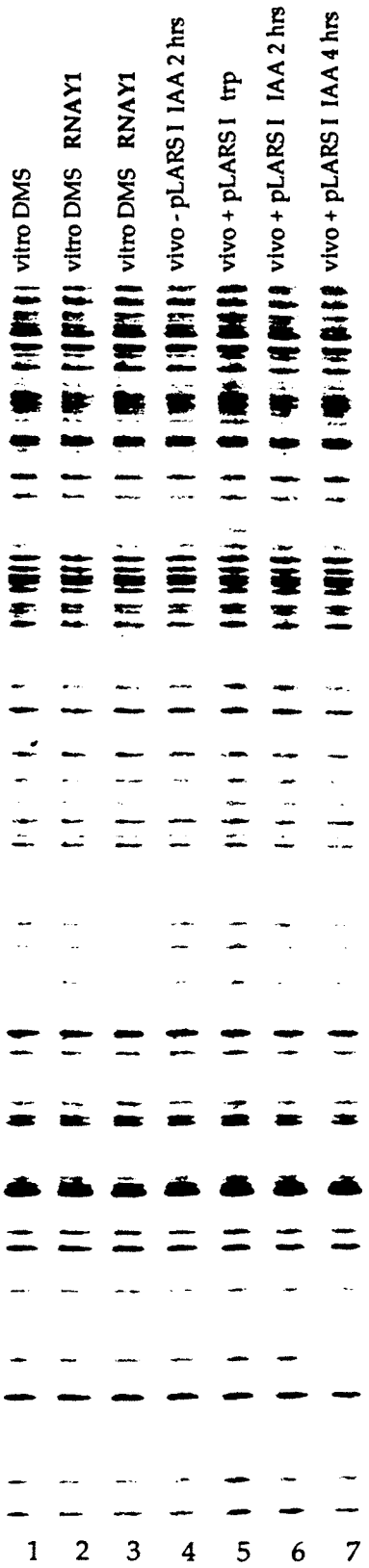
vitro DMS
vitro DMS RNAY1
vitro DMS RNAY1
vivo - pLARS I IAA 2 hrs
vivo + pLARS I trp
vivo + pLARS I IAA 2 hrs
vivo + pLARS I IAA 4 hrs
1 2 3 4 5 6 7

DISCUSSION

We have found that overexpression of a small uridine-rich oligoribonucleotide, which can form a triple helical complex with double helical DNA *in vitro* under nonstringent conditions, in *E. coli* cells does not promote triple helix formation *in vivo* with its cognate homopurine tract. *In vivo* DMS footprinting analysis shows that the presence of micromolar concentrations of this intact small RNA does not cause protection of specific guanines in the target site from *in vivo* methylation. Attempts to assay the effect of *in vivo* triple helix formation on transcriptional elongation by *E. coli* RNA polymerase were hindered by the fact that these complexes were not forming.

Speculation on Possible Biological Roles of RNA-Directed Triple Helical Complexes. A number of arguments for potential biological roles of three stranded complexes composed of an RNA third strand binding to genomic DNA have been made. Early studies on the molecular basis of gene regulation lead Jacob and Monod to speculate that the lac repressor was a ribonucleoprotein which recognized its lac operator binding site through Watson-Crick hydrogen bonding interactions (Jacob & Monod, 1961). This model was modified by Miller and Sobell who proposed that the lac repressor was a ribonucleoprotein which bound to its operator sequence through triple helix formation (Miller & Sobell, 1966). The putative oligoribonucleotide portion of the lac repressor bound in the major groove of the duplex DNA through the formation of U•AT and rC^{+}•GC base triplets. The authors surmised that these interactions allowed for high selectivity of target site recognition and thus would be useful for gene regulation.

Britten and Davidson proposed a model of higher cell gene regulation involving activator RNA species which could form sequence-specific complexes with double helical DNA (Britten & Davidson, 1969). Although the molecular basis of this interaction was not commented upon, the role of distinct activator RNA species was to bind to genomic DNA and activate transcription of downstream genes normally repressed due to histone interactions. Despite the fact that further experimentation has shown that the activator role is played by DNA binding proteins, the theory still has evolutionary implications for gene regulation in a putative RNA world.

Minton speculated that RNA directed triple helix formation may preferentially serve a role in the modulation of eukaryotic rather than prokaryotic gene expression (Minton, 1985). He surmised that prokaryotic systems may be biased against RNA directed triple helix fomation since the rapidity of protein production and convenient site of synthesis (essentially on the DNA itself) predisposes itself to short and reliable feedback mechanisms. Minton reasoned that the lengthy processes of eukaryotic RNA processing, export into the cytoplasm, translation, and reimport of proteins back into the nucleus may bias the cell towards directly using RNA as a transcriptional regulatory molecule. He proposed that transcriptional termination of eukaryotic RNA polymerase II and III elongation may involve triple helix formation at homopurine tracts. It was proposed that RNA-directed triple helix formation may inhibit transcription factors from binding to DNA or translocating in critical promoter regions.

Recent studies have implicated ribonucleoproteins as transcription factors in eukaryotic cells. Kinniburgh and co-workers have shown that a ribonucleoprotein binds to the c-*myc NSE* (nuclease-sensitive element) (Davis et al., 1989). It was hypothesized that the ribonucleoprotein as well as other

protein that can bind to the NSE may not act as traditional transcription factors but rather as topology-altering factors that allow alternative forms of transcriptional promotion. Another study implicated a ribonucleoprotein in the negative regulation of the erythropoietin gene (Beru et al., 1990). Finally, Sprague and co-workers proposed the existence of a class III transcription factor that was composed of RNA (Young et al., 1991). In all these cases, the role of the RNA component of the ribonucleoprotein complex is unclear. However, it is possible that the RNA may be involved in the recognition of double-helical DNA through the formation of base triplets. Further experimentation is necessary to discriminate between this model and the multitude of others in which RNA components may be involved.

Possible Reasons for the Inability to Form RNA-Directed Triple Helical Complexes In Vivo. There are a significant number of reasons why the oligoribonucleotide generated in this study is unable to bind to the plasmid present in *E. coli.* Although Northern blot analysis showed that micromolar levels of intact uridine-rich RNA are produced in this system, it is not clear how much of the oligoribonucleotide is free to hybridize and not bound by intracellular components, such as proteins or other nucleic acids. The effective concentration of free oligoribonucleotide may be substantially lower than the amount detected by Northern blot analysis. There have been a number of reports suggesting that *E. coli* may contain a number of polyadenylated RNA species (Gopalakrishna et al., 1981; Karnik et al., 1987; Cao & Sarkar, 1992). If these substantial cellular levels of these species do exist, then they could competitively hybridize with the overexpressed uridine-rich RNA to inhibit triple helix formation.

The oligoribonucleotide may not interact with the plasmid target site due to improper intracellular localization. If the uridine-rich RNA species is sequestered away from the plasmid DNA then its effective concentration would be substantially lower. This is less likely to occur in a prokaryotic cell due to the lesser amount of intracellular compartmentalization, such as the lack of a nucleus, compared to a eukaryotic cell. Since transcriptional and translational machinery are coupled near the genomic and episomal DNA in prokaryotic cells, it is reasonable to assume that the newly transcribed uridine-rich RNA should have significant access to the target site.

Triple helical complexes may be disrupted by intracellular repair machinery or by polymerases that unwind the three-stranded structures as they track along the helix. Although oligodeoxyribonucleotide-directed triple helix formation can inhibit Klenow fragment DNA polymerase mediated strand displacement DNA synthesis at the identical homopurine tract, there is no evidence that triple helical structures can inhibit DNA synthesis by the intact replication machinery (Hacia et al., 1994). Purified DNA helicases can effectively unwind triple helical complexes (Maine & Kodadek, 1994). Furthermore, intermolecular triple helices have either no blocking effect or minimal ones on transcriptional elongation (Young et al., 1991; Maher, 1992; Duval-Valentin et al., 1992). Triple helices do not appear to be very effective in blocking elongation by either prokaryotic or eukaryotic RNA polymerases, and this may reflect the fact that these polymerases are multiprotein holoenzyme complexes replete with DNA melting and helicase activities (Lewin, 1990). Finally, it is possible that multistranded complexes may be sensed as potential genetic lesions subject to repair mechanisms. However, intramolecular H-form DNA triple helical structures can form on plasmid DNA inside *E. coli* cells (Kohwi et al., 1992; Ussery & Sinden, 1993). Although

they are structurally different from intermolecular triple helical complexes, this indicates that some triple helical structures may be stable in *E. coli.*

Finally, it is possible that the target site is no longer accessible to oligonucleotide hybridization since it is coated with DNA binding proteins. It has not been clearly demonstrated that oligonucleotides can bind to sequences packaged into higher order structures. They may not bind due to steric blockade or by dramatically slowing the kinetics of the search process by which the oligonucleotide locates its target site. It is known that plasmids carried in *E. coli* become coated with a number of different DNA binding proteins such as the HU protein (Berthold & Geider, 1976; Rouviere-Yaniv et al., 1979; Broyles & Pettijohn, 1986). The HU protein is a heterotypic dimer composed of the closely related HUα and HUβ subunits. It can package DNA into nucleosome-like structures and is the primary protein constituent associated with the bacterial chromosome (Varshavsky et al., 1977; Rouviere-Yaniv et al., 1978; Mensa-Wilmot et al., 1989; Shellman & Pettijohn, 1991).

BIBLIOGRAPHY

Arraiano, C. M., Yancey, S. D., & Kushner, S. R. (1988) *J. Bact. 170*, 4625-4633.

Babitzke, P., & Kushner, S. R. (1991) *Proc. Natl. Acad. Sci. U. S. A. 88*, 1-5.

Baga, M., Goransson, M., Normark, S., & Uhlin, B. E. (1988) *Cell 52*, 197-206.

Belasco, J. G., & Higgins, C. F. (1988) *Gene 72*, 15-23.

Berthold, V., & Geider, K. (1976) *Eur. J. Biochem. 71*, 443-449.

Beru, N., Smith, D., & Goldwasser, E. (1990) *J. Biol. Chem. 265*, 14100-14104.

Besse, M., von Wilcken-Bergmann, & Muller-Hill, B. (1986) *EMBO J. 5*, 1377-1381.

Bogosian, G., Somerville, R. L., Nishi, K., Kano, Y., & Imamoto, F. (1984) *Mol. Gen. Gent. 193*, 244-250.

Booth, I. R. (1985) *Microbiol. Rev. 49*, 359-378.

Borowiec, J. A., & Gralla, J. D. (1986) *Biochemistry 25*, 5051-5057.

Borowiec, J. A., Zhang, L., Sasse-Dwight, S., & Gralla, J. D. (1987) *J. Mol. Biol. 196*, 101-111.

Britten, R. J., & Davidson, E. H. (1969) *Science 165*, 349-357.

Breyles, S. S., & Pettijohn, D. E. (1986) *J. Mol. Biol. 187*, 47-60.

Cao, G.-J., & Srakar, N. (1992) *Proc. Natl. Acad. U. S. A. 89*, 7546-7550.

Castle, A. M., Macnab, R. M., & Shulman, R. G. (1986) *J. Biol. Chem. 261*, 3288-3294.

Castle, A. M., & Macnab, R. M., & Shulman, R. G. (1986) *J. Biol. Chem. 261*, 7797-7806.

Cayley, S., Lewis, B. A., Guttman, H. J., Record, M. T. (1991) *J. Mol. Biol. 222*, 281-300.

Collier, D. A., Mergny, J. L., Thuong, N. T., & Helene, C. (1991) *Nucleic Acids Res. 19*, 4219-4224.

Davis, T. L., Firulli, A. B., & Kinniburgh, A. J. (1989) *Proc. Natl. Acad. Sci. U. S. A. 86*, 9682-9686.

Davis, R. W., Botstein, D., & Roth, J. R. (1980) *Advanced Bacterial Genetics*, Cold Spring Harbor Laboratory, Cold Spring Harbor, New York.

Deutscher, M. P. (1985) *Cell 40*, 731-732.

Deutscher, M. P., Marlor, C. W., & Zaniewski, R. (1984) *Proc. Natl. Acad. Sci. U. S. A. 81*, 4290-4293.

Deutscher, M. P., Marlor, C. W., & Zaniewski, R. (1985) *Proc. Natl. Acad. Sci. U. S. A. 82*, 6427-6430.

Donovan, W. P., & Kushner, S. R. (1986) *Proc. Natl. Acad. Sci. U. S. A. 83*, 120-124.

Duval-Valentin, G., Thuong, N. T., & Helene, C. (1992) *Proc. Natl. Acad. Sci. U. S. A. 89*, 504-508.

Escude, C., Francois, J.-C., Sun, J.-S., Ott, G., Sprinzl, M., Garestier, T., & Helene, C. (1993) *Nucleic Acids Res. 21*, 5547-5553.

Flashner, Y., & Gralla, J. D. (1988) *Proc. Natl. Acad. U. S. A. 85*, 8968-8972.

Gopalakrishna, Y., Langley, D., & Sarkar, N. (1981) *Nucleic Acids Res. 9*, 3545-3554.

Gunsalus, R. P., Miguel, A, G., & Gunsalus, G. L. (1986) *J. Bact. 167*, 272-278.

Gunsalas, R. P., & Yanofsky, C. (1979) *Proc. Natl. Acad. Sci. U. S. A. 77*, 7117-7121.

Gunsalas, R. P., Zurawski, G., & Yanofsky, C. (1979) *J. Bact. 140*, 106-113.

Guyer, C. A., Morgan, D. G., & Staros, J. V. (1986) *J. Bact. 168*, 775-779.

Hacia, J. G., Dervan, P. B., & Wold, B. J. (1994) *Biochemistry 33*, 6192-6200.

Han, H. & Dervan, P. B. (1993) *Proc. Natl. Acad. Sci. 90*, 3806-3810.

Higgins, C. F., McLaren, R. S., & Newbury, S. F. (1988) *Gene 72*, 3-14.

Hurwitz, C., & Rosano, C. L. (1967) *J. Biol. Chem. 242*, 3719-3722.

Jacob, F., & Monod, J. (1961) *J. Mol. Biol. 3*, 318-356.

Karnik, P., Taljanidisz, J., Sasvari-Szakely, M., & Sarkar, N. (1987) *J. Mol. Biol. 196*, 347-354.

Kelley, R. L., & Yanofsky, C. (1982) *Proc. Natl. Acad. Sci. U. S. A. 79*, 3120-3124.

Kohwi, Y., Malkhosyan, S. R., Kohwi-Shigamatsu, T. (1992) *J. Mol. Biol. 223*, 817-822.

Krulwich, T. A., Agus, R., Schneier, M., & Guffanti, A. A. (1985) *J. Bact. 162*, 768-772.

Latta, M., Philit, M., Maury, I., Soubrier, F., Denefle, P., Mayaux, J.-F. (1990) *DNA Cell Biol. 9*, 129-137.

Lee, J. S., & Morgan, A. R. (1982) *Can. J. Biochem. 60*, 952-961.

Lewin, B. (1990) *Genes IV*, Oxford University Press, New York.

Lusk, J. E., Williams, R. J. P., & Kennedy, E. P. (1968) *J. Biol. Chem. 243*, 2618-2624.

Mackie, G. A. (1989) *J. Bact. 171*, 4112-4120.

Maher, L. J. (1992) *Biochemistry 31*, 7587-7594.

Maher, L. J., III, Dervan, P. B., & Wold, B. J. (1990) *Biochemistry 29*, 8820-8826.

Maher, L. J., III, Dervan, P. B., & Wold, B. (1992) *Biochemistry 31* 70-81.

Maine, I. P., & Kodadek, T. (1994) *Biochem. Biophys. Res. Comm. 204*, 1119-1124.

Martinez, E., Bartolome, B., & de la Cruz, F. (1988) *Gene 68*, 159-162.

McLaren, R. S., Newbury, S. F., Dance, G. S. C., Causton, H. C., & Higgins, C. F. (1991) *J. Mol. Biol. 221*, 81-95.

Melefors, O., & von Gabain. A. (1988) *Cell 52*, 893-901.

Mensa-Wilmot, K., Carroll, K., & McMacken, R. (1989) *EMBO J. 8*, 2393-2402.

Miller, J. H. (1992) *A Short Course in Bacterial Genetics*, Cold Spring Harbor Laboratory Press, Cold Spring Harbor, NY.

Miller, J. H. & Sobell, H. M. (1966) *Proc. Natl. Acad. Sci. U. S. A. 55*, 1201-1205.

Milligan, J. F., Groebe, D. R., Witherell, G. W., & Uhlenbeck, O. C. (1987) *Nucleic Acids Res. 15*, 8783-8798.

Minton, K. W. (1985) *J. Exptl. Path. 2*, 135-148.

Muller-Hill, B. (1975) *Prog. Biophys. Molec. Biol. 30*, 227-252.

Munro, G. F., Hercules, K., Morgan, J., & Sauerbier, W. (1972) *J. Biol. Chem. 247*, 1272-1280.

Newbury, S. F., Smith, N. H., Robinson, E. C., Hiles, I. D., & Higgins, C. F. (1987) *Cell 48*, 297-310.

Nichols, B. P., & Yanofsky, C. (1983) in *Methods in Enzymology 101*, pp. 155-164, Academic Press.

Oehler, S., Eismann, E. R., Kramer, H., & Muller-Hill, B. (1990) *EMBO J. 9*, 973-979.

Ohlsen, K. L., & Gralla, J. D. (1992) *J. Bact. 174*, 6071-6075.

Paluh, J. L., & Yanofsky, C. (1986) *Nucleic Acids Res. 14*, 7851-7860.

Park, M. H., Wong, B. B., Lusk, J. E. (1976) *J. Bact. 126*, 1096-1103.

Plamann, M. D., & Stauffer, G. V. (1990) *Mol. Gen. Genet. 220*, 301-306.

Platt, T. (1986) *Annu. Rev. Biochem. 55*, 339-372.

Repaske, D. R., & Adler, J. (1981) *J. Bact. 145*, 1196-1208.

Richey, B., Cayley, D. S., Mossing, M. C., Kolka, C., Anderson, C. F., Farrar, T. C., Record, M. T. (1987) *J. Biol. Chem. 262*, 7157-7164.

Roberts, J. W. (1993) *Cell 72*, 653-655.

Roberts, R. W., & Crothers, D. M. (1992) *Science 258*, 1463-1466.

Rosenberg, M., & Court, D. (1979) *Ann. Rev. Genet. 13*, 319-353.

Rouviere-Yaniv, J. (1978) *Cold Spring Harbor Symp. Quant. Biol. 421*, 439-447.

Rouviere-Yaniv, J., Yaniv, M., & Germond, J. E. (1979) *Cell 17*, 265-274.

Sambrook, J., Fritsch, E. F., & Maniatis, T. (1989) *Molecular Cloning, A Laboratory Manual*, 2nd ed., Cold Spring Harbor Laboratory, Cold Spring Harbor, NY.

Sasse-Dwight, S., & Gralla, J. D. (1988) *J. Mol. Biol. 202*, 107-119.

Shellman, V. L., & Pettijohn, D. E. (1991) *J. Bact. 173*, 3047-3059.

Singleton, S. F., & Dervan, P. B. (1992) *J. Am. Chem. Soc. 114*, 6957-6965.

Stern, M. J., Ames, G. F.-L., Smith, N. H., Robinson, E. C., & Higgins, C. F. (1984) *Cell 37*, 1015-1026.

Strobel, S. A., & Dervan, P. B. (1991) *Nature 350*, 172-174.

Summers, W. C. (1970) *Anal. Biochem. 33*, 459-463.

Telesnitsky, A. P. W., & Chamberlin, M. J. (1989) *J. Mol. Biol. 205*, 315-330.

Ussery, D. W., & Sinden, R. R. (1993) *Biochemistry 32*, 6206-6213.

Varshavsky, A. J., Nedospasov, S. A., Bakayev, V. V., Bakayeva, T. G., & Georgiev, G. (1977) *Nucleic Acids Res. 4*, 2725-2745.

von Hippel, P. H., Bear, D. G., Morgan, W. D., & McSwiggen, J. A. (1984) *Annu. Rev. Biochem. 53*, 389-446.

Wagner, L. A., Weiss, R. B., Driscoll, R., Dunn, D., & Gesteland, R. F. (1990) *Nucleic Acids Res. 18*, 3529-3535.

Warne, S. R., Thomas, C. M., Nugent, M. E., & Tacon, W. C. A. (1986) *Gene 46*, 103-112.

Yansura, D. G., & Henner, D. J. (1990) in *Methods in Enzymology 185*, pp. 54-60, Academic Press.

Young, L. S., Dunstan, H. M., Witte, P. R., Smith, T., Ottonello, S., & Sprague, K. U. (1991) *Science 252*, 542-546.

Young, S. L., Krawczyk, S. H., Matteucci, M. D., & Toole, J. J. (1991) *Proc. Natl. Acad. Sci. U. S. A. 88*, 10023-10026.

Zaniewski, R., Petkaitis, E., & Deutscher, M. P. (1984) *J. Biol. Chem. 259*, 11651-11653.

Zilberstein, D., Agmon, A., Schuldiner, S., & Padan, E. (1984) *J. Bact. 158*, 246-252.

Chapter V

Inhibition of Klenow Fragment DNA Polymerase On Double Helical Templates By Oligonucleotide-Directed Triple Helix Formation

INTRODUCTION

Triple helical DNA structures can be formed by the sequence specific interaction of deoxyoligonucleotides with their cognate target sites in double stranded DNA (Moser & Dervan, 1987; Le Doan et al., 1987). The third strand oligonucleotide, which may be either purine rich or pyrimidine rich, interacts with exposed purine residues in the major groove of the target duplex. Pyrimidine oligonucleotides bind in a parallel orientation relative to the purine rich strand duplex strand through the formation of T•AT and C^+•GC triplets (Moser & Dervan, 1987; Rajagopal & Feigon, 1989; de los Santos et al., 1989). Purine-rich oligonucleotides bind in an antiparallel orientation relative to the purine rich duplex strand through the formation of G•GC and A•AT or T•AT triplets (Cooney et al., 1988; Beal & Dervan, 1991; Radhakrishnan et al., 1991). Oligonucleotide-directed triple helix formation has recently been used to study interactions between DNA and various DNA binding proteins, including restriction endonucleases (Maher et al., 1989, 1990; Hanvey et al., 1990; Francois et al., 1989), transcription factors (Maher et al., 1989, 1992), viral replication proteins (Huang et al., 1992), and RNA polymerases (Young et al., 1991; Maher et al., 1992; Maher, 1993). Effects of intermolecular triple helix formation with double helical templates on the

function of DNA polymerases have not previously been reported, and these are the focus of this work.

The interaction of DNA polymerases with different forms of DNA is central for their DNA repair and replication functions. Recent studies have used structural, biochemical, genetic, and pharmacological approaches to focus on different aspects of this important protein:DNA interaction. X-ray co-crystal structures of *Escherichia coli* DNA polymerase I large fragment with DNA substrates have provided atomic level resolution and led to detailed molecular models for the interaction of polymerase with primer and single stranded template (Ollis et al., 1985; Joyce & Steitz, 1987; Derbyshire et al., 1988; Beese & Steitz, 1991; Beese et al., 1993), but similar structural data is not yet available for polymerase on a double stranded DNA substrate. Others have probed the interactions of polymerase and double stranded templates by studying effects that different site specific noncoding template lesions have on the processivity and fidelity of *in vitro* DNA synthesis systems (Bhanot et al., 1991; Simha et al., 1991; Comess et al., 1992; Grevatt et al., 1991; Shibutani et al., 1993). In general these lesions lead to very efficient blocks to elongation; however, they can be bypassed by the incorporation of bases, usually adenine, across from these modified sites (Strauss, 1991). Other studies have noted sequence specific inhibition of DNA polymerase by small molecules that have high affinity, noncovalent interactions with DNA (Wartell et al., 1974; Weiland & Dooley, 1991; Sun & Hurley, 1992) or by replication termination proteins such as the *E. coli ter*-binding protein (Lee & Kornberg, 1992). Furthermore there has been recent interest in potentially inhibitory template structures and sequence composition effects such as homopurine tracts (Abbotts et al., 1988; Bedinger et al., 1989;

Weisman-Shomer et al., 1989; Brinton et al., 1991). In some cases blocks to extension occur at sites where intramolecular triple helices or local intermolecular triple helices, formed on single stranded templates, can potentially be formed (Lapidot et al., 1989; Baran et al., 1991; Brinton et al., 1991; Dayn et al., 1992; Giovannangeli et al., 1993; Samadashwily et al., 1993).

In this study we report efficient, sequence specific inhibition of DNA synthesis on a double stranded template through intermolecular pyrimidine oligonucleotide-directed triple helix formation. Triple helix forming oligonucleotides of lengths ranging from 17 nt to 27 nt were used to map blocks to synthesis catalyzed by either *E. coli* Klenow fragment or a modified T7 DNA polymerase. This system has allowed us to study sequence specific inhibition of primer extension without introducing chemical lesions.

EXPERIMENTAL PROCEDURES

Materials. All DNA synthesis reagents were obtained from Applied Biosystems Inc. except for 5-methylcytosine phosphoramidite obtained from Cruachem Inc. and Chemical Phosphorylation Reagent obtained from Glen Research. Restriction enzymes, T4 polynucleotide kinase, T4 DNA ligase, and DNase I were purchased from Boehringer Mannheim. Sequenase Version 2.0 DNA Sequencing Kit and *E. coli* DNA Polymerase I large (Klenow) fragment were purchased from U. S. Biochemicals. Adenosine 5'- [γ^{32}P] - triphosphate and deoxyadenosine - [α^{32}P] - triphosphate were obtained from New England Nuclear.

Synthesis of Oligonucleotides. Oligodeoxyribonucleotides were synthesized on an Applied Biosystems Model 380B DNA synthesizer using β-cyanoethyl phosphoramidite chemistry. Oligonucleotides were purified by denaturing polyacrylamide gel electrophoresis, visualized by UV shadowing, and electroeluted from gel slices using an Elu-trap apparatus (Schleicher & Schuell). They were ethanol precipitated and resuspended in 0.5X TE before storing at -80 °C. The concentration of oligonucleotides were determined by A_{260} measurements using the following molar extinction coefficients: 15,400 (A), 11,700 (G), 7,300 (C), 8,800 (T), and 5,800 (^{me}C).

Plasmid Construction. The plasmid pTER I was obtained by cloning the oligonucleotides 5'-pTCGACTTTTTTTCTTTTTCTTTCTTTTTTTTTTT TGGCGCATG-3' and 5'-pCGCCAAAAAAAAAAAAGAAAGAAAAAGA AAAAAAG-3' into the large Sal I/Sph I restriction fragment of pUC19.

Large scale preparation of plasmid was performed using Qiagen purification kits. The sequence of the insert was confirmed by dideoxynucleotide sequencing.

Construction of Synthetic Templates for Inhibition of DNA Synthesis. The synthetic template shown in Figure 1 was made by mixing 2 nmoles of oligonucleotides **S1** 5'-CGACGGCCAGTGAATTCGAGCTCGGTACCCG GGGATCCTCTAGAGTCGACTTTTTTTCTTTTTCTTTCTTTTTTT-3', **S2** 5'-pAAAAAGTCGACTCTAGAGGATCCCCGGGTACCGAGCTCGAATTC ACTGGCCGTCGTTTTACAAGCTCGTGACTGG-3', **S3** 5'-pTTTTTGGCGC ATGCAAGCTTGGCGTAATCATGGTCATAGCTGTTTCCTGTGTGAAAT TGTTATCCGCTCACAATT-3' , and **S4** 5'-TTCACACAGGAAACAGCTAT GACCATGATTACGCCAAGCTTGCATGCGCCAAAAAAAAAAAAAGAA AGAAAAAGAA-3' in a total volume of 50 µL 1X TNE. The reaction was heated to 100 °C for 2 minutes and slowly cooled to room temperature. To the reaction was added 38 µL of water, 10 µL of 10X ligation buffer, 1 µL of 100 mM ATP and 10 U of T4 DNA ligase. It was placed at 37 °C for 8 hours, terminated by ethanol precipitation, and resuspended in 40 µL of nondenaturing load dye (0.25% bromophenol blue, 0.25% xylene cyanol FF, 30% glycerol). The samples were heated to 70 °C for 2 minutes and chilled on ice prior to electrophoresis on a 10% nondenaturing polyacrylamide gel. The annealed full length target duplex was visualized by UV shadowing, excised, and extracted through electroelution. The duplex was ethanol precipitated and resuspended in 1X TE buffer prior to storage at -80 °C.

DNase I Footprinting. The 438-bp Afl III-EcoR I restriction fragment of

pTER I was 3'-end labeled with deoxyadenosine - [α^{32}P] - triphosphate, and chemical sequencing A + G specific reactions were carried out by standard procedures (Sambrook et al., 1991). Labeled DNA (50,000 cpm) in 9 μL of 1.1X Sequenase Reaction Buffer (44 mM Tris-Cl pH 7.5, 55 mM NaCl, and 22 mM $MgCl_2$) was either heated to 100 °C under mineral oil for 2 minutes prior to slow cooling to room temperature or incubated for an equivalent amount of time at 37 °C, as indicated. Oligonucleotide (1 μL) was added and the reaction was allowed to equilibrate for 2 hours at 37 °C. Immediately prior to addition of 2 μL of DNase I (0.01 U/μL in 1X TE) , 1 mL of 100 mM $CaCl_2$ was added to the reaction. Digestion proceeded for 2 minutes at room temperature before termination by ethanol precipitation and resuspension in Sequenase Stop Buffer (95% formamide, 20 mM EDTA, 0.05% Bromophenol Blue, 0.05% Xylene Cyanol FF). The samples were analyzed by electrophoresis on 8% denaturing polyacrylamide gels.

Inhibition of DNA Synthesis Using Synthetic Templates. DNA template (0.1 pmole) was added to either 5'-end labeled primer **A** 5'-CCAGTCACGAGCTTGTAAAA-3' or 5'-end labeled primer **B** 5'-AATTGTGAGCGGATAACAAT-3' (20,000 cpm/reaction) in a volume of 9 μL of 1.1X Sequenase Reaction Buffer. The mixture was heated to 70 °C for 2 minutes and slow cooled to 37 °C. Oligonucleotide was added in a volume of 1 μL and incubated at 37 °C for 2 hours. A 15 μL volume of primer extension buffer (12.5 mM DTT, 50 mM in each dNTP, 15 mM NaCl, 2.5 mM Tris-Cl pH 7.5, 12.5 μg/mL BSA, 3.25 U of either Klenow fragment or Sequenase 2.0) was added to each reaction and allowed to incubate for the specified time at 37 °C. This amount of polymerase theoretically represents a 10-fold excess of enzyme to third strand

oligonucleotide (present at 50 nM concentration). Addition of 10-fold greater amounts of polymerase did not change experimental results (data not shown), implying that the primer extension reactions are done with saturating amounts of DNA polymerase. Reactions were stopped by the addition of 14 µL of Sequenase Stop Buffer. Molecular weight markers were generated by terminating primer extension reactions by ethanol precipitation and resuspension in 40 µL of nondenaturing load dye. The samples were heated to 70 °C for 2 minutes and chilled on ice prior to electrophoresis on a 10% nondenaturing gel. 5'-end labeled full length target duplex was visualized by autoradiography, excised, and electroeluted. Chemical sequencing A+G and C+T specific reactions were carried out as described (Sambrook et al., 1989). Samples were electrophoresed on 8% denaturing polyacrylamide gels that were dried and placed on film upon completion. Afterward, gels were exposed to storage phosphor screen (Kodak storage screen S0230, obtained from Molecular Dynamics) and data were analyzed on a Molecular Dynamics 400S PhosphorImager using ImageQuant v. 3.22 software.

Inhibition of DNA Synthesis Using Restriction Fragments. Molecular weight markers consisted of dideoxy sequencing reactions performed on alkaline denatured pTER I supercoiled template using 5'-end labeled primers. The 349 bp Pvu II restriction fragment of pTER I was isolated by electrophoresis on a 1% agarose gel followed by electroelution. Restriction fragment (10 ng) was added to either 5'-end labeled primer **C** 5'-TGCTTCCGGCTCGTATGTTGTGTGG-3' or 5'-end labeled primer **D** 5'-ACGCCAGGGTTTTCCCAGTCACGAC-3' (200,000 cpm/9 µL final reaction) in a volume of 9 µL of 1.1X Sequenase Reaction Buffer per final reaction.

The mixture was heated to 100 °C under mineral oil for 2 minutes and slow cooled to 37 °C. Reaction aliquots (9 μL) were placed in separate tubes and oligonucleotide was added in a volume of 1 mL. The triple helix annealing reaction was allowed to equilibrate for 2 hours at 37 °C. Primer extension buffer (15 μL) was added to each reaction and incubated for the specified time at 37 °C. Reactions were stopped by the addition of 14 μL of Sequenase Stop Buffer and heated at 100 °C for 2 minutes. Samples were electrophoresed on 8% denaturing polyacrylamide gels that were dried and placed on film and storage phosphor screen for analysis as stated above.

RESULTS

Design of a Duplex DNA Target Site and Corresponding Third Strand Oligonucleotides. To examine whether and how intermolecular triplex structures affect DNA synthesis reactions, a thirty-one base pair homopurine tract was designed to act as the target site. The large size of this purine sequence allows for the formation of several different triple helical complexes nested within the target site. Potential third strand oligonucleotides used in all triplex formation and primer extension assays are shown in Table 1. Reagents **y1-y4** are all expected to occupy the target in the orientation shown. However, their individual lengths and frame of occupancy on the target are anticipated to be different. Together, these probes provide the means to map termination patterns positioned across the target site in a predictable manner and to compare how well triple helical complexes of varying stability inhibit polymerase. Reagents **y5**, **r1**, and **r2**, which are not expected to bind to the target site under the conditions used in this study, serve to measure polymerase termination that is unrelated to triple helix formation but might depend on template composition or the mere presence of oligonucleotides. Reagent **y5** has the same sequence composition as **y1** but is antisense to the purine rich target strand, so it can be used to test for possible Watson-Crick interactions and their effects on the polymerase reactions. Reagents **r1** and **r2** are purine-rich oligonucleotides, with **r1** being antisense to the homopyrimidine target strand.

Occupancy of Triple Helix Target Sequence. DNase I footprinting assays were performed to show that the target site is occupied by oligonucleotides

Figure 1. Representation of the two systems used in the primer extension inhibition assays. Oligonucleotides **S1** and **S3** are ligated together to form the pyrimidine-rich strand of the synthetic template while oligonucleotides **S2** and **S4** are ligated together to form the purine-rich strand of the synthetic template with **S2** and **S3** providing the 3'-overhangs complementary to Primers **A** and **B** respectively. Py Tract refers to the pyrimidine-rich strand of the target site while Pu Tract refers to the purine-rich strand.

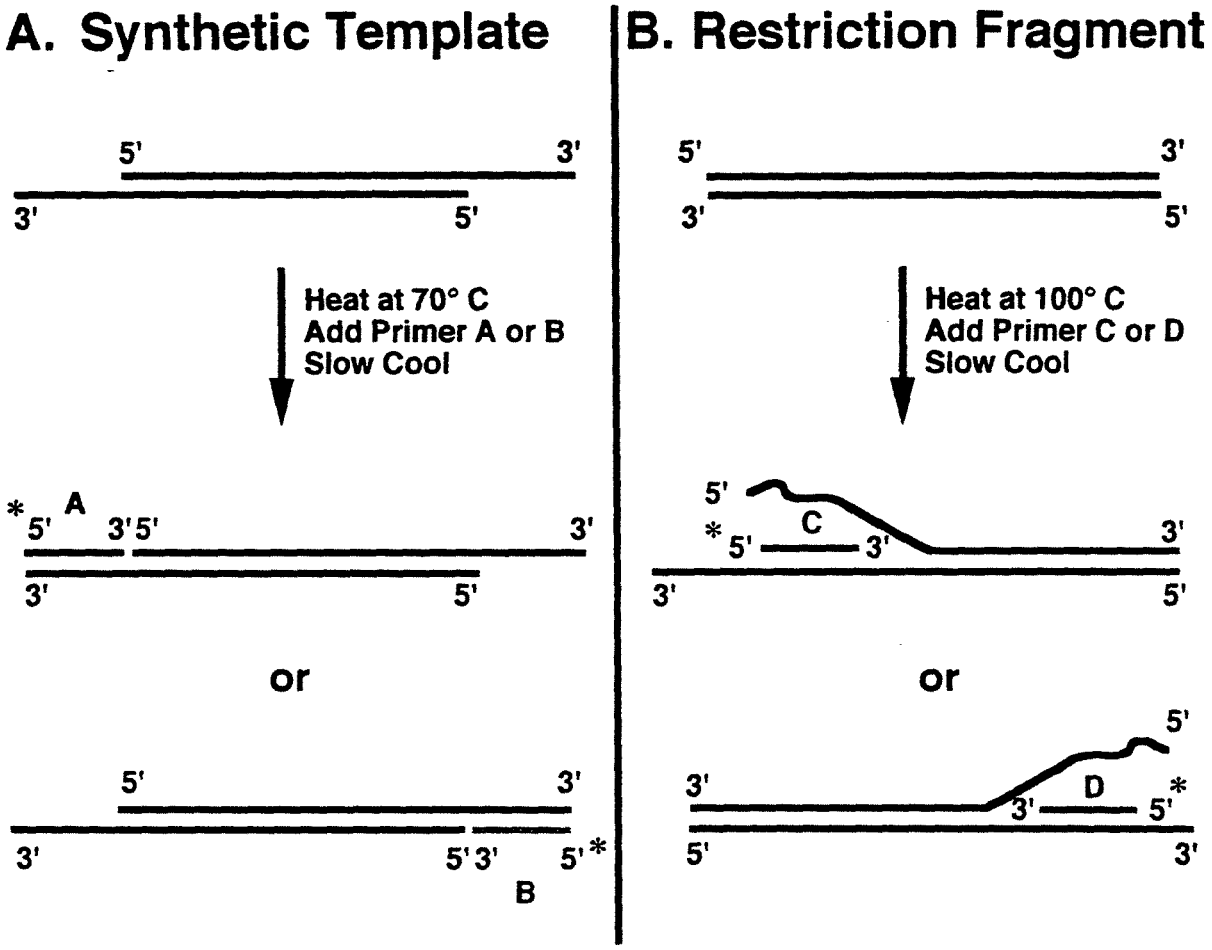
A. Synthetic Template
B. Restriction Fragment
5'
3'
3'
5'
Heat at 70° C
Add Primer A or B
Slow Cool
Heat at 100° C
Add Primer C or D
Slow Cool
A
C
D
B
or
or

Table 1: Sequences of Oligonucleotides and 31-bp Target Site

Homopurine Target Site

5' A A A A A A A A A A A A G A A A G A A A A A G A A A A A A A A G 3'
3' T T T T T T T T T T T T C T T T C T T T T T C T T T T T T T C 5'

Oligonucleotides

Oligo			Length
y1	5'	T T T T T T T T T C T T T C T T T T T C T T T T T T T T 3'	27 nt
y2	5'	T T T T T T T T T T T C T T T C T T T T T C T T T T T 3'	27 nt
y3	5'	T T T T T T T T T C T T T C T T T T T T 3'	19 nt
y4	5'	T T T C T T T T T C T T T T T T T T 3'	17 nt
y5	5'	T T T T T T T C T T T T T C T T T C T T T T T T T T T 3'	27 nt
r1	5'	A A A A A A A A A G A A A G A A A A A G A A A A A A A A 3'	27 nt
r2	5'	A A A A A A A G A A A A A G A A A G A A A A A A A A A 3'	27 nt

y1-y4, as expected from their design, and that negative control oligonucleotides did not form triplexes. The target duplex is embedded in a restriction fragment (EcoR I -Afl III) from the plasmid pTER I. It consists of a 31-bp homopurine run flanked by sequences common to the small Pvu II fragment from pTER I and the synthetic oligonucleotide duplex depicted in Figure 1. Studies using the native fragment shown in Figure 2A demonstrate complete occupancy of the target site by oligonucleotides y1, y2, y3 and y4 under the same conditions that are used for DNA polymerase assays. The size and location of the protected regions correlate with the formation of expected oligonucleotide directed triple helices. Moreover there is a distinctive hypersensitive cleavage site present at the 3'-end of the triple helical complexes in Figure 2A lanes 3, 5, and 6. Oligonucleotides y5, r1 and r2 show no protection of the triple helix target site, as expected since they have no triple helical homology to the target site. Studies performed on the renatured target fragment shown in Figure

B further demonstrate complete occupancy of the target site by the triple helix forming oligonucleotides. The control oligonucleotides **y5**, **r1** and **r2** do not occupy the target site. The similarity of DNase I patterns in panels A and B indicate that, within the limits of detection, the vast majority of the heat denatured template has reannealed to completion. The anticipated orientation of the third strand was confirmed for oligonucleotide **y1** by standard affinity cleavage analysis (Dreyer & Dervan, 1985; Moser & Dervan, 1987) (data not shown).

Synthetic Gapped Template System of DNA Synthesis Inhibition. Two templates carrying the same target sequence were used in this study (Figure 1). These substrates differ in the manner in which they provide an entry and initiation point for DNA polymerase. The first was designed to provide a nick in an otherwise perfect duplex. The nick is positioned upstream of the triplex target site and is expected to serve as a specific entry site and primer for the DNA polymerase. To create a homogeneous population of this substrate, its components were each synthesized chemically, followed by annealing reactions and subsequent gel purification (Materials and Methods). Preliminary experiments verified that the nick acts as a primer for DNA synthesis using Klenow Fragment (Figures 3 and 4). Triple helix forming oligonucleotides were added to the annealed template to test for inhibition of DNA synthesis. The sequence of the template's double stranded region is identical to that of the pTER I restriction fragment used in the footprinting and restriction fragment termination assays. This should permit direct comparison of the synthetic gapped template system and the restriction fragment system described below.

Figure 2A: Autoradiogram of an 8% denaturing polyacrylamide gel showing DNase I footprinting patterns of the oligonucleotides listed in Table 1. Footprinting reactions performed on the native Afl III-EcoR I restriction fragment of pTER I are represented. Lane 1, A + G specific chemical sequencing lanes; lane 2, DNase I control lane; lanes 3, 0.05 μM **y1**; lane 4, 0.05 μM **y2**; lane 5, 1 μM **y3**; lane 6, 1 μM **y4**; lane 7, 0.05 μM **y5**; lane 8, 0.05 μM **r6**; lane 9, 0.05 μM **r7**; lane 10, untreated DNA control lane.

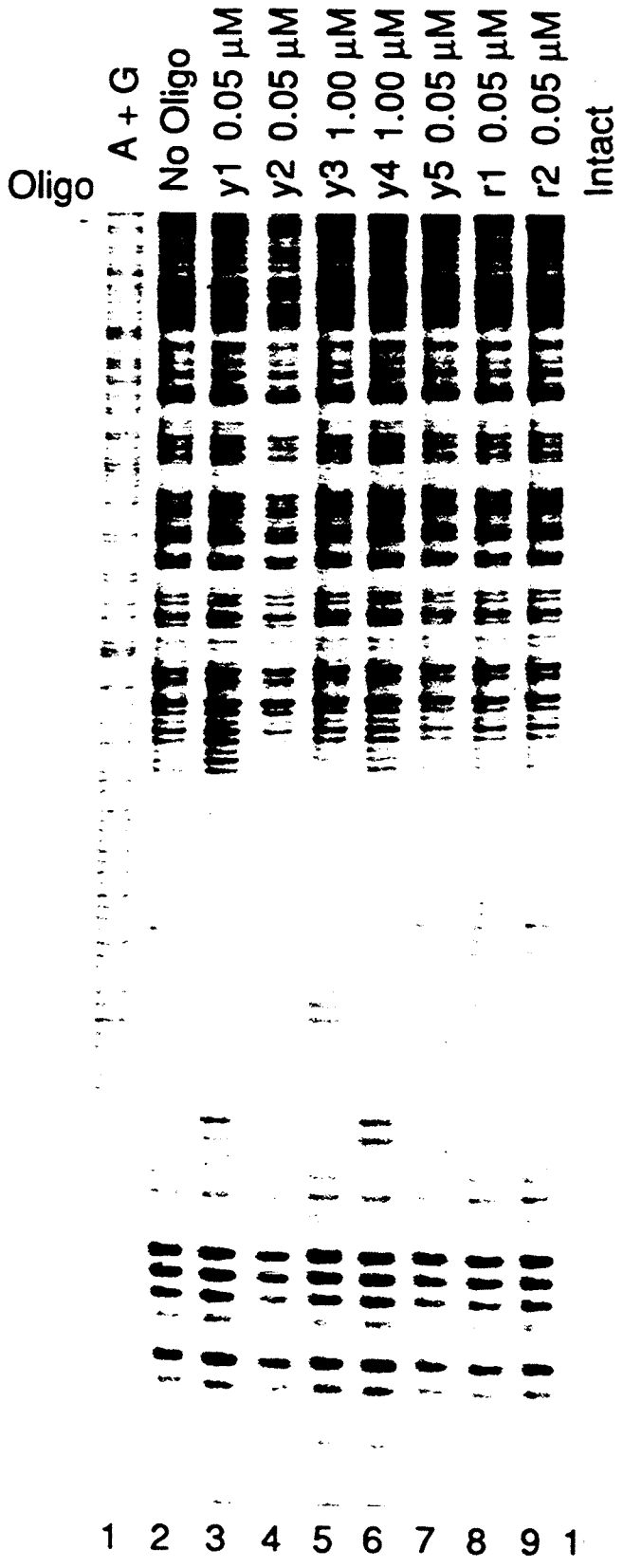
Oligo
A + G
No Oligo
y1 0.05 µM
y2 0.05 µM
y3 1.00 µM
y4 1.00 µM
y5 0.05 µM
r1 0.05 µM
r2 0.05 µM
Intact
1 2 3 4 5 6 7 8 9 1

Figure 2B. Autoradiogram of an 8% denaturing polyacrylamide gel showing DNase I footprinting patterns of the oligonucleotides listed in Table 1. The reactions performed on the denatured and reannealed fragment are represented. Lane 1, A + G specific chemical sequencing lanes; lane 2, DNase I control lane; lanes 3, 0.05 μM **y1**; lane 4, 0.05 μM **y2**; lane 5, 1 μM **y3**; lane 6, 1 μM **y4**; lane 7, 0.05 μM **y5**; lane 8, 0.05 μM **r6**; lane 9, 0.05 μM **r7**; lane 10, untreated DNA control lane.

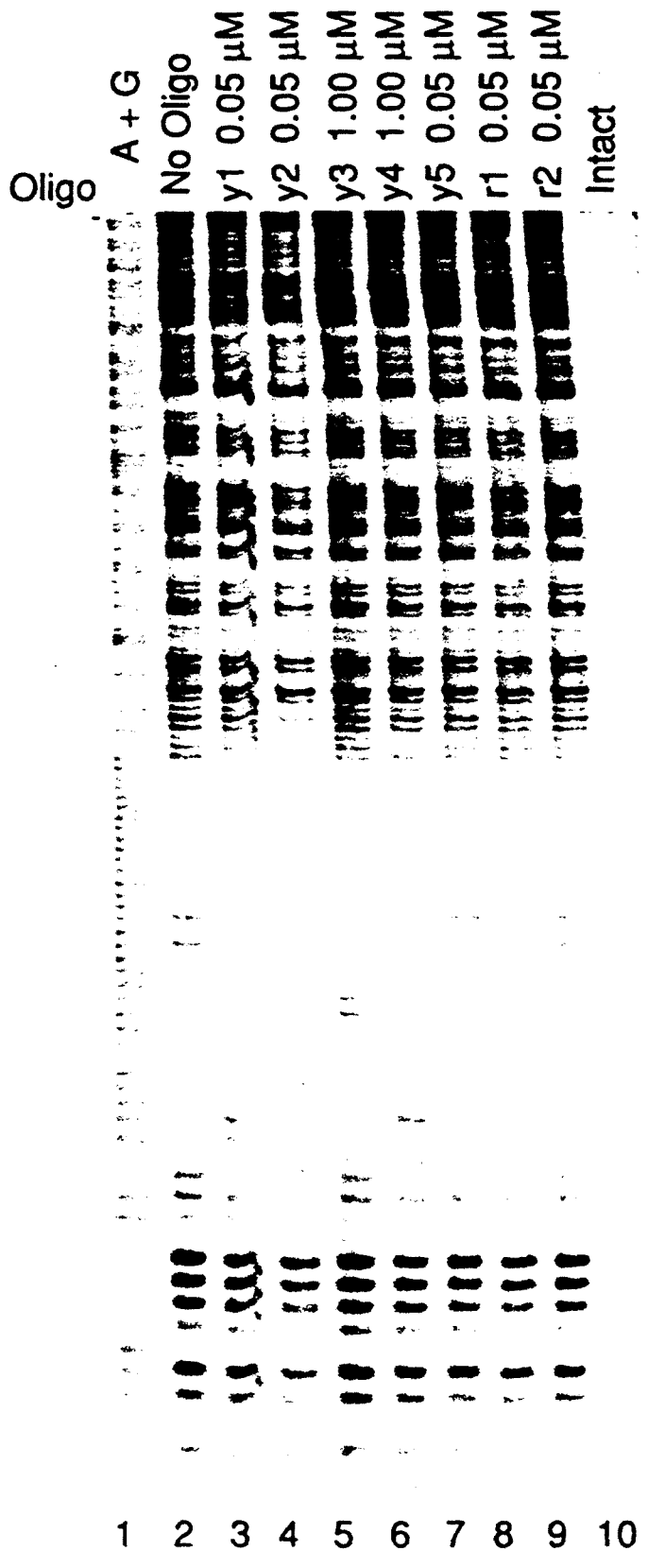
Oligo
A + G
No Oligo
y1 0.05 µM
y2 0.05 µM
y3 1.00 µM
y4 1.00 µM
y5 0.05 µM
r1 0.05 µM
r2 0.05 µM
Intact
1 2 3 4 5 6 7 8 9 10

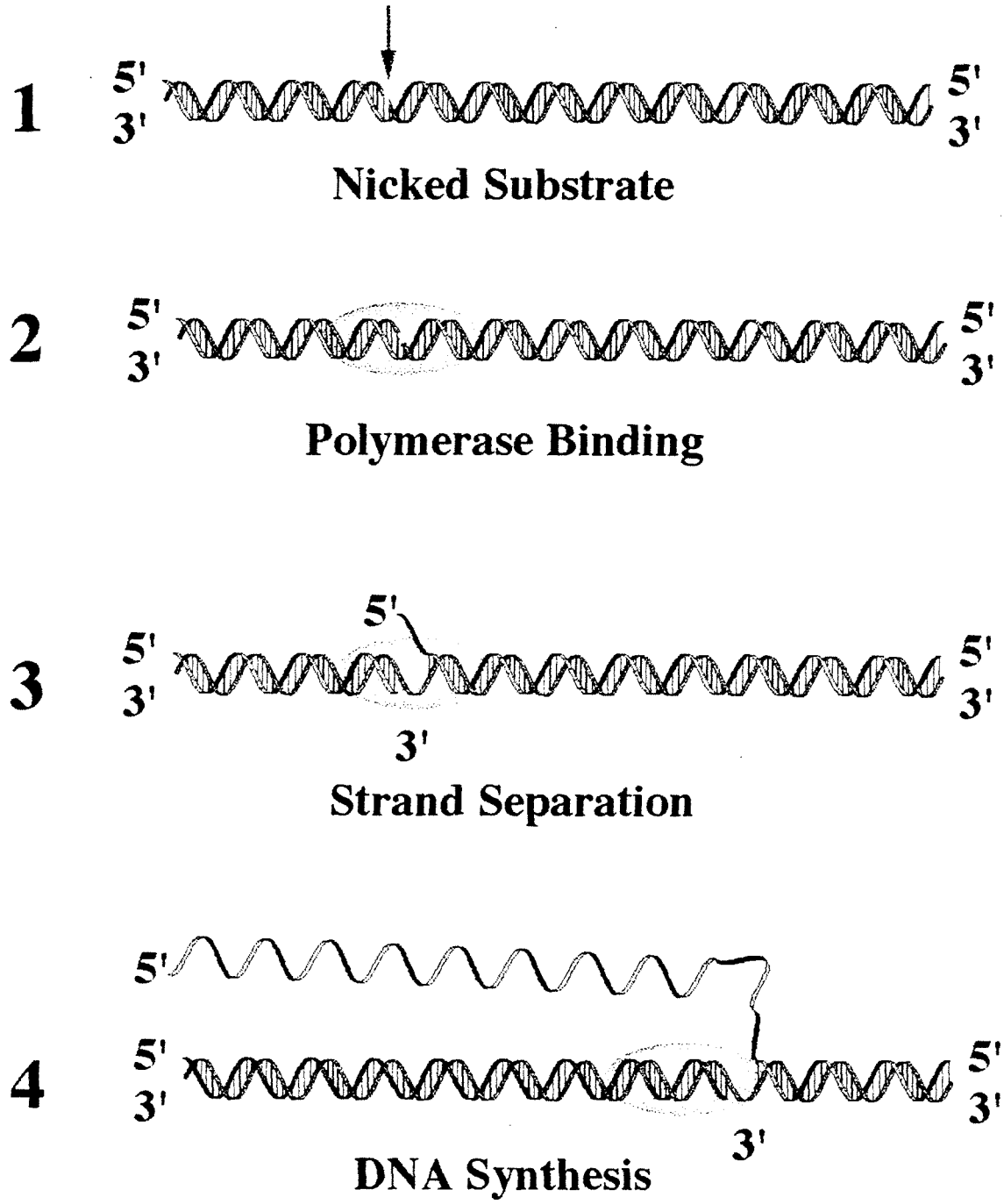

Figure 3. Strand displacement DNA synthesis.

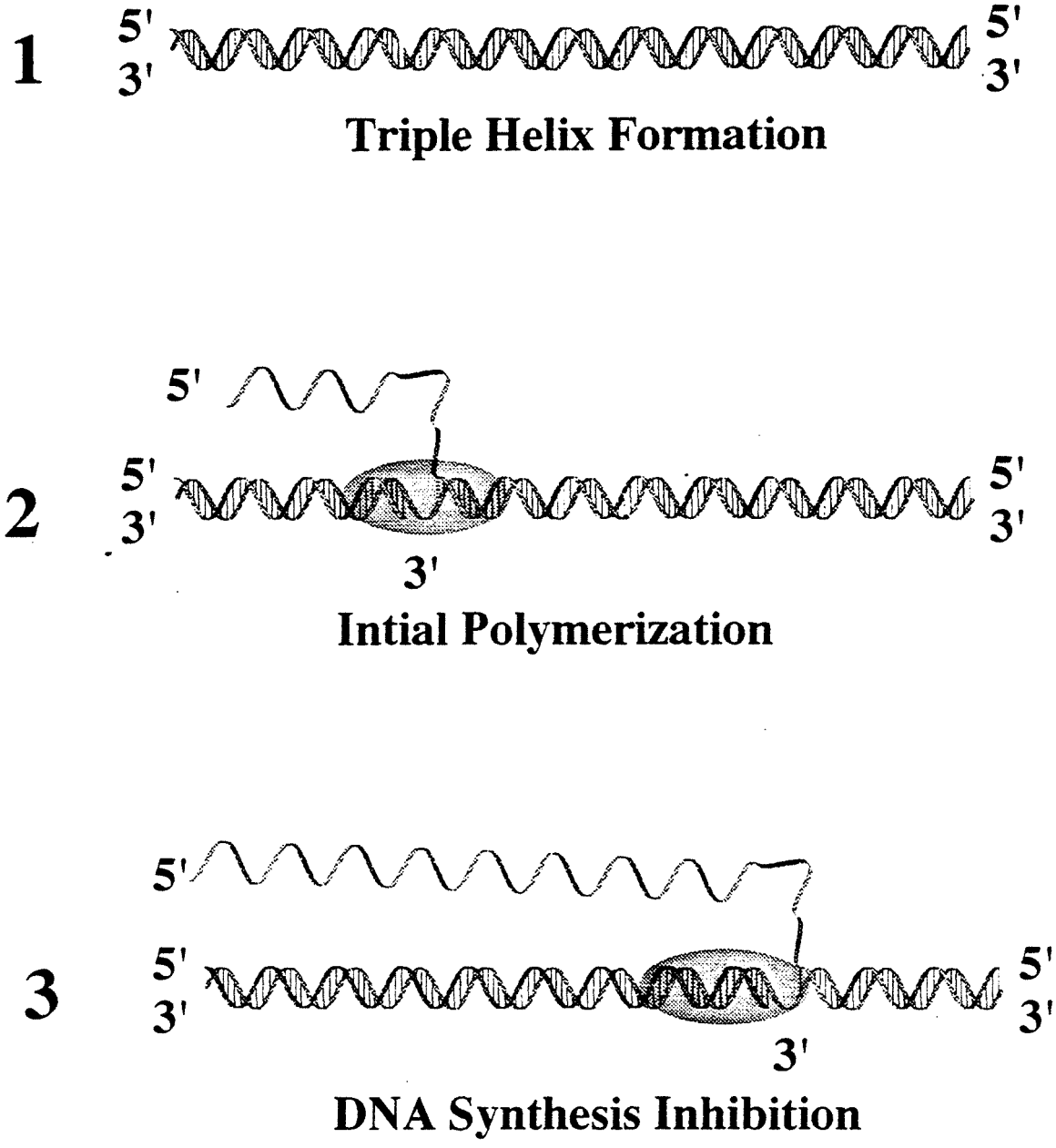

Figure 4. Triple helix inhibition of strand displacement DNA synthesis.

Restriction Fragment System of DNA Synthesis Inhibition. In this alternative system the small Pvu II fragment of pTER I is heat denatured in the presence of excess primer, as depicted schematically in Figure 1. After annealing, primer bound to the fragment template can be extended with either the Klenow fragment of DNA polymerase I or Sequenase 2.0 (data not shown), as would be expected from prior studies showing the ability of these enzymes to execute strand displacement synthesis (Tabor & Richardson, 1989; Kornberg & Baker, 1992). For reasons detailed below, this class of substrates was used only to provide initial observations which were then verified on the better defined synthetic template described above. However this substrate should have the advantage of most nearly approximating the region upstream of DNA polymerase performing strand displacement synthesis, and all major conclusions proved the same in both systems. For this set of templates, there is clearly greater uncertainty concerning substrate homogeneity and conformation because the majority of primer is expected to be branch migrated off the template strand during the reannealing stage. This means that priming and DNA synthesis will come from a minority of the DNA in the reaction. For this reason, it is not possible to definitively and directly characterize the conformation of DNA (and its triple-stranded status where appropriate oligonucleotides are present) at positions downstream of the primer termini. It is easy to imagine that competing side reactions on higher order structures could become significant in this system. Nevertheless, as shown below, both substrate types gave remarkably similar results when triple helix forming oligonucleotides are added to the reaction followed by challenge with polymerase. Effects of the same set of oligonucleotides tested on the fully defined, nicked substrate were determined for the

restriction fragment substrates.

Inhibition of DNA Polymerases Priming From the Pyrimidine Rich Strand. In the synthetic template system, primer extension terminates efficiently and quite abruptly a few bases internal to the 5'-end of the triple helix as shown in Figure 5A and Figure 6. This stoppage is distinct in position and efficiency from the intrinsic polymerase pausing (Figure 4, lane 11) characteristic of homopurine tracts (Weisman-Shomar et al., 1989). Both oligonucleotide probes **y1** and **y2** cause greater than 95% inhibition of primer extension at the homopurine target site (Figure 4, lanes 2 and 3). The shorter oligonucleotides **y3** and **y4** show termination efficiencies of 85% and 40% respectively when present at concentrations sufficient to saturate the target site by the criterion of in parallel DNase I footprinting (Figure 4, lanes 4 and 5). At oligonucleotide concentrations no longer sufficient for full occupancy of the target site there is a further decrease in termination efficiency (Figure 4, lanes 6 and 7). Oligonucleotides with identical 5'-ends (**y1** and **y3**) show similar patterns of inhibition. This appears to be due to the position of the triple helical region itself, rather than an effect due to a particular sequence in the context of the helix. Thus, oligonucleotide **y2**, which has a different 5'-end than **y1** and **y3**, yields a different termination pattern in the same homopurine run. That termination is similarly positioned a few bases downstream from the 5'-end of the triplex. Of the oligonucleotides that do not bind the target site significantly, only **y5** displays slight (less than 5%) inhibition of DNA synthesis localized near the 3'-end of the homopurine run (Figure 4, lane 8).

Using the restriction fragment system, similar results were obtained

Figure 5: Histograms representing oligonucleotide mediated termination patterns. Arrows indicate the location and relative intensities of polymerase stoppage. The upper arrows indicate pauses observed with primers **B** and **C** in the synthetic template and restriction fragment systems respectively. The lower arrows indicate pauses observed with primers **A** and **D** in the synthetic template and restriction fragment systems respectively. Pause sites that appear in the control and are independent of the oligonucleotide have been subtracted as backround. Panel A. Synthetic template system using oligonucleotides **y1, y2, y5, r1,** and **r2** at 0.05 μM concentration and oligonucleotides **y3** and **y4** at 1 μM concentration. Reactions were allowed to proceed for 2 minutes. Panel B. Same conditions as panel A using the restriction fragment template. Panel C. Oligonucleotide mediated termination kinetics using the synthetic template system. Oligonucleotide **y1** is present at 0.05 μM concentration in all cases with the reaction time given. Panel D. Same conditions as panel C using the restriction fragment template.

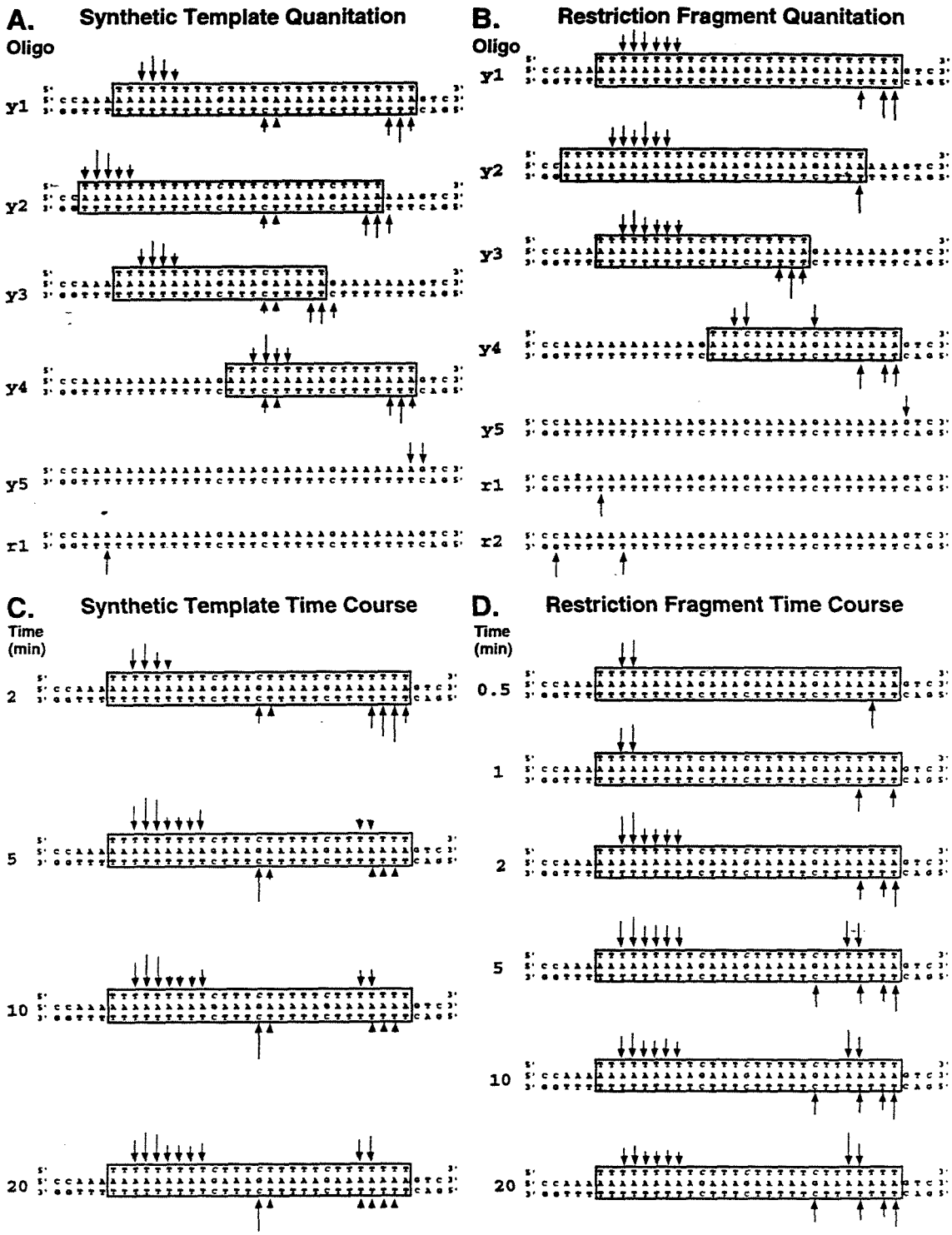
A.
Synthetic Template Quanitation
Oligo
y1
y2
y3
y4
y5
r1
B.
Restriction Fragment Quanitation
Oligo
y1
y2
y3
y4
y5
r1
r2
C.
Synthetic Template Time Course
Time
(min)
2
5
10
20
D.
Restriction Fragment Time Course
Time
(min)
0.5
1
2
5
10
20

Figure 6: Autoradiogram of an 8% denaturing polyacrylamide gel showing the effect of oligonucleotides on primer extension reactions performed on a synthetic template. Klenow fragment was used to extend Primer **B** off the strand containing pyrimidine-rich tract in this two minute reaction. Lane 1, A + G specific chemical sequencing lane performed on the extension product of 5'-end labeled Primer **B**; lane 2, 0.05 μM **y1**; lane 3, 0.05 μM **y2**; lane 4, 1 μM **y3**; lane 5, 1 μM **y4**; lane 6, 0.05 μM **y3**; lane 7, 0.05 μM **y4**; lane 8, 0.05 μM **y5**; lane 9, 0.05 μM **r1**; lane 10, 0.05 μM **r2**; lane 11, no oligonucleotide control.

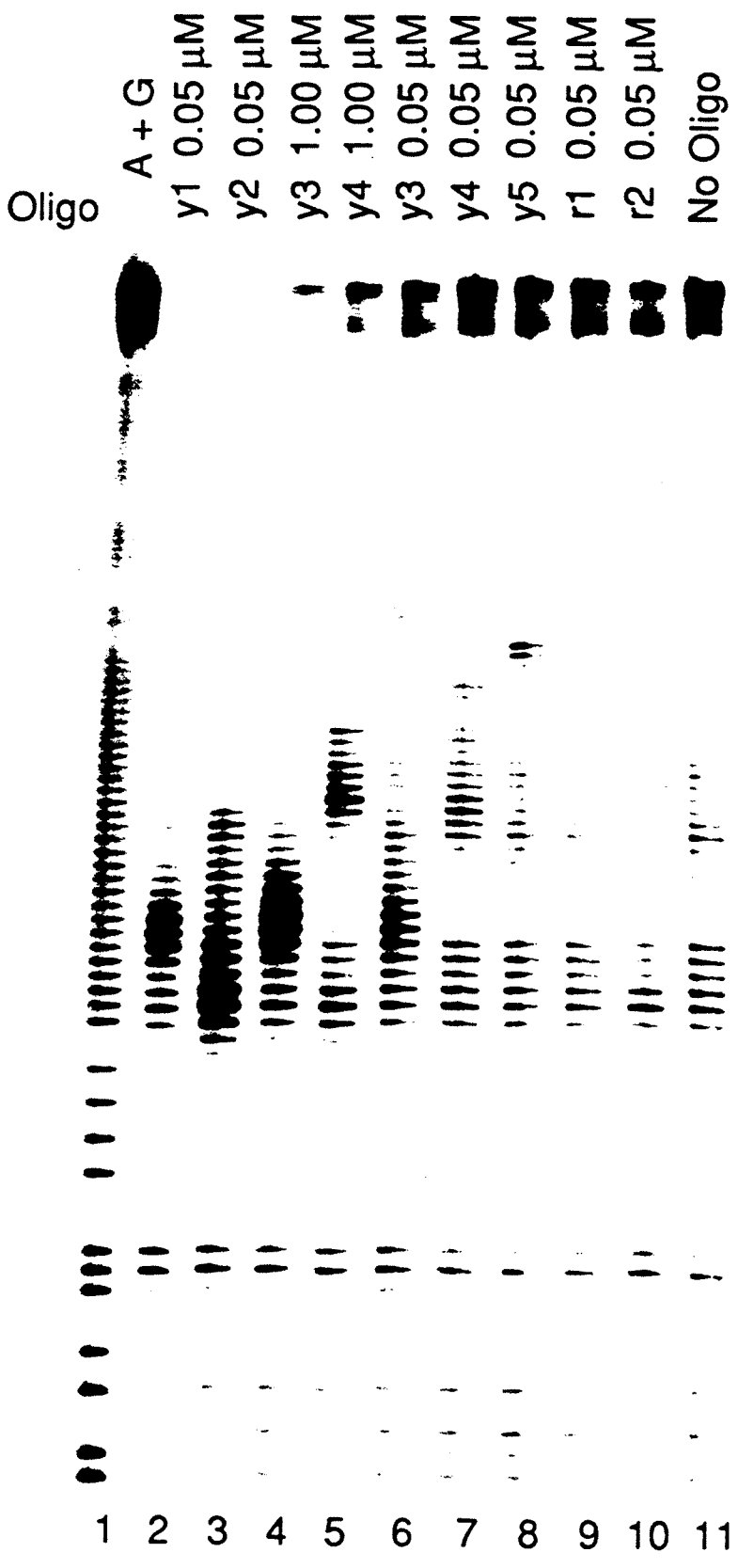
Oligo
A + G
y1 0.05 µM
y2 0.05 µM
y3 1.00 µM
y4 1.00 µM
y3 0.05 µM
y4 0.05 µM
y5 0.05 µM
r1 0.05 µM
r2 0.05 µM
No Oligo
1 2 3 4 5 6 7 8 9 10 11

(Fig. 5B). Again the extension process is halted several bases internal to the 5'- terminus of the triple helix. Oligonucleotides **y1** and **y2** cause greater than 95% inhibition of primer extension past the homopurine target site. The shorter triple helix forming oligonucleotides **y3** and **y4** show significant termination efficiencies of 75% and 60% respectively. An unanticipated result, novel to this substrate, was that oligonucleotide **y5** caused significant polymerase stoppage, even though it does not form a stable triplex complex as measured by footprinting. This may be due to interactions of the oligonucleotide with the displaced strand during the primer extension reaction or to incomplete reanealing of the template yielding oligonucleotide stabilized higher order structures.

Inhibition of DNA Polymerases Priming From the Purine Rich Strand. Using the synthetic template system, primer extension terminates directly internal to the 3'-end of the triple helix (Figure 5A). Both oligonucleotide probes **y1** and **y2** cause greater than 95% inhibition of primer extension past the target site. The shorter oligonucleotides **y3** and **y4** show a decreased amount of inhibition with termination efficiencies of 75% and 70% respectively when present at concentrations sufficient for full binding site occupancy. At lower concentrations there is a further decrease in termination efficiency. Oligonucleotides with identical 3'-ends (**y1** and **y4**) show similar patterns of inhibition. Of the oligonucleotides that do not bind to the target site, only **r1** displays slight (less than 5%) inhibition of primer extension near the 5'-end of the homopurine run.

The restriction fragment system gave similar termination patterns with the extension process again being halted nearby the 3'-terminus of the triple helix as shown in Figure 5B and Figure 5. Both oligonucleotide

Figure 7: Autoradiogram of an 8% denaturing polyacrylamide gel showing the effect of oligonucleotides on primer extension reactions performed on a restriction fragment. Klenow fragment was used to extend 5'-end labeled Primer **D** off the strand containing the purine-rich tract in this two minute reaction. Lane 1, T dideoxynucleotide sequencing reaction performed on plasmid pTER I; lane 2, 0.05 μM **y1**; lane 3, 0.05 μM **y2**; lane 4, 1 μM **y3**; lane 5, 1 μM **y4**; lane 6, 0.05 μM **y3**; lane 7, 0.05 μM **y4**; lane 8, 0.05 μM **y5**; lane 9, 0.05 μM **r1**; lane 10, 0.05 μM **r2**; lane 11, no oligonucleotide control.

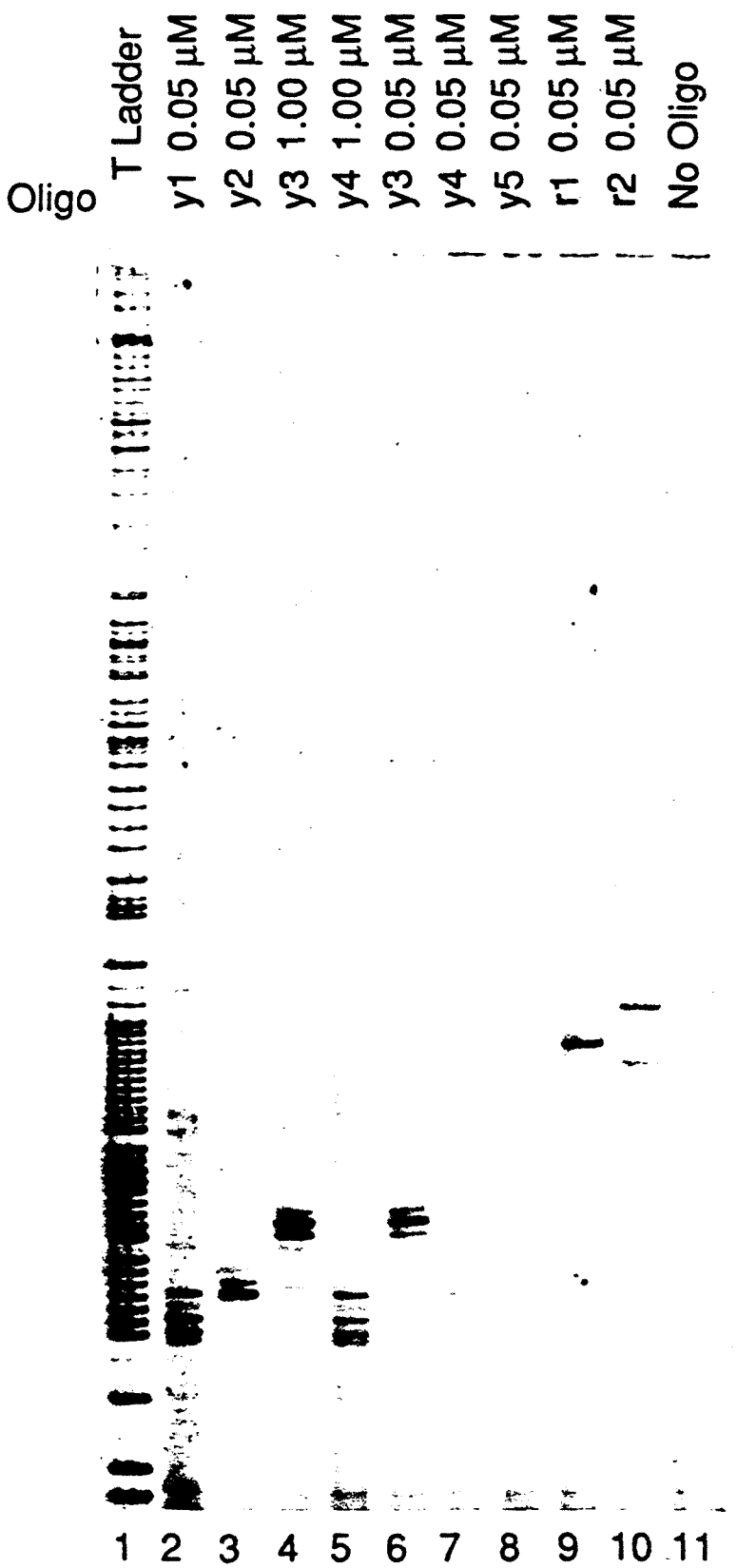
Oligo
T Ladder
y1 0.05 µM
y2 0.05 µM
y3 1.00 µM
y4 1.00 µM
y3 0.05 µM
y4 0.05 µM
y5 0.05 µM
r1 0.05 µM
r2 0.05 µM
No Oligo
1 2 3 4 5 6 7 8 9 10 11

probes **y1** and **y2** cause greater than 95% inhibition of primer extension past the homopurine target site (Figure 5, lanes 2 and 3). The shorter triple helix forming oligonucleotides **y3** and **y4** still show significant termination efficiencies of 95% and 85% respectively (Figure 5, lanes 4 and 5). Oligonucleotides with identical 3'-ends show similar patterns of extension inhibition. Although having no affinity for the duplex target site, the homopyrimidine antisense oligonucleotides **r1** and **r2** cause significant stoppage. Again it may reflect interactions of the oligonucleotide with the displaced strand during primer extension or more complicated higher order structures.

Kinetics of DNA Synthesis Inhibition Priming From the Pyrimidine Rich Strand. Using the synthetic template system triple helix formation with oligonucleotide **y1** blocks primer extension at greater than 95% efficiency for at least 20 minutes as shown in Figure 3C and Figure 6. During this twenty minute time span (37 °C), the minor stop sites toward the 3'-end of the triple helix present at the 2 minute time point become more prominent (Figure 6, lanes 2-5). Similar results are found using the restriction fragment based assay as shown in Figure 3D.

Kinetics of DNA Synthesis Inhibition Priming From the Purine Rich Strand. The synthetic template system used in mapping termination events demonstrates that the triple helix formed with **y1** can block primer extension at greater than 95% efficiency for at least 20 minutes (Figure 3C). Once again the minor stop sites toward the 5'-end of the triple helix present at the earlier 2 minute time point become more prominent during the course of this time span. The restriction fragment system yields

Figure 8: Autoradiogram of an 8% denaturing polyacrylamide gel showing the kinetics of a Klenow fragment primer extension reaction priming off the strand containing the pyrimidine-rich tract in the synthetic template system. The time of the reaction is given and when indicated reactions were done in the presence of 0.05 μM **y1**. Lane 1, A + G specific chemical sequencing lane performed on the extension product of 5'-end labeled Primer **B**; lane 2, 2 minutes with **y1**; lane 3, 5 minutes with **y1**; lane 4, 10 minutes with **y1**; lane 5, 20 minutes with **y1**; lane 6, 2 minutes; lane 7, 20 minutes.

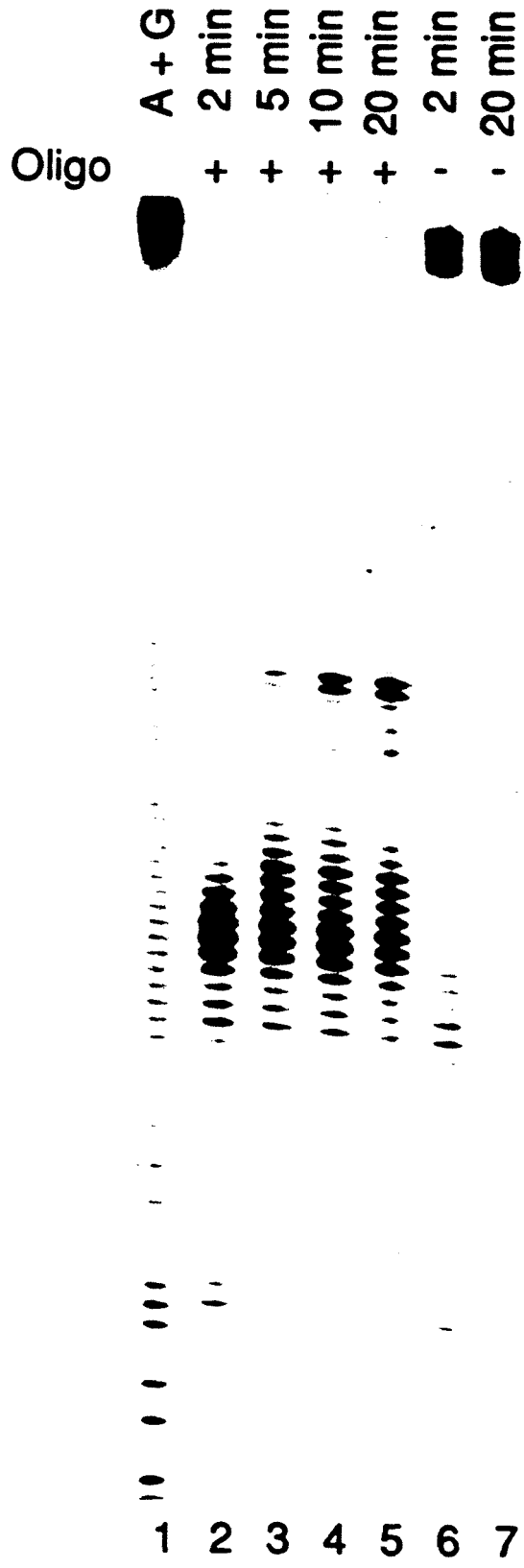
A+G
2 min
5 min
10 min
20 min
2 min
20 min
Oligo
+ + + + - -
1 2 3 4 5 6 7

similar results as shown in Figure 3D.

DISCUSSION

We have found that triple helical complexes of lengths ranging from 17 nt to 27 nt and of differing sequence composition inhibit primer extension by Klenow or modified T7 DNA polymerases. DNase I footprinting showed that only those oligonucleotides that stably occupied the target sequence were able to inhibit polymerase extension. Primer extension that copied from either strand of the duplex target in the synthetic template system was efficiently stalled adjacent to the first junction between triplex and duplex in the substrate. This block was stable for at least twenty minutes in the cases studied, although at longer time points there was an increase in larger termination products implying entry into the triplex or possible polymerase stuttering at the triplex junction. Interestingly, the efficiency of the polymerase blocks depended not only on triple helix occupancy, but also on the length of the triplex. When priming from either strand, shorter complexes were less efficient than longer ones. This length dependence is not a simple reflection of steady-state occupancy since DNase I footprinting assays showed complete occupancy of the target site by these oligonucleotides under polymerase assay conditions. However it may indicate that polymerase remains on the blocked complex and can complete read-through upon oligonucleotide dissociation, thereby revealing more rapid dissociation-rates for shorter oligonucleotides. An alternative or additional mechanism is that partial unwinding of the triple helices by polymerase is an active process which ultimately destabilizes the block, an effect that would more efficiently disrupt disruptive to shorter complexes than longer ones.

A possible precedent for similar partial read-through by Klenow

fragment has been observed in the blockage of an *in vitro* DNA replication fork by the *E. coli ter*-binding protein (Lee & Kornberg, 1992). In this case, the *ter*-binding protein (TBP) was shown to occupy a 22 base pair stretch of DNA, but allowed the T7 DNA polymerase to read 3 or 4 bp into the protected region in either direction. Interestingly the same *ter* complex was effective in preventing any read-through into the 22 bp protected site by an *in vitro* DNA replication system containing DNA polymerase III holoenzyme, helicases, and single-strand binding proteins. This observation was attributed to TBP mediated helicase inhibition in conjunction with the relative lack of strand displacing activity of the DNA polymerase III holoenzyme. The inherent T7 or Klenow fragment strand displacing activities, whose mechanism is not yet understood, may carry a local DNA melting activity that secondarily disrupts interaction of either oligonucleotide or protein in its path. Alternatively, the ability to make partial progress into such obstacles might be revealing their capacity to physically disrupt diverse noncovalent interactions.

Oligonucleotides that could not stably occupy the double helical DNA target, defined by DNase I footprinting criteria, had virtually no effect on primer extension in the synthetic fragment system. This included **y5** and **r1** which are antisense complements to the two strands of the triple helix target site and **r2** which shares partial Watson:Crick homology to the homopyrimidine strand. However, these reagents did display significant differences on the two substrate types studied: in the denaturation and annealing paradigm, presence of an oligonucleotide that is the direct complement of the displaced strand target region gave a significant block to DNA synthesis. We believe that a competing Watson:Crick pairing of the oligonucleotide generates alternative structures which then compete

with the desired template product in the substrate preparation.

Possible Mechanisms of the Triplex Mediated DNA Polymerase Block. There are several potential models for oligonucleotide directed triple helix inhibition of primer extension on duplex templates. In the systems we have studied, DNA synthesis occurs through a strand displacement mechanism. In order for the polymerase to continue primer extension, it must disrupt the downstream template duplex region. Although Klenow frgament lacks intrinsic helicase activity, it is able to perform strand displacement synthesis (Kornberg & Baker, 1992). One explanation for this phenomenon is that Klenow fragment may be able to exploit breathing of the template duplex beginning at a nick or gap and extending into the fraying branch. Such end melting effects are not fully understood, but it seems possible that the presence of a third strand together with the hydrogen bonding and stacking interactions that accompany triplex formation might reduce this melting or fraying effect. In this model, the polymerase block would be secondary to enhanced duplex stability. One would predict from this model that if short triple helices could be generated using oligonucleotides with enhanced binding affinities due to improved third strand stacking interactions, the efficiency of termination would be correspondingly improved.

An alternative model for the triplex mediated polymerase blockade would be a significant distortion of the duplex template structure near the duplex/triplex junction. Previous chemical footprinting studies have shown that the double helical regions near the triple helical termini are structurally distorted from B-form geometry (Francois et al., 1988; Collier et al., 1991). Such distortion is also suggested by the DNase I footprinting

experiment in this work; it revealed pronounced hypersensitivities at the 3'-junction of triple helices formed with oligonucleotides **y1**, **y2**, and **y4**. DNA polymerases may encounter such alterations in template topology and terminate the polymerization reaction. Other reports have suggested that Z-DNA forming sequences adjacent to intramolecular triple helical structures can cause stoppage that may be due to changes in template topology (Brinton et al., 1991). Nevertheless the fact that shorter triple helical complexes that share identical 5'- or 3'-termini with longer complexes gave the same pattern of DNA synthesis blockage, but have lesser termination efficiency, indicates that the junction by itself cannot be solely responsible for efficient termination.

There is no reported high resolution structure of a paused DNA replication fork. In the most current crystal structure of the Klenow fragment, polymerase is bound to an 11 bp duplex with a single-stranded three base 3'-overhang (Beese et al., 1993). Although this provides no information on structure downstream of the 3'-end of an active extending primer, the dimensions of cleft 1 (containing the polymerase active site) and 2 (formed upon binding duplex DNA) suggest that two DNA strands may be a tight fit, and this leads to speculation that three strands might be sterically disallowed. Indirect evidence concerning polymerase:DNA interactions at the displacement junction has come from DNase I footprinting on a nicked duplex template (Joyce et al., 1986). In this context, Klenow fragment protects 4 base pair non-contact zone on the template strand. These investigators suggest that this is a region where the DNA strand curves away from the polymerase. If correct and important for function, it seems likely that such curvature would be altered by the presence of a third strand agent that can stiffen or distort the

helix. This may account for the observed termination by the triple helix since the complex may prevent the polymerase from accepting the template into the polymerase active site. Moreover, while the current model for the Klenow fragment structure from crystallographic data does not provide guidance for strand displacement, it does suggest that double helical DNA must bend 80° to enter the cleft containing the polymerase active site. This again presents a bending event that may be inhibited by the presence of a preformed triplex.

Inhibition of DNA Synthesis by Intramolecular Triple Helix Formation. Several prior studies have reported that templates that can form intramolecular, rather than intermolecular, triplexes, and that these can inhibit DNA polymerase elongation (Lapidot et al., 1989; Baran et al., 1991; Brinton et al., 1991; Dayn et al., 1992). In all cases, these observations support the central conclusions from this study, although the intramolecular substrates undergo topological changes under triplex-favoring conditions, and the contributions due to such ancillary changes are difficult to clearly separate from direct triplex effects.

The Effect of Triple Helical Complexes on RNA Polymerases. A number of studies have focused on the ability of triple helical complexes to alter transcription by preventing the binding of transcription factors, and this invites comparison with effects on DNA polymerase activities reported here. Several have shown that intermolecular triple helices positioned sufficiently far downstream so that they are presumed to be testing for effects on elongation showed either no blocking effect or minimal ones (Young et al., 1991; Maher, 1992; Duval-Valentin et al.,

1992). Effects on transcriptional initiation are much more robust, and have been generated using triplex sites positioned either upstream (Maher et al., 1990; Maher, 1992) or just downstream (Duval-Valentin et al., 1993) of initiation sites. Not surprisingly, some of the inhibitory effects could be enhanced by covalently linking the third strand reagent to the duplex target (Duval-Valentin et al., 1993). Thus triple helices by themselves do not appear to be very effective in blocking elongation by either prokaryotic or eukaryotic RNA polymerases, and this result might reflect the fact that these polymerases are multiprotein holoenzyme complexes replete with DNA melting and helicase activities (Lewin, 1990). In contrast, triple helices substantially blocked elongation by the DNA polymerases studied in this work. It will now be interesting to extend this to additional DNA polymerase activities in the presence and absence of supporting activities provided by SSBs and helicases. A recent report has indicated that DNA helicases can unwind triple helical complexes (Maine & Kodadek, 1994). Similarly, it will be interesting to test the effects of specifically modified third strand oligonucleotides to discern how they block polymerase progress.

REFERENCES

Abbots, J., SenGupta, D. N., Zon, G., & Wilson, S. H. (1988) *J. Biol. Chem. 263*, 15094-15103.

Baran, N., Lapidot, A., & Manor, H. (1991) *Proc. Natl. Acad. Sci. U. S. A. 88*, 507-511.

Beal, P. A., & Dervan, P. B. (1991) *Science 251*, 1360-1363.

Bedinger, P., Munn, M., & Alberts, B. M. (1989) *J. Biol. Chem. 264*, 16880-16886.

Beese, L. S., Derbyshire, V., & Steitz, T. A. (1993) *Science 260*, 352-355.

Beese, L. S., & Steitz, T. A. (1991) *EMBO-J 10*, 25-33.

Bhanot, O. S., Grevatt, P. C., Donahue, J. M., Gabrielides, C. N., & Solomon, J. J. (1990) *Biochemistry 29*, 10357-10364.

Brinton, B. T., Caddle, M. S., & Heintz, N. H. (1991) *J. Biol. Chem. 266*, 5153-5161.

Collier, D. A., Mergny, J. L., Thuong, N. T., & Helene, C. (1991) *Nucleic Acids Res. 19*, 4219-4224.

Comess, K. M., Burstyn, J. N., Essigmann, J. M., & Lippard, S. J. (1992)

Biochemistry 31, 3975-3990.

Cooney, M., Czernuszewicz, G., Postel, E. H., Flint, S. J., & Hogan, M. E. (1988)*Science 241*, 456-459.

Dayn, A., Samadashwily, G. M., & Mirkin, S. M. (1992) *Proc. Natl. Acad. Sci. U. S. A. 89*, 11406-11410.

de los Santos, C., Rosen, M., & Patel, D. (1989) *Biochemistry 28*, 7282-7289.

Derbyshire, V., Freemont, P. S., Sanderson, M. R., Beese, L., Friedman, J. M., Joyce, C. M., & Steitz, T. A. (1988) *Science 240*, 199-201.

Dreyer, G. B., & Dervan, P. B. (1985) *Proc. Natl. Acad. Sci. U. S. A. 82*, 968-972.

Duval-Valentin, G., Thuong, N. T., & Helene, C. (1992) *Proc. Natl. Acad. Sci. U. S. A. 89*, 504-508.

Francois, J.-C., Saison-B. T., & Helene, C. (1989) *Nucleic Acids Res. 16*, 11431-11440.

Francois, J.-C., Saison-Behmoaras, T., Thuong, N. T., & Helene, C. (1989) *Biochemistry 28*, 9617-9619.

Giovannangeli, C., Thuong, N. T., & Helene, C. (1993) *Proc. Natl. Acad. Sci. U. S. A. 90*, 10013-10017.

Grevatt, P. C., Donahue, J. M., & Bhanot, O. S. (1991) *J. Biol. Chem. 266,* 1269-1275.

Hanvey, J. C., Shimizu, M., & Wells, R. D. (1990) *Nucleic Acids Res. 18,* 157-161.

Huang, C. C., Nguyen, D., Martinez, R., & Edwards, C. A. (1992) *Biochemistry 31,* 993-998.

Joyce, C. M., Ollis, D. L., Rush, J., Steitz, T. A., Konigsberg, W. H., & Grindley, N. D. F. (1986) in *Protein Structure, Folding and Design* (UCLA Symposia on Molecular and Cellular Biology, Vol. 32) (D. Oxender, ed.), pp. 197-205, Alan R. Liss.

Joyce, C. M., & Steitz, T. A. (1987) *TIBS* 12, 288-292.

Kornberg, A., & Baker, T. A. (1992) *DNA Replication,* 2nd ed., W. H. Freeman and Company, New York.

Lapidot, A., Baran, N., & Manor, H. (1989) *Nucleic Acids Res. 17,* 883-900.

Le Doan, T., Perrouault, L., Praseuth, D., Habhoub, N., Decout, J.-L., Thuong, N. T., Lhomme, J., & Helene, C. (1987) *Nucleic Acids Res. 15,* 7749-7760.

Lee, E. H. & Kornberg, A. (1992) *J. Biol. Chem. 267,* 8778-8784.

Lewin, B. (1990) *Genes IV*, Oxford University Press, New York.

Maher, L. J. (1992) *Biochemistry 31*, 7587-7594.

Maher, L. J., III, Wold, B., & Dervan, P. B. (1989) *Science 245*, 725-730.

Maher, L. J., III, Dervan, P. B., & Wold, B. J. (1990) *Biochemistry 29*, 8820-8826.

Maher, L. J., III, Dervan, P. B., & Wold, B. (1992) *Biochemistry 31* 70-81.

Maine, I. P., & Kodadek, T. (1994) *Biochem. Biophys. Res. Comm. 204*, 1119-1124.

Moser, H. E., & Dervan, P. B. (1987) *Science 238*, 645-650.

Ollis, D. L., Brick, P., Hamlin, R., Xuong, N. G., & Steitz, T. A. (1985) *Nature 313*, 762-766.

Radhakrishnan, I., de los Santos, C., & Patel, D. J. (1991) *J. Mol. Biol. 221*, 1403-1418.

Rajagopal, P., & Feignon, J. (1989) *Nature 339*, 637-640.

Sambrook, J., Fritsch, E. F., & Maniatis, T. (1989) *Molecular Cloning, A Laboratory Manual*, 2nd ed., Cold Spring Harbor Laboratory, Cold Spring Harbor, NY.

Samadashwily, G. M., Dayn, A., & Mirkin, S. M. (1993) *EMBO J. 12*, 4975-4983.

Shibutani, S., Bodepudi, V., Johnson, F., & Grollman, A. P. (1993) *Biochemistry 32*, 4615-4621.

Simha, D., Vaseem, A. P., & Humayun, M. Z. (1991) *Biochemistry 30*, 8727-8735.

Sun, D., & Hurley, L. H. (1992) *Biochemistry 31*, 2822-2829.

Strauss, B. S. (1991) *BioEssays 13*, 79-84.

Tabor, S., & Richardson, C. C. (1989) *J. Biol. Chem. 264*, 6447-6458.

Wartell, R. M., Larson, J. E., & Wells, R. D. (1974) *J. Biol. Chem. 249*, 6719-6731.

Weiland, K. L., & Dooley, T. P. (1991) *Biochemistry 30*, 7559-7565.

Weisman, S-. P., Dube, D. K., Perrino, F. W., Stokes, K., Loeb, L. A. & Fry, M. (1989) *Biochem. Biophys. Res. Commun. 164*, 1149-1156.

Young, S. L., Krawczyk, S. H., Matteucci, M. D., & Toole, J. J. (1991) *Proc. Natl. Acad. Sci. U. S. A. 88*, 10023-10026.

Chapter VI

Phosphorothioate Oligonucleotide-Directed Triple Helix Formation

INTRODUCTION

Oligonucleotide-directed triple helix formation is a powerful chemical approach for the sequence-specific recognition of double-helical DNA. Two distinct structural motifs are known to exist for triple helix formation. Pyrimidine-rich oligonucleotides bind in a parallel orientation to purine rich strands in double-helical DNA through the formation of specific Hoogsteen hydrogen bonds (T•AT and C^+•GC base triplets) in pyrimidine•purine•pyrimidine triple helices (Moser & Dervan, 1987; Le Doan et al., 1987; Rajagopal & Feigon, 1989; de los Santos et al., 1989). Alternatively, purine-rich oligonucleotides bind in an antiparallel orientation relative to purine rich strands in double-helical DNA through the formation of reverse Hoogsteen hydrogen bonds (G•GC and T•AT or A•AT base triplets) in purine•purine•pyrimidine triple helices (Beal & Dervan, 1991; Chen, 1991; Pilch et al., 1991; Durland et al., 1991; Radhakrishnan et al., 1991; Radhakrishnan et al., 1993; Radhakrishnan & Patel, 1993a).

Phosphorothioate internucleotide linkages have been among the most widely examined oligonucleotide backbone modifications in both biophysical and pharmacological studies (Stein & Cheng, 1993). Phosphorothioate modified oligonucleotides have played key roles in

studies of nucleic acid recognition and processing (Eckstein, 1983). Although they possess many favorable attributes such as increased stability to cellular nucleases, phosphorothioate modifications introduce a chiral center at each internucleotide linkage that can lead to the formation of 2^n diastereomers per n internucleotide linkages. Interest in synthesizing oligonucleotides with stereoregular phosphorothioate linkages has been encouraged by biophysical studies that suggest phosphorothioate oligonucleotides exclusively containing all *R*P or *S*P diastereomer linkages have different affinities for single-stranded and double-stranded nucleic acids (Cosstick & Eckstein, 1985; LaPlanche et al., 1986; Latimer et al., 1989; Kim et al., 1992).

In this chapter, the ability of oligonucleotides containing diastereomeric mixtures of phosphorothioate linkages to form triple-helical complexes in both the pyrimidine and purine motifs is examined. A method for the enzymatic production of pure *R*P phosphorothioate oligonucleotides based on the work of Eckstein and coworkers and the effectiveness of these nonnatural nuclease resistant oligonucleotides for triple helix formation is reported. Furthermore, phosphorothioate pyrimidine-rich and purine-rich oligonucleotides containing modified nucleosides were designed to promote triple helix formation *in vitro* under physiological ionic conditions. These nucleic acid analogs may prove useful for *in vitro* and *in vivo* biological model systems.

EXPERIMENTAL

Materials. All DNA synthesis reagents, including tetraethylthiuram disulfide, were obtained from Applied Biosystems Inc. except for uridine phosphoramidite obtained from BioGenex and 5-methyl-2'-deoxycytidine phosphoramidite , 5-(1-propynyl)-2'-deoxyuridine phosphoramidite, 5-(1-propynyl)-2'-OMe-uridine phosphoramidite, 2'-OMe-cytidine phosphoramidite, and S6-DNP-dG-phosphoramidite obtained from Glen Research. P1 phosphoramidite and P1 CPG were the generous gifts of Scott Priestley, All restriction enzymes, T4 DNA ligase, and DNase I were purchased from Boehringer Mannheim. Sequenase 2.0 was obtained from U. S. Biochemicals. The *S*P isomers of 2'-deoxynucleoside 5'-O-(1-thiotriphosphates) were obtained from Amersham.

Synthesis and Purification Of Oligonucleotides. Oligonucleotides were synthesized on an Applied Biosystems 380B DNA Synthesizer using β-cyanoethyl phosphoramidite chemistry. Oligonucleotides containing a diastereomeric mixture of phosphorothioate linkages were prepared using β-cyanoethyl phosphoramidite chemistry and oxidation with tetraethylthiuram disulfide (Vu & Hirschbein, 1991). Oligonucleotide **RS1**, containing 6-thioguanosine nucleosides, was deprotected according to the method of Xu (Xu et al., 1992). The solid support was removed from the column and treated with 10 mL of 10% β-mercaptoethanol/ ammonium hydroxide in a closed 15-mL Falcon tube. The reaction was incubated in a 37 °C incubator shaking at 200 rpm for 48 hours. The solution was spun in a clinical centrifuge and the supernatant dried through lyophilization. Oligonucleotides were purified on 20% denaturing polyacrylamide gels,

visualized by UV shadowing, and electroeluted from gel slices using an Elu-trap apparatus (Schleicher & Schuell). They were desalted using Sep-Pak reverse pahse chromatography (Waters) and resuspended in 0.5X TE before storing at -80 °C (Sambrook et al., 1989). The concentration of oligonucleotides were determined by A_{260} measurements using the following molar extinction coefficients: 15,400 (A), 11,700 (G), 7,300 (C), 8,800 (T), 5,800 (^{me}C), 9,700 (PU), 2,500 (P1), and 9,000 (^{s}G) (Fox et al., 1958).

Plasmid Construction. The plasmid pTER I was obtained by cloning the oligonucleotides 5'-pTCGACTTTTTTTCTTTTCTTTCTTTTTTTTTTTTGG CGCATG-3' and 5'-pCGCCAAAAAAAAAAAAGAAAGAAAAAGAAAA AAAG-3' into the large Sal I-Sph I restriction fragment of pUC19. The plasmid pTER 3 was obtained by cloning the oligonucleotides 5'-pGGGAAAAAGAGAGAGAGAGCTGCAGGCGGCCGCCACTAGTGAGG GAGGGGAGGGGAGGGAGCTGCT-3' and 5'-pCTAGAGCAGCTCCCTCCC CTCCCCTCCCTCACTAGTGGCGGCCGCCTGCAGCTCTCTCTCTCTTTTTC CC-3' into the large Sma I-Xba I restriction fragment of pTER I.

DNase I Footprinting. Either the 438-bp EcoR I-Afl III restriction fragment of pTER I or the 338-bp Hind III-Nar I restriction fragment of pTER 3 was 3'-end labeled with deoxyadenosine -[α^{32}P]- triphosphate (New England Nuclear) and chemically sequenced (Sambrook et al., 1989). Labeled DNA (30,000 cpm) and oligonucleotide were incubated in either association buffer I (Table I), association buffer II (Table II), or association buffer III (Table III) for 24 hours at 25 °C. A 1 µL volume of DNase I (0.1 U/µL in 10 mM $MgCl_2$, 10 mM $CaCl_2$, 20 mM Tris-Cl pH 8.0) was added to the reaction and incubated for 3 minutes at 25 °C before termination by

ethanol precipitation and resuspension in formamide/TBE loading buffer. Samples were analyzed by electrophoresis on 8% denaturing polyacrylamide gels. Gels were dried and placed on film or photostimulable phosphor imaging plates and quantitated as described (Singleton & Dervan, 1992).

Synthesis Of Stereoregular Phosphorothioate Oligonucleotides. DNA template **R1** 5'-ACCCACCCCACCCCACCCAAGGGTTGATGGAAGG-3' or **Y1** 5'-AAAAAAAGAAAAAGAAAAGGGTTGATGGAAGG-3' (5 nmoles) was added to 5 nmoles of oligonucleotide primer **S1** 5'-CCTTCCATCAACCCrUT-3' in a 20 μL volume of 1X Sequenase Buffer. The mixture was heated to 80 °C for 2 minutes prior to slow cooling to 37 °C. The reaction was brought up to a final volume of 100 μL in 1X Sequenase Buffer containing 4 mM DTT with the addition of 1 mM deoxyguanosine 5' (αthio) triphosphate and 1 mM thymidine 5' (αthio) triphosphate in the case of template **R1** or 1 mM thymidine 5' (αthio) triphosphate and 1 mM deoxycytidine 5' (αthio) triphosphate in the case of template **Y1**. Sequenase 2.0 (10 U) was added and the reaction was allowed to proceed for 5 hours at 37 °C. The reaction was terminated by ethanol precipitation, dissolved in 500 μL ammonium hydroxide solution, and incubated at 55 °C overnight. The DNA products were dried and resuspended in formamide/TBE loading buffer before purification on a 20% denaturing polyacrylamide gel.

RESULTS

Design of Stereoregular Phosphorothioate Oligonucleotides. Oligonucleotides containing exclusively *R*P phosphorothioate linkages were made according to the scheme in Figure 1. All reported DNA polymerases accept only the *S*P isomers of 2'-deoxynucleoside 5'-O-(1-thiotriphosphates), producing the *R*P linkage by inversion of configuration at phosphorus (Burgers & Eckstein, 1979; Romaniuk & Eckstein, 1982; Brody et al., 1982; Eckstein, 1985). A primer extension system was designed with a DNA primer containing a single ribonucleotide as the penultimate residue. Extension in the presence of 2'-deoxynucleoside 5'-O-(1-thiotriphosphates) yields a full length duplex with one strand the DNA template and the other strand the elongated primer containing *R*P deoxyribophosphorothioate internucleotide linkages. Treatment of this chimeric duplex with base cleaves the labile ribophosphodiester linkage to separate the DNA primer from the stereoregular (*R*P) phosphorothioate oligonucleotide extension product. Denaturing polyacrylamide gel electrophoresis separates the three strands to isolate the stereoregular (*R*P) phosphorothioate oligonucleotide.

Design of Physiological Ionic Conditions to Assay for Triple Helix Formation. To determine if oligonucleotides have the potential to hybridize *in vivo* with double stranded DNA, *in vitro* DNase I assays were performed under physiological nuclear ionic conditions. The nuclear ionic conditions of Stage IV *Xenopus* oocytes were chosen since they closely mimic those found in most other eukaryotic cells and also because these oocytes were used to examine *in vivo* triple helix formation

(Chapter 6). The oocyte nucleus contains a higher concentration of potassium and lower concentrations of sodium than the cytoplasm (Horowitz et al., 1979; Horowitz & Paine, 1979; Paine et al., 1981; Ibrahim & Dick, 1984; Paine et al., 1992). It has been estimated that the nucleus contains 130 mM KCl and 15 mM NaCl while the cytoplasm contains 30 mM KCl and 80 mM NaCl (Paine et al., 1992). The asymmetric distribution of monovalent cations may be due to either the exclusion or sequestration of the cations in a cellular compartment. There is no active transport of potassium into the nucleus and a significant portion of potassium in the nucleus may be bound by protein (Paine et al., 1992). The intracellular concentration of magnesium in *Xenopus* oocytes has been estimated to be approximately 3 mM (Belle et al., 1986). The intraceullar levels of the polyamines spermine, spermidine, and putrescine have been estimated to be approximately 0.1 mM, 0.8 mM, and 1.4 mM, respectively (Sunkara et al., 1981; Osborne et al., 1989). The intracellular pH of the *Xenopus* oocyte has been estimated to be approximately pH 7.45 (Webb & Nuccitelli, 1981; Giaume & Kado, 1983). All these parameters will vary according to the stage of oocyte development and culture conditions. However, these estimates provide guidelines to assay if oligonucleotides have a reasonable chance to form triple helical structures *in vivo*.

Effect of Phosphorothioate Backbone on Triple Helix Formation By Oligonucleotides Containing Natural Nucleosides. Quantitative DNase I footprint titration experiments reveal that a purine-rich oligonucleotide with stereoregular (*R*P) or diastereomeric mixtures of phosphorothioate linkages had similar affinity for the purine target site relative to the phosphodiester oligonucleotide (figure 2, Table I). In sharp contrast,

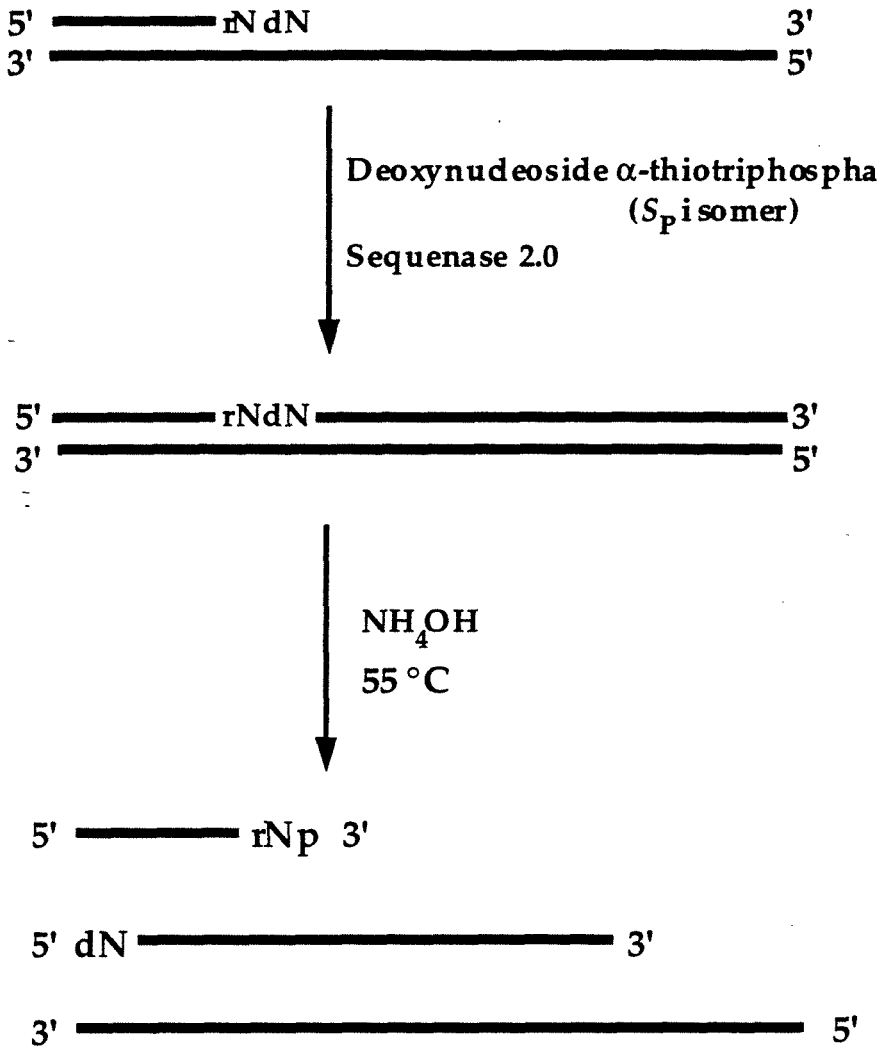

Figure 1: Synthetic scheme for the stereoregular (*R*P) phosphorothioate oligonucleotide synthesis. N refers to any base complementary to the template.

neither pure *R*P nor diastereomeric phosphorothioate pyrimidine oligonucleotide had measurable affinity for the homopurine target site which differs markedly from the energetics of the corresponding phosphodiesters (figure 3, Table II).

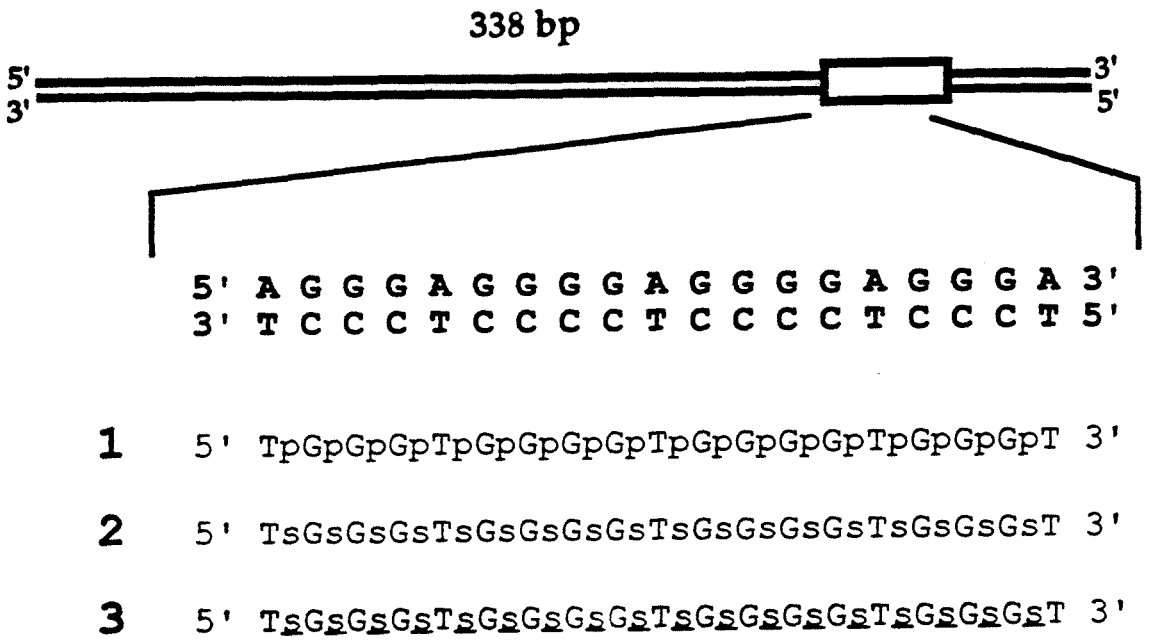

Figure 2: Sequence of the 21-bp purine motif target site along with the relative position of the target site within the radiolabeled duplex and modified oligonucleotides tested. Key: p = phosphodiester, s = phosphorothioate mixed diastereomers.

Table I. Equilibrium association constants for purine-rich oligonucleotides[a]

oligonucleotide	K (M^{-1})	ΔG (kcal mol^{-1})
1	1.6 (± 0.2) X 10^7	-9.8 (± 0.1)
2	2.8 (± 0.3) X 10^7	-10.2 (± 0.1)
3	2.6 (± 0.3) X 10^7	-10.1 (± 0.1)

[a]Values reported in the table are mean values measured from four repetitions of DNase I titration experiments performed in association buffer I (20 mM NaCl, 100 μM spermine, 25 mM Tris-OAc, pH 7.2, 25 °C)

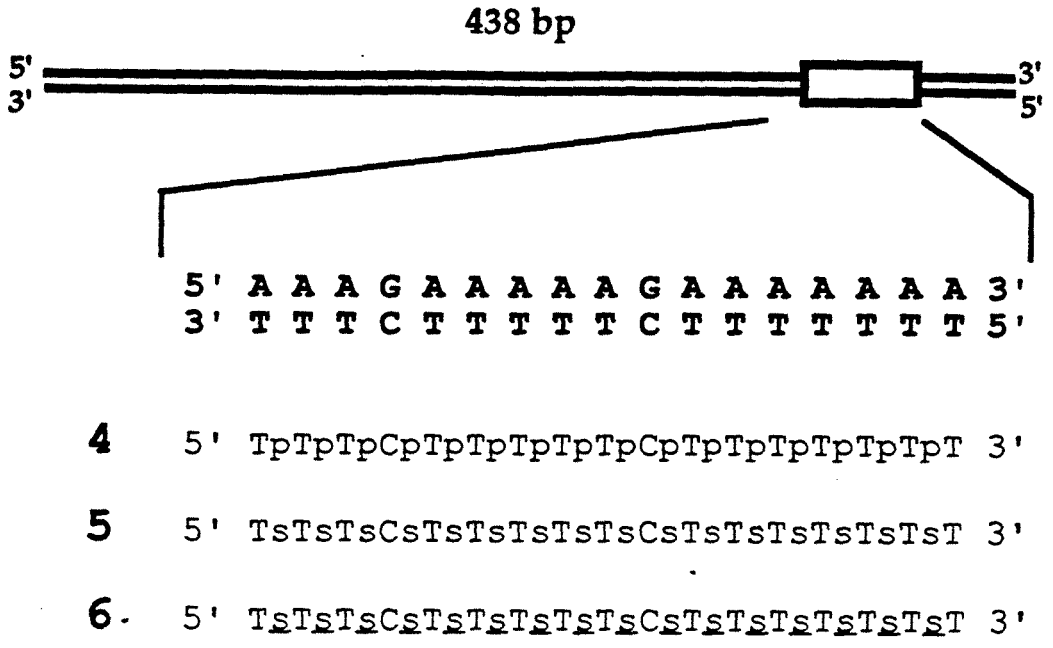

Figure 3: Sequence of the 17-bp pyrimidine motif target site along with the relative position of the target site within the radiolabeled duplex and oligonucleotides tested. Key: p = phosphodiester, s = phosphorothioate mixed diastereomers, s = phosphorothioate *R*P diastereomer.

Table II. Equilibrium association constants for pyrimidine-rich oligonucleotides[a]

oligonucleotide	K (M^{-1})	ΔG (kcal mol^{-1})
4	4.9 (± 0.6) X 10^7	-10.5 (± 0.1)
5	<1 X 10^5	
6	<1 X 10^5	

[a]Values reported in the table are mean values measured from four repetitions of DNase I titration experiments performed in association buffer II (20 mM NaCl, 20 mM $MgCl_2$, 100 μM spermine, 50 mM Tris-Cl, pH 7.2, 25 °C)

Effect of Modified Purine Nucleosides on Phosphorothioate Oligonucleotide-Directed Triple Helix Formation Under Physiological Ionic Conditions. Under physiological ionic conditions, purine-rich oligonucleotides containing guanine nucleosides and either phosphodiester or a diastereomeric mixture of phosphorothioate internucleotide linkages do not have measurable affinity for the homopurine target site (Figure 4 and Table III). The inclusion of either thymidine, adenine, 5-bromo-2'-deoxyuridine, or 5-(1-propynyl)-2'-deoxyuridine nucleosides (oligonucleotides **SR2**, **SR3**, **SR4**, and **SR5**, respectively) for AT base pair recognition does not measurably enhance binding. Although the modified nucleoside P1 was incorporated into oligonucleotide **SR6** for GC base pair recognition along with 5-(1-propynyl)-2'-deoxyuridine nucleosides for AT base pair recognition, no binding was detected. The P1 nucleoside has been used for parallel triple helix formation for the pH independent recognition of GC base pairs (Koh & Dervan, 1992). On the other hand, inclusion of 6-thio-2'-deoxyguanosine nucleosides (oligonucleotide **RS1**) for GC base pair recognition rescues binding to the triple helix target site (Figure 5 and Table III).

Effect of Modified Pyrimidine Nucleosides on Phosphorothioate Oligonucleotide-Directed Triple Helix Formation Under Physiological Ionic Conditions. Under physiological ionic conditions, phosphodiester oligonucleotide **SY1** (containing thymidine and 5-methyl-2'-deoxycytidine nucleosides) has moderate affinity for the homopurine target site (Figures 6-7 and Table III). The introduction of a phosphorothioate backbone creates oligonucleotide **SY2** which lacks measurable affinity for the target

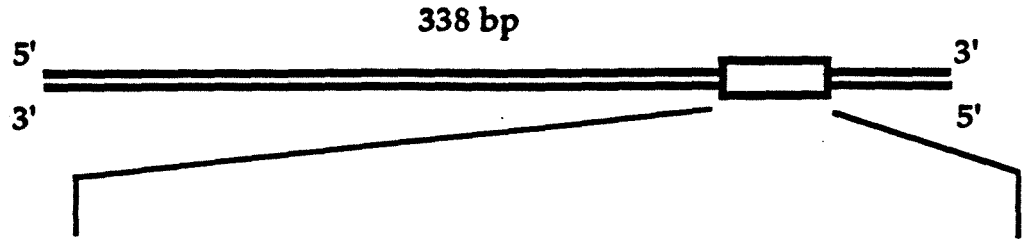

SR1 5' GpTpGpGpGpTpGpGpGpGpTpGpGpGpGpTpGpGpGpTpG 3'

SR2 5' GsTsGsGsGsTsGsGsGsGsTsGsGsGsGsTsGsGsGsTsG 3'

SR3 5' GsAsGsGsGsAsGsGsGsGsAsGsGsGsGsAsGsGsGsAsG 3'

SR4 5' GsUsGsGsGsUsGsGsGsGsUsGsGsGsGsUsGsGsGsUsG 3' (Br at U positions)

SR5 5' GsUsGsGsGsUsGsGsGsGsUsGsGsGsGsUsGsGsGsUsG 3' (p at U positions)

SR6 5' PsUsPsPsPsUsPsPsPsPsUsPsPsPsPsUsPsPsPsUsP 3' (p at U positions)

RS1 5' GsTsGsGsGsTsGsGsGsGsTsGsGsGsGsTsGsGsGsTsG 3' (s at all positions)

Figure 4: Sequence of the 21-bp purine motif target site along with the relative position of the target site within the radiolabeled duplex and modified oligonucleotides tested. Key: p = phosphodiester, s = phosphorothioate mixed diastereomers, ^{Br}U = 5-bromo-2'-deoxyuridine, PU = 5-(1-propynyl)-2'-deoxyuridine, P1 = 3-methyl-5-amino-7H-pyrazolo (4, 3-d) pyrimidine-7-one.

site. However, inclusion of 5-(1-propynyl)-2'-deoxyuridine and 5-methyl-2'-deoxycytidine nucleosides with either a phosphodiester or phosphorothioate backbone (oligonucleotides **SY3** and **YS1**) causes a dramatic increase in binding affinity (Table III). The association constants were not measured for these tightly binding oligonucleotides since the concentration of radiolabelled template becomes significant under assay conditions.

Figure 5: Quantitative *in vitro* DNaseI footprinting analysis of oligonucleotide **RS1** under physiological ionic conditions. Oligonucleotide **RS1** was allowed to equilibrate with the ^{32}P 3'-end labelled 338-bp Nar I-Hind III restriction fragment from pTER I for 24 hours at room temperature prior to analysis. Lane 1, A + G specific chemical sequencing lane; lane 2, DNase I control lane; lane 3, 1 nM **RS1**; lane 4, 5 nM **RS1**; lane 5, 10 nM **RS1**; lane 6, 25 nM **RS1**; lane 7, 40 nM **RS1**; lane 8, 50 nM **RS1**; lane 9, 75 nM **RS1**; lane 10, 100 nM **RS1**; lane 11, 200 nM **RS1**; lane 12, 400 nM **RS1**; lane 13, 500 nM **RS1**; lane 14, DNase I control lane; lane 15, no DNase I control.

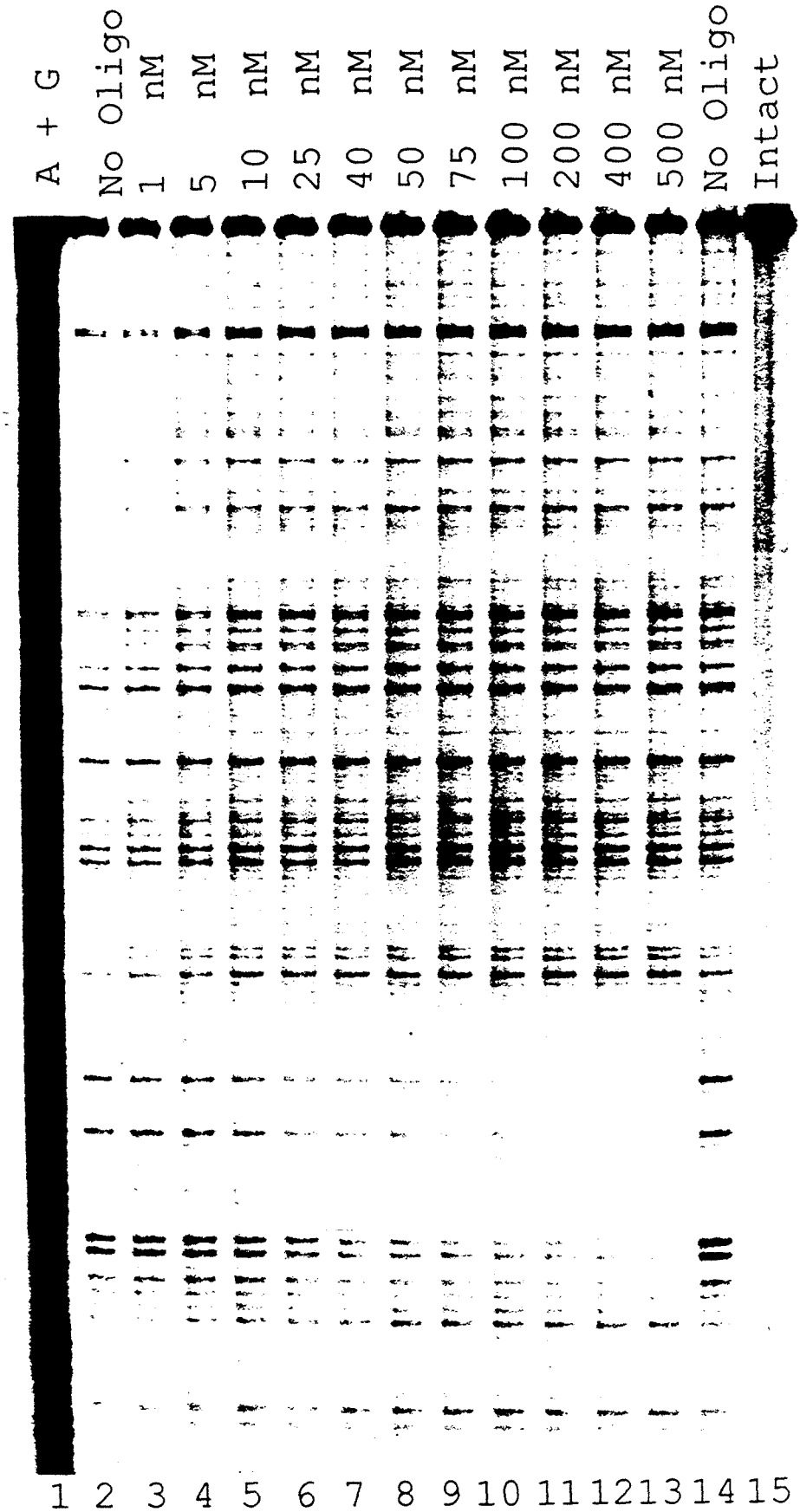
A + G
No Oligo
1 nM
5 nM
10 nM
25 nM
40 nM
50 nM
75 nM
100 nM
200 nM
400 nM
500 nM
No Oligo
Intact
1 2 3 4 5 6 7 8 9 10 11 12 13 14 15

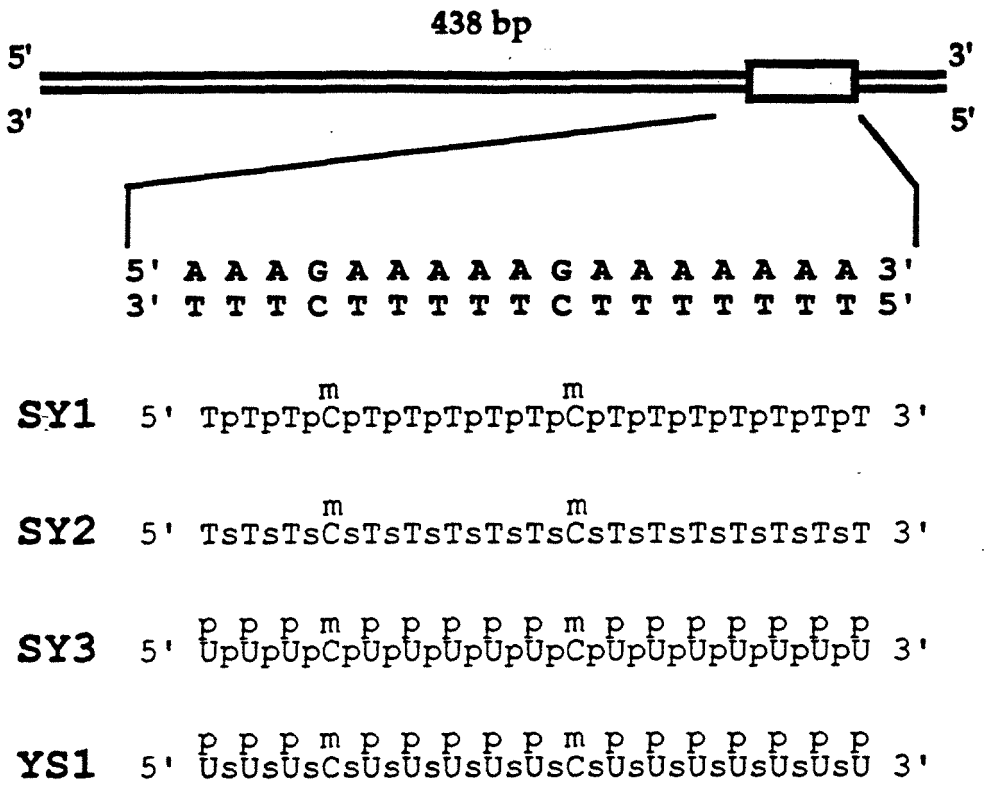

Figure 6: Sequence of the 17-bp pyrimidine motif target site along with the relative position of the target site within the radiolabeled duplex and modified oligonucleotides tested. Key: p = phosphodiester, s = phosphorothioate mixed diastereomers, ^{me}C = 5-methyl-2'-deoxycytidine, PU = 5-(1-propynyl)-2'-deoxyuridine.

Figure 7: Quantitative *in vitro* DNaseI footprinting analysis of oligonucleotide **SY1** under physiological ionic conditions. Oligonucleotide **SY1** was allowed to equilibrate with the ^{32}P 3'-end labelled 438-bp EcoR I-Afl III restriction fragment from pTER I for 24 hours at room temperature prior to analysis. Lane 1, A + G specific chemical sequencing lane; lane 2, DNase I control lane; lane 3, 1 nM **SY1**; lane 4, 4 nM **SY1**; lane 5, 10 nM **SY1**; lane 6, 15 nM **SY1**; lane 7, 25 nM **SY1**; lane 8, 40 nM **SY1**; lane 9, 50 nM **SY1**; lane 10, 75 nM **SY1**; lane 11, 100 nM **SY1**; lane 12, 300 nM **SY1**; lane 13, DNase I control; lane 14, no DNase I control.

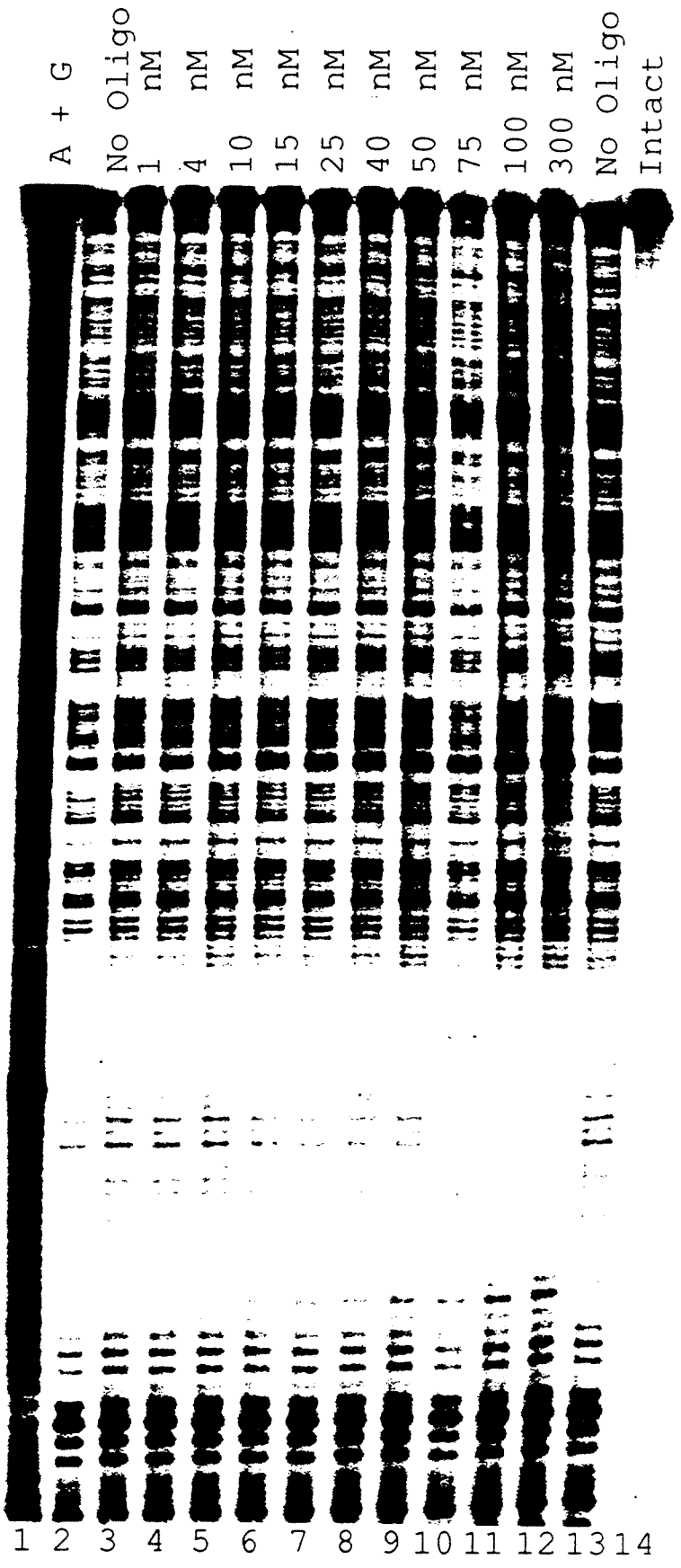
A + G
No Oligo
1 nM
4 nM
10 nM
15 nM
25 nM
40 nM
50 nM
75 nM
100 nM
300 nM
No Oligo
Intact
1 2 3 4 5 6 7 8 9 10 11 12 13 14

Table III. Equilibrium association constants for modified pyrimidine and purine oligonucleotides[a]

oligonucleotide	K (M^{-1})	ΔG (kcal mol^{-1})
SY1	1.2 (±0.2) X 10^7	-9.7 (± 0.1)
SY2	<1 X 10^5	
SY3	>2 X 10^8	
YS1	>2 X 10^8	
SR1	<1 X 10^5	
SR2	<1 X 10^5	
SR3	<1 X 10^5	
SR4	<1 X 10^5	
SR5	<1 X 10^5	
SR6	<1 X 10^5	
RS1	1.6 (±0.3) X 10^7	-9.8 (± 0.1)

[a]Values reported in the table are mean values measured from four repetitions of DNase I titration experiments performed in *Xenopus* Ionic buffer (130 mM KCl, 15 mM NaCl, 3 mM $MgCl_2$, 0.1 mM spermine, 0.8 mM spermidine, 1.4 mM putrescine, 20 mM Tris-Cl, pH 7.45, 25 °C)

DISCUSSION

Two different structural motifs previously defined for phosphodiester oligonucleotides were considered in analyzing the effect of phosphorothioate internucleotide linkages on triple helix formation. The sequences of the triple helical target sites are given in Figures 2, 3, 4 and 6. Both modified purine-rich and modified pyrimidine rich oligonucleotides containing a diastereomeric mixture of internucleotide linkages were found to bind double helical DNA with high affinity under physiological ionic conditions (Figure 8, Table III).

Other Reports of Phosphorothioate Triple Helix Formation. There have been several reports involving the use of phosphorothioate oligonucleotides to form triple helical complexes. Lee and co-workers reported the effect of stereoregular (all *R*P) phosphorothioate polymers on triple helix formation through UV melting experiments (Latimer et al., 1989). The authors concluded that all phosphorothioate DNA polymers containing a phosphorothioate modification 5' to a purine have a higher Tm than if the modification is 5' to a pyrimidine. Furthermore, having the phosphorothioate modification 5' to a purine promotes triple helix formation while having it 5' to a pyrimidine destabilizes the triple helix. No experiments examined triple helix formation between a phosphorothioate containing polymer and an all-phosphodiester polymeric duplex due to the limitations of the polymeric system. Nevertheless, this study provided the first insight that the stability of phosphorothioate triple helical complexes may be subject to sequence composition effects.

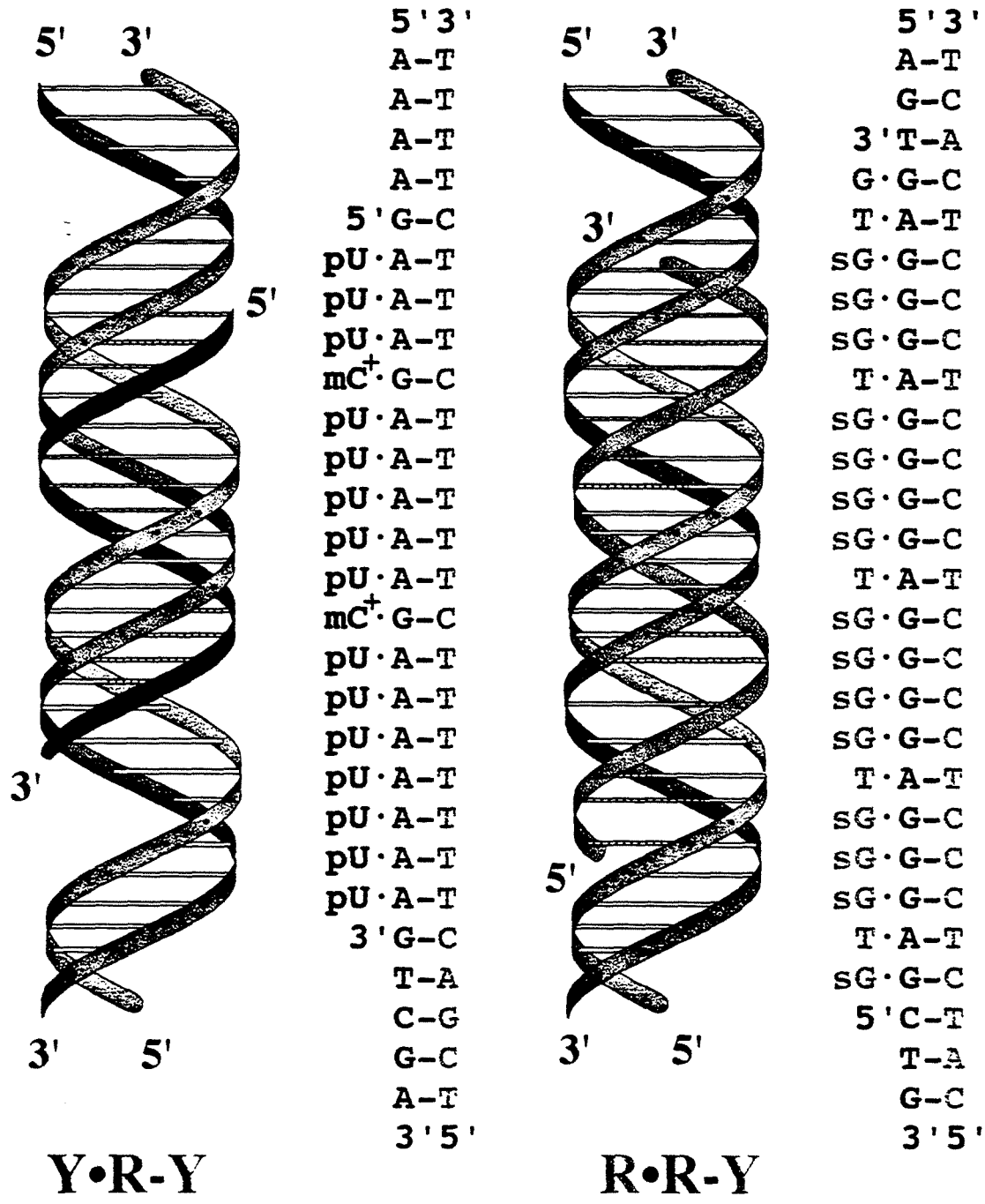

Figure 8. Ribbon Model Of Modified Phosphorothioate Triple Helical Complexes.

Takaku and co-workers demonstrated that introducing a single phosphorothioate linkage in an all-thymidine 15mer oligodeoxyribonucleotide dramatically decreases triple helix formation through UV melting experiments (Kim et al., 1992). Inclusion of a single phosphorothioate linkage in the *R*P configuration was more energetically favorable towards triple helix formation, producing a 13 °C decrease in T_m, than a linkage in the *S*P configuration, producing a 23 °C decrease in T_m. An all-thymidine 15mer oligodeoxyribonucleotide, containing a diasteremeric mixture of phosphorothioate internucleotide linkages, could not form a detectable triple helical complex with its target site under standard assay conditions (10 mM phosphate buffer, pH 7.2, 100 mM NaCl). The fact that single phsophorothioate modifications do not completely inhibit triple helix formation was used by Takaku and co-workers to design 3'- and 5'-end capped phosphorothioate oligonucleotides (Tsukahara et al., 1993). Such oligonucleotides were shown to bind to double helical DNA with lessened affinity than the phosphodiester counterparts.

Quadrifoglio and co-workers examined the ability of short pyrimidine-rich oligonucleotides, with a diastereomeric mixture of phosphorothioate internucleotide linkages, to form triple helical complexes with a target hairpin duplex through CD and UV melting experiments (Xodo et al., 1994). An 11mer phosphorothioate oligonucleotide, containing six cytosines and five thymidines, was shown to form a weak triple helical complex with the target hairpin under nonstringent conditions (0.1 M sodium acetate, pH 5.0, 50 mM NaCl, 10 mM $MgCl_2$). However, under slightly more stringent conditions (0.1 M sodium acetate, pH 6.0, 50 mM NaCl, 10 mM $MgCl_2$) the phosphorothioate oligonucleotide, unlike its

phosphodiester counterpart, could no longer form a triple helical complex. Furthermore, the authors show that under the pH 5.0 conditions there is an approximate 2 °C depression in T_m per phosphorothioate internucleotide linkage.

Strekowski and co-workers examined the effect of triple helix stabilizing ligands on pyrimidine-rich phosphorothioate triple helix formation through UV melting analysis (Wilson et al., 1993). In the absence of stabilizing ligand, an oligodeoxyribonucleotide containing a diastereomeric mixture of phosphorothioate internucleotide linkages was shown to lack affinity for double helical DNA. However, the triple helix stabilizing quinoline intercalator causes a triple helical complex of modest energetic stability was found to form. These stabilizing ligands potentially could be used with other modified oligonucleotide which have low affinity for double-helical DNA.

Possible Explanations for Differences Between Pyrimidine-Rich and Purine-Rich Phosphorothioate Oligonucleotide-Directed Triple Helix Formation Using Natural Nucleosides. Model building and NMR studies suggest that the placement of the third strand oligonucleotide in the major groove of DNA only slightly differs for purine•purine•pyrimidine and pyrimidine•purine•pyrimidine triple helical structures. Both the purine•purine•pyrimidine and pyrimidine•purine•pyrimidine third strand phosphodiesters are displaced toward the purine strand of the Watson-Crick double helix (Radhakrishnan & Patel, 1993b). It is possible that the replacement of either the *pro-R*P or *pro-S*P oxygen atoms for a larger sulfur atom leads to steric crowding in the pyrimidine•purine•pyrimidine triple helix. However, analysis NMR

structural models of pyrimidine and purine motif triple helical complexes, does not indicate any significant negative steric interactions due to a stereoregular all *R*P phosphorothioate backbone (figures 9 and 10). Alternatively, since hydrogen bonds to sulfur are likely weaker than those to oxygen, it is possible that the phosphorothioate modifications disturb specific backbone hydrogen bonding interactions such as localized binding of water in the major groove (Cosstick & Eckstein, 1985). Furthermore, the charge distribution on the phosphodiester backbone is changed in the phosphorothioate linkages. The major resonance form of the phosphorothioate backbone appears to be one in which the phosphorus nonbridging oxygen bond order is close to 2 and sulfur carries a full negative charge (Frey & Sammons, 1985). Coulombic repulsion due to phosphorothioate substitutions could possibly be energetically destabilizing in the pyrimidine motif. Moreover, the increased polarizability of sulfur relative to oxygen may alter the specificity of stabilizing cations binding to the phosphorothioate internucleotide linkages. These structural implications are non-exclusive, and the relative contributions of each to triplex stability will require further studies. The distinction between the effects of the phosphorothioate backbone in the pyrimidine versus purine motifs is sufficiently large that we expect it to generalize to other target sequences and their corresponding oligonucleotides. However, the modest differences between phosphodiester and phosphorothioate oligonucleotides in the purine motif suggest that sequence composition effects must be examined further.

Possible Reasons for Purine-Rich Phosphorothioate Triple Helix

Figure 9: Modified NMR structural model of a purine•purine•pyrimidine intramolecular triple helix in which sulfur atoms are introduced via molecular modelling to produce a stereoregular (all *R*P) phosphorothioate third strand (Radhakrishnan & Patel, 1993b). The purine and pyrimidine strands of the double-helical target are depicted in blue and green, respectively. The third purine-rich strand is depicted in light red with sulfurs atoms shaded in darker red.

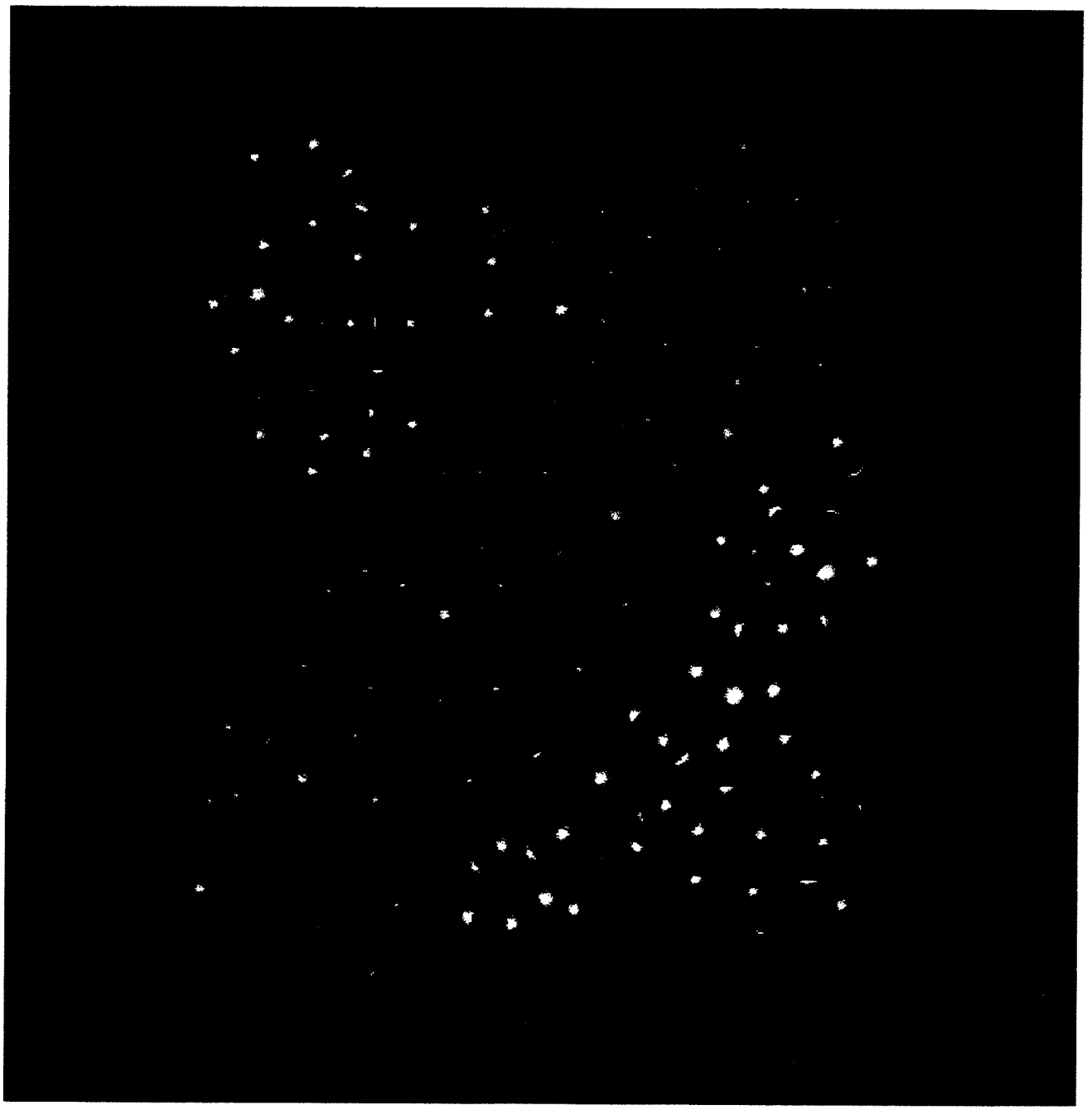

Figure 10: Modified NMR structural model of a pyrimidine•purine•pyrimidine intramolecular triple helix in which sulfur atoms are introduced via molecular modelling to produce a stereoregular (all *R*P) phosphorothioate third strand (Radhakrishnan & Patel, 1994). The purine and pyrimidine strands of the double-helical target are depicted in blue and green, respectively. The third pyrimidine-rich strand is depicted in light red with sulfurs atoms shaded in darker red.

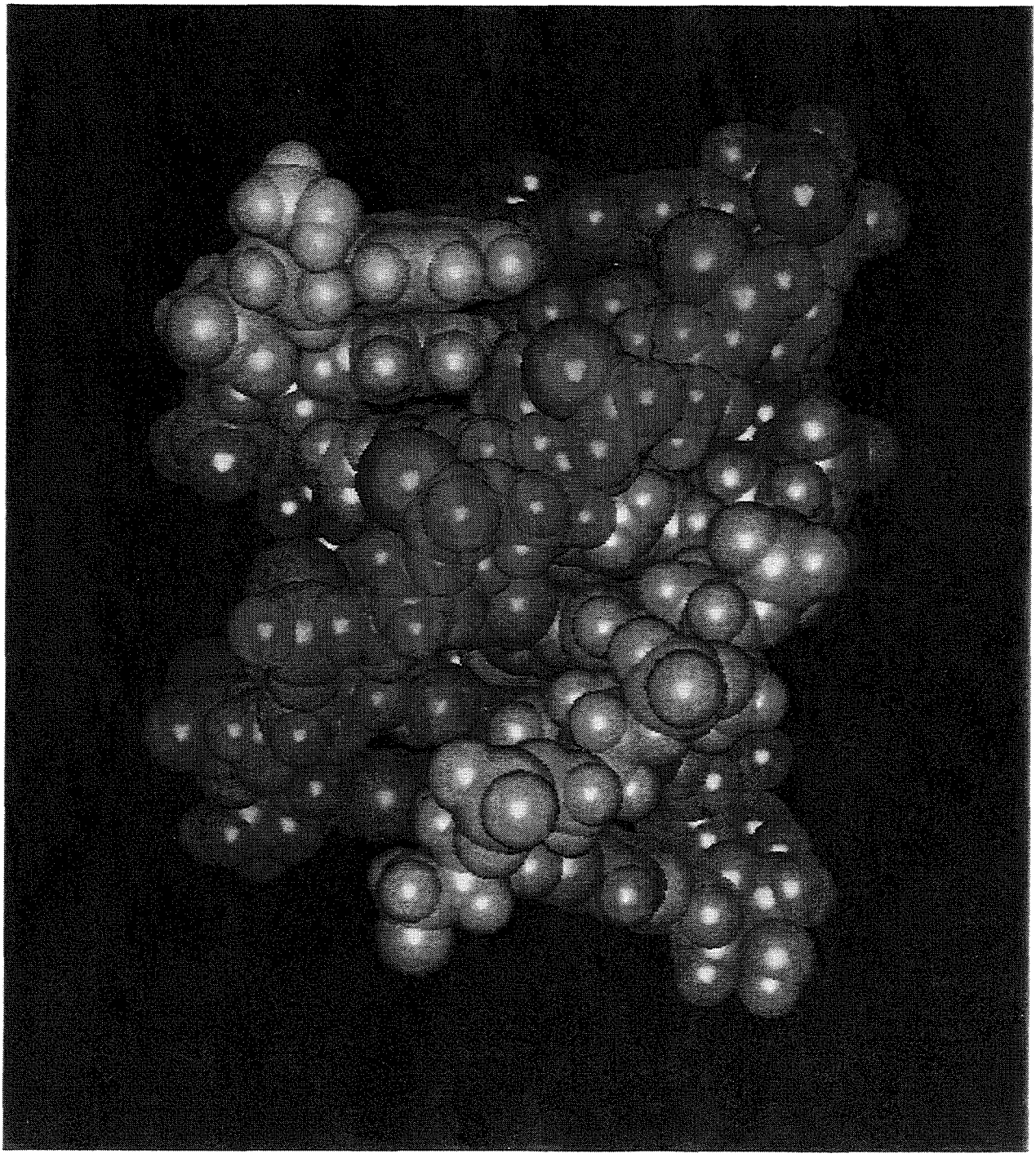

Formation Stabilization by 6-Thioguanosine Under Physiological Ionic Conditions. Although the guanine-rich phosphorothioate oligonucleotides examined can bind with great affinity to the double-helical target site under non-stringent conditions, they do not have measurable affinity for the target site under physiological ionic conditions. It has been reported that potassium inhibits triple helix formation with guanine-rich oligonucleotides (Cheng & Van Dyke, 1993; Milligan et al., 1993). This has been attributed to the formation of potassium dependent higher order structures, such as tetraplexes, between the guanine-rich oligonucleotides (Williamson et al., 1989; Sen & Gilbert, 1990). These structures will compete with oligonucleotide hybridization to the triple helix target site. This is supported by the fact that the guanine-rich oligonucleotides **SR2-SR5** all have no affinity for the target site. Figure 14 depicts the structure of a guanine quartet that may form between these oligonucleotides.

In order to facilitate guanine-rich triple helix formation in the presence of potassium, studies have used modified guanines that potentially can form two reverse Hoogsteen hydrogen bonds with guanines in the target site yet inhibit tetraplex formation. One of these strategies involves incorporating 7-deaza-2'-deoxyguanosine into oligonucleotides for GC basepair recognition (Milligan et al., 1993). Suprisingly, this inhibits triple helix formation even under low salt conditions. Since the atomic charge pattern of 7-deaza-2'-deoxyguanosine is different from 2'-deoxyguanosine, it is possible that it may produce less favorable base stacking interactions.

Another guanine analog, 6-thio-2'-deoxyguanosine, was proposed as a potential means of enhancing triple helix formation in the presence of potassium (Rao et al., 1992). As can be seen in Figure 6, the O6 position of

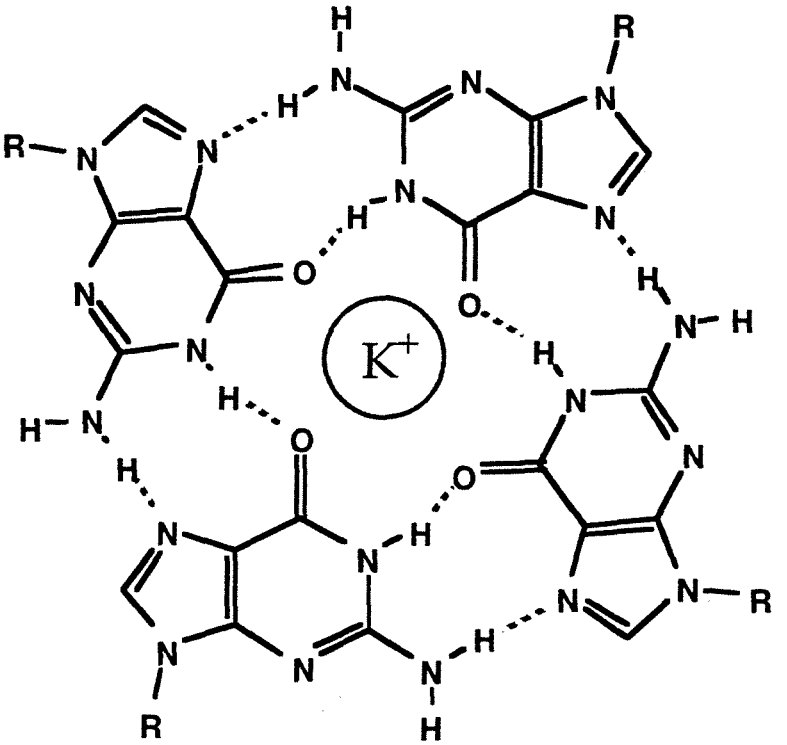

Figure 11: Structure of a guanine quartet. The O6 position of each guanine is highlighted in red.

guanine is important in guanine quartet formation. However, it is not involved in reverse Hoogsteen hydrogen boding interactions with the triple helix target site (Figure 11). Other studies have shown that 6-thioguanosine forms a less stable base pair with cytosine than does guanine (Rappaport, 1988; Christopherson & Broom, 1991; Ling et al., 1992a; Ling et al., 1992b; Xu et al., 1992a; Xu et al., 1992b). A number of different reasons such as weaker hydrogen bonding to sulfur relative to oxygen or steric interactions due to the larger size of the sulfur atom may account for this observation. In any case, this subsitution should not have as major an effect on ring electronics as does 7-deaza-2'-deoxyguanosine. This is consistent with oligonucleotide **RS1** having high affinity for the target site in the presence of physiological concentrations of potassium.

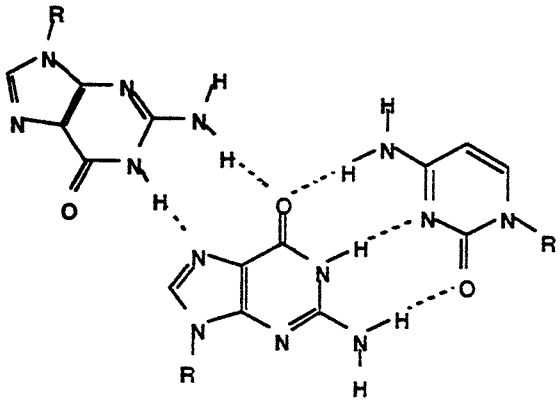

G•GC

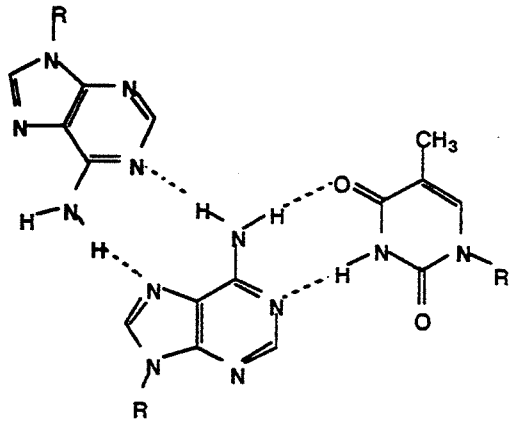

A•AT

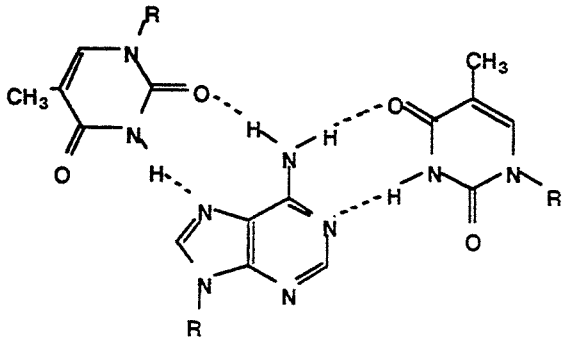

T•AT

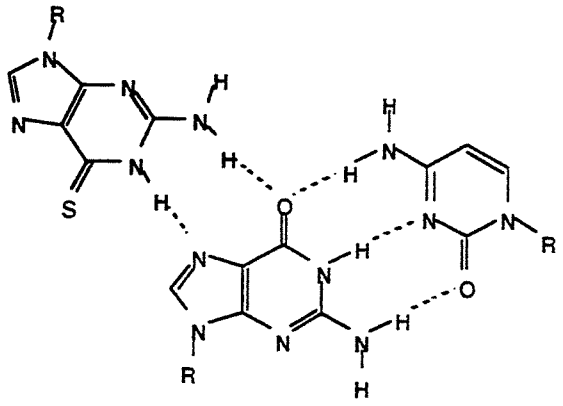

^{S}G•GC

Figure 11 . Modified Pu•Pu•Py Base Triplets.

Possible Reasons for Pyrimidine-Rich Phosphorothioate Triple Helix Formation Stabilization by 5-propynyl-2'-deoxyuridine Under Physiological Ionic Conditions. The energetic penalty towards triple helix formation caused by introducing a diastereomeric mixture of phosphorothioate internucleotide linkages into pyrimidine-rich oligonucleotides is compensated by the introduction of modified pyrimidine nucleosides. The modified nucleoside 5-(1-propynyl)-2'-deoxyuridine stabilizes hybridization to single-stranded RNA and DNA, relative to thymidine (Froehler et al., 1992; Froehler et al., 1993; Gutierrez et al., 1994; Lin et al., 1994). Furthermore it enhances triple helix formation with third strand oligodeoxyribonucleotides (Froehler et al., 1992). The base triplet formed between this nucleoside and an AT base pair is shown in Figure 12. This stabilization has enabled cooperative interactions between adjacent triple helix forming 8-mer oligonucleotides to be measured (Colocci & Dervan, 1994). Furthermore, oligonucleotides containing the C-5 propyne 2'-deoxyuridine analog with formacetal and 3'-thioformacetal linkages show substantially enhanced triple helix formation relative to their thymidine containing counterparts (Lin et al., 1994). This indicates that C-5 propyne 2'-deoxyuridine analogs may be compatible with a range of phosphodiester backbone modifications. This stabilization may be due to increased base stacking interactions since the propyne modification is planar with respect to the heterocyclic ring. Other studies utilizing 5-alkyl-substituted uridines have attributed increased triple helix formation to these base stacking effects (Povsic, 1992). Furthermore, the hydrophobic propyne group allows for an increase in the entropy of binding which favors triple helix formation.

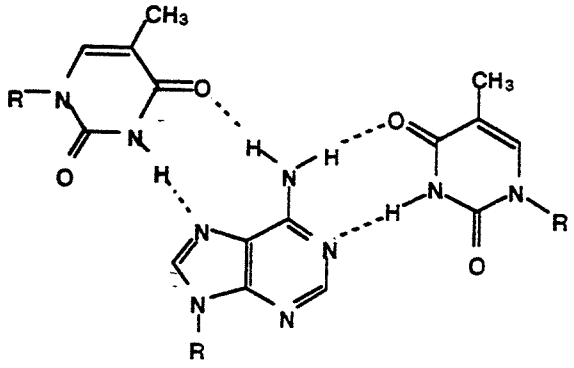

T•AT

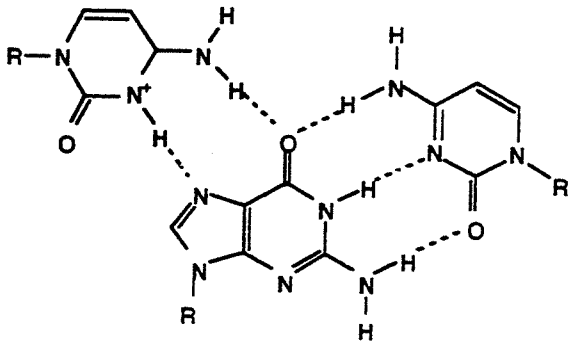

C^{+}•GC

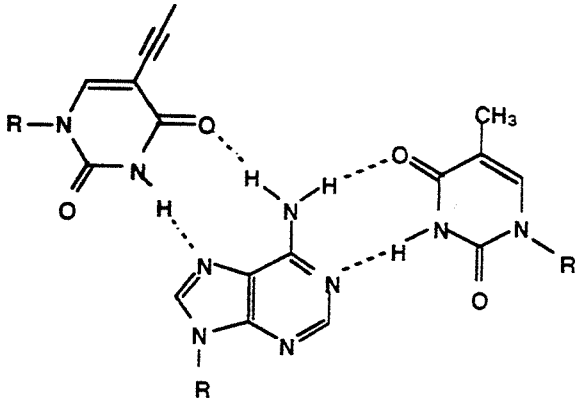

PU•AT

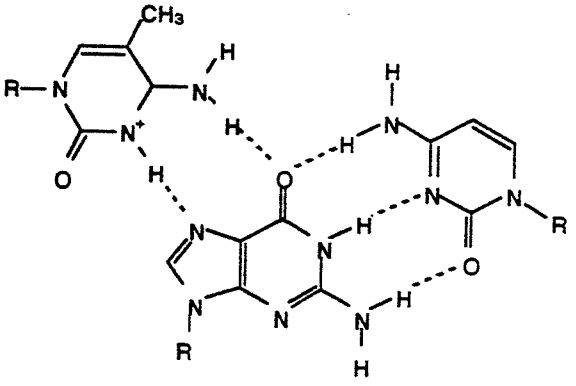

$^{me}C^{+}$•GC

Figure 12. Modified Py•Pu•Py Base Triplets

Chemical Synthesis of Stereoregular Phosphorothioate Backbones. There is considerable interest in developing efficient synthetic methodologies for the stereocontrolled synthesis of phosphorothioate oligonucleotides. Stec and co-workers have reported a methodology for this type of synthesis based on a stereospecific (>99%) base catalyzed nucleophilic substitution at a pentavalent phosphorothioyl center (Stec et al., 1991). Although this provides a significant advance, the authors note that 99% stereospecificity for each phosphorothioate linkage would not be sufficient for the production of longer oligonucleotides. For example, the synthesis of a 28mer with a 99% stereospecificity of a single coupling would yield a product with only 76% of single diastereomer having predetermined chirality at each phosphorus atom.

Effect of Other Phosphodiester Backbone Modifications on Triple Helix Formation. Other oligonucleotides with modified internucleotide linkages have been tested for triple helix formation. Studies have focused on the ability of pyrimidine-rich methylphosphonate oligonucleotides to form triple helical complexes. Wilson and co-workers examined the ability of the oligonucleotides dA_{19} and dT_{19} and their methylphosphonate analogs to form triple helical complexes through UV melting analysis (Kibler-Herzog et al., 1990). It was concluded that no triple helices could be formed if any of the phosphodiester strands were replaced with a methylphosphonate strand. A later study by Wilson and co-workers concluded from circular dichroism (CD) experiments that triple helical complexes could form between dT_{19} and the methylphosphonate dA_{19} (Kibler-Herzog et al., 1993). Overall these findings contrast reports of complex formation using much shorter

oligonucleotides (Miller et al., 1979; Miller et al., 1980; Miller et al., 1981). Triplex formation between $d(CT)_8$ and $d(AG)_8$, in which the pyrimidine strand consisted of methylphosphonates, was found to require a lower pH for stability relative to its all phosphodiester analog (Callahan et al., 1991). More relevant work showed through DNase I footprinting that introducing a diastereomeric mixture of methylphosphonate internucleotide linkages into oligodeoxyribonucleotides inhibits triple helix formation on DNA target sites (Jones et al., 1993a). Strekowski and co-workers also showed that an all thymidine 19mer methylphosphonate oligonucleotide could not bind to its cognate DNA target site through UV melting analysis (Wilson et al., 1993). However, the addition of a quinoline intercalating agent appeared to stabilize the complex.

Helene and co-workers have investigated the ability of α-oligonucleotides, containing the α-anomers of each nucleotide, to bind to double helical DNA (Le Doan et al., 1987; Praseuth et al., 1988; Sun et al., 1991). Third strand α-oligonucleotides composed entirely of thymine bind parallel to the purine-rich strand of DNA while those composed of both thymine and cytosine bind in an antiparallel orientation. Triple helical complexes formed by α-oligonucleotides were found to be less stable than those formed by the natural β-oligodeoxyribonucleotides.

Oligonucleotide analogs containing riboacetal internucleotide linkages bind avidly to double-helical DNA (Jones et al., 1993b). A 15-nt chimeric oligonucleotide which contained seven riboacetal linkages alternating with seven phosphodiester linkages displayed a 100-fold increase in affinity for a triple helix target site relative to its all phosphodiester counterpart, but decreased affinity for its cognate single-stranded RNA. This may be due in part to reduced electrostatic repulsion due to the

neutral riboacetal linkages. However, the related neutral phosphate mimics such as formacetal and 3'-thioformacetal linkages tested under identical experimental conditions do not greatly enhance triple helix formation (Jones et al., 1993a). The authors propose that the covalent conformational restriction of the riboacetal linkage along with the perturbation of the ribose sugar pucker are responsible for tighter binding.

Studies have focused modifying the sugar portion of the phosphodiester internucleotide linkages. As described in Chapter 1, oligoribonucleotide third strands in general have been found to form more stable triple helical complexes than the oligodeoxyribonucleotide counterparts (Roberts & Crothers, 1992; Escude et al., 1992; Escude et al., 1993; Han et al., 1993). Ohtsuka and co-workers examined the effect of several sugar modifications on triple helix formation (Shimizu, et al., 1992). Modified oligonucleotides 15-nt long, composed of eight cytosines and seven uridines or thymidines (in the case of DNA), were tested for hybridization to a 17-bp oligodeoxyribonucleotide duplex at either pH 6.1 or pH 5.5 in the presence of 100 mM NaCl and 1 mM EDTA. Oligonucleotides containing 2'-deoxy, 2'-OH, 2'-OMe, and 2'-fluoro substituted ribose sugars were synthesized. At pH 5.0, the rank order of oligonucleotide binding was: 2'-OMe > 2'-OH > 2'-F > 2'-H. However at pH 6.1, the rank order of binding was: 2'-OH ≥ 2'-OMe > 2'-H > 2'-F. This indicates that hybridization conditions effect the energetics of oligonucleotide modifications, in agreement with the effects of pH on the stability of 2'-OMe complexes shown in Chapter 1. Others have reported that 2'-OMe oligonucleotides form more stable triple helical structures with duplex DNA than either their oligoribonucleotide or oligodeoxyribonucleotide counterparts (Escude et al., 1992).

Other 2'-alkyl substituted oligonucleotides have been assayed for binding to single-stranded DNA and RNA oligonucleotides. Nuclease resistant 2'-O-allyl derivatives have low non-specific binding to HeLa cell nuclear extracts and are not a substrate for RNase H cleavage (Inoue et al., 1987; Irabarren et al., 1990; Barabino et al., 1992; Froehler et al., 1993). There are no reports of 2'-O-allyl oligonucleotides forming triple helical complexes with DNA targets. The 2'-O-allyl oligonucleotide **rUrC** 5'-$U_aU_aU_aC_aU_aU_aU_aU_aU_a\ C_aU_aU_aU_aU_aU_aU_a$-3' and its phosphodiester analog **dUdC** 5'-UUUCUUUUUCUUUUUUU-3' were synthesized and tested for binding to the DNA target site shown in Figure 1. When incubated with the target site for 24 hours at 25 °C in 1X Sequenase Reaction Buffer (40 mM Tris-Cl pH 7.5, 50 mM NaCl, and 20 mM $MgCl_2$), 1 μM oligonucleotide **dUdC** provided complete protection of the target site from DNase I digestion (figure 17). On the other hand, up to 30 μM oligonucleotide **rUrC** did not protect the target site from DNase I digestion. The 2'-O-allyl substitution appears to destabilize triple helix formation. Nevertheless, based on the results found for pyrimidine phosphorothioate oligonucleotides, inclusion of 5-(1-propynyl)-2'-O-allyl-uridine and 5-methyl-2'-O-allyl-cytidine nucleosides would probably rescue binding.

Figure 14. *In vitro* DNase I footprinting analysis of modified oligonucleotides under nonstringent ionic conditions (40 mM Tris-Cl pH 7.5, 50 mM NaCl, and 20 mM $MgCl_2$). Oligodeoxyribonucleotides **UdC** 5'-UUUCUUUUUCUUUUUUU-3', **dTdC** 5'-TTTCTTTTTCTTTTTTT-3', and **dTdmC** 5'-TTT^{m}CTTTTT^{m}CTTTTTTT-3' and the oligo-2'-O-allyl-ribonucleotide rUrC 5'-UaUaUaCaUaUaUaUaUaCaUaUaUaUaUaUa-3' were allowed to equilibrate with the ^{32}P 3'-end labelled 438-bp EcoRI-AflIII restriction fragment from pTERI for 24 hours at room temperature prior to analysis. Lane 1, A + G specific chemical sequencing lane; lane 2, 10 nM **dTdC**; lane 3, 10 nM **dTdmC**; lane 4, 10 μM **rUrC**; lane 5, 20 μM **rUrC**; lane 6, 30 μM **rUrC**; lane 7, 10 μM **dUdC**; lane 8, 20 μM **dUdC**; lane 9, 30 μM **dUdC**; lane 10, no oligonucleotide; lane 11, no DNase I.

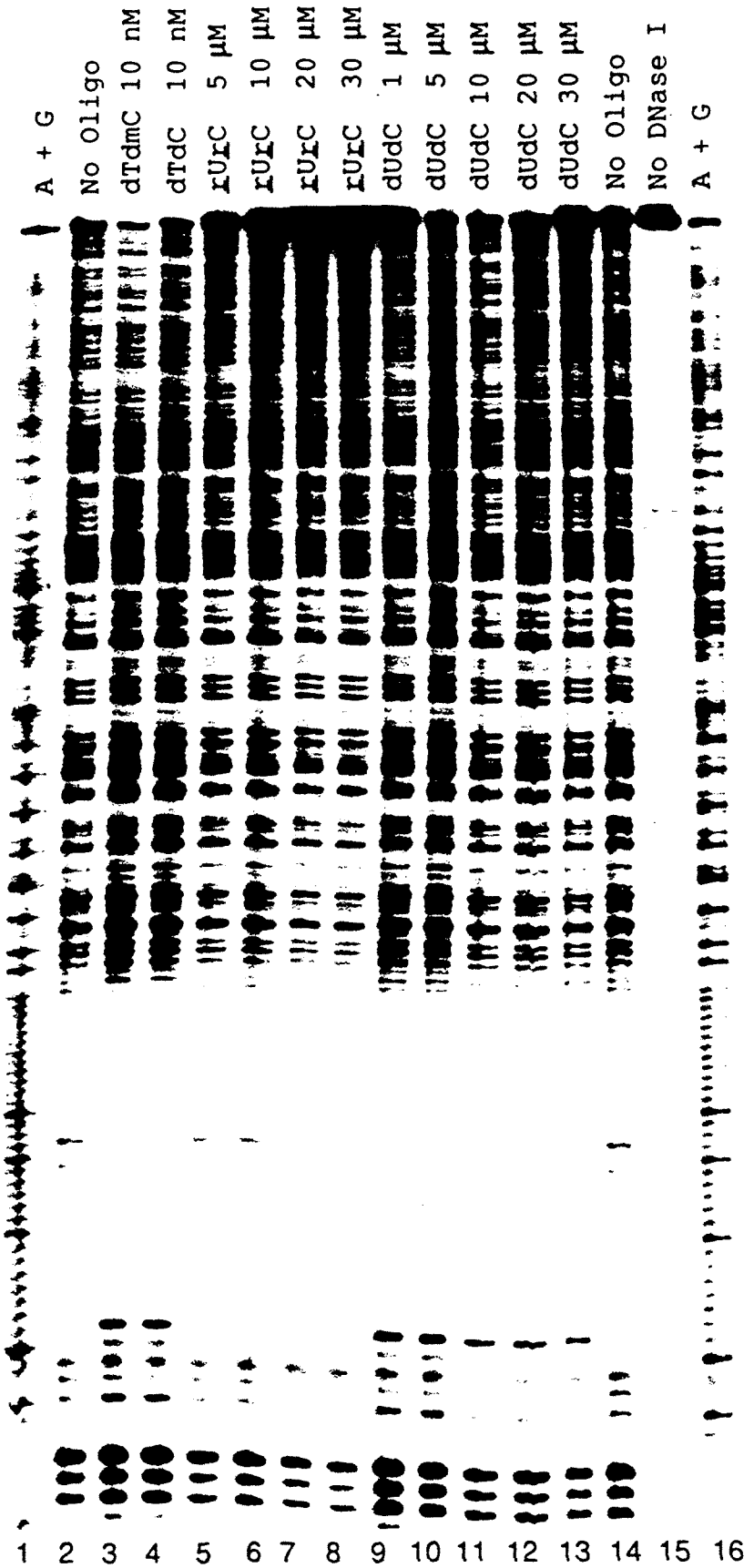
A + G
No Oligo
dTdmC 10 nM
dTdC 10 nM
rUrC 5 μM
rUrC 10 μM
rUrC 20 μM
rUrC 30 μM
dUdC 1 μM
dUdC 5 μM
dUdC 10 μM
dUdC 20 μM
dUdC 30 μM
No Oligo
No DNase I
A + G
1 2 3 4 5 6 7 8 9 10 11 12 13 14 15 16

REFERENCES

Barabino, S. M. L., Sproat, B. S., Lamond, A. I. (1992) *Nucleic Acids Res. 20*, 4457-4464.

Beal, P. A., & Dervan, P. B. (1991) *Science 251*, 1360-1363.

Belle, R., Mulner-Lorillon, O., Marot, J., & Ozon, R. (1986) *Cell Diff. 19*, 253-261.

Brody, R. S., Adler, S., Modrich, P., Stec, W. J., Leznikowski, Z. J., & Frey, P. A. (1982) *Biochemistry 21*, 2570-2572.

Burgers, P. M. J., & Eckstein, F. (1979) *J. Biol. Chem. 254*, 6889-6893.

Callahan, D. E., Trapane, T. L., Miller, P. S., T'so, P. O. P., Kan, L. S. (1991) *Biochemistry 30*, 1650-1655.

Chen, F. -M. (1991) *Biochemistry 30*, 4472-4479.

Cheng, A.-J., & Van Dyke, M. W. (1993) *Nucleic Acids Res. 21*, 5630-5635.

Christopherson, M. S., & Broom, A. D. (1991) *Nucleic Acids Res. 19*, 5719-5724.

Colocci, N.; Dervan, P. B. (1994) *J. Am. Chem. Soc. 116*, 785-786.

Cosstick, R. & Eckstein, F. (1985) *Biochemistry 24*, 3630-3638.

de los Santos, C., Rosen, M., & Patel, D. (1989) *Biochemistry 28*, 7282-7289.

Durland, R. H., Kessler, D. J., Gunnell, S., Duvic, M., Pettitt, B. M. & Hogan, M. E. (1991) *Biochemistry 30*, 9246-9255.

Eckstein, F. (1983) *Angew. Chem. Int. Ed. Engl. 22*, 423-506.

Eckstein, F. (1985) *Ann. Rev. Biochem. 54*, 367-402.

Escude, C., Francois, J.-C., Sun, J.-S., Ott, G., Sprinzl, M., Garestier, T., & Helene, C. (1993) *Nucleic Acids Res. 21*, 5547-5553.

Escude, C., Sun, J-. S., Rougee, M., Garestier, T., & Helene, C. (1992) *C. R. Acad. Sci. Paris 315*, 521-525.

Fox, J. J., Wempen, I., Hampton, A., Doerr, I. L. (1958) 80, 1669-1675.

Frey, P. A., & Sammons, R. D. (1985) *Science 228*, 541-545.

Froehler, B. C., Jones, R. J., Cao, X., & Terhorst, T. J. (1993) *Tetrahedron Lett. 34*, 1003-1006.

Froehler, B. C., Wadwani, S., Terhorst, T. J., & Gerrard, S. R. (1992) *Tetrahedron Lett. 33*, 5307-5310.

Giaume, C., & Kado, R. T. (1983) *Biochim. Biophys. Acta 762*, 337-343.

Gutierrez, A. J., Terhorst, T. J., Matteucci, M. D., & Froehler, B. C. (1994) *J. Am. Chem. Soc. 116*, 5540-5544.

Han, H. & Dervan, P. B. (1993) *Proc. Natl. Acad. Sci. 90*, 3806-3810.

Horowitz, S. B., & Paine, P. L. (1979) *Biophys. J. 25*, 45-62.

Horowitz, S. B., Paine, P. L., Tluczek, L., & Reynhout, J. K. (1979) *Biophys. J.* 25, 33-44.

Ibrahim, K. B., & Dick, D. A. T. (1984) *Carlsberg Res. Commun. 49*, 273-292.

Inoue, H., Hayase, Y., Iwai, S., & Ohtsuka, E. (1987) *FEBS Lett. 15*, 327-330.

Irabarren, A. M., Sproat, B. S., Neuner, P., Sulston, I., Ryder, U., & Lamond, A. I. (1990) *Proc. Natl. Acad. Sci. U. S. A. 87*, 7747-7751.

Jones, R. J., Lin, K.-Y., Milligan, J. F., Wadwani, S., & Matteucci, M. D. (1993a) *J. Org. Chem. 58*, 2983-2991.

Jones, R. J., Swaminathan, S., Milligan, J. F., Wadwani, S., Froehler, B. C., & Matteucci, M. D. (1993b) *J. Am. Chem. Soc. 115*, 9816-9817.

Kibler-Herzog, L., Kell, B., Zon, G., Shinozuka, K., Mizan, S., & Wilson, W.

D. (1990) *Nucleic Acids Res. 18,* 3545-3555.

Kibler-Herzog, L., Zon, G., Whittier, G., Mizan, S., & Wilson, W. D. (1993) *Anti-Cancer Drug Design 8,* 65-79.

Kim, S.-G., Tsukahara, S., Yokoyama, S., & Takaku, H., (1992) *FEBS Letters 314,* 29-32.

Koh, J. S., & Dervan, P. B. (1992) *J. Am. Chem. Soc. 114,* 1470-1478.

Latimer, L. J. P., Hampel, K., & Lee, J. S. (1989) *Nucleic Acids Res. 17,* 1549-1561.

LaPlanche, L. A., James, T. L., Powell, C., Wilson, W. D., Uznanski, B., Stec, W. J., Summers, M. F., & Zon, G. (1986) *Nucleic Acids Res. 14,* 9081-9093.

Le Doan, T., Perrouault, L., Praseuth, D., Habhoub, N., Decout, J.-L., Thuong, N. T., Lhomme, J., & Helene, C. (1987) *Nucleic Acids Res. 15,* 7749-7760.

Lee, J. S., Woodsworth, M. L., Katimer, L.J. P., & Morgan, A. R. (1984) *Nucleic Acids Res. 12,* 6603-6614.

Lin, K.-Y., Pudlo, J. S., Jones, R. J., Bischofberger, N., Matteucci, M. D., & Froehler, B. C. (1994) *Bioorg. Med. Chem. Lett. 4,* 1061-1064.

Ling, Y.-H., Chan, J. Y., Beattie, K. L., & Nelson, J. A. (1992a) *Mol. Pharm. 42*, 802-807.

Ling, Y.-H., Nelson, J. A., Fraquhar, D., Beattie, K. L. (1992b) *Nucleosides Nucleotides 11*, 23-35.

Miller, P. S., Dreon, N., Pulford, S. M., & McParland, K. B. (1980) *J. Biol. Chem. 255*, 9659-9665.

Miller, P. S., McParland, K. B., Jayaraman, K., & T'so, P. O. P. (1981) *Biochemistry 20*, 1874-1880.

Miller, P. S., Yano, E., Yano, E., Carroll, C., Jayaraman, K., & T'so, P. O. P. (1979) *Biochemistry 18*, 5134-5143.

Milligan, J. F., Krawczyk, S. H., Wadwani, S., & Matteucci, M. D. (1993) *Nucleic Acids Res. 21*, 327-333.

Moser, H. E., & Dervan, P. B. (1987) *Science 238*, 645-650.

Osborne, H. B., Mulner-Lorillon, O., Marot, J., & Belle, R. (1989) *Biochem. Biophy. Res. Commun. 158*, 520-526.

Paine, P. L., Johnson, M. E., Lau, Y. -T., Tluczek, L. J. M., & Miller, D. S. (1992) *BioTechniques 13*, 238-246.

Paine, P. L., Pearson, T. W., Tluczek, L. J. M., & Horowitz, S. B. (1981)

Nature 291, 258-261.

Pilch, D. S., Levenson, C., & Shafer, R. H. (1991) *Biochemistry 30*, 6081-6087.

Povisc, T. J. Ph. D. Thesis, California Institute of Technology, 1992.

Praseuth, D., Perrouault, L., Le Doan, T., Chassignol, M., Thuong, N. T., Helene, C. (1988) *Proc. Natl. Acad. Sci. U. S. A. 85*, 1349-1353.

Radhakrishnan, I., de los Santos, C., & Patel, D. J. (1991) *J. Mol. Biol. 221*, 1403-1418.

Radhakrishnan, I., de los Santos, C., & Patel, D. J. (1993) *J. Mol. Biol. 234*, 188-197.

Radhakrishnan, I., & Patel, D. J. (1993a) *J. Am. Chem. Soc.115*, 1615-1617.

Radhakrishnan, I., & Patel, D. J. (1993b) *Structure 1*, 135-152.

Radhakrishnan, I., & Patel, D. J. (1994) *Structure 2*, 17-32.

Rajagopal, P., & Feigon, J. (1989) *Nature 339*, 637-640.

Rao, T. S., Jayaraman, K., Durland, R. H., & Revankar, G. R. (1992) *Tetrahedron Lett. 33*, 7651-7654.

Rappaport, H. P. (1988) *Nucleic Acids Res. 16*, 7253-7267.

Roberts, R. W., & Crothers, D. M. (1992) *Science 258*, 1463-1466.

Romaniuk, P. J., & Eckstein, F. (1982) *J. Biol. Chem. 257*, 7684-7688.

Sambrook, J., Fritsch, E. F., & Maniatis, T. (1989) in Molecular Cloning: A Laboratory Manual, 2nd ed., Cold Spring Harbor Laboratory Press, Cold Spring Harbor, NY.

Sen, D., & Gilbert, W. (1990) *Nature 344*, 410-414.

Shimizu, M., Konishi, A., Shimada, Y., Inoue, H., & Ohtsuka, E. (1992) *FEBS Lett. 302*, 155-158.

Singleton, S. F., & Dervan, P. B. (1992) *J. Am. Chem. Soc. 114*, 6957-6965.

Stec, W. J., Grajkowski, A., Koziolkiewicz, M., & Uznanski, B. (1991) *Nucleic Acids Res. 19*, 5883-5888.

Stein, C. A. & Cheng, Y. -C. (1993) *Science 261*, 1004-1012.

Sun, J. S., Giovannangeli, C., Francois, J. C., Kurfurst, R., Montenay-Garestier, T., Asseline, U., Saison-Behmoaras, T., Thuong, N. T., & Helene, C. (1991) *Proc. Natl Acad. Sci. U. S. A. 88*, 6023-6027.

Sunkara, P. S., Wright, D. A., & Nishioka, K. (1981) *Devel. Biol. 87*, 351-355.

Tsukahara, S., Kim, S.-G., & Takaku, H. (1993) *Biochem. Biophys. Res. Commun. 196,* 990-996.

Vu, H., & Hirschbein, B. L. (1991) *Tetrahedron Lett. 32,* 3005-3008.

Webb, D. J., & Nuccitelli, R. (1981) *J. Cell Biol. 91,* 562-567.

Williamson, J. R., Raghuraman, M. K., & Cech, T. R. (1989) *Cell 59,* 871-880.

Wilson, W. D., Tanious, F. A., Mizan, S., Yao, S., Kiselyov, A. S., Zon, G., & Strekowski (1993) *Biochemistry 32,* 10614-10621.

Xodo, L., Alunni-Fabbroni, M., Manzini, G., & Quadrifoglio, F. (1994) *Nucleic Acids Res. 22,* 3322-3330.

Xu, Y.-Z., Zheng, Q., & Swann, P. F. (1992a) *Tetrahedron 48,* 1729-1740.

Xu, Y.-Z., Zheng, Q., & Swann, P. F. (1992b) *Tetrahedron Lett. 33,* 5837-5840.

Chapter VII

In Vivo Footprinting Analysis of Triple Helix Formation Using Modified Oligodeoxyribonucleotides

INTRODUCTION

The sequence-specific recognition of nucleic acids by proteins plays a crucial role in the regulation of gene expression. DNA-binding proteins that can bind to distinct DNA sequences have pivotal roles in the processes of transcription, replication, and recombination (Lewin, 1990). Synthesizing molecules that bind sequence-specifically to DNA and inhibit proteins binding could allow for the selective modulation of gene expression leading to controlled alterations in cell metabolism and division. Besides a long-term goal of using such molecules as therapeutic agents, there is great interest in using them as biological tools to examine gene function and regulation.

Oligonucleotide-directed triple helix formation provides a powerful chemical approach towards the sequence-specific recognition of double helical DNA. Rationally designed oligonucleotides can bind to unique 15-bp target sites with high selectivity against single base pair mismatches (Singleton & Dervan, 1992 a, b; Singleton & Dervan, 1993). This specificity allows targeting of a single unique sequence on gigabase pair size DNA, such as the human genome (Strobel & Dervan, 1990; Strobel & Dervan, 1991; Strobel et al., 1991). *In vitro* studies have utilized triple helices to prevent DNA binding proteins such as restriction endonucleases,

methylases, and transcription factors from interacting with DNA binding sites (Maher et al., 1989; Maher et al., 1990; Maher et al., 1992; Strobel & Dervan, 1991). Furthermore, triple helix formation can specifically inhibit *in vitro* transcription and primer extension reactions (Young et al., 1991; Maher et al., 1992; Duval-Valentin et al., 1993; Maher, 1992; Hacia et al., 1994).

Although triple helix formation has shown great promise as a means of modulating gene expression, there is no convincing experimental evidence that these structures can form within a cell. In this study, we examine the ability of oligonucleotide analogs to bind to minichromosomes present in *Xenopus* oocytes through *in vivo* footprinting analysis. Although these oligonucleotides bound with high affinity *in vitro* to naked templates, they were unable to bind *in vivo* to the same templates. Nevertheless, the *Xenopus* oocyte minichromosome system appears to have potential as a well controlled and flexible model system for measuring the affinity of designed DNA binders for chromatin *in vivo*.

EXPERIMENTAL

Materials. All DNA synthesis reagents were obtained from Applied Biosystems Inc. except for 5-methylcytosine phosphoramidite , 5-(1-propynyl)-2'-deoxyuridine phosphoramidite, 2'-OMe-cytidine phosphoramidite, 5-(1-propynyl)-2'-OMe-uridine phosphoramidite, and S6-DNP-dG-phosphoramidite obtained from Glen Research. The modified 5-amino-thymidine phosphoramidite was a generous gift from Matt Taylor. Pfu DNA polymerase was obtained from Stratagene. Adenosine 5'- [γ^{32}P] - triphosphate was obtained from New England Nuclear.

Plasmid Construction. The recombinant plasmid pTER3 was constructed as described in the chapter 5 of this thesis. It contains three distinct homopurine tracts along with a distal sequence element normally found upstream of the *Xenopus laevis* U3 snRNA genes cloned into pUC19 (Savino et al., 1992). Figure 1 shows a simplified map of plasmid pMTCAT-TH1 along with some of the compounds tested.

Chemical Synthesis of Oligodeoxyribonucleotides. The oligodeoxyribonucleotides used in this study are shown in Tables 1 and 2. All oligodeoxyribonucleotides as well as 2'-OMe oligonucleotides and phosphorothioate oligodeoxyribonucleotides were prepared on an Applied Biosystems 380B DNA Synthesizer with β-cyanoethyl phosphoramidites. Oligonucleotides were purified by denaturing polyacrylamide gel electrophoresis, visualized by UV shadowing, and electroeluted from gel slices using an Elu-trap apparatus (Schleicher & Schuell). They were

desalted by C18 Reverse Phase chromatography using Sep-Pak cartridges (Waters) and resuspended in Milli-Q before storing at -80 °C. The concentration of oligonucleotides were determined by A_{260} measurements using the following molar extinction coefficients: 15,400 (A), 11,700 (G), 7,300 (C), 8,800 (T), 5,800 (^{me}C), and 9,700 (PU).

Microinjection into Oocytes. Large adult females of *Xenopus laevis* were supplied by Dr. Norman Davidson's laboratory at the California Institute of Technology. Stage VI oocytes were used and germinal vesicle injections were performed using standard methods (Dumont, 1972; Gargiulo et al., 1983; Gargiulo & Worcel 1983; Skeiky et al., 1987; Dargemont et al., 1992; Lehman & Carroll, 1993). After microinjecting plasmid into the germinal vesicle, oocytes were incubated at 20 °C for 24 hours in 0.2 micron filtered ND96 medium (2 mM NaCl, 96 mM NaCl, 1 mM $MgCl_2$, 1.8 mM $CaCl_2$, 2.5 mM Na-pyruvate, 50 µg/ml gentamycin, 5 mM HEPES pH 7.5). Data was obtained by pooling the plasmid DNA reisolated from four oocytes.

Reisolation of Plasmid DNA from Xenopus Oocytes. Oocytes were quickly homogenized in 100 µL of *Xenopus* Extraction Buffer (30 mM Tris-Cl pH 7.4, 20 mM EDTA pH 8.0, 1% SDS, 1 mM β-mercaptoethanol, and 15 µg proteinase K) per oocyte by vortexing in a 1.5 mL microfuge tube. The homogenates were incubated for 4 hours at 37 °C. A 200 µL volume of Buffer P1 (5 mM Tris-Cl pH 8.0, 0.5 mM EDTA, 5 µg/ml RNase A) was added to each tube followed by 100 µL of Buffer P3 (2.55M KOAc pH 5.2). The extracts were spun at 4 °C in a microfuge for 20 minutes. The supernatant was applied to a Qiagen Tip-20 column pre-equilibrated with

Table I. Pyrimidine-rich triple helix-forming oligonucleotides[a]

		Homopurine Tract 3	
	5'	A A A G A A A A A G A A A A A A G	3'
	3'	T T T C T T T T T C T T T T T T C	5'
ys1	5'	p p p m p p p p p m p p p p p p p UsUsUsCsUsUsUsUsUsCsUsUsUsUsUsU	3'
ys2	5'	p p p m p p p p p m p p p p p p p UpUpUpCpUpUpUpUpUpCpUpUpUpUpUpU	3'
yk1	5'	a p m p p p p p p m p p p p p p p TpUpCpUpUpUpUpUpUpCpUpUpUpUpUpUpC	3'
yk2	5'	e p m p p p p p m p p p p p p p p TpUpCpUpUpUpUpUpUpCpUpUpUpUpUpUpC	3'

[a]Key: s = phosphorothioate mixed diastereomers, p = 2'-OMe, PU = 5-(1-propynyl)-uridine, ^{m}C = 5-methylcytosine, ^{a}T = modified 5-amino-thymidine, ^{e}T = N-bromoacetamide modified thymidine

2 mL of Buffer QBT (750 mM NaCl, 50 mM MOPS, 15% ethanol, 0.15% Triton X-100; pH 7.0). The column was washed with 3 mL of Buffer QC (1 M NaCl, 50 mM MOPS, 15% ethanol, pH 7.0) and the plasmid DNA was eluted with 0.7 mL of Buffer QF (1.2 M NaCl, 50 mM MOPS, 15% ethanol, pH 8.0). The sample was precipitated by adding 0.7 mL of isopropanol and microcentrifuging at 4 °C for 20 minutes. The pellet was washed with 70% ethanol and dried in a Speed-Vac (Savant). The sample was resuspended in 100 µL of piperidine and incubated at 90 °C for 20 minutes. The samples were dried in a Speed-Vac and resuspended in 100 µL of Milli-Q prior to reevaporation. The pellet was resuspended in 400 µL of Milli-Q water and extracted twice with phenol:chlorofom:isoamyl alcohol (25:24:1). DNA

Table II. Purine-rich triple helix-forming oligonucleotides[b]

Homopurine Tract 2	
	5' G A G G G A G G G G A G G G G A G G G A G 3'
	3' C T C C C T C C C C C T C C C C T C C C T C 5'
	s s s s s s s s s s s s s s s s s
RS1	5' GsTsGsGsGsTsGsGsGsGsTsGsGsGsGsTsGsGsGsTsG 3'
RS2	5' GsTsGsGsGsTsGsGsGsGsTsGsGsGsGsTsGsGsGsTsG 3'

[b]Key: s = phosphorothioate mixed diastereomers, ^{s}G = 6-thioguanosine

was precipitated by adding 40 µL of 3M NaOAc pH 5.5 and 1 mL of ethanol prior to incubation at -80 °C for 15 minutes. The samples were centrifuged at 4 °C for 20 minutes and the pellets were washed with 70% ethanol. Samples were dried in a Speed-Vac and resuspended in 100 µL of Mill-Q water prior to storage at -80 °C.

Primer Extension Analysis. Primer extension reactions were assembled in a 650 µL microfuge tube by combining 30 µL of reisolated plasmid, 7 µL of dNTP mix (2.5 mM in each dNTP), 7 µL of 10X Pfu Polymerase Buffer (20 mM Tris-Cl (pH 8.5), 100 mM $(NH_4)_2SO_4$, 20 mM $MgCl_2$, 1 mg/ml BSA, 1% Triton X-100), the indicated ^{32}P 5'-end-labeled primer (100,000 cpm), and 1 U of Pfu DNA polymerase in a 70 µL total volume. Primer **YP1** 5'-G GTGTGACACATGCAAATGAGC-3' was used to read homopurine tract 3 while primer **RP1** 5'-TGCGGATAACAATTTCACACAGG-3' was used to read homopurine tract 2. A PCR wax gem (Perkin Elmer-Cetus) was placed on top of the reaction solution and the microfuge tube was placed in a thermocycler. The reactions were subjected to three cycles of primer extension (99 °C denaturation for 1 minute, 68 °C annealing for 1 minute,

and 74 °C extension for 2 minutes). The reactions were removed from under the wax layer and transferred to a fresh 1.5 mL microfuge tube. To each reaction was added 330 µL of Milli-Q water, 40 µL of 3M NaOAc pH 5.2, and 1 mL of ethanol prior to incubation at -80 °C for 20 minutes. The reactions were centrifuged at 4 °C for 20 minutes and the pellets were washed with 70% ethanol. Samples were dried in a Speed-Vac and resuspended in 10 µL of 1X Stop Buffer (1X TAE, 100 mM EDTA, 56% glycerol, 0.2% SDS, and 1% bromophenol blue) prior to electrophoretic separation on 8% denaturing polyacrylamide gels. Gels were dried and placed on film or photostimulable phosphor imaging plates and quantitated as described (Singleton & Dervan, 1992).

Synthesis of Modified N-Bromoacetyloligonucleotides. Five nanomoles of oligonucleotide **yk1** were dissolved in 10 µL of 200 mM borate buffer, pH 8.9. A 10 µL volume of freshly prepared 30 mM N-hydroxysuccinimidyl bromoacetate in N, N,-dimethylformamide (stored over molecular sieves) was added and reacted for 30 seconds. The reaction was diluted to 0.5 ml with water and passed through a NAP-5 column (Sephadex G-25, equilibrated with water). Following elution with 1 mL of water the sample volume was reduced to 800 µL in a Speed-Vac. The eluate was aliquoted into two separate 1.5 mL microfuge tubes. To each tube was added 40 µL of 3M NaOAc pH 5.5 and 1 mL of ethanol prior to storage at -80 °C for 20 minutes. The oligonucleotide was centrifuged at 4 °C for 20 minutes and the pellet was carefully washed with 70% ethanol. The oligonucleotide was dried in a Speed-Vac and resuspended in 100 µL of Milli-Q water. The concentration of the modified oligonucleotide **yk2** was determined by A_{260} measurements and the sample redried in a Speed-

Vac. It was resuspended in 20 µL of Milli-Q water to give a 5 mM solution of modified oligonucleotide which was stored at -80 °C.

In Vitro Alkylation Reaction. In vitro alkylation reaction were assembled by combining 250 ng of pTER3, 2 µL of 10X Alkylation Buffer (200 mM HEPES pH 7.4, 8 mM $Co(NH_3)_6^{+3}$), and 2 µL of 10 µM oligonucleotide **yk2** in a 20 µL total volume. The reaction was incubated at 37 °C for 36 hours. Afterwards, the reactions were quenched by adding 100 µL of *Xenopus* Extraction Buffer. The reaction was purified by Qiagen anion exchange chromatography and treated with piperidine by the same protocol for the isolation of plasmid DNA from *Xenopus* oocytes. The samples was analyzed by primer extension reactions.

In Vivo Alkylation Reaction. After microinjecting 10 nL of a 1 mg/ml stock solution of pTER3 into the germinal vesicles of 200 oocytes, the oocytes were incubated at 20 °C for 24 hours. Approximately 180 healthy oocytes (showing distinct animal and vegetal poles with no discoloration) were chosen for oligonucleotide injections. When indicated, 100 nL of 10 mM oligonucleotide **yk2** was injected into the vegetal pole cytoplasm of each oocyte. Alternatively, 20 nL of 10 µM oligonucleotide **yk2** was injected into the germinal vesicle of each oocyte. After cytoplasmic or nuclear injections, oocytes were incubated at 22 °C for the indicated times. Plasmid DNA was isolated from the oocytes and the reactions were evaluated by primer extension analysis.

In Vitro Methylation Reaction. In vitro methylation reactions were assembled by combining 250 ng of pTER3, 2 µL of 10X *Xenopus* Salts (1.3M

KCl, 150 mM NaCl, 30 mM $MgCl_2$), and 2 µL of a 10 mM solution of the indicated oligonucleotide in a 20 µL total volume. For oligonucleotide **rs2**, 2 µL of 10X Purine Salts (20 mM NaCl, 100 mM spermine, 25 mM Tris-OAc, pH 7.2) was used in place of 10X *Xenopus* salts. A 2 µL volume of a 10% DMS solution was added to the reaction and incubated for four minutes at room temperature. The methylation reaction was terminated by adding 50 µL of DMS stop solution (10 mM β-mercaptoethanol, 10 mM Tris-Cl pH 8.0) and 750 µL of ethanol. Reactions were incubated on dry ice for 15 minutes prior to spinning in a microcentrifuge at 4 °C for 20 minutes. Supernatants were discarded and the pellets were washed once with 70% ethanol prior to drying in a Speed-Vac. The pellets were resuspended in 80 µL of 10% piperidine and incubated at 90 °C for 30 minutes. The reactions were spun briefly in a microcentrifuge and dried in a Speed-Vac. The pellets were resuspended in 100 µL of Milli-Q water and dried again in a Speed-Vac prior to final resuspension in 10 µL Milli-Q water. *In vitro* alkylation reactions were evaluated by primer extension analysis as described above.

In Vivo Methylation Reaction. After microinjecting 10 nL of a 1 mg/ml stock solution of pTER3 into the germinal vesicles of 500 oocytes, the oocytes were incubated at 20 °C for 24 hours. Approximately 480 healthy oocytes (showing distinct animal and vegetal poles with no discoloration) were chosen for oligonucleotide injections. When indicated, 100 nL of the indicated oligonucleotide solution was injected into the vegetal pole cytoplasm of each oocyte. Alternatively, 20 nL of the indicated oligonucleotide solution was injected into each oocyte germinal vesicle. Prebound oligonucleotide:pTER3 complexes were injected in a 20

nL volume into the oocyte germinal vesicle. Complexes were formed under the in vitro methylation conditions. After cytoplasmic or nuclear injections, oocytes were incubated at 22 °C for the indicated times. Groups of four similarly injected oocytes were removed and placed in a 1.5 mL microfuge tube. The culture media was carefully removed with a micropipetter and the oocytes were gently resuspended in 100 µL of 10% DMS for two minutes at room temperature. Afterwards, the DMS solution was removed and plasmid DNA was isolated.

RESULTS

Design of an Experimental System to Assay for In Vivo Triple Helix Formation. To examine whether oligonucleotide-directed triple helix formation can occur *in vivo* on chromatinized DNA, an experimental system using *Xenopus* oocytes containing artificial minichromosomes was designed. The large size of *Xenopus* oocytes (1 mm in diameter) makes them amenable studies involving the microinjection of chemical reagents and biological macromolecules. Figure 1 displays a typical *Xenopus* oocyte that is undergoing microdissection to remove the germinal vesicle. Within several hours of injection, nearly all circular DNA deposited in the *Xenopus* oocyte germinal vesicle is assembled into minichromosomal structures containing the DNA template assembled around nucleosomes at the typical 200 base-pair spacing (Woodland et al., 1977; Wyllie, et al., 1977, Wyllie et al., 1978, Cortese, et al., 1980; Gurdon & Melton; 1981; Gargiulo et al., 1983; Gargiulo & Worcel, 1983; Glikan et al., 1984; Ryoji & Worcel, 1984; Etkin et al., 1987). Figure 2 shows the fate of various DNA topological forms injected into either the oocyte cytoplasm or germinal vesicle. The same supercoiled DNA templates that are amenable to oligonucleotide-directed triple helix formation *in vitro* may be utilized for *in vivo* triple helix formation. A 3420-bp plasmid pTER3 (Figure 3) serves as the target for both *in vitro* and *in vivo* studies. It contains three distinct homopurine tracts which support *in vitro* triple helix formation. Homopurine tract 1 contains the 15-bp sequence shown by Moser and Dervan to form triple helices with pyrimidine-rich oligonucleotides (Moser & Dervan, 1987). Homopurine tract 2 contains a 21-bp sequence shown by Beal and Dervan to be recognized by purine-rich

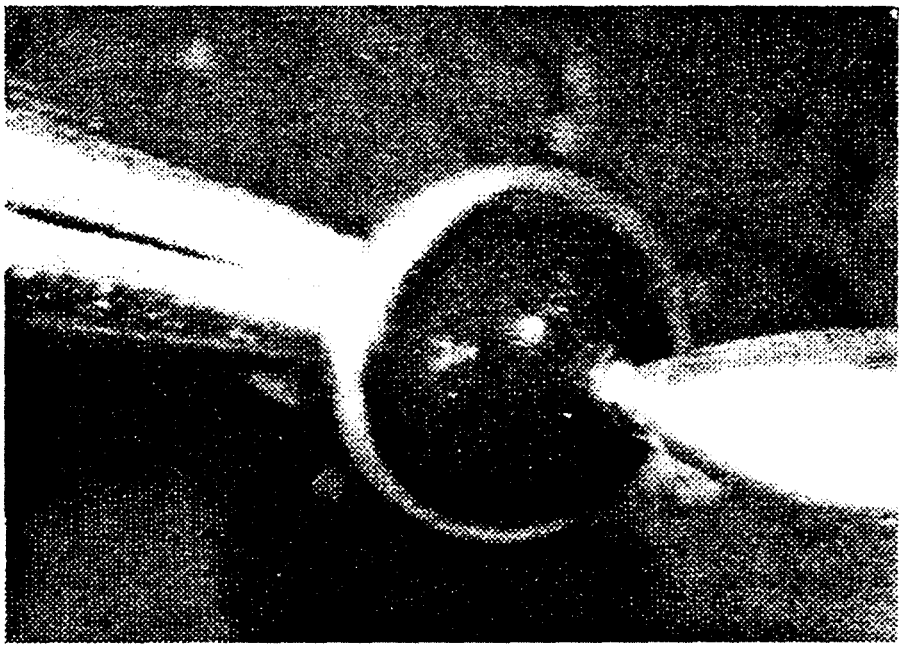

Oocyte punctured at the animal pole

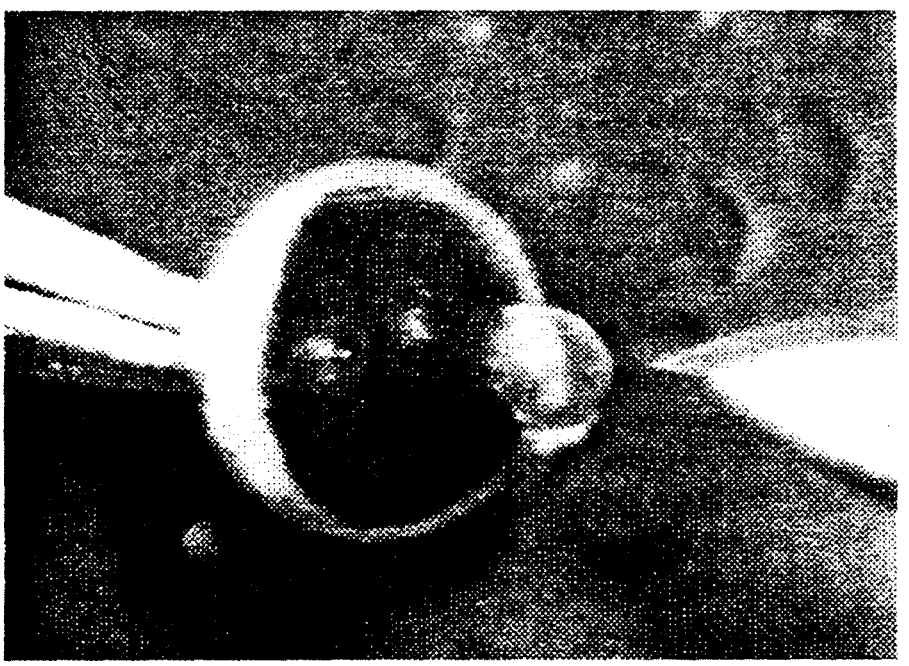

Germinal vesicle removal

Figure 1. ***Xenopus*** **oocyte microdissection.**

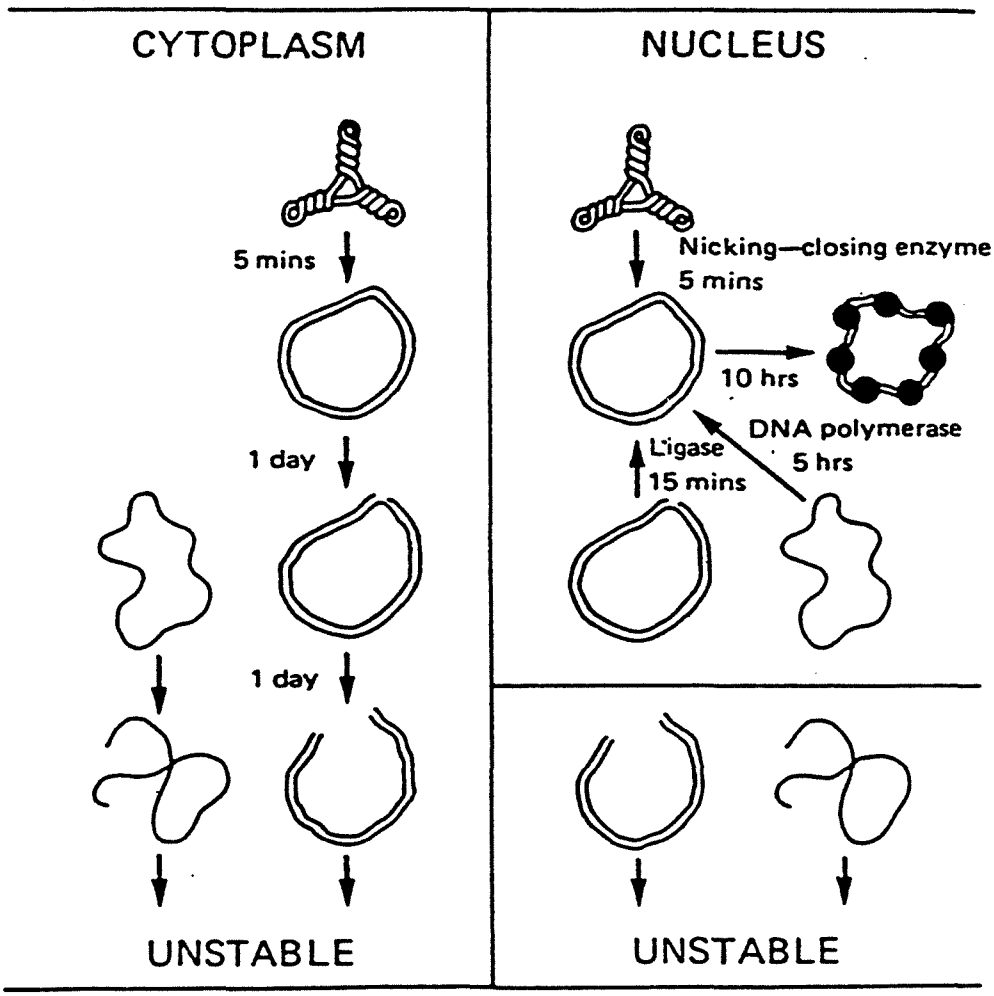

Injected DNA is assembled around nucleosomes at the typical 200 bp spacing. At least 10 ng of plasmid can be assembled into chromatin.

Figure 2. Fate of DNA Microinjected into *Xenopus* Oocytes.

oligonucleotides (Beal & Dervan, 1991; Beal & Dervan, 1992). Homopurine tract 3 contains the 31-bp sequence shown in Chapter 5 form triple-helical complexes that inhibits read-through by Klenow fragment DNA polymerase (Hacia et al., 1994). A 60 base pair insert containing a distal sequence element found upstream of the *Xenopus* laevis U3 snRNA genes assays if oocyte DNA binding proteins can recognize the template DNA (Savino et al., 1992).

In vivo footprinting experiments were chosen as the primary analytical technique to determine if triple helices can form *in vivo* on the microinjected plasmid DNA. A previous study showed that the *Xenopus* oocyte minichromosome system is amenable to *in vivo* footprinting techniques using DNase I and topoisomerase I as DNA damaging agents (Ryoji & Worcel, 1984). Dimethyl sulfate, which preferentially methylates N7 of guanine in the major groove of the double helix, was chosen for this assay. Studies have proven it to be an effective reagent for detecting protein:DNA complexes inside living cells (Mueller et al., 1988; Garrity & Wold, 1992; Garrity et al., 1994). Triple helix formation by either pyrimidine-rich or purine-rich third stands protects N7 of guanine from methylation by alkylating agents through the formation of specific Hoogsteen or reverse Hoogsteen hydrogen bonds. Triple helical complexes may be detected in cells by determining the protection of specific guanines from methylation by dimethyl sulfate in the target site.

In Vivo Footprinting of Triple Helical Target Sites in the Presence of Pyrimidine-Rich Oligonucleotides. Two different pyrimidine-rich oligonucleotides were tested by *in vivo* footprinting analysis for triple helix formation on homopurine site 3 (Table 1 and Figures 5 and 6).

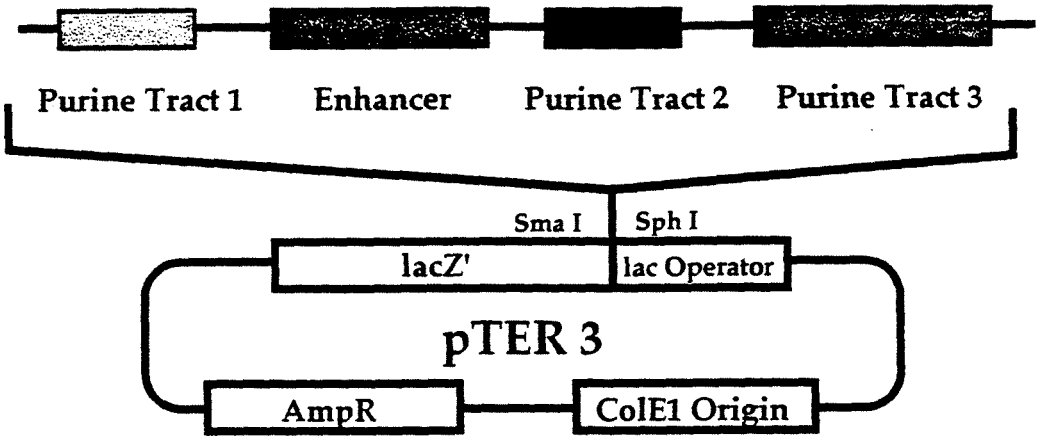


```
       p p p m p p p p p m p p p p p p p
5'     U U U C U U U U U C U U U U U U U   3'
5' A G A A A G A A A A A G A A A A A A G 3'
3' T C T T T C T T T T T C T T T T T T C 5'
```

Phosphorothioate Oligonucleotide YS1

```
3' G T G G G T G G G G T G G G G T G G G T G 5'
5' G A G G G A G G G G A G G G G A G G G A G 3'
3' C T C C C T C C C C T C C C C T C C C T C 3'
```

Phosphorothioate Oligonucleotide RS1

```
         p   p p p p p   p p p p p p p p
5'   (E) T U C U U U U U C U U U U U U U C  3'
5' A G A A A G A A A A A G A A A A A A A G  3'
3' T C T T T C T T T T T C T T T T T T T C  5'
```

2 '-OMe Alkylator Oligonucleotide YA1

Figure 1: Simplified Map of pTER3 along with representative oligonucleotides used in this study.

Phosphorothioate oligonucleotide **ys1** has high affinity for the target site *in vitro* (>1 X 10^9) under ionic conditions approximating those found inside *Xenopus* oocytes (Chapter 5). Furthermore, phosphorothioate oligonucleotides have extended half-lives inside the *Xenopus* oocyte (>8 hours) relative to their phosphodiester counterparts (<30 minutes) (Woolf et al., 1990). Figure 4 outlines the manipulations involved in the *in vivo* footprinting experiments. These experiments require *in vivo* reaction assembly, *in vivo* methylation reaction, template reisolation, and primer extension analysis. In most cases, pTER3 is injected into the oocyte germinal vesicle 24 hours prior to subsequent injections. This allows the template to become coated with histones and eliminates plasmid unintentionally injected into the cytoplasm (Figure 3). When indicated, oligonucleotide is injected into either the oocyte germinal vesicle or cytoplasm and incubated for the allotted time. Afterwards, *in vivo* methylation reactions are initiated by soaking the oocytes in DMS. pTER3 is reisolated and the samples are analyzed by primer extension reactions.

Figure 5 displays the results of both *in vitro* and *in vivo* footprinting reactions using oligonucleotide **ys1** and the pTER3 DNA template. In lane 12, oligonucleotide **ys1** protects the two guanosines in the triple helical complex from DMS alkylation *in vitro* under physiological ionic conditions. However, if oligonucleotide **ys1** is injected into either the oocyte cytoplasm (lanes 3, 5, 7, and 9) or the germinal vesicle (lanes 2, 4, 6, and 8) there is no protection of the targeted guanines from alkylation. Preformed triple helical complexes injected into the oocyte germinal vesicle are not protected from methylation after a one hour incubation (lane 10).

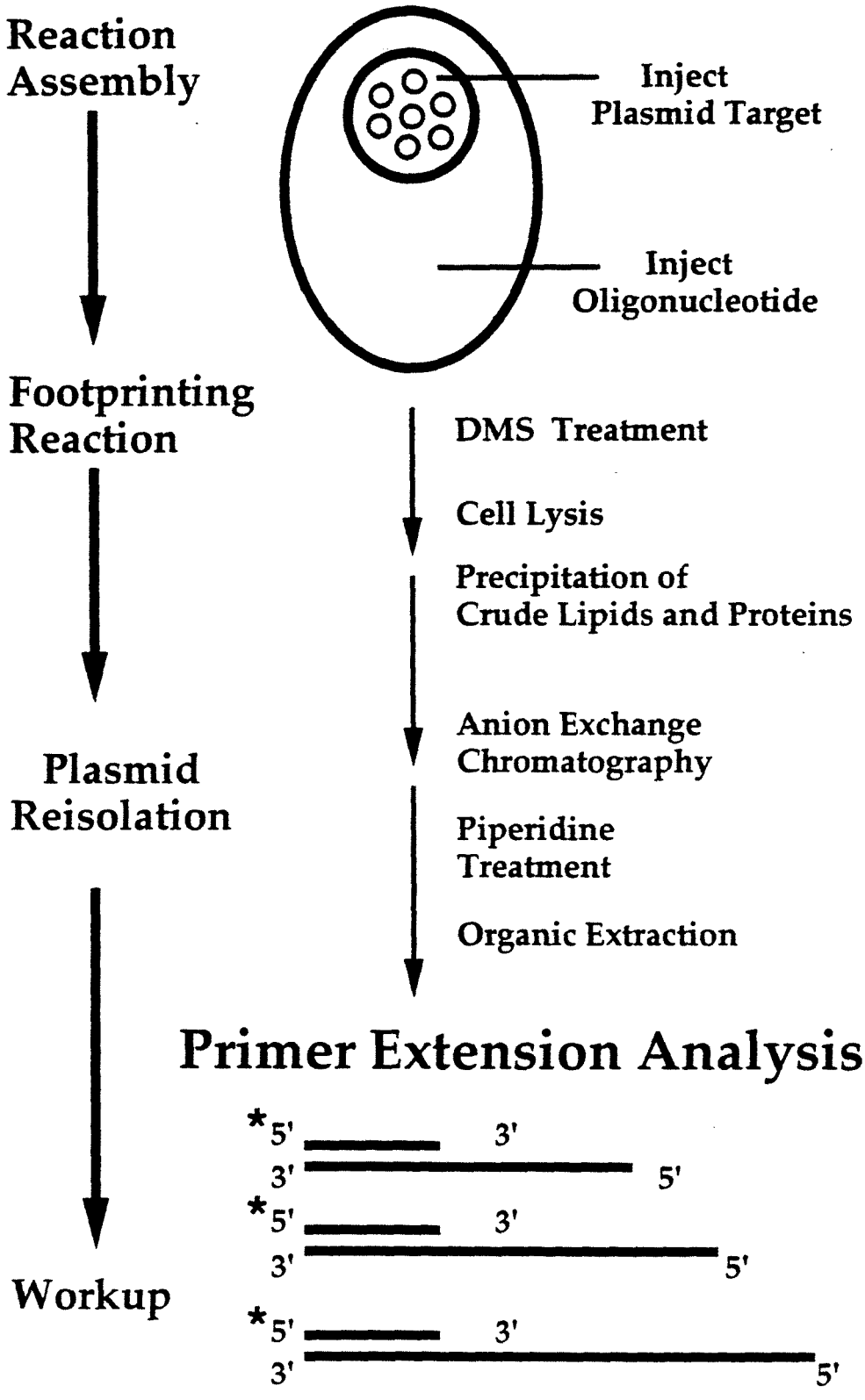
Reaction Assembly
Inject Plasmid Target
Inject Oligonucleotide
Footprinting Reaction
DMS Treatment
Cell Lysis
Precipitation of Crude Lipids and Proteins
Anion Exchange Chromatography
Plasmid Reisolation
Piperidine Treatment
Organic Extraction
Primer Extension Analysis
Workup
*5'
3'
3'
5'
*5'
3'
3'
5'
*5'
3'
3'
5'

In an analogous experiment, Figure 6 displays both *in vitro* and *in vivo* footprinting reactions using oligonucleotide **ys2** and the pTER3 DNA template. In lane 11, oligonucleotide **ys2** protects the two guanosines in the triple helical complex from DMS alkylation *in vitro* under physiological ionic conditions. As before, if oligonucleotide **ys2** is injected into the oocyte cytoplasm (lanes 3, 5, 7, and 9) or the germinal vesicle (lanes 2, 4, 6, and 8) targeted guanines are not protected from alkylation.

Figure 5: Autoradiogram of an 8% denaturing polyacrylamide gel showing results of *in vivo* footprinting reactions using oligonucleotide **ys1**. For all *in vivo* reactions, 10 ng of pTER3 was injected into the *Xenopus* oocyte germinal vesicle 24 hours prior to subsequent injections. When indicated, either 100 nL of 400 μM oligonucleotide **ys1** was injected into the oocyte cytoplasm or 20 nL of 400 μM oligonucleotide **ys1** was injected in the oocyte germinal vesicle. All samples were generated through primer extension reactions on reisolated pTER3 using 5'-end labeled primer **YP1**. Lane 1, *in vivo* DMS footprinting reaction; lane 2, *in vivo DMS* footprinting reaction with nuclear injected oligonucleotide **ys1** with a 2 hour incubation; lane 3, *in vivo* DMS footprinting reaction with cytoplasmically injected oligonucleotide **ys1** with a 2 hour incubation; lane 4, *in vivo* DMS footprinting reaction with nuclear injected oligonucleotide **ys1** with a 4 hour incubation; lane 5, *in vivo* DMS footprinting reaction with cytoplasmically injected oligonucleotide **ys1** with a 4 hour incubation; lane 6, *in vivo* footprinting reaction with nuclear injected oligonucleotide **ys1** with a 8 hour incubation; lane 7, *in vivo* DMS footprinting reaction with cytoplasmically injected oligonucleotide **ys1** with a 8 hour incubation; lane 8, *in vivo* DMS footprinting reaction with nuclear injected oligonucleotide **ys1** with a 12 hour incubation; lane 9, *in vivo* DMS footprinting reaction with cytoplasmically injected oligonucleotide **ys1** with a 12 hour incubation; lane 10, *in vivo* footprinting reaction with nuclear injected pTER3:oligonucleotide **ys1** triple helical complex with a 1 hour incubation; lane 11, *in vitro* DMS chemical sequencing reaction; lane 12, *in vitro* footprinting reaction with 1 μM oligonucleotide **ys1**.

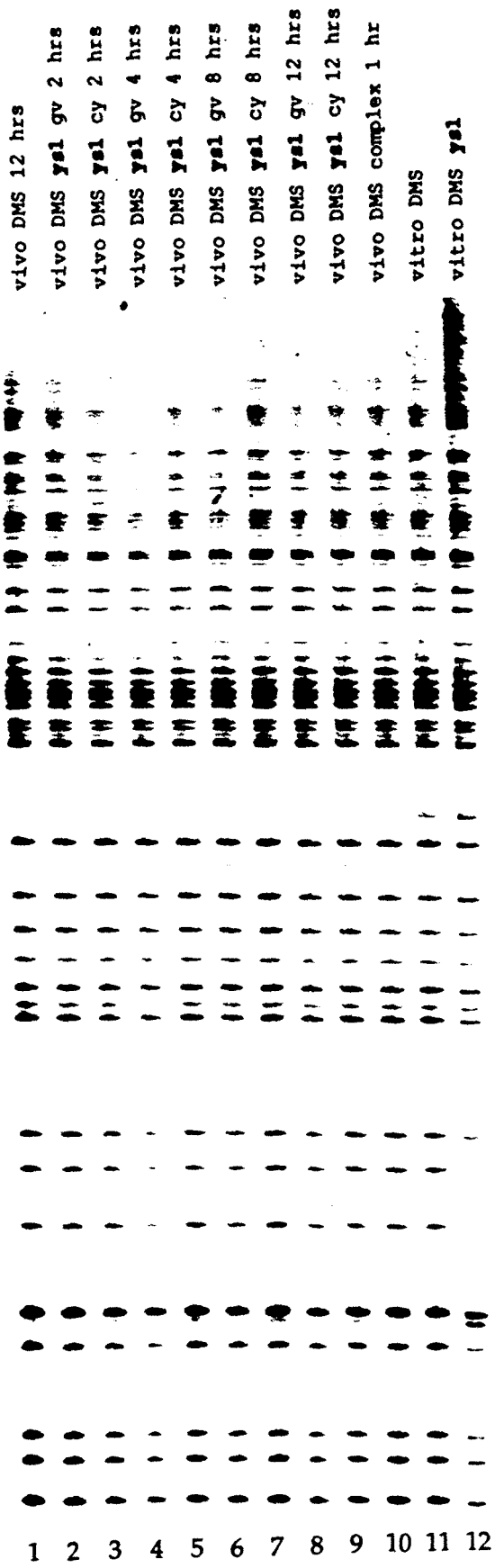
vivo DMS 12 hrs
vivo DMS ysl gv 2 hrs
vivo DMS ysl cy 2 hrs
vivo DMS ysl gv 4 hrs
vivo DMS ysl cy 4 hrs
vivo DMS ysl gv 8 hrs
vivo DMS ysl cy 8 hrs
vivo DMS ysl gv 12 hrs
vivo DMS ysl cy 12 hrs
vivo DMS complex 1 hr
vitro DMS
vitro DMS ysl
1 2 3 4 5 6 7 8 9 10 11 12

Figure 6: Autoradiogram of an 8% denaturing polyacrylamide gel showing results of *in vivo* footprinting reactions using oligonucleotide **ys2**. For all *in vivo* reactions, 10 ng of pTER3 was injected into the *Xenopus* oocyte germinal vesicle 24 hours prior to subsequent injections. When indicated, either 100 nL of 400 μM oligonucleotide **ys2** was injected into the oocyte cytoplasm or 20 nL of 400 μM oligonucleotide **ys2** was injected in the oocyte germinal vesicle. All samples were generated through primer extension reactions on reisolated pTER3 using 5'-end labelled primer **YP1**. Lane 1, *in vivo* DMS footprinting reaction; lane 2, *in vivo DMS* footprinting reaction with nuclear injected oligonucleotide **ys2** with a 2 hour incubation; lane 3, *in vivo* DMS footprinting reaction with cytoplasmically injected oligonucleotide **ys2** with a 2 hour incubation; lane 4, *in vivo* DMS footprinting reaction with nuclear injected oligonucleotide **ys2** with a 4 hour incubation; lane 5, *in vivo* DMS footprinting reaction with cytoplasmically injected oligonucleotide **ys2**; lane 6, *in vivo* footprinting reaction with nuclear injected oligonucleotide **ys2** with a 8 hour incubation; lane 7, *in vivo* DMS footprinting reaction with cytoplasmically injected oligonucleotide **ys2** with a 8 hour incubation; lane 8, *in vivo* DMS footprinting reaction with nuclear injected oligonucleotide **ys2** with a 12 hour incubation; lane 9, *in vivo* DMS footprinting reaction with cytoplasmically injected oligonucleotide **ys2** with a 12 hour incubation; lane 10, *in vitro* DMS chemical sequencing reaction; lane 11, *in vitro* footprinting reaction with 1 μM oligonucleotide **ys2**.

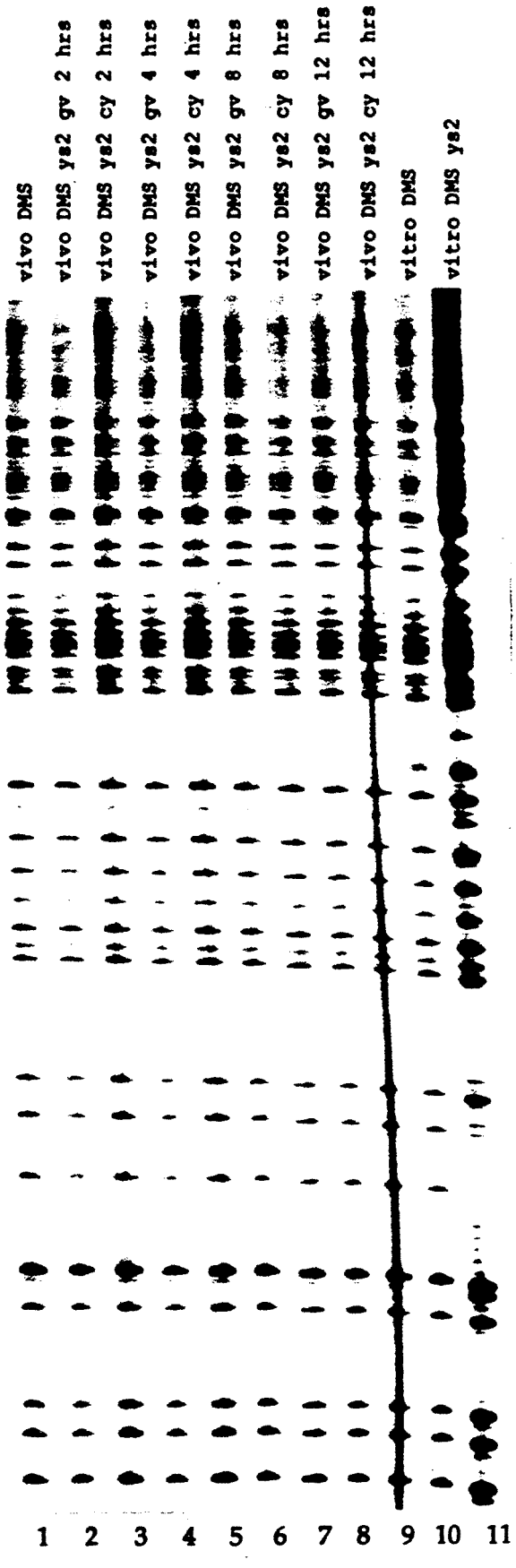
vivo DMS
vivo DMS ys2 gv 2 hrs
vivo DMS ys2 cy 2 hrs
vivo DMS ys2 gv 4 hrs
vivo DMS ys2 cy 4 hrs
vivo DMS ys2 gv 8 hrs
vivo DMS ys2 cy 8 hrs
vivo DMS ys2 gv 12 hrs
vivo DMS ys2 cy 12 hrs
vitro DMS
vitro DMS ys2
1 2 3 4 5 6 7 8 9 10 11

In Vivo Footprinting of Purine-Rich Oligonucleotide Triple Helical Targets. The purine-rich phosphorothioate oligonucleotide **rs1** was assayed by *in vivo* footprinting for triple helix formation at homopurine tract 2. Figure 7 displays the results of *in vitro* and *in vivo* footprinting reactions using oligonucleotide **rs1**. In lane 2, oligonucleotide **rs1** protects the seventeen guanosines in the triple helical complex from DMS alkylation *in vitro* under physiological ionic conditions. However, if oligonucleotide **rs1** is injected into the oocyte cytoplasm (lanes 4, 6, 8, and 10) or the germinal vesicle (lanes 3, 5, 7, and 9) there is no protection of the targeted guanines from methylation. Preformed triple helical complexes injected into the oocyte germinal vesicle are not protected from methylation after a one hour incubation (lane 11).

In an analogous experiment, Figure 8 displays the results of both *in vitro* and *in vivo* footprinting reactions using oligonucleotide **rs2**. In lane 11, oligonucleotide **rs2** protects the two guanosines in the triple helical complex from DMS alkylation *in vitro* under physiological ionic conditions. As before, if oligonucleotide **rs2** is injected into the oocyte cytoplasm (lanes 2, 4, 6, and 8) or the germinal vesicle (lanes 3, 5, 7, and 9) targeted guanines are not protected from alkylation.

In Vivo Alkylation Studies. A series of experiments were performed to determine if triple helix formation can direct the alkylation of a specific guanine on a minichromosome inside *Xenopus* oocytes. Oligonucleotide **yk1** containing 5-(1-propynyl)-2'-OMe-uridine and 2'-OMe-cytosine nucleosides was synthesized and post-synthetically modified with the N-hydroxy-succinimide ester of bromoacetaldehyde to create oligonucleotide **yk2** (Povsic & Dervan, 1990). This oligonucleotide carries a N-bromoacteyl

Figure 7: Autoradiogram of an 8% denaturing polyacrylamide gel showing results of *in vivo* footprinting reactions using oligonucleotide **rs1**. For all *in vivo* reactions, 10 ng of pTER3 was injected into the *Xenopus* oocyte germinal vesicle 24 hours prior to subsequent injections. When indicated, either 100 nL of 400 μM oligonucleotide **rs1** was injected into the oocyte cytoplasm or 20 nL of 400 μM oligonucleotide **rs1** was injected in the oocyte germinal vesicle. All samples were generated through primer extension reactions on reisolated pTER3 using 5'-end labelled primer **RP1**. Lane 1 , *in vitro* DMS chemical sequencing lane; lane 2, *in vitro* footprinting reaction with 1 μM oligonucleotide **rs1**; lane 3, *in vivo* DMS footprinting reaction with nuclear injected oligonucleotide **rs1** with a 2 hour incubation; lane 4, *in vivo* DMS footprinting reaction with cytoplasmically injected oligonucleotide **rs1** with a 2 hour incubation; lane 5, *in vivo* DMS footprinting reaction with nuclear injected oligonucleotide **rs1** with a 4 hour incubation; lane 6,*in vivo* DMS footprinting reaction with cytoplasmically injected oligonucleotide **rs1** with a 4 hour incubation; lane 7, *in vivo* DMS footprinting reaction with nuclear injected oligonucleotide **rs1** with a 8 hour incubation; lane 8, *in vivo* DMS footprinting reaction with cytoplasmically injected oligonucleotide **rs1** with a 8 hour incubation; lane 9, *in vivo* DMS footprinting reaction with nuclear injected oligonucleotide **rs1** with a 12 hour incubation; lane 10, *in vivo* DMS footprinting reaction with cytoplasmically injected oligonucleotide **rs1** with a 12 hour incubation; lane 11, *in vivo* footprinting reaction with nuclear injected pTER3:oligonucleotide **rs1** triple helical complex with a 1 hour incubation; lane 12, *in vivo* footprinting reaction with a 12 hour incubation.

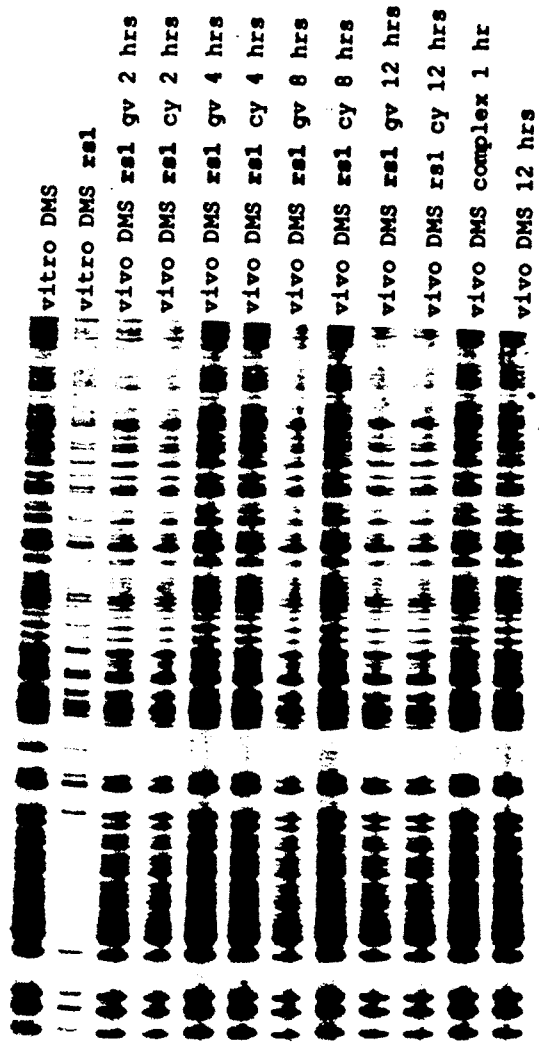

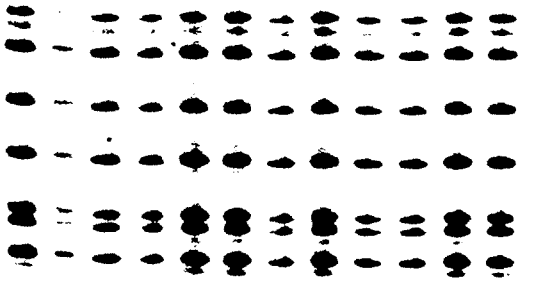

1 2 3 4 5 6 7 8 9 10 11 12

Figure 8: Autoradiogram of an 8% denaturing polyacrylamide gel showing results of *in vivo* footprinting reactions using oligonucleotide **rs2**. For all *in vivo* reactions, 10 ng of pTER3 was injected into the *Xenopus* oocyte germinal vesicle 24 hours prior to subsequent injections. When indicated, either 100 nL of 400 μM oligonucleotide **rs2** was injected into the oocyte cytoplasm or 20 nL of 400 μM oligonucleotide **rs2** was injected in the oocyte germinal vesicle. All samples were generated through primer extension reactions on reisolated pTER3 using 5'-end labelled primer **RP1**. Lane 1, *in vivo* DMS footprinting reaction with a 12 hour incubation; lane 2, *in vivo* DMS footprinting reaction with nuclear injected oligonucleotide **rs2** with a 2 hour incubation; lane 3, *in vivo* DMS footprinting reaction with cytoplasmically oligonucleotide **rs2** with a 2 hour incubation; lane 4, *in vivo* DMS footprinting reaction with nuclear injected oligonucleotide **rs2** with a 4 hour incubation; lane 5, *in vivo* DMS footprinting reaction with cytoplasmically injected oligonucleotide **rs2** with a 4 hour incubation; lane 6, *in vivo* DMS footprinting reaction with nuclear injected oligonucleotide **rs2** with a 8 hour incubation; lane 7, *in vivo* DMS footprinting reaction with cytoplasmically injected oligonucleotide **rs2** with a 8 hour incubation; lane 8, *in vivo* DMS footprinting reaction with nuclear injected oligonucleotide **rs2** with a 12 hour incubation; lane 9, *in vivo* DMS footprinting reaction with cytoplasmically injected oligonucleotide **rs2** with a 12 hour incubation; lane 10, *in vitro* DMS footprinting reaction; lane 11, *in vitro* footprinting reaction with 1 μM oligonucleotide **rs2**.

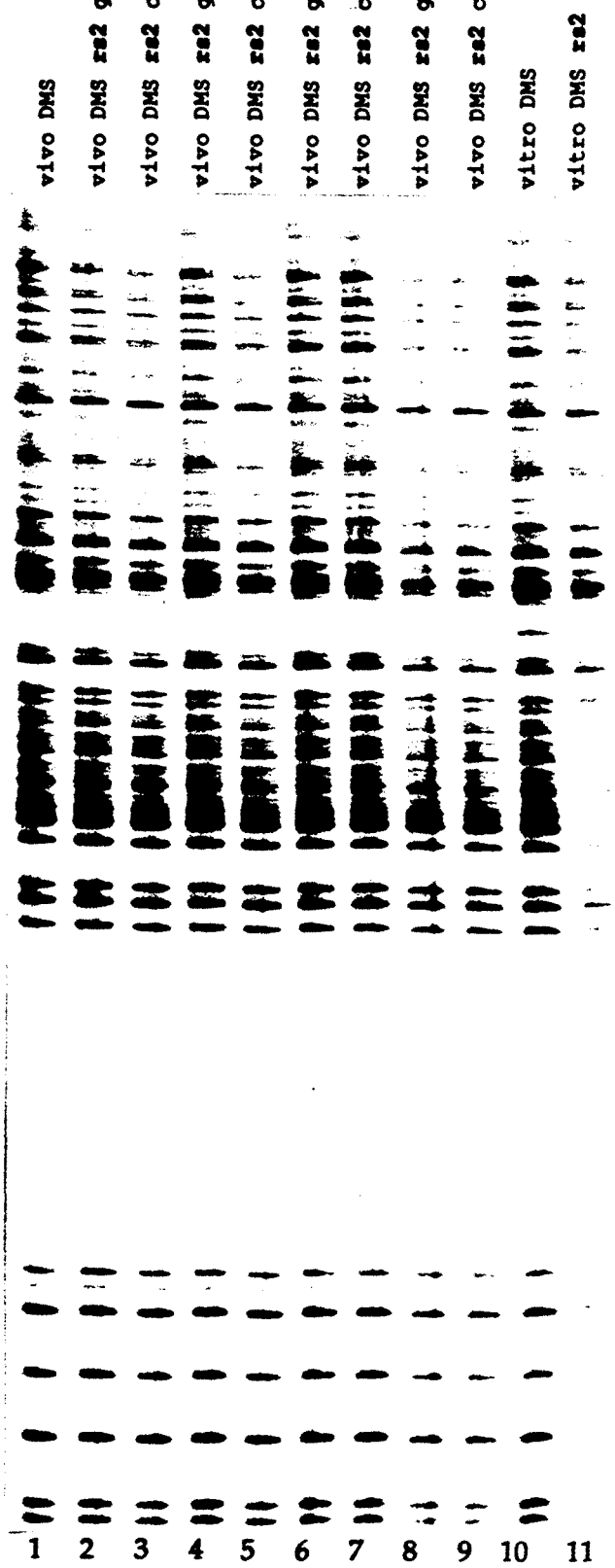
vivo DMS
vivo DMS rs2 gv 2 hrs
vivo DMS rs2 cy 2 hrs
vivo DMS rs2 gv 4 hrs
vivo DMS rs2 cy 4 hrs
vivo DMS rs2 gv 8 hrs
vivo DMS rs2 cy 8 hrs
vivo DMS rs2 gv 12 hrs
vivo DMS rs2 cy 12 hrs
vitro DMS
vitro DMS rs2
1 2 3 4 5 6 7 8 9 10 11

moiety tethered to the 5-position of the terminal 5'-modified 2'-deoxythymidine. Oligonucleotide **yk2** binds to a 16 base pair double helical target site through the formation of specific Hoogsteen hydrogen bonds and alkylate a single guanine two bases upstream from the 5'-end of the triple helix (Figure 1, Table 1). Figure 9 shows the results of both *in vitro* and *in vivo* alkylation reactions using this modified oligonucleotide and the pTER3 DNA template. In lane 2, oligonucleotide **yk2** directs nearly quantitative alkylation of the desired guanosine adjacent to the target site *in vitro* after 48 hours. However, if oligonucleotide **yk2** is injected into the oocyte cytoplasm (lanes 5, 7, 9, 11, and 13) or the germinal vesicle (lanes 6, 8, 10, 12, and 14) no alkylation of the desired guanosine is detected *in vivo*. In all cases, the pTER3 DNA template is almost completely intact without any detectable lesions attributable to the presence of the modified oligonucleotide.

Figure 9: Autoradiogram of an 8% denaturing polyacrylamide gel showing results of *in vivo* alkylation reactions using oligonucleotide **yk2**. For all *in vivo* reactions, 10 ng of pTER3 was injected into the *Xenopus* oocyte germinal vesicle 24 hours prior to subsequent injections. When indicated, either 100 nL of 400 μM oligonucleotide **yk2** was injected into the oocyte cytoplasm or 20 nL of 400 μM oligonucleotide **yk2** was injected in the oocyte germinal vesicle for the indicated incubation times. All samples were generated through primer extension reactions using 5'-end labelled primer **YP1**. Lanes 1 and 15, *in vitro* DMS chemical sequencing reaction; lane 2, *in vitro* alkylation reaction with 1 μM oligonucleotide **yk2** after 48 hours; lane 3, *in vitro* reaction without oligonucleotide **yk2** after 48 hours; lane 4, *in vivo* alkylation reaction with nuclear injected oligonucleotide **yk2** after 2 hours; lane 5, *in vivo* alkylation reaction with cytoplasmically injected oligonucleotide **yk2** after 2 hours; lane 6, *in vivo* footprinting reaction with nuclear injected oligonucleotide **yk2** after 4 hours; lane 7, *in vivo* alkylation reaction with cytoplasmically injected oligonucleotide **yk2** after 4 hours; lane 8, *in vivo* alkylation reaction with nuclear injected oligonucleotide **yk2** after 8 hours; lane 9, *in vivo* alkylation reaction with cytoplasmically injected oligonucleotide **yk2** after 8 hours; lane 10, *in vivo* alkylation reaction with nuclear injected oligonucleotide **yk2** after 12 hours; lane 11, *in vivo* alkylation reaction with cytoplasmically injected oligonucleotide **yk2** after 12 hours; lane 12, *in vivo* alkylation reaction with nuclear injected oligonucleotide **yk2** after 24 hours; lane 13, *in vivo* alkylation reaction with cytoplasmically injected oligonucleotide **yk2** after 24 hours; lane 14, *in vivo* reaction without oligonucleotide **yk2** after 24 hours.

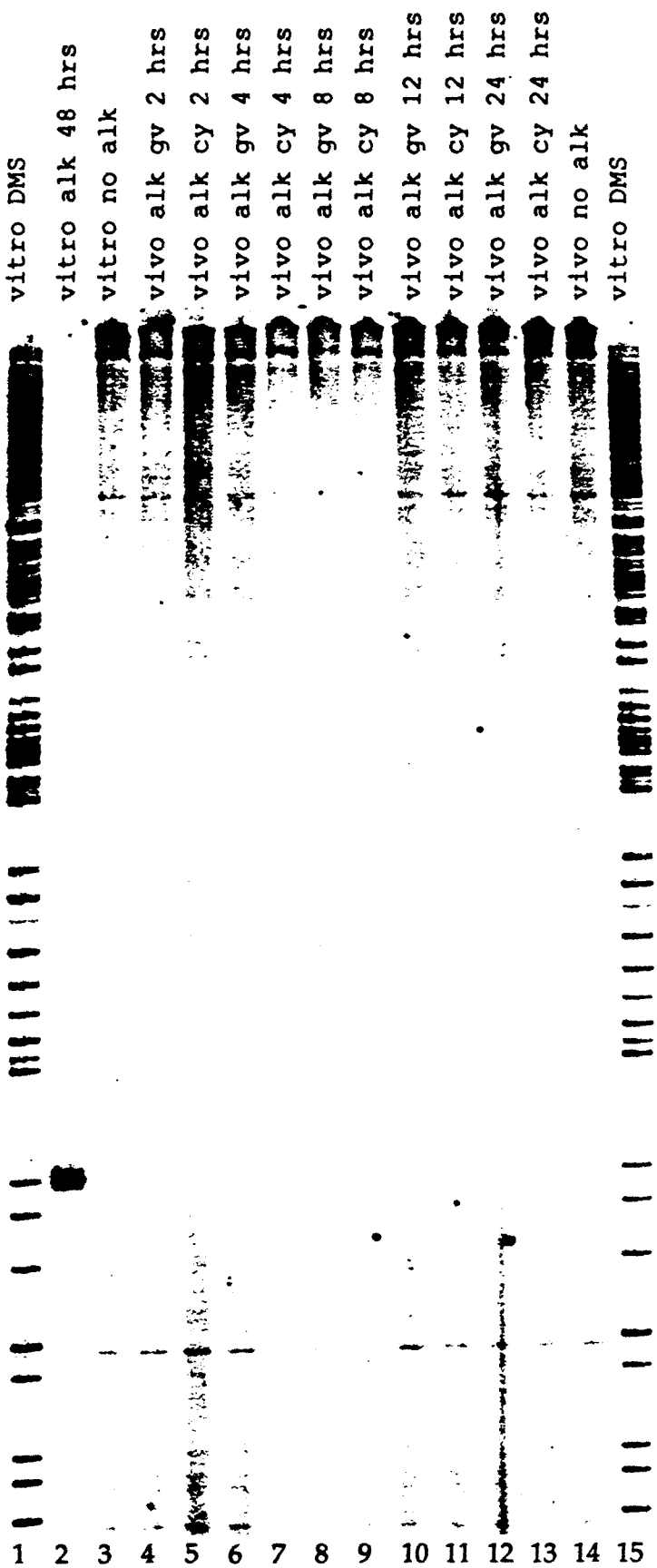
vitro DMS
vitro alk 48 hrs
vitro no alk
vivo alk gv 2 hrs
vivo alk cy 2 hrs
vivo alk gv 4 hrs
vivo alk cy 4 hrs
vivo alk gv 8 hrs
vivo alk cy 8 hrs
vivo alk gv 12 hrs
vivo alk cy 12 hrs
vivo alk gv 24 hrs
vivo alk cy 24 hrs
vivo no alk
vitro DMS
1 2 3 4 5 6 7 8 9 10 11 12 13 14 15

DISCUSSION

We have found that nuclease resistant phosphorothioate oligonucleotides which display high affinity for double helical DNA under physiological ionic conditions *in vitro* do not form triple helical structures with the same target sites inside *Xenopus* oocytes. *In vivo* footprinting analysis showed that the modified oligonucleotides injected either into the oocyte germinal vesicle or cytoplasm were unable to form detectable triple helical complexes with a target plasmid localized in the germinal vesicle. Preformed triple helical complexes, containing either pyrimidine-rich or purine-rich oligonucleotides, injected into the oocyte germinal vesicle were completely disrupted after one hour. Attempts to specifically alkylate the template at a single guanine *in vivo* were unsuccessful despite the fact that the reaction works efficiently (>95%) *in vitro.*

Potential Reasons for the Inability of Oligonucleotides to Bind Chromatinized DNA Templates In Vivo. There are a significant number of reasons why the oligonucleotides used in this study are unable to bind *in vivo* to the plasmid. Although phosphorothioate oligonucleotides have long half-lives in *Xenopus* oocytes, it is not clear how much of the oligonucleotide is free in solution and not bound by intracellular components, such as proteins or other nucleic acids (Baker et al., 1990; Dagle et al., 1990; Woolf et al., 1990). Oligonucleotides with 2'-OMe modifications have increased resistance to nucleases and long intracellular half-lives (Sproat et al., 1989; Monia et al., 1993; Morvan et al., 1993). The effective concentration of free oligonucleotide may be substantially lower than the amount injected. However, the fact that phosphorothioate

oligonucleotides are effective antisense reagents in *Xenopus* oocytes argues that a fraction of injected oligonucleotides is available for hybridization. In addition, the oligonucleotides may not have the proper intracellular localization to interact with the target site. Again, antisense studies in *Xenopus* oocytes show that mRNA localized in either the germinal vesicle or cytoplasmic compartments are susceptible to RNase H-mediated degradation directed by oligonucleotides injected into the cytoplasm (Cazenave et al., 1987; Jessus et al., 1988; Walder, 1988; Baker et al., 1990; Dagle et al., 1990; Smith et al., 1990; Woolf et al., 1990; Dagle et al., 1991; Chipev & Wolffe, 1992; Jenkins et al., 1992; Tsvetkov et al., 1992; Woolf et al., 1992). This indicates that some oligonucleotides are free to enter the germinal vesicle and hybridize with other nucleic acids.

Triple helical complexes may be disrupted by intracellular repair machinery or by polymerases that unwind the structures as they track along the helix (Maine & Kodakek, 1994). Preformed triple helical complexes involving both a pyrimidine-rich oligonucleotide **ys1** and a purine-rich oligonucleotide **rs1** were completely disrupted after one hour in the oocyte germinal vesicle. The *Xenopus* system was chosen to minimize any problems related to polymerase mediated triple helix destabilization. Plasmids injected into the oocyte germinal nucleus are not replicated by DNA polymerases. In addition, these plasmids are not actively transcribed unless specific promoter sequences are present. Since the plasmid used in this study lacks these sequences, it is unlikely that RNA polymerases are actively interacting with the triple helical target sequences. Transcription would likely result only from weak cryptic promoter sequences in the plasmid.

Finally, the target site may not be accessible to oligonucleotide

hybridization since it is coated with nucleosomes. It has not been demonstrated that oligonucleotides can bind to sequences packaged in histones. This may be due to steric blockade or by slowing the search process by which the oligonucleotide finds its target site. Plasmids injected into *Xenopus* oocytes become coated with histones than are normally not in phase with respect to one another. Most probably the target sites are in the linker region between histone octameric cores in some templates. It would be expected that these linker regions would be more accessible to oligonucleotide hybridization since they are not as directly associated with proteins. Nevertheless, chromatin structure may present a formidable challenge towards *in vivo* triple helix formation.

Potential Reasons for the Inability of Oligonucleotides to Direct Specific Alkylation In Vivo. The N-bromoacetimide modified 2'-OMe oligonucleotides were able to efficiently alkylate a specific guanine located two nucleotides upstream of the 5'-end of the triple helix *in vitro* utilizing the buffer conditions of Povisic and Dervan (Povsic & Dervan, 1990). These buffer conditions (20 mM HEPES pH 7.4, 0.8 mM $Co(NH_3)_6^{+3}$) were permit triple helix formation in a non-nucleophilic environment. Increasing the nucleophilicity of the hybridization conditions, by including Tris buffers or polyamines, decreases the efficiency of oligonucleotide-directed alkylation of the template (Povsic, 1992). This is presumably due to the reaction of oligonucleotide with buffer components which inhibit alkylation of the template. The reducing environment inside eukaryotic cells is due to the presence of large amounts (>5 mM) glutathione. Triple helix forming N-bromoacetamide oligonucleotides are deactivated *in vitro* when incubated in the presence of 5 mM cysteine

(Kutyavin et al., 1993). Thus the alkylator oligonucleotide conjugates used in this study may react with the excess glutathione or other nucleophilic oocyte components and be prevented from alkyating the DNA template. Also, if the oligonucleotide were able to alkylate the template DNA then the lesions would be susceptible to DNA repair. Abasic sites incorporated into SV40 derived plasmids are repaired with high fidelity (up to 99%) (Gentil et al., 1992; Cabral Neto et al., 1994). Repair activity in the oocyte may oblate lesions generated by the oligonucleotide conjugate. *Xenopus* oocytes have highly efficient DNA repair systems for lesions caused by UV irradiation (Saxena et al., 1991). Furthermore, *in vivo* footprinting experiments have shown that the unmodified alkylator oligonucleotides are unable to occupy the target homopurine tract. This would also prevent the site-specific alkylation chemistry from occurring. In order to address this issue, activatable N-bromoactetamide oligonucleotides would have to be designed to ensure that alkylation chemistry only occurs after template hybridization.

Reports on In Vivo Repair of DNA Adducts Targeted by Triple Helix Formation. Triple helix forming oligonucleotides have been used to create localized lesions on double helical DNA as a way of measuring intracellular DNA repair activity. Glazer and co-workers have focused on using psoralen derivatized oligonucleotides to create photoactivatable adduct formation on λ as well as SV40 DNA (Havre et al., 1993; Havre & Glazer, 1993). Targeted mutagenesis was more efficient in COS-7 cells transfected with SV40 DNA (6% of SV40 genomes incurred targeted mutations) than *E. coli* cells transfected with λ DNA (0.2% of λ genomes incurred targeted mutations). Bredberg and co-workers showed a 1.3%

targeted mutational rate in damaged plasmids transfected into a Jurkat human cell line (Sandor & Bredberg, 1994). The mutations generated are proximal to the triple helix binding site but are neither localized to a single position or predictable. Leonetti and co-workers reported that oligonucleotide-directed psoralen damage to the β-galactosidase gene cloned into a SV40 plasmid was rapidly repaired within one day of transfection into HeLa cells (Degols et al., 1994). However, damaged plasmid transfected into *Xeroderma pigmentosa* cells deficient in UV repair function was not repaired within 48 hours. This indicates that the intracellular repair of targeted psoralen adducts is directed by repair functions missing in the *Xeroderma pigmentosa* cell line.

Reports of In Vivo Triple Helix Formation. Although reports claiming biological effects of oligonucleotide-directed triple helix formation *in vivo* have been made, none have presented direct and clear evidence for complex formation. Helene and co-workers raised the possibility that a phosphodiester octathymadylate linked via its 3'-end to an acridine derivative could form a triple helical complex with SV40 DNA in CV1 monkey cells and inhibit viral DNA replication (Birg et al., 1990). However, other mechanisms that may explain their findings involving alternative nucleic acid hybridization schemes were proposed. More experimentation is necessary to discriminate between these numerous explanations.

Hogan and co-workers provided evidence that a guanine-rich 27-mer oligodeoxyribonucleotide designed to bind to the human c-*myc* P1 promoter, through the formation of G•GC, T•AT, A•TA, G•AT, and A•GC triplets, can cause a differential reduction of c-*myc* RNA levels in

HeLa cells 2.5 hours after addition to the media (Postel et al., 1991). DNase I hypersensitive site analysis showed an oligonucleotide-dependent alteration in DNaseI protection in the c-*myc* promoter region. This change may be attributed to a number of different phenomena unrelated to triple helix formation. The c-*myc* promoter element has been found to have an unusual, H-DNA (protonated triplex DNA) structure in vitro that has been called a nuclease-sensitive element (*NSE*) (Kinniburgh et al., 1994). Such structures contain both triple helical and single-stranded regions of DNA. Guanine-rich oligonucleotides that could bind to transcription factors such as the nuclease sensitive element protein-1, NSEP-1, or heterogeneous nuclear ribonuclear protein K, hnRNP K, would competitively inhibit binding of these factors to the *NSE* promoter element (Kinniburgh et al., 1994). This could lead to the oligonucleotide-dependent change in the c-*myc* promoter DNase I hypersensitivity pattern.

Two separate studies have been made claiming triple helix-mediated *in vivo* transcriptional inhibition of the IL2Rα gene. Hogan and co-workers claimed that a 28-mer guanine-rich phosphodiester oligonucleotide, designed to occupy the promoter region of the IL2Rα gene, caused a 30% decrease of IL2Rα mRNA levels in PHA-stimulated T lymphocytes (Orsen et al., 1991). However, these 3'-amine oligonucleotides were designed to bind parallel to the purine strand of the target site through the formation of G•GC, T•AT, G•CG, and T•TA triplets. Since purine-rich oligonucleotides preferentially bind in an antiparallel orientation to the target site and are destabilized by mismatches, it is difficult to conclude that triple helix formation is the reason for transcriptional inhibition. Again, nonspecific interactions between guanine-rich oligonucleotides and other biological macromolecules may cause these effects. Helene and

co-workers claimed that a 5'-acridine derivatized 15-nt pyrimidine-rich oligonucleotide could specifically inhibit transcription of an IL2Rα-CAT promoter-reporter gene construct in a human tumor T cell line (HSB2 cells) (Grigoriev et al., 1992). Although the authors show that the oligonucleotide binds the homopurine tract , through the formation of T•AT and $^{me}C^{+}$•GC triplets, which overlaps 4-bp of a NF-κB binding site *in vitro*, oligonucleotide and construct are cotransfected in the *in vivo* transcriptional inhibition experiments. This leaves open the possibility that the triple helical complexes are preformed prior to transfection or are forming during the transfection process.

Hogan and co-workers proposed that 31-nt and 38-nt 3'-amine modified guanine-rich phosphodiester oligonucleotides could bind to purine-rich HIV-1 viral promoters and inhibit expression of viral genes (McShan et al., 1992). The 31-nt oligonucleotide was designed to bind antiparallel to the purine-rich target site through the formation of G•GC, T•AT, G•CG, and T•TA triplets. On the other hand, the 38-nt oligonucleotide was designed to bind parallel to the purine-rich target site through the formation of G•GC, T•AT, G•CG, and T•TA triplets. The authors claim that there is ambiguity as to the orientation of guanine-rich third strand oligonucleotides with respect to the purine-rich strand of the duplex target site, in contrast to much of the published literature. Although evidence for oligonucleotide-dependent decreases in viral gene expression are made, no direct proof is offered that this inhibition is due to triple helix formation. Indeed, Rando and co-workers showed that independent of sequence composition, guanine-rich oligonucleotides were able to significantly inhibit HIV-1 induced syncytium formation and viral production in an acute infection assay system (Ojwang et al., 1994). The

oligonucleotides directly inhibited HIV-1 reverse transcriptase activity, HIV-1 integrase enzyme activity, and interactions between gp120 and CD4 without binding to double-helical DNA. This study raises questions to the cause of the anti-HIV-1 activity of the guanine-rich oligonucleotides used by Hogan and co-workers. Non-specific effects of guanine-rich oligonucleotides always must be considered when evaluating studies investigating *in vivo* triple helix formation.

Hogan and co-workers claimed that a 38-mer 3'-amine guanine-rich phosphodiester oligonucleotide cholesterol modified could bind to progesterone response elements controlling the expression of a chloramphenicol acetyl transferase reporter gene in transiently transfected monkey kidney-derived CV-1 cells (Ing et al., 1993). This antiparallel triple helical complex would be comprised of G•GC, T•AT, T•TA, and G•CG triplets. The authors claim that 3'-amine guanine-rich oligonucleotides that form triple helices *in vitro* do not effect the expression of a CAT reporter gene controlled by progesterone response elements *in vivo*. However, cholesterol derivatized triple helix forming oligonucleotides present at 20 mM in the culture medium could induce a two-fold reduction of CAT activity. This contrasts with other work from Hogan and co-workers that claim guanine-rich oligonucleotides not tethered to cholesterol could form triple helical structures *in vivo* and influence transcription of target genes (Postel et al., 1991; Orsen et al., 1991; McShan et al., 1992). The authors claim that the increased cell permeability of cholesterol modified oligonucleotides accounts for this phenomena. Further controls will be necessary to prove if triple helix formation is responsible for the decrease in promoter activity.

Hobbs and Yoon proposed that guanine-rich phosphodiester

oligonucleotides could bind to purine-rich target sites found on a plasmid tranfected in CHO cells and direct *in vivo* cleavage of the target by a triple-helix specific nuclease (Hobbs & Yoon, 1994). These guanine-rich oligonucleotides were designed to bind parallel to the purine-rich strand of the target site through the formation of G•GC, T•AT or A•AT, and G•TA triplets. The authors propose that guanine-rich oligonucleotides can bind to double helical DNA through G•GC triplet formation and maintain triple helix formation independent of other mismatched triplets, in contrast to other published data (Beal & Dervan, 1992). Southern blot analysis shows increasing amounts of guanine-rich oligonucleotide decreased the copy number of reporter plasmid in CHO cells. However, no controls utilizing other nonspecific guanine-rich oligonucleotides were used in these studies. The decrease in plasmid copy number may be attributable other unrelated effects such as cellular toxicity.

Roy reported that a purine-rich oligonucleotide designed to bind antiparallel to the purine-rich strand of the interferon response element (IRE) of the 6-16 gene located upstream of a CAT gene could decrease reporter gene activity in HeLa cells (Roy, 1994). The 21-nt oligonucleotide could bind the target site *in vitro* through the formation of G•GC, A•AT, and T•TA triplets. Like the 1991 study by Helene and co-workers involving the interleukin-2 receptor α-regulatory sequence, plasmid and oligonucleotide were co-transfected into mammalian cells prior to measuring CAT reporter gene inhibition (Grigoriev et al., 1992). Again triple helix formation may be occurring prior to introduction into the cellular environment. Furthermore, the author proposes that the plasmid used in this study may adopt a H-DNA conformation. It is difficult to prove that the oligonucleotide is not involved in other types of

hybridization reactions unrelated to intermolecular triple helix formation.

BIBLIOGRAPHY

Baker, C., Holland, D., Edge, M., & Colman, A. (1990) *Nucleic Acids Res. 18*, 3537-3543.

Beal, P. A. & Dervan, P. B. (1991) *Science 251*, 1360-1363.

Beal, P. A., & Dervan, P. B. (1992) *Nucleic Acids Res. 20*, 2773-2776.

Birg, F., Praseuth, D., Zerial, A., Thuong, N. T., Asseline, U., Le Doan, T., & Helene, C. (1990) *Nucl. Acids Res. 18*, 2901-2907.

Cabral Neto, J. B., Caseira Cabral, R. E., Margot, A., Le Page, F., Sarasin, A., & Gentil, A. (1994) *J. Mol. Biol. 240*, 416-420.

Cazenave, C., Chevrier, M., Thuong, N. T., & Helene, C. (1987) *Nucleic Acids Res. 15*, 10507-105021.

Chipev, C. C., & Wolffe, A. P. (1992) *Mol. Cell. Biol. 12*, 45-55.

Cortese, R., Harland, R., & Melton, D. (1980) *Proc. Natl. Acad. Sci. U. S. A. 77*, 4147-4151.

Dagle, J. M., Walder, J. A., & Weeks, D. L. (1990) *Nucleic Acids Res. 18*, 4751-4757.

Dagle, J. M., Weeks, D. L., & Walder, J. A. (1991) *Antisense Res. Devel. 1*,

11-20.

Dargemont, C., & Kuhn, L. C. (1992) *J. Cell Biol. 118*, 1-9.

Degols, G., Clarenc, J.-P., Lebleu, B., & Leonetti, J.-P. (1994) *J. Biol. Chem. 269*, 16933-16937.

Dumont, J. N. (1972) *J. Morph. 136*, 153-180.

Duval-Valentin, G., Thuong, N. T., & Helene, C. (1992) *Proc. Natl. Acad. Sci. U.S.A. 89*, 504-508.

Etkin, L. D., & Pearman, B. (1987) *Development 99*, 15-23.

Gargiulo, G., Wasserman, W., & Worcel, A. (1983) *Cold Spring Harbor Symp. Quant. Biol. 47*, 549-556.

Gargiulo, G., & Worcel, A. (1983) *J. Mol. Biol. 170*, 699-722.

Garrity, P. A., Chen, D., Rothenberg, E. V., & Wold, B. J. (1994) *Mol. Cell. Biol. 14*, 2159-2164.

Garrity, P. A., & Wold, B. J. (1992) *Proc. Natl. Acad. Sci. U. S. A. 89*, 1021-1025.

Gentil, A., Cabral-Neto, J. B., Mariage-Samson, R., Margot, A., Imbach, J. L., Rayner, B., & Sarasin, A. (1992) *J. Mol. Biol. 227*, 981-984.

Glikin, G. C., Ruberti, I., & Worcel, A. (1984) *Cell 37*, 33-41.

Grigoriev, M., Praseuth, D., Robin, P., Hemar, A., Saison-Behmoaras, T., Dautry-Varsat, A., Thuong, N. T., & Helene, C. (1992) *J. Biol. Chem. 267*, 3389-3395.

Gurdon, J. B. & Melton, D. A. (1981) *Ann. Rev. Genet. 15*, 189-218.

Hacia, J. G., Dervan, P. B., & Wold, B. J. (1994) *Biochemistry 33*, 6192-6200.

Havre, P. A., & Glazer, P. M. (1993) *J. of Virology 67*, 7324-7331.

Havre, P. A., Gunther, E. J., Gasparro, F. P., & Glazer, P. M. (1993) *Proc. Natl. Acad. Sci. U. S. A. 90*, 7879-7883.

Hobbs, C. A., & Yoon, K. (1994) *Antisene Res. and Devel. 4*, 1-8.

Ing, N. H., Beekman, J. M., Kessler, D. J., Murphy, M., Jayaraman, K., Zendegui, J. G., Hogan, M. E., O'Malley, B. W., & Tsai, M.-J. (1993) *Nucleic Acids Res. 21*, 2789-2796.

Jenkins, T. M., Saxena, J. K., Kumar, A., Wilson, S. H., & Ackerman, E. J. (1992) *Science 258*, 475-478.

Jessus, C., Cazenave, Ozon, R., & Helene, C. (1988) *Nucleic Acids Res. 16*, 2225-2233.

Kinninburgh, A. J., Firulli, A. B., & Kolluri, R. (1994) *Gene 149*, 93-100.

Kutyavin, I. V., Gamper, H. B., Gall, A. A. , & Meyer, R. B. (1993) *J. Am. Chem. Soc. 115*, 9303-9304.

Lamond, A. I., & Sproat, B. S. (1993) *FEBS Lett. 325*, 123-127.

Lehman, C. W., & Carroll, D. (1993) *Anal. Biochem. 211*, 311-319.

Lewin, B. (1990) *Genes IV*, Oxford University Press, New York.

Maher, L. J. (1992) *Biochemistry 31*, 7587-7594.

Maher, L. J., III, Wold, B., & Dervan, P. B. (1989) *Science 245*, 725-730.

Maher, L. J., III, Dervan, P. B., Wold, B. J. (1990) *Biochemistry 29*, 8820-8826.

Maher, L. J., III, Dervan, P. B., & Wold, B. (1992) *Biochemistry 31*, 70-81.

McShan, W. M., Rossen, R. D., Laughter, A. H., Trial, J., Kessler, D. J., Zendegui, J. G., Hogan, M. E., & Orson, F. M. (1992) *J. Biol. Chem. 267*, 5712-5721.

Maine, I. P., & Kodadek, T. (1994) *Biochem. Biophys. Res. Comm. 204*, 1119-1124.

Monia, B. P., Lesnik, E. A., Gonzalez, C., Lima, W. F., McGee, D., Guinosso, C. J., Kawasaki, A. M., Cook, P. D., & Freier, S. M. (1993) *J. Biol. Chem. 268*, 14514-14522.

Morvan, F., Porumb, H., Degols, G., Lefebvre, I., Pompon, A., Sproat, B. S., Rayner, B., Malvy, C., Lebleu, B., & Imbach, J. -L. (1993) *J. Med. Chem. 36*, 280-287.

Moser, H. E., & Dervan, P. B. (1987) *Science 238*, 645-650.

Mueller, P. R., Salser, S. J., & Wold, B. (1988) *Genes Devel. 2*, 412-427.

Ojwang, J., Elbaggari, A., Marshall, H. B., Jayaraman, K., McGrath, M. S., & Rando, R. F. (1994) *J. Acq. Imm. Def. Syn. 7*, 560-570.

Orsen, F. M., Thomas, D. W., McShan, W. M., Kessler, D. J., & Hogan, M. E. (1991) *Nucl. Acids Res. 19*, 3435-3441.

Postel, E. H., Flint, S. J., Kessler, D. J., & Hogan, M. E. (1991) *Proc. Natl. Acad. Sci. U. S. A. 88*, 8227-8231.

Povisc, T. J. Ph. D. Thesis, California Institute of Technology, 1992.

Povsic, T. J., & Dervan, P. B. (1990) *J. Am. Chem. Soc. 112*, 9428-9430.

Roy, C. (1994) *Eur. J. Biochem. 220*, 493-503.

Ryoji, M., & Worcel, A. (1984) *Cell 37*, 21-32.

Sandor, Z., & Bredberg, A. (1994) *Nucleic Acids Res. 22*, 2051-2056.

Savino, R., Hitti, Y., & Gerbi, S. A. (1992) *Nucleic Acids Res. 20*, 5435-5442.

Saxena, J. K., Hays, J. B., & Ackerman, E. J. (1991) *Nucleic Acids Res. 18*, 7425-7432.

Singleton, S. F. & Dervan, P. B. (1992a) *Biochemistry 31*, 10995-11003.

Singleton, S. F., & Dervan, P. B. (1992b) *J. Am. Chem. Soc. 114*, 6957-6965.

Singleton, S. F., & Dervan, P. B. (1993) *Biochemistry 32*, 13171-13179.

Skeiky, Y. A. W., & Iatrou, K. (1987) *J. Biol Chem. 262*, 6628-6636.

Smith, R. C., Bement, W. M., Dersch, M. A., Dworkin-Rastl, E., Dowrkin, M. B., & Capco, D. G. (1990) *Develop. 110*, 769-779.

Sproat, B. S., Lamond, A. I., Beijer, B., Neuner, P., & Ryder, U. (1989) *Nucleic Acids Res. 17*. 3373-3386.

Strobel, S. A., & Dervan, P. B. (1990) *Science 249*, 73-75.

Strobel, S. A., & Dervan, P. B. (1991) *Nature 350*, 172-174.

Strobel, S. A., Douchette-Stamm, L. A., Riba, L., Housman, D. E., & Dervan, P. B. (1991) *Science 254*, 1639-1642.

Tsvetkov, A., Jantsch, M., Wu, Z., Murphy, C., & Gall, J. C. (1992) *Mol. Biol. Cell 3*, 249-261.

Walder, J. (1988) *Genes Dev 2*, 502-504.

Woodland, H. R., & Adamson, E. D. (1977) *Dev. Biol. 57*, 118-135.

Woolf, T. M., Jennings, C. G. B., Rebagliati, M., & Melton, D. A. (1990) *Nucleic Acids Res. 18*, 1763-1769.

Woolf, T. M., Melton, D. A., & Jennings, C. B. (1992) *Proc. Natl. Acad. Sci. U.S.A. 89*, 7305-7309.

Wyllie, A. H., Gurdon, J. B., & Price, J. (1977) *Nature 268*, 150-151.

Wyllie, A. H., Laskey, R. A., Finch, J., & Gurdon, J. B. (1978) *Develop. Biol. 64*, 178-188.

Young, S. L., Krawczyk, S. H., Matteucci, M. D., & Toole, J. J. (1991) *Proc. Natl. Acad. Sci. U. S. A. 88*, 10023-10026.